Romanian Journal of
GEOPHYSICS

continuation of

STUDII TEHNICE ŞI ECONOMICE
(Seria D)

Founded 1947 by the Geological Institute of Romania

ISSN 1220-5680

Vol. 16

CONTENTS

I.G.G. 45° N
24° E

Institutul de Geologie şi Geofizică
Bucureşti – 1993

Romanian Journal of GEOPHYSICS

Published by the Institute of Geology and Geophysics, Bucharest
Director Ion Rădulescu

Editorial Office:
Institute of Geology and Geophysics
Str. Caransebeş 1
78344 Bucureşti–32, Romania
Tel. 65 75 30; 65 66 25
Fax. 010-40-0-12 84 44

The manuscripts should be sent to the scientific editor and/or executive secretary and the correspondence concerning advertisements, announcements and subscriptions to the executive secretary.

The **Romanian Journal of Geophysics** (Rom. J. Geophysics) is now at its first volume in the new form. However, the publication goes back to 1947, as the first volume of the "Studii tehnice şi economice, seria D" has appeared as proceedings of geophysicists' working with the Geological Institute of Romania.

The editor has changed the name as follows: Institutul Geologic al României (vol. I, 1947), Comitetul Geologic (vol. II–VI, 1950–1966), Institutul Geologic (vol. VII–X, 1970–1974), Institutul de Geologie şi Geofizică (vol. XI–XV, 1976–1988).

The **Institute of Geology and Geophysics** is now publishing the following periodicals:

- Romanian Journal of Mineralogy
- Romanian Journal of Petrology
- Romanian Journal of Mineral Deposits
- Romanian Journal of Paleontology
- Romanian Journal of Stratigraphy
- Romanian Journal of Tectonics and Regional Geology
- Romanian Journal of Geophysics

as well as other publications.

Classification index for libraries 55(058)

Printed by the Institute of Geology and Geophysics

Rom. J. Geophysics, 1993, 16, p. 1–8

L'INFLUENCE DES BRUITS INDUSTRIELS PRODUITS PAR L'ACTIVITÉ MINIÈRE SUR LES RÉSULTATS DE LA PROSPECTION MAGNÉTOMÉTRIQUE

Dan ALEXANDRESCU, Mioara ALEXANDRESCU

Institutul de Geologie şi Geofizică. Str. Caransebeş 1, 78344 Bucureşti 32.

Key words: Magnetic surveys. Magnetic field. Electromagnetic field. Noise.

Abstract: *Considerations on the Influence of the Industrial Noise Produced by Mining on the Results of Magnetometrical Prospecting.* A difficult problem is the separation between the natural fields and the industrial ones because of the large variety of electromagnetical sources with the same frequency. Our theoretical and practical studies have underlined the influence of the mining on the results of magnetometrical prospecting because of the stationary noise created by the buildings and even because of the transitory noise due to the variation of the continuous and/or alternative current.

La délimitation des champs naturels de ceux industriels est assez difficile, étant donné que la gamme des sources éléctromagnétiques rencontrées dans la même bande de fréquence est très large. Pour ce fait les recherches entreprises ont été dirigées vers l'observation et la connaissance des caractéristiques spatio-temporelles des bruits industriels, ainsi que l'influence de ceux-ci sur les mésurages magnétométriques exécutés au sol.

Les courants industriels (continu, alternatif) engendrent des champs très puissants parfois. De tels phénomènes perturbateurs, engendrés par le passage du courant électrique par les conducteurs (bruits industriels et régimes transitoires) sont doublés par des bruits à caractère stationnaire (ceux des anomalies constantes en temps) produits par les constructions et d'autres objets métalliques. Les effets magnétiques engendrés par les sources susmentionnées ajouttés au champ magnétique terrestre s'enterfèrent avec celuici et conduisent à des résultats qui peuvent etre interprétés d'une manière erronée.

À la différence des champs naturels qui ont les sources dans la profondeur, ou à l'extérieur de la Terre, les sources des champs industriels sont localisées à la surface du sol ou immédiatement au-dessous de celuici, à des distances très réduites de la zone à investiguer. La séparation des champs naturels de ceux industriels pose des problèmes quant aux apareils employés, ceuxci devrant etre capables d'enregistrer simultanément le champ magnétique en plus de trois stations.

L'investigation de l'influence des bruits industriels (en régime transitoire) générés par les activités minières sur les mesurages magnétométriques éxécutés au sol représente une continuation aux études effectués par Beşuţiu (1983, 1985, données nonpubl.). Pour l'étude de ce problème on doit prendre en considération les deux aspects des perturbations: celles stationnaires (produites par le soutènement d'une galerie, par les voies ferrées, par les diverses annexes des travaux miniers) et celles transitoires, dûes aux courants électriques.

Les lignes électriques sont représentées dans notre pays par les systèmes de transport en courant alternatif et par ceux en courant continu. Les systèmes électriques de transport comportent des installations à des implications dans la détermination des caractéristiques du champ électromagnétique qui se propage dans le milieu ambiant (Beşuţiu, 1986, données nonpubl.). Les lignes de transport en courant continu, amplement utilisées dans le transport minier sont semblables au système de transport en courant alternatif, avec la seule particularité que les amplitudes des composants du champ présentent des variations irrégulières (Condacse, 1980).

La recherche des anomalies magnétiques générées par l'acier du soutènement de la galerie, ainsi que par les courants électriques qui circulent par les conducteurs de la galerie, relève l'importance des perturbations stationaires et transitoires pour tout le phénomène anomal.

Les anomalies engendrées par l'induction magnétique de l'acier présent dans les galeries sont en général dipolaires, présentant de hautes magnétisations et, adjacentement, de basses magnétisations (par l'approximation d'une galerie à un cylindre infinit horizontal). L'amplitude A (en nT) de la courbe anomale donnée par l'acier d'un conducteur, définie comme la différence entre les points de maximum et minimum résulte de la relation (Gay, 1982):

$$A = \frac{2KT'_0 S}{Z^2}\frac{\sin I_0}{\sin I'_0} a \qquad (1)$$

où

K = la susceptibilité magnétique (qui inclut aussi la démagnétisation);

T'_0 = l'intensité du vecteur du champ magnétique terrestre au plan vertical du conducteur;

S = l'aire de la section de l'acier du conducteur;

Z = la distance à la verticale dès le niveau d'observation au centre du conducteur;

I_0 = le penchant du champ magnétique terrestre;

I'_0 = le penchant du champ magnétique terrestre au plan vertical qui renferme le conducteur;

a = le coeficient dont la valeur varie entre 1.125 et 1.299, fonction du penchant du champ et l'orientation du conducteur.

L'effet anomal produit par les conduits d'acier peut être determiné aussi en utilisant la relation (Glebovskii, Vasiutocikin, 1981):

$$A = \frac{K\pi F d l}{r^2} \qquad (2)$$

où

r = la distance du centre du conduit (en centimètres);

F = la valeur normale du champ géomagnétique;

d = le diamètre du conduit;

l = l'épaisseur des parois du conduit;

K = le coéficient qui dépende de l'acier du conduit, $10 \leq K \leq 20$.

En calculant l'effet donnée par l'acier du conduit on a constaté qu'en général il est néglijable, représentant la dixième partie de nT pour les distances, dès le point d'observation vers le centre du conduit, sur des distances de centaines de mètres.

L'anomalie magnétique dûe au courant qui circule par les conducteurs de la galerie peut être estimée, en considérant la galerie un cylindre horizontal infini. La figure 1 représente une section transversale à la galerie. Selon "la règle de la main droite" de la physique élémentaire, les lignes du flux magnétique sont circulaires et mouvent dans le sens des aiguilles du montre, notamment quand le courant s'écoule le long de l'axe x' (dans le plan du papier).

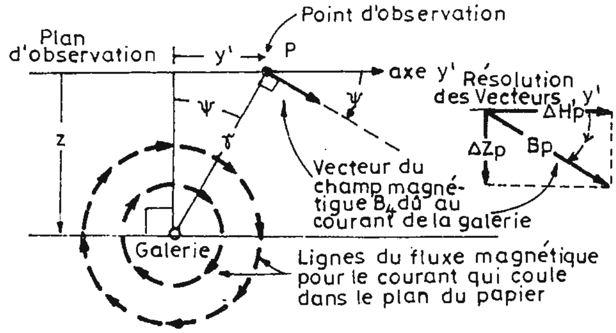

Fig. 1 – La géométrie du flux magnétique et les vecteurs du champ magnétique produits par le courant électrique qui circule dans la galerie horizontale.

La direction du vecteur de l'intensité du champ magnétique B est tangente au cercle – c'est à dire à la galerie – en n'importe quel point P, ayant la suivante valeur facilement à déduire de la loi d'Ampère:

$$B = \frac{0,2I}{r} \qquad (3)$$

où

B = l'intensité du champ magnétique engendrée par le passage du courant électrique continu, en nT;

I = l'intensité du courant électrique continu, en A;

r = la distance radiale de la galerie, en km.

Conformément à l'équation susmentionnée l'intensité du champ magnétique généré par le passage du courant électrique continu diminue uniquement avec la première puissance de la distance, pendant que le champ dû aux objets métalliques afférents à la galerie diminue avec le carré de la distance. Ce taux de diminution lent constitue la cause principale des ennuis engendrés par la présence des galeries dans les périmètres investigués envers les mesurages magnétométriques exécutés au sol.

On doit souligner encore une fois que la principale source des anomalies magnétiques, dans les zones à galeries minières où le transport est électrique, la constitue le courant continu, sans tenir compte de la présence d'autres sources en liaison avec les conducteurs existents: magnétisation induite, magnétisation rémanente, courant électrique alternatif, mais aussi celui qui s'écoule loin du conducteur dans le sol. Les calcules effectués sont valables pour une longueur considérée infinie de la galerie. Mais quelques changements dans les valeurs doivent intervenir pour une longueur finie.

Ayant en vue les considérations teoriques antérieures on a calculé les effets du courant électrique continu à la surface. Les paramètres variables pris en considération ont été: x (la distance en km en plan horizontal du centre de la galerie au point d'enregistrement P) et Z (la distance en km, à la verticale, dès le point d'enregistrement P à la côte de la galerie). Pour un courant continu de 100 A, on a calculé les effets produits par celui-ci pour que les résultats obtenus soient aisément d'interpréter pour n'importe quel autre courant. Dans le tableau qui suit sont présentés quelques résultats pour observer la manière de dépendence de l'intensité du champ magnétique B des x et Z (en nT).

x(km) / z(km)	0.0	0.20	0.40	0.60	0.80
0.010	2000.0	99.9	50.0	33.3	25.0
0.250	800.0	99.2	49.9	33.3	25.0
0.050	400.0	97.0	49.6	33.2	25.0
0.075	266.7	93.6	49.1	33.1	24.9
0.100	200.0	89.4	48.5	32.9	24.8
0.125	160.0	84.8	47.7	32.6	24.7
0.150	133.3	80.0	46.8	32.3	24.6

On observe que pour une distance de plus de 400 m entre le point d'observation et la galerie, l'influence de la profondeur dans le calcul de la valeur de l'intensité du champ magnétique B diminue de manière qu'à 600 m la valeur se modifie avec 1 nT pour une profondeur variable de la galerie, de 10 à 150 m. Pour une même profondeur de la galerie, 0,01 km par exemple, sur les premières centaines de mètres la diminution est importante (des centaines de nT). Pour des distances dépassant 0,5 km entre la galerie et le point d'enregistrement, la modification de l'intensité du champ magnétique présente des valeurs unitaires ou même subunitaires. Des données présentées on observe comme le gradient magnétique diminue avec chaque centaine de mètres.

0.5 - 0.6 km	6.6 nT/100 m
0.6 - 0.7	4.7
0.7 - 0.8	3.6
0.8 - 0.9	2.8
0.9 - 1.0	2.2
1.0 - 1.5	1.4
1.5 - 2.0	0.6
2.0 - 5.0	0.2
5.0 - 10.0	0.04

Les études effectuées ne se sont axées uniquement sur des considérations téoriques sur les sources et les caractéristiques des champs magnétiques naturels et industriels, mais ont suivi aussi la possibilité d'effectuer des mesurages magnétométriques dans la présence des bruits industriels de l'activité minière. Les expériments ont été entrepris en deux provinces différentes du point de vue géologique – le bassin sédimentaire de Comăneşti et la zone de l'éruptif néogène de Baia Mare.

De la large gamme d'expériments effectués – des mesurages classiques ou simultanés dans les reseaux de micropanneaux magnétiques, mesurages dans des profiles magnétiques ou dans des points fixes situés à des différentes distances par rapport à la galerie – les plus significantifs seront détaillées à continuation.

Pour le bassin sédimentaire de Comăneşti, deux des résultats obtenus sont représentatifs. Dans la figure 3 on présente deux enregistrements simultanés du champ magnétique, enregistrements exécutés dans deux points fixes – l'un situé sur la galerie et l'autre à 50 m du premier. On a enregistré de variation de l'ordre de centaines de nT dans le premier cas et de l'ordre de dizaines de nT dans le deuxième cas. Représentative est la figure 4 où les variations du champ magnétique enregistrées en trois points fixes emplacées sur la galerie, à 100 m et à 300 m de celle-ci, diminuent fortement une fois avec l'éloignement de la source de perturbation.

Dans la figure 2 on présente des enregistrements synchrones avec deux magnétomètres emplacés à des distances différentes de la source du bruit (50 m, 250 m, 500 m) (1 et 2) qui ont été effectués dans les périmètres des exploitations minières de Rudnîi Altai et Karatau (Busnev, 1977). Ces enregistrements ont été comparés en permanence avec ceux exécutés dans un point de référence situé à approximativement 12 km de l'aire polluée (3). Les investigations entreprises ont conduit à des résultats remarquables: on peut exécuter des prospections magnétométriques de précision ($e = \pm 2nT$) à une distance de plus de 500 m des installations de l'exploitation minière.

Dans la zone de l'éruptif néogène, une des zones interessantes a été délimitée dans le cadre du périmètre minier de Băiţa. La galerie de Tüzoşa – située à 4 km vers le nord de la localité de Băiţa – a représenté une autre source perturbateure dont on a suivi la manière d'influence. Les mesurages ont été exécutés en deux panneaux micromagnétiques, disposés transversalement sur la galerie et emplacés à 50 m de l'entrée dans la galerie (A) et, respectivement, à 25 m du premier (B). On a effectué les mesurages tant dans la manière classique, la base pour l'enregistrement de la variation diurne étant emplacée en dehors de la zone polluée magnétiquement (5 km environ), aussi bien que synchrones avec 4 magnétomètres protoniques, deux pour chaque panneau, mais sans un dispositif spécial de synchronisation. Dans la planche sont représentées les images du champ magnétique pour les deux pan-

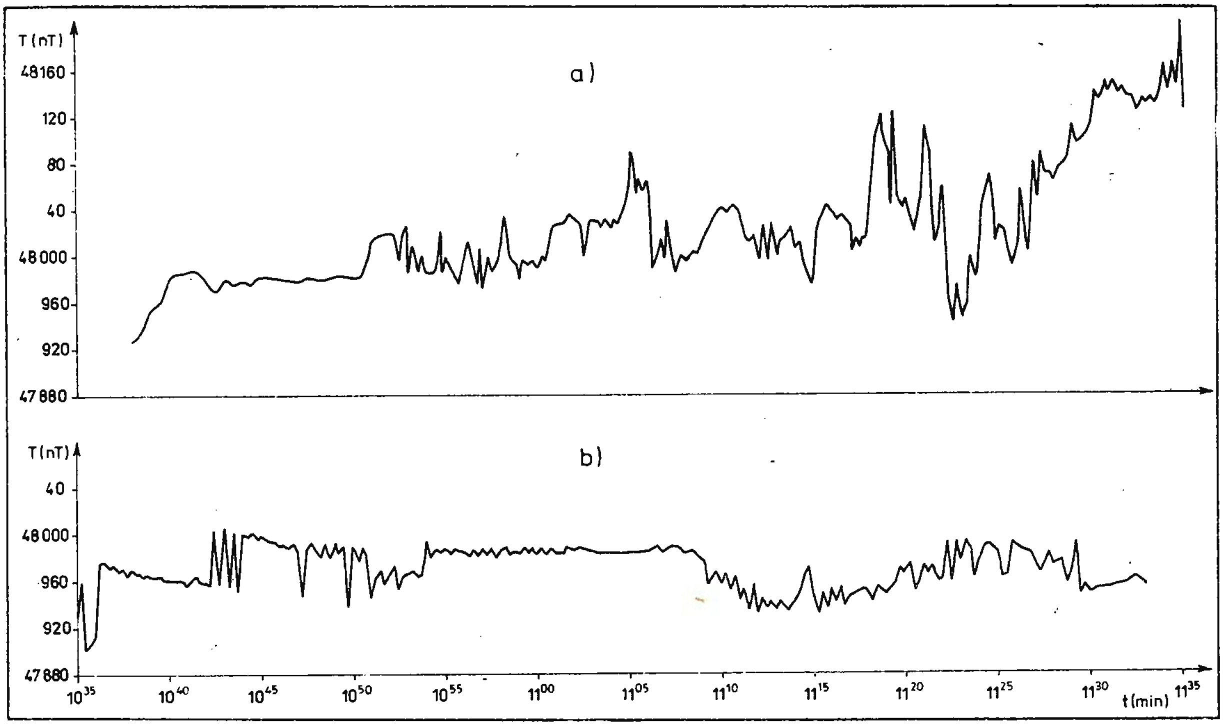

Fig. 2 – L'enregistrement du champ magnétique au-dessus (a) et à 50 m (b) de la galerie RAL-Comăneşti.

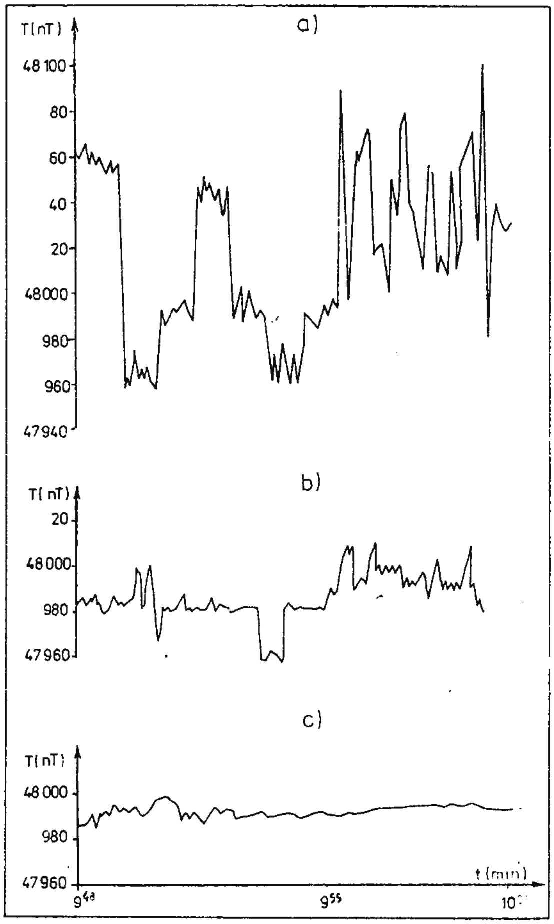

Fig. 3 – L'enregistrement simultané des variations du champ magnétique dans 3 points emplacés dans la zone de la galerie RAL-Comăneşti.

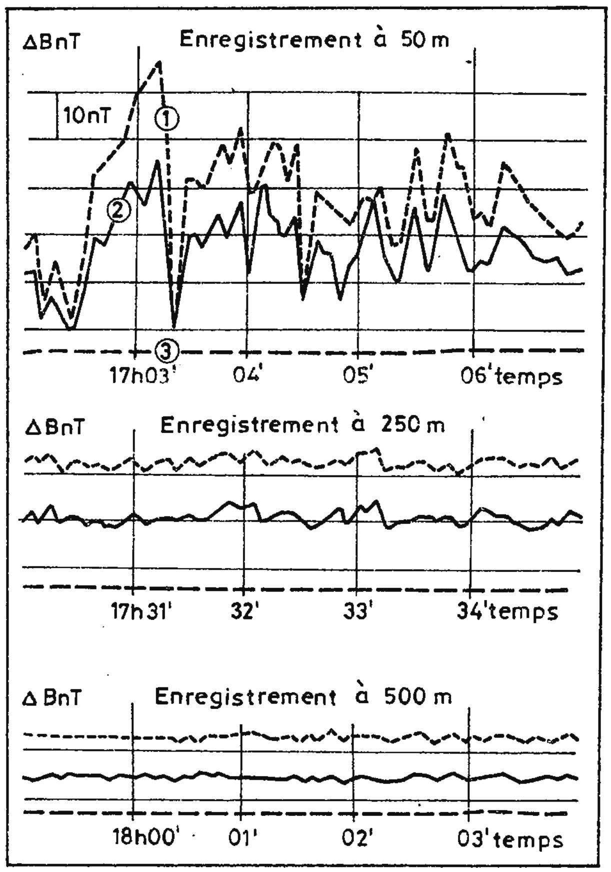

Fig. 4 – Séquences du bruit engendré par l'activité minière (après Busuev, 1970)

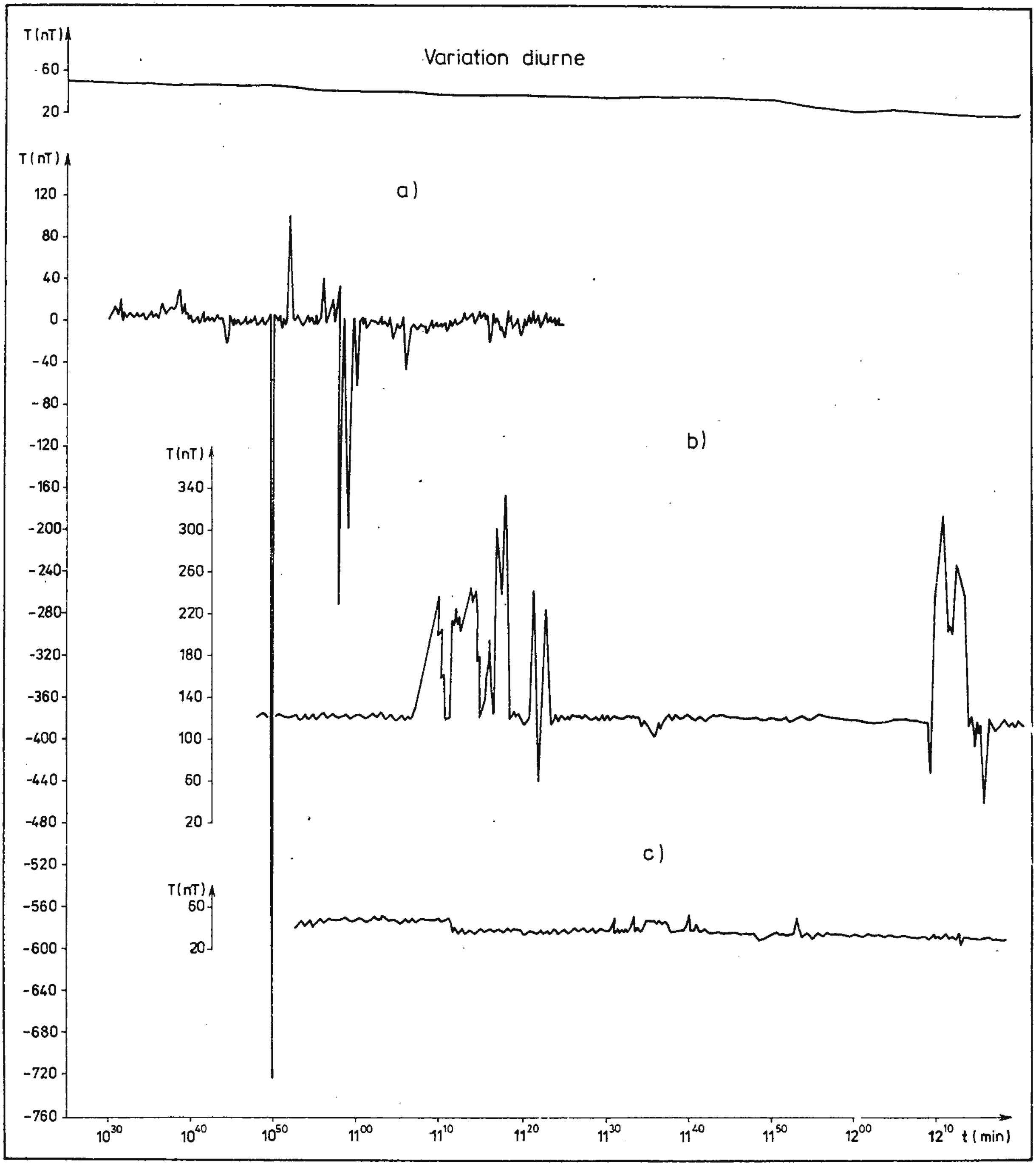

Fig. 5 - Enregistrement des variations temporaires du champ magnétique dans la zone de la galerie Tüzoşa-Băiţa.

neaux: A – des mesurages synchrones avec deux magnétomètres protoniques, et B – des mesurages en deux variantes (classique-2 et synchrone-1).

Dans l'intervalle où on a exécuté les enregistrements des deux panneaux, la locomotive électrique est restée au puits d'extraction de Tüzoşa, donc l'intensité du courant électrique continu a été quasiconstante. On observe, dans l'image présentée, que la partie centrale du panneau est caractérisée par une zone anomale, disposée au-dessus de la galerie, en représentant l'effet du à celle-ci. Pour le panneau apparait un effet cumulé dû tant à la galerie que par le conduit métallique enfoui à une profondeur réduite. L'emplacement de ces micropanneaux a eu comme but l'obtention des images du champ magnétique dans la zone d'une mine. Tenant compte de la nature des phénomènes perturbateurs (des bruits à des régims transitoires) les résultats ne sont pas si concluants. Ainsi on a considéré utile l'emplacement de certains points permanents de mesurage, ayant en vue aussi la variation des phénomènes qui perturbent le champ magnétique terrestre dans de telles zones polluées (fig. 5).

Il est digne d'attention le fait que l'enregistrement effectué dans les points situés à 50 m et, respectivement, 400 m de la galerie a été réalisé pendant le passage de la locomotive électrique, ainsi qu'au stationnement de celle-ci.

Les variations de l'amplitude de l'intensité du champ magnétique enregistrées dans ce point sont de l'ordre de 10 à 12 nT, en démontrant la diminution accentuée de l'effet perturbateur le long des premières centaines de mètres par rapport à la galerie.

De la comparaison du profile mesuré dans la zone du système de galeries de la vallée de Tüzoşa Mare avec les profils théoriques calculés pour trois intensités du courant électrique continu (I = 40, 70 et 100 A) on observe que les amplitudes maximums sont présentes dans la zone de la galerie, les effets étant de centaines de nT tant pour les cas théorique que ceux réels aussi.

Une autre zone investiguée, qui nous a fourni des résultats très intéressants, est située dans le périmètre minier de Ilba (les galeries de Firiza I et de Ţapu).

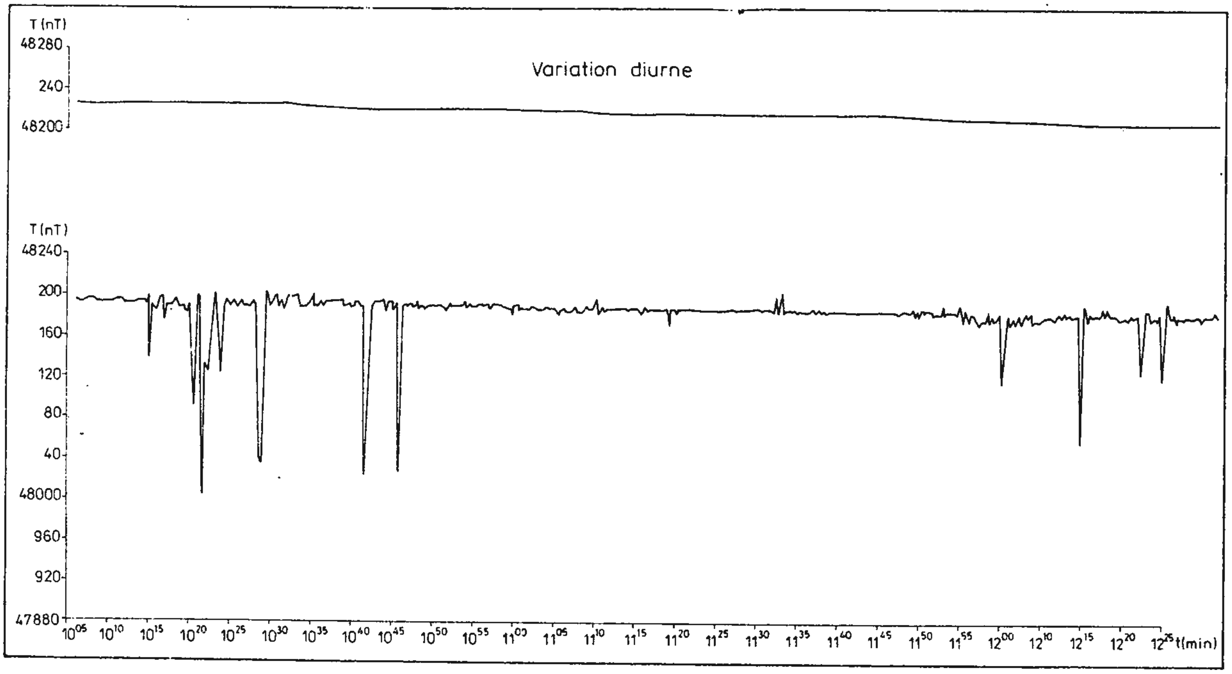

Fig. 6 - La variation temporaire du champ magnétique enregistrée dans la zone de la galerie Firizan I - Ilba.

Le diagramme (a) représente l'enregistrement des variations du champ magnétique dans un point situé immédiatement au-dessus de la galerie à 40 m environ à la verticale. Sur le diagramme (b) de la variation en temps du champ magnétique enregistré à 50 m de la galerie on observe deux intervalles de temps, entre 11^{07} h et 11^{25} h et 12^{00} h et 12^{18} h à de grandes variations (300 nT environ) de l'amplitude de l'intensité du champ magnétique, dus au déplacement de la locomotive électrique, ce qui implique de grandes variations de l'intensité du courant électrique continu. Le diagramme (c) représente la variation en temps du champ magnétique, dans un point situé à 400 m de la galerie.

Les figures 6 et 7 représentent les variations du champ magnétique en deux points fixes emplacés dans la zone des galeries susmentionnées, ainsi que les courbes de variation diurne pour le meme intervalle de temps.

Le point de l'enregistrement présenté dans la figure 6 est emplacé à approximativement 135 m de l'ouverture de la galerie, à 25 m latéralement de celle-ci et à 95 m à la verticale. L'enregistrement est caractérisé par l'existence de quelques perturbations à de grandes amplitudes, jusqu'à 200 nT, sur le fond de certaines variations à des amplitudes petites, quelques dizaines de nT.

Le point fixe dans lequel on a obtenu la variation

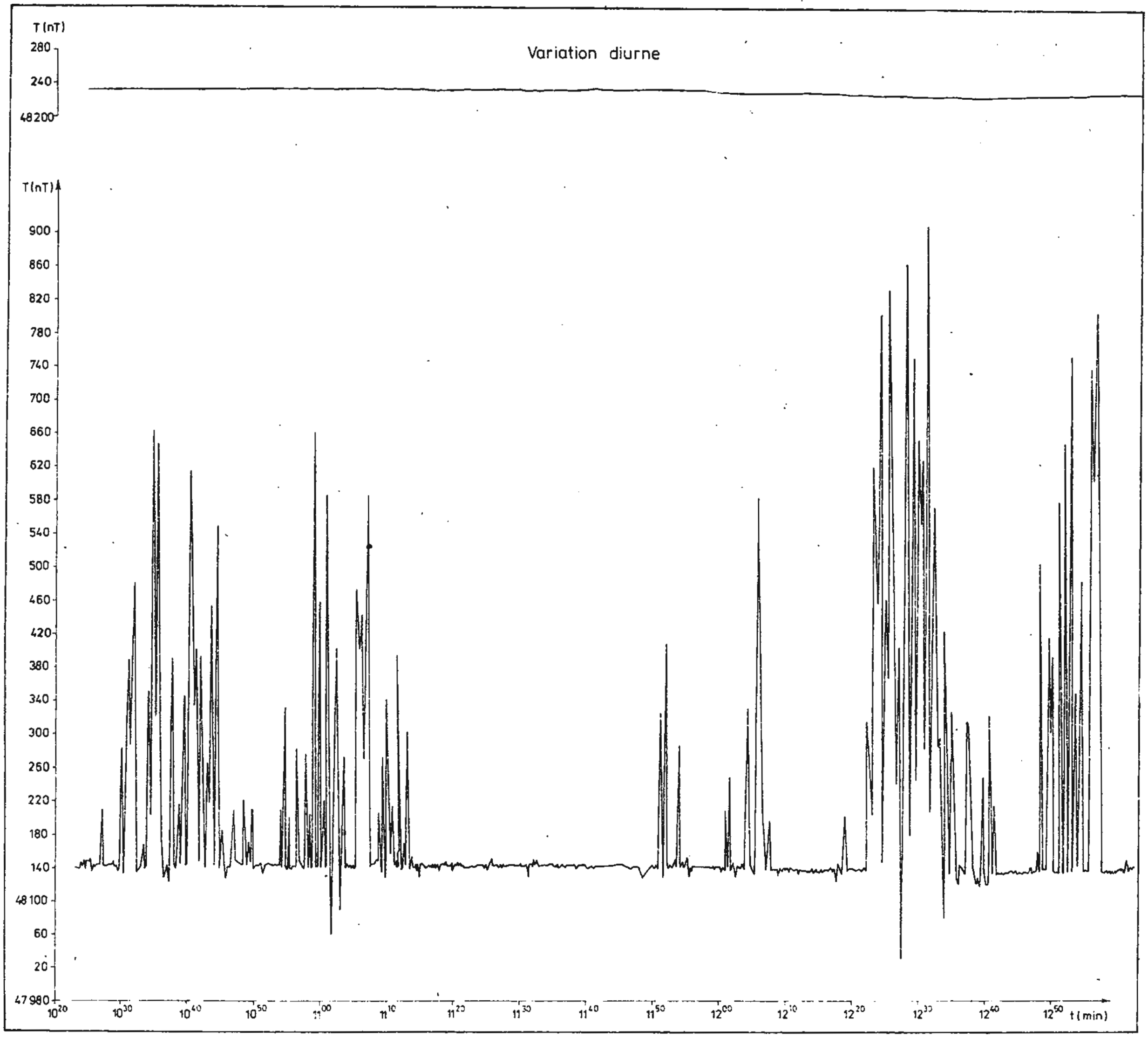

Fig. 7 - La variation temporaire du champ magnétique au-dessus de la galerie Ţapului - Ilba.

du champ magnétique présentée dans la figure 7, est emplacé à 50 m de l'ouverture de la galerie de Ţapu, au dessus de celle-ci, la galerie étant à une profondeur de 22 m. A la différence de ce cas on observe des variations de l'intensité du champ magnétique à de très grandes amplitudes, jusqu'à 900 nT environ, sur le fond des variations à de petites amplitudes de l'ordre des dizaines de nT.

On a recourt à ces expériments pour une vérification des considérations théoriques présentées et pour mettre en évidence les conclusions ci-dessous.

Les études entreprises, théoriques et pratiques, ont déterminé la manière dans laquelle les résultats de la prospection magnétométrique sont influencés par l'activité minière du périmètre respectif (le bruit stationnaire produit par les constructions métalliques de la galerie, le bruit transitoire produit par les variations du courant électrique continu et celui alternatif de haute tension.

Les variations en temps du champ magnétique dans les zones fortement polluées n'ont pas évidentié des particularités concernant l'amplitude ou la fréquence des effets perturbateurs qui permet une séparation ou une élimination de ceux-ci. Étant donnée que l'intensité du champ magnétique due au passage du courant électrique diminue uniquement avec la première puissance de la distance et celle dûe aux objets métalliques avec la deuxième puissance de la distance, on souligne que ce taux d'abaissement lent du bruit du premier cas constitue la principale cause des perturbations engendrés par la présence des galeries dans la prospection magnétométrique au sol.

Les calcules théoriques et les expériments effectués ont délimité une zone de 400 à 500 m environ au tour de la galerie, où les variations du champ magnétique perturbateur sont grandes; au dehors de cette zone les modifications de l'intensité du champ magnétique sont réduites de l'ordre des unités et même subunités. À 400 ou 500 m de la galerie l'intensité du champ magnétique dépend plus ou moins de la profondeur par rapport à la source perturbatrice.

Dans les zones minières donc, on peut appliquer la méthode de la prospection magnétométrique à des distances de plus de 500 m des sources perturbatrices du souterraine, la meme distance étant mentionnée aussi par les études effectuées par les chercheurs russes (Busuev, 1970).

Bibliographie

Busuev A. V. (1977) Vozmojnosti vîsokotocinîh magnitnîh izmerenii pri nalicii promîşlennîh pomeh. V sb., "Voprosî rudnoi gheofiziki v Kazahstane i Srednii Azii", *NPO "Gheofizika"*, Sankt Petersburg.

Condacse N. (1980) Locomotive şi trenuri electrice. Ed. didact. ped., Bucureşti.

Gay S. P. Jr. (1982) The effect of cathodically protected pipelines on aeromagnetic surveys. *Geophysics*, 51, 8, p. 1671-1684, Tulsa.

Glebovskii I. S., Vasiutocikin G. S. (1981) Instrukţia po magnitorazvedke. Nazemnaia siomka. Ghidromagnitnaia siomka. Aeromagnitnaia siomka., izd. Nedra, 263 p., Sankt Petersburg.

Received: November 7, 1989
Accepted: November 7, 1989
Presented at the XV-th Symposium of Earth's Physics and Applied Geophysics-Bucureşti: June 8-10, 1989

Rom. J. Geophysics, 1993, 16, p. 9–14

PROSPECTAREA MAGNETOMETRICĂ A ARIILOR ACOPERITE DE APE DE MICĂ ADÎNCIME. LACUL BABADAG

Lucian BEŞUŢIU, Vlad ROŞCA, Corneliu MARAN
Institutul de Geologie şi Geofizică. Str. Caransebeş 1, 78 344 Bucureşti.

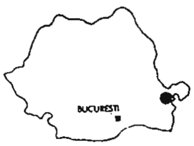

Key words: Magnetic surveys. Shallow-water environment. Dobrogea.

Abstract: *Magnetics in areas covered by shallow waters. Babadag Lake.* Shallow waters investigations on the Babadag Lake were carried out to establish a suitable method for magnetic prospecting of such areas. By the help of the achieved methodology more than 30 sq. km. were mapped and a consistent set of data for both land and water areas has been obtained allowing the compilation of a high accuracy magnetic map ΔT. The outlined magnetic anomalies revealed the existence of some hidden magmatic bodies located at depths of 40–60 m. Discussions are made on their geological significance.

Introducere

Apele de mică adîncime - *shallow waters* - cum sint ele numite in literatura anglo-saxonă, sint acele ape a căror adincime nu depăşeşte, de regulă, 2–3 metri. În ţara noastră ele constituie, in principal, Delta Dunării şi complexul lagunar Razelm-Sinoe. Numai ultimul ansamblu de lacuri menţionat totalizează peste 70.000 ha, ceea ce oferă o imagine concludentă asupra răspîndirii acestor zone şi, implicit, a necesităţii prospectării lor.

Situate la contactul dintre uscatul nord-dobrogean şi apele Mării Negre, investigarea acestor arii ar putea conduce la descifrarea raporturilor corecte dintre structurile nord-dobrogene şi cele ale platformei continentale a Mării Negre, prin corelarea datelor geologice pe care le deţinem asupra teritoriului dobrogean cu informaţiile recent furnizate de cercetările geologice şi geofizice intreprinse in domeniul marin.

Studiul la care se referă lucrarea de faţă a urmărit punerea la punct a unei metodologii care să permită cartarea magnetometrică de semidetaliu (scara 1:25.000) a acestor zone. Viabilitatea şi fiabilitatea metodei elaborate au fost testate prin cartarea lacului Babagad (cca 3.000 ha), soldată şi cu unele rezultate interesante din punct de vedere geologic.

1. Lucrări anterioare

Primele cercetări magnetometrice in domeniul acvatic au fost realizate in ţara noastră in perioada 1969–1970 (Romanescu et al., 1972) şi s-au concretizat intr-o hartă magnetometrică de recunoaştere a platformei continentale a Mării Negre in zona litoralului romanesc. A fost utilizat in acest scop un magnetometru protonic marin de construcţie britanică (ELSEC). Reţeaua de observaţie consta, in principal, dintr-un evantai de profile convergente in zona portului Constanţa, iar poziţionarea şi dirijarea navei se făcea cu mijloace clasice de navigaţie.

În perioada care a urmat (1976–1978) au fost întreprinse investigaţii geomagnetice de detaliu pentru evidenţierea acumulărilor de minerale grele, în imediata vecinătate a litoralului (Velcescu et al., 1979, date nepubl.). Dirijarea şi poziţionarea navei se făcea mult mai exact, cu ajutorul unor mijloace optice, de pe mal. Tractarea senzorului pe fundul apei s-a dovedit insă neinspirată, acceleraţiile şi deceleraţiile bruşte, la care era supus senzorul, producind "salturi" în indicaţiile magnetometrului fără legătură cu substratul geologic.

O altă metodologie de achiziţionare a datelor magnetometrice in domeniul marin a fost experimentată de Sava (1981, date nepubl.), care a utilizat magnetometre terestre de tip MPP-78, avînd senzorii montaţi pe catargul unei bărci tractate de o navă remorcher. Poziţionarea s-a făcut cu mijloace moderne de radionavigaţie de tip HI-FIX. Cu ajutorul acestui sistem s-a lucrat ani la rind la realizarea unor foi de hartă magnetometrică la scara 1:200.000. Plasarea senzorilor magnetometrelor in virful unui catarg de 10 metri conducea, insă, la amplificarea mişcărilor datorate tangajului şi ruliului ambarcaţiunii purtătoare, înrăutăţind astfel raportul semnal/zgomot. De aceea, ulterior s-a trecut la utilizarea unui magnetometru marin MPM-2S, produs în cadrul I.G.G., cu o arhitectură similară celui utilizat de Romanescu şi colab. (1969–1970).

În domeniul lacustru propriu-zis, investigaţiile magnetice au debutat cu determinări de susceptibilitate efectuate pe probe prelevate din sedimentele recente (Rădan, Rădan în Mihăilescu et al., 1978, date nepubl.). Cercetările s-au desfăşurat în diverse perimetre din Delta Dunării şi din ansamblul lacustru Razelm-Sinoe.

Paralel cu aceste preocupări, autorii menţionaţi au iniţiat şi studii asupra repartiţiei cîmpului geomagnetic în aceste arii. Primele tentative, întreprinse cu ajutorul unui magnetometru protonic cu senzorul tractat pe fundul apei, s-au lovit de aceleaşi impedimente ca şi cercetările efectuate de Velcescu et al.(1979, date nepubl.). Obstacolele intîlnite de senzor în calea sa produceau salturi artificiale în indicaţiile magnetometrului, iar apropierea prea mare de surse făcea metoda mai adecvată determinărilor de susceptibilitate decît de cîmp geomagnetic. De aceea, începînd cu anul 1982, s-a trecut la utilizarea unui senzor plutitor, ceea ce a îmbunătăţit considerabil calitatea determinărilor (Rădan, Rădan în Mihăilescu et al., 1983, date nepubl.). Cu ajutorul acestei metodologii şi folosind mijloace clasice de navigaţie au fost realizate o serie de profile magnetometrice Δ T de recunoaştere în Delta Dunării şi complexul lagunar Razelm-Sinoe.

2. Metodologia de lucru

2. 1. Sistemul de achiziţionare a datelor

Prin sistem de achiziţionare a datelor (SAD) am definit ansamblul elementelor care permit efectuarea determinărilor magnetometrice în condiţiile specifice domeniului menţionat. Elementele constitutive ale SAD sînt:

- magnetometrul propriu-zis,
- mijloacele de radiocomunicaţie,
- ambarcaţiunea (vectorul purtător).

Arhitectura versiunii finale a SAD este prezentată în figura 1. Soluţia adoptată derivă dintr-o variantă a cercetării aeromagnetice. Opţiunea pentru "totul la bord" a fost impusă de condiţiile de lucru specifice. Dacă în zonele lacustre propriu-zise, caracterizate de oglinzi de apă largi, metodologia "clasică", cu senzor tractat la o distanţă convenabilă de ambarcaţiunea purtătoare, funcţionează, în ariile denumite de noi "deltaice", acoperite de stuf, în care circulaţia se face doar pe canale sau japşe (ceea ce oferă posibilităţi restrînse de manevră) utilizarea sa devine greoaie sau chiar imposibilă. Cu SAD adoptat s-au putut carta cu uşurinţă aceste zone, vectorul purtător permiţînd schimbări bruşte de direcţie şi chiar întoarceri în loc în cazul canalelor înfundate.

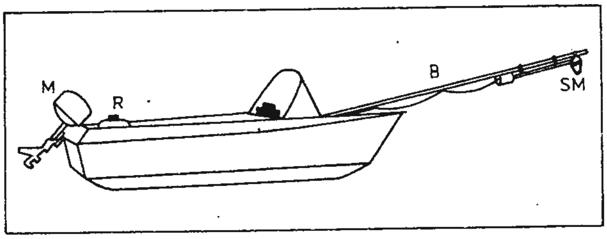

Fig. 1 – Configuraţia sistemului de achiziţionare a datelor (SAD): SM, senzorul magnetometrului; B, bompres nemagnetic; R, rezervor de carburant; M, motorul ambarcaţiunii.

Înaintea începerii lucrărilor propriu-zise au fost întreprinse cercetări speciale asupra viabilităţii soluţiei adoptate, examinîndu-se influenţa diverselor surse de zgomot ce ar putea altera semnalul magnetometric.

2.1.1. Zgomotul magnetic cu caracter staţionar

Influenţa elementelor feromagnetice din constituţia SAD (motor, rezervor de carburant, acumulatori, staţie de radio etc.) a fost examinată prin microcartarea cîmpului magnetic din jurul acestuia (fig. 2). Plasarea senzorului la extremitatea bompresului nemagnetic îl fereşte complet de aria contaminată.

2.1.2. Zgomotul magnetic cu caracter tranzitoriu

Plasarea senzorului la bordul ambarcaţiunii ridică problema delicată a perturbaţiilor datorate cîmpului electromagnetic creat de funcţionarea motorului, a cărui influenţă se resimte dincolo de raza de acţiune a cîmpului staţionar.

Pe baza unor experienţe realizate la punct fix cu diverse tipuri de aparatură, s-a demonstrat capabilitatea magnetometrului cu pompaj optic M-33 de a funcţiona în aceste condiţii. Constatarea este astfel în deplină concordanţă cu rezultatele unor studii anterioare privind comportarea magnetometrelor terestre în cîmpuri electromagnetice perturbatoare (Beşuţiu, 1986) (fig. 3).

2.1.3. Zgomotul provocat de mişcările de ruliu şi tangaj

Spre deosebire de cercetările magnetometrice întreprinse pe uscat, în domeniul acvatic senzorul magnetometrului este permanent supus la diverse acceleraţii pe care le suportă vectorul purtător. Spre a evita amplificarea acestor mişcări nedorite, senzorul magnetometrului a fost plasat pe un catarg-bompres confecţionat din materiale nemagnetice. Simularea unor mişcări de ruliu şi tangaj şi înregistrarea comportamentului magnetometrelor la punct fix au demonstrat din nou superioritatea magnetometrului M-33,

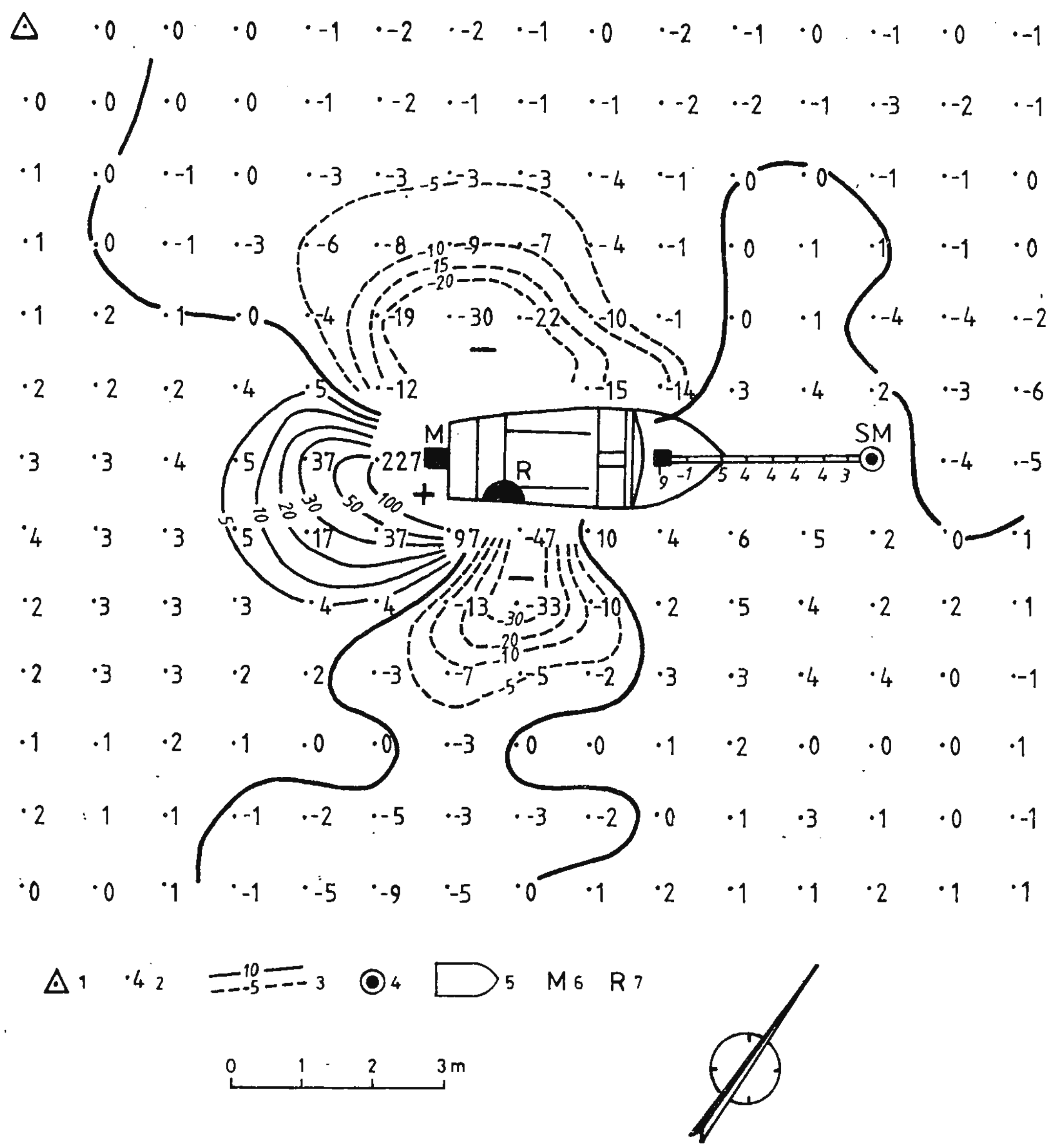

Fig. 2 – Cartarea zgomotului magnetic cu caracter staţionar din jurul SAD.
1, baza panoului; 2, locaţia staţiei magnetometrice şi valoarea Δ T (în nT); 3, izolinii Δ T (în nT); 4, senzor magnetometru; 5, conturul ambarcaţiunii; 6, motor; 7, rezervor de carburant.

care a funcţionat stabil pînă la oscilaţii de 10–15°.

2.2. Tehnica de lucru

Înaintea începerii lucrărilor de cartare magnetometrică a lacului Babadag a fost realizată pichetarea şi ridicarea topografică a capetelor de profile pe ţărmul de nord şi de sud al acestuia. In conformitate cu cerinţele lucrărilor magnetometrice efectuate pe uscat de I.P.G.G., distanţa între profilele de observaţie a fost de 200 m.

Dirijarea şi poziţionarea SAD pe profilele de lucru s-a realizat de pe mal, cu ajutorul unor mijloace optice, similar metodei utilizate de Velcescu et al. (1979, date nepubl.). Astfel, la extremităţile profilului de lucru au fost amplasaţi doi operatori dotaţi cu teodolite şi mijloace de radiocomunicaţie, care dirijau pe rînd, în raza lor de vizibilitate, ambarcaţiunea, comunicînd prin radio cu timonierul. Un al treilea operator era plasat lateral, stabilind la intervale de timp regulate poziţia ambarcaţiunii pe profilul respectiv. După cum au demonstrat-o, însă, testele efectuate pe cca. 20 profile, ambarcaţiunea circula cu viteză constantă, ceea ce permitea identificarea poziţiei punctului de măsură de pe un profil numai pe baza etichetei de timp a înregistrării (menţionăm că determinările de cîmp geomagnetic se făceau în regim automat, la fiecare 15 secunde, ceea ce, la o viteză de 10 km/h, înseamnă cca 40 m între staţii.

În zonele de tip "deltaic" poziţia SAD a fost stabilită prin cartare directă pe hărţi la scara 1:5.000. Între detaliile planimetrice identificate, la diverse momente, de-a lungul unui profil (intersecţii şi schimbări de direcţie ale canalelor, capete de canal etc.) poziţia punctelor de observaţie a fost stabilită în ipoteza unei deplasări cu viteză constantă.

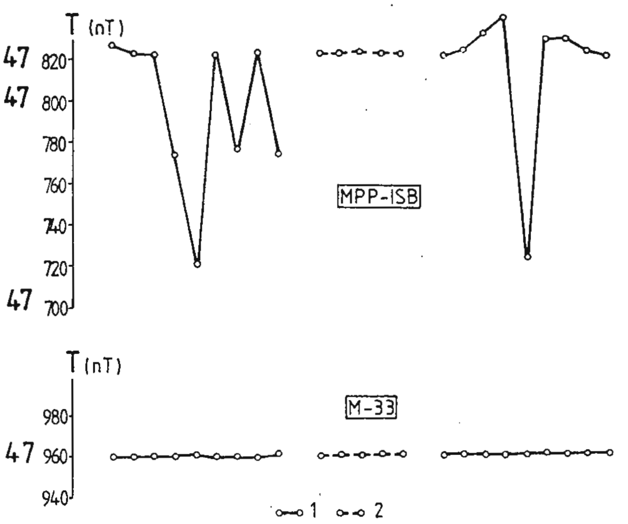

Fig. 3 Influenţa cîmpului electromagnetic creat de motorul ambarcaţiunii asupra magnetometrelor protonice (a) şi cuantice (b).
1, determinări efectuate cu motorul oprit; 2, determinări efectuate cu motorul pornit.

3.3. *Calitatea determinărilor magnetometrice*

Despre rolul şi semnificaţia acestui parametru în întocmirea şi interpretarea hărţilor magnetometrice, precum şi a modului de evaluare a sa, s-a vorbit pe larg într-o lucrare recentă (Beşuţiu, 1988).

Estimarea calităţii lucrărilor magnetometrice lacustre efectuate pe lacul Babadag a fost realizată cu ajutorul unor profile de control repetate în zile diferite, cu sensuri diverse de parcurgere. Abaterea standard calculată pe baza acestor teste a fost sub ± 1,5 nT, ceea ce a permis construirea hărţii magnetometrice cu un interval de interpolare de 5 nT.

4. Particularităţi ale morfologiei cîmpului geomagnetic în aria investigată. Asupra naturii geologice a surselor anomale

Morfologia cîmpului magnetic terestru în aria lacului Babadag confirmă parţial informaţiile furnizate de cercetarea aeromagnetică regională (Cristescu, Ştefănciuc, 1967, date nepubl.) completîndu-le cu detalii inerente achiziţionării datelor pe o suprafaţă mult mai apropiată de sursele anomale şi la un grad de detaliere mai ridicat.

Larga anomalie regională de maxim din aria lacului Razelm, pe a cărei terminaţie estică se află situat lacul Babadag, relevă, într-un plan situat la 600 m sub nivelul la care a fost realizată harta aeromagnetică, o serie de complicaţii morfologice datorate, fără îndoială, unor surse situate relativ aproape de suprafaţă. Estimări de adîncime efectuate cu ajutorul procedeului Peters (Glebovskii, Vasiutocikin, 1981) au arătat că faţa superioară a corpurilor perturbatoare se situează la adîncimi de 40–60 m, în toate cazurile anomaliilor semnalate pe lac.

Principalele efecte anomale cartate (fig. 4) sînt următoarele:

- prima grupă o constituie efectele conturate în centrul lacului, la sud-vest de punctul geodezic Uriaşul;
- a doua grupă se află pe rama sudică a lacului, în imediata vecinătate a ariei de aflorare a calcarelor cenomaniene, între profilele 56–61;
- a treia grupă apare pe terminaţia sud-estică a lacului, într-o arie denumită de noi "deltaică", fiind acoperită de stuf. Efectul conturat aici, pe baza determinărilor efectuate pe canale şi japşe, rămîne deschis în promontoriul de la nord de localitatea Enisala. Profile executate pe ţărm au regăsit valorile anomale constatate în domeniul acvatic, la o amplitudine ceva mai atenuată şi fără pronunţatul termen de minim care caracterizează anomalia obţinută pe lac, ceea ce arată limitarea sau, cel puţin, afundarea sudică a sursei anomale.

Prima tentativă de interpretare geologică a acestor anomalii a pornit de la un model de simulare a efectului magnetometric produs de sedimentele recente de pe fundul lacului. Prezenţa unor minerale grele în cadrul acestor depozite le conferă susceptibilităţi magnetice de pînă la 40.10^{-6} uCGS (Rădan, Rădan în Mihăilescu et al., 1983, date nepubl.). Modelarea a arătat însă că, pentru a atinge amplitudinea anomaliilor observate în centrul lacului, de exemplu, grosimea acestor sedimente ar trebui să depăşească 2.000 m (!), ceea ce este inacceptabil, morfologia cîmpului modelat fiind oricum deosebită de efectul observat, datorită adîncimii reduse luate în considerare la simulare.

Privite în contextul mai larg oferit de hărţile magnetometrice realizate în regiune (Manea, 1986; Manea,

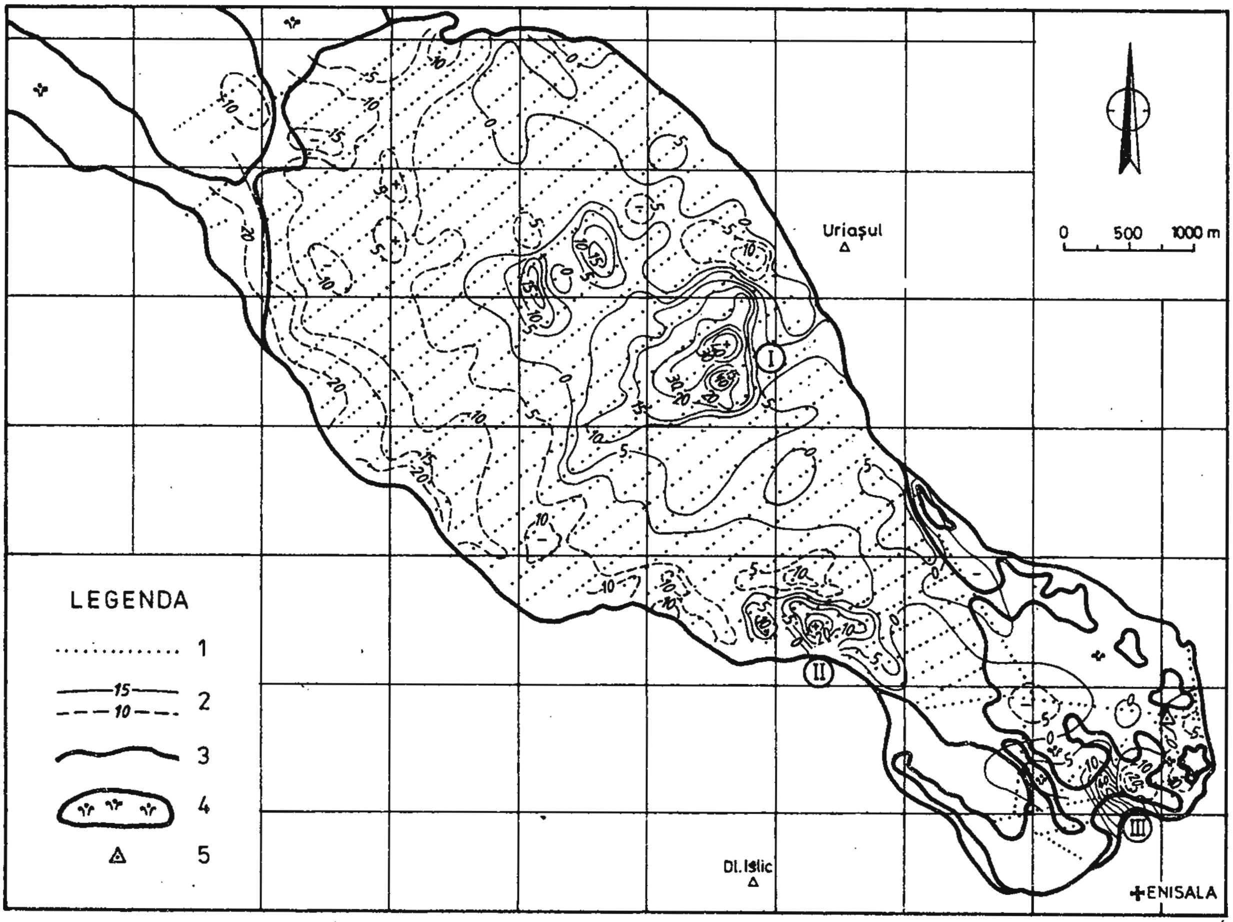

Fig. 4 - Harta magnetometrică Δ T a lacului Babadag (nivelul de referinţă = baza Heracleea, epoca ridicării magnetometrice = 1988,0).
1, profile magnetometrice; 2, izolinii Δ T (în nT); 3, conturul oglinzii de apă; 4, arii acoperite de stuf; 5, locaţia bazei Heracleea.

Manea, 1987, date nepubl.) grupele anomale din arealul lacului Babadag se încadrează într-un şir mai larg de anomalii care se desfăşoară paralel cu linia de încălecare dintre unitatea de Niculiţel şi unitatea de Tulcea (am numit aici efectele conturate la sud-est de dealul Lisii Hora, sud şi sud-est de localitatea Mihai Bravu, nord-vest de localitatea Babadag). Plasarea lor între ivirile de bazalte (recunoscute pentru susceptibilitatea lor magnetică ridicată) de la sud-vest de Mihai Bravu şi nord de Enisala, conduce, aparent fără dubii, la desemnarea acestui tip de rocă ca sursă a anomaliilor conturate.

Apar, însă, în acest caz, o serie de aspecte mai greu de explicat. Astfel, aproape toate anomaliile din şirul menţionat manifestă unele tendinţe de orientare perpendiculară pe direcţia planului de încălecare menţionat (lucru evident şi în cazul primei grupe anomale).

Al doilea aspect, care intrigă, este faptul că anomaliile cele mai intense ale şirului, cele de lîngă Mihai Bravu, se termină tocmai în zona de aflorare a bazaltelor considerate ca sursă ! Bazaltele din zona Enisala au demonstrat proprietăţi magnetice relativ modeste (susceptibilităţi sub 10^{-4} uCGS şi remanenţe neglijabile), iar corpurile de microgabbrouri şi dolerite cu care se însoţesc au un comportament magnetic similar. Avînd însă în vedere gradul foarte avansat de tectonizare şi alterare supergenă la care au fost supuse, se poate accepta totuşi că, în stare proaspătă, ar putea atinge susceptibilităţi magnetice comparabile cu cele ale bazaltelor de la Mihai Bravu ($150-180 \cdot 10^{-6}$ uCGS), suficiente pentru a explica anomaliile conturate în cadrul celei de-a treia grupe. Rămîne însă, şi în acest caz, problema reducerii amplitudinii anomaliei magnetice pe ţărm, în aria de aflorare a presupuselor surse (reamintim că estimările de adîncime au arătat că, în domeniul lacustru, faţa superioară a corpului perturbator este situată la 50–60 m adîncime). De altfel, profile executate pe ţărm nu au arătat acea morfologie agitată a cîmpului, tipică în cazul unor surse amplasate superficial.

O altă ipoteză în legătură cu natura geologică a surselor anomaliilor magnetice conturate pe lac face apel la existenţa unor roci necunoscute în aria respectivă, aparţinînd unui magmatism cretacic-superior sau post-cretacic.

Întreaga zonă pusă în discuţie se află pe un puternic cordon gravimetric, care a fost interpretat ca fiind suprapus flancului sudic al unui graben (Roşca in Visarion et al., 1986, date nepubl.) sau limitei unui batholit granodioritic (Andrei in Borcoş et al., 1987, date nepubl.). In ambele ipoteze, regiunea lacului Babadag apare ca o zonă de minimă rezistenţă, favorabilă insinuării materialului magmatic de-a lungul unor falii. Astfel s-ar putea explica şi orientările perpendiculare pe planul de încălecare ale axelor anomale menţionate anterior.

Opţiunea pentru unul din modelele amintite este dificilă, iar datele de flux geotermic nu pot ridica ambiguitatea interpretării, datorită lipsei de aport caloric al granitelor nord-dobrogene (Veliciu in Visarion et al., 1986, date nepubl.). Este de remarcat, totuşi, tendinţa de maxim pe care o înregistrează harta de flux geotermic în zona lacului, grefată pe un minim regional ce acoperă aria presupusului graben şi care s-ar putea explica prin prezenţa în această arie a unei fracturi profunde, încă circulate, posibilă cale de acces pentru magmele menţionate. In favoarea existenţei unui rezervor magmatic, care să fi alimentat insinuările de material eruptiv din zona lacului Babadag, pare a pleda marea anomalie magnetică ce se extinde spre est, în domeniul lacului Razelm. De notat, de asemenea, tendinţa gravimetrică de maxim, exprimată în anomalia reziduală (Roşca, Ştefănescu in Visarion et al., 1986, date nepubl.) din aria lacului Babadag, condiţionată, probabil, de existenţa unor roci de natură bazică sau ultrabazică, capabile să ofere contrastul de masă necesar apariţiei sale.

Concluzii

Corectitudinea şi fiabilitatea unei metodologii de cercetare magnetometrică a ariilor acoperite de ape de mică adîncime a fost elaborată şi testată prin cartarea lacului Babadag.

Spre deosebire de prospecţiunea aeromagnetică, ce evidenţiase în această regiune doar terminaţia vestică a unei anomalii regionale, a cărei cauză părea situată la mare adîncime, cercetările întreprinse pe lac au relevat cel puţin o categorie de surse anomale locale, mult mai apropiate de suprafaţă (50–60 m), reprezentate probabil de roci bazice sau ultrabazice. Asupra naturii lor au fost formulate două ipoteze principale:

a) magmatite bazice triasice alohtone, cantonate în fruntea pînzei de Niculiţel;

b) roci necunoscute în prezent în zonă, aparţinînd unui magmatism mai nou, poate de tipul andezitelor cenomaniene întîlnite de forajul marin de pe structura Lotus, insinuate de-a lungul unor linii de fractură, semnalate de cordonul de gradient gravimetric ce acoperă aria lacului Babadag.

Bibliografie

Beşuţiu L. (1988) Asupra estimării calităţii prospecţiunilor magnetometrice. *St. tehn. econ.*, D, 15, p. 27–34, Bucureşti.

Glebovskii I. S., Vasiutocikin G. S. (1981) Instrukţia po magnitorazvedke. Izd. Nedra, 263 p., Sankt Petersburg.

Romanescu D., Roşca Vl., Soare A. (1972) Recherches magnetométriques sur la platforme continentale de la Mer Noire au large des côtes roumaines. *Rev. roum. géol., géophys., géogr., Géophys.*, 16, 1, Bucureşti.

Received: May 10, 1988
Accepted: May 10, 1988
Presented at the XV-th Symposium of Earth's Physics and Applied Geophysics–Bucureşti: June 8–10, 1989

Rom. J. Geophysics, 1993, 16, p. 15–21

MAGNETIC AND GAMMA-RAY SPECTROMETRIC STUDY OF SOME HYDROTHERMAL HALOES IN THE METALIFERI MOUNTAINS

Dumitru IOANE, Justin ANDREI

Institutul de Geologie şi Geofizică. Str. Caransebeş 1, 78344, Bucureşti 32.

Key words: Magnetic surveys. Gamma-ray spectrometry. Hydrothermal alteration. Haloes. Metaliferi Mountains. Apuseni Mountains.

Abstract: The argillization-silicification hydrothermal processes affecting the eruptive rocks of the Metaliferi Mts induced the substitution of the accessory magnetite with iron sulfides and, sometimes, an enrichment of the rocks in potassium minerals. These transformations are auspicious for a good application of the magnetic and gamma-ray spectrometry methods in the hydrothermal haloes study.

Introduction

The geological studies effectuated in the Metaliferi Mts revealed a close correlation between the hydrothermal haloes and the ore bodies, in the sense that the base-metal and/or auro-argentiferous veins or stocks are included in such haloes (Ghiţulescu, Socolescu, 1941; Ianovici et al., 1969).

The direct mapping of the hydrothermal haloes being sometimes difficult, it was necessary to obtain indirect, geophysical information. In this respect, in the Metaliferi Mts it has been emphasized the capacity of the magnetic method to outline the hydrothermal alteration areas of argillization, sericitization, silicification, pyritization type (Romanescu, 1963; Calotă, Romanescu, 1963), because the mentioned transformations lead to the substitution of the accessory magnetite from the volcanic rocks with paramagnetic minerals.

The hydrothermal haloes cover large areas and consequently their geological or magnetical delimitation is not enough for the location of the ore bodies. Taking into account that the hydrothermal mineralizations are often closely linked spatially with a potassium metasomatosis (adularization, sericitization, illitization), it has been considered that the radiometric method can offer useful data for indirectly locating the ore bodies as due to the radioactive properties of a potassium isotope (K_{40}).

The complexity of outlining the hydrothermal haloes and the highly metallogenic areas within them, by means of the mentioned geophysical methods, determined us to effectuate experimental works in the Metaliferi Mts. This paper presents the results of the researches carried out in the period 1979–1981 in the Bocşa–Săcărîmb, Coranda Mare and Pîrîul lui Avram zones, geologically situated in the southernmost part of the Neogene volcanic belt related to the Brad–Săcărîmb basin, between the Hondol and Săcărîmb deposits.

Bocşa–Săcărîmb Zone

From the geological point of view Săcărîmb quartz andesites crop out in the Bocşa–Săcărîmb zone (Ungureanu, Aldea, 1972, unpubl. report). The south-eastern part is characterized by biotite-bearing amphibole andesites and the north-western part by pyroxene-bearing amphibole andesites in intrusive facies (Fig. 1). On a NW–SE striking strip the andesites are highly hydrothermalized (argillized, silicified, pyritized); a stock-type lead-zinc mineralization intensely illitized (Udubaşa et al., 1976) occurs in the Bocşa ore deposit.

The petrophysical determinations of magnetic susceptibility and the K, U, Th contents have been effectuated on andesite samples from outcrops and drillings (Ioane, Andrei, 1980, unpubl. report). The pyroxene-hornblende quartz andesites of Dealul Grozii type (north-western sector) show different magnetic susceptibilities, generally determined by the hydrothermal alteration degree. Thus, on unaltered rocks or affected by autometamorphic propylitization, values of $500–2200.10^{-6}$ uCGS have been obtained (average ca 1300.10^{-6} uCGS) whereas on highly argillized rocks the values range between 0 and 75.10^{-6} uCGS (average 15.10^{-6} uCGS). The magnetic anomalous effect

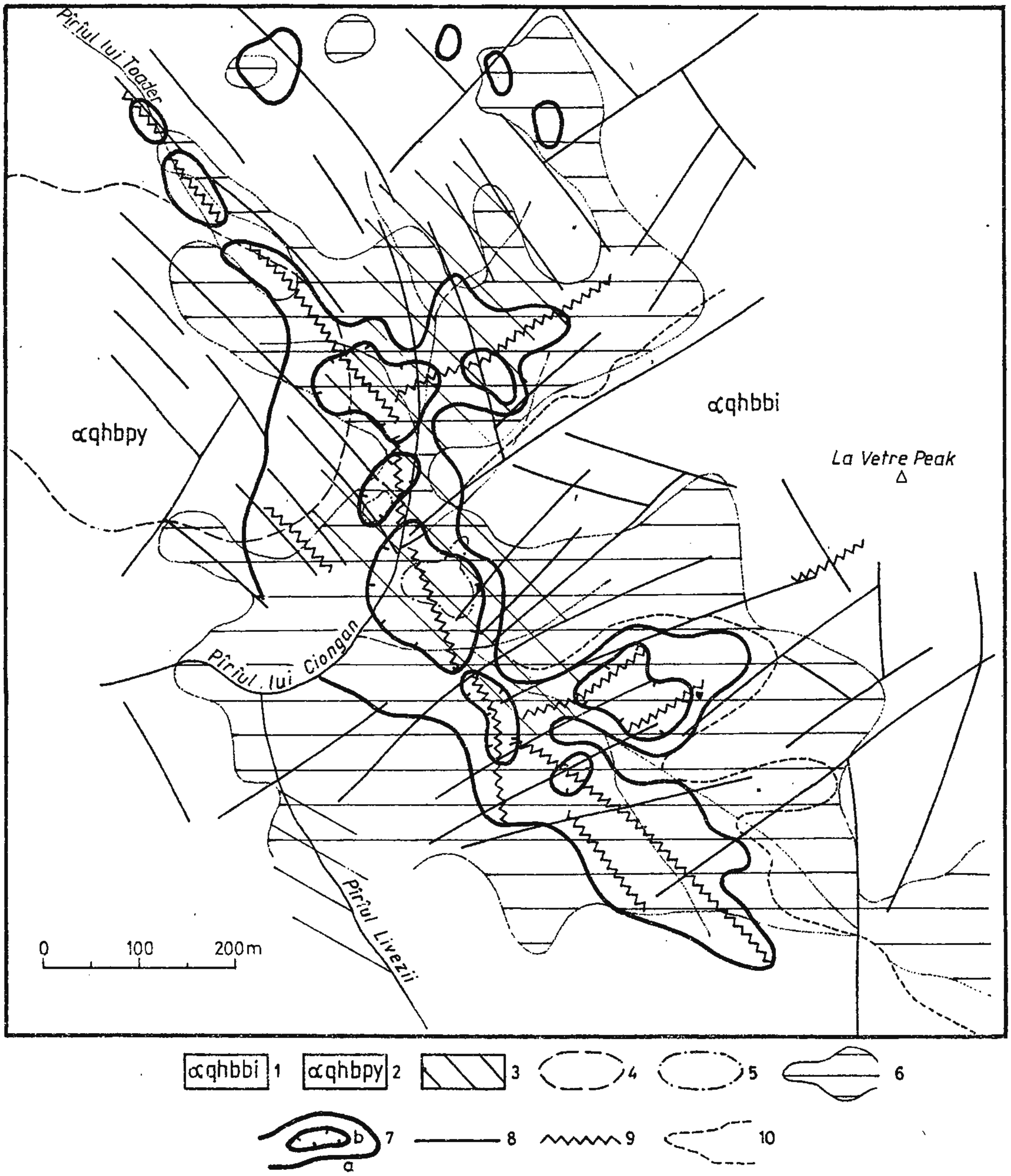

Fig. 1 – Structural and metallogenetical sketch-map of the Bocşa–Săcărîmb zone elaborated on the basis of ΔT magnetic and gamma-ray spectrometric data.
Neogene volcanics: 1, hornblende+biotite quartz andesite; 2, hornblende+pyroxenes quartz andesite; 3, intense hydrothermal alterations (argillization, silicification, pyritization); 4, eruptive body boundary, geologically traced; 5, lead-zinc stock outline in a mine horizon; 6, hydrothermal alteration halo inferred from ΔT magnetic data; 7, potassium hydrometasomatosis halo, inferred from gamma-ray spectrometric data: a, intense; b, highly intense; 8, fractures inferred from magnetic data; 9, fractures with metallogenetic functions inferred from gamma ray spectrometric data; 10, geological boundary inferred from gamma ray spectrometric data.

of the hydrothermally unaltered andesites is amplified by a significant remanent magnetization (the Q coefficient determined on a sample was 3.12). Laboratory spectral radiometric measurements pointed out for these rocks contents of 1–2 ppm U, 5–6 ppm Th and 1–4 per cent K, the K amount varying according to the intensity of the potassium hydrometasomatosis. The biotite+hornblende quartz andesites of "La Vetre type", unaltered, are characterized by magnetic susceptibility values of $800–1250.10^{-6}$ uCGS (average 1000.10^{-6} uCGS) as well as by a strong remanent magnetization (Q coefficients values between 3 and 4). Values of $30–570.10^{-6}$ uCGS have been obtained on andesites of the above-mentioned type with different degrees of hydrothermal alteration. The laboratory radiometric determinations indicated for unaltered andesites contents of 5 ppm U, 20 ppm Th and 2.5 per cent K and for altered andesites values of 2.5–3 ppm U, 9 ppm Th and 1.5 per cent K. All this shows that the andesitic rocks in the study zone present similar magnetic properties; however, significant differentiations are observed as regards the U, Th and K content.

The petrophysical data make us consider that the magnetic map ΔT outlines, with intense anomalies, the unaltered volcanics or affected by autometamorphic propylitization, the areas with weak magnetic disturbances reflecting the hydrothermal halo. The maps with the gamma radiation and its components (K, Th, U) highlight maximum anomalies in the outcropping and suboutcropping areas of the andesites with a high biotite content in the "La Vetre" summit area. The map with the potassium component gives information on the potassic hydrometasomatosis but its effect is included in the larger maximum "anomaly" determined by andesites with a high content of primary biotite. In order to overpass this situation we started from the observation that for a certain type of unaltered andesitic rock the contents of U, Th and K vary within restricted limits and they can be practically considered constant. In the areas with unaltered rocks the values of the K/U and K/Th ratios are relatively constant, whereas in the areas affected by hydrothermal alterations in potassic facies the values are higher according to the amount of the secondary potassium. The major anomalies on the maps with the K/U or K/Th ratios (excepting those obtained on the known mineralized stocks) are susceptible to indicate new lead-zinc mineralizations similar to those worked off in the Bocşa mine. Thus, K/Th maximum anomaly located at about 250 m ESE of the main stock has been investigated by two drillings, a weak Pb and Zn mineralization being identified.

Figure 1 presents interpretative aspects resulting from magnetic and gamma-ray spectrometric measurements carried out in the Bocşa–Săcărîmb Zone. It is of note that the hydrothermal halo delimited by means of magnetic evidence has a wider spreading area than the one with potassic facies alterations and, moreover, the areas of intense potassic hydrometasomatosis corresponds to the mineralized stocks.

Coranda Mare Zone

Coranda Mare zone consists of Cretaceous sedimentary deposits of Barremian-Aptian age (sandstones, clays, siltites) overlain by Almaşu Mare gravels (conglomerates, gravels, sandstones, clays) of Carpathian age. They are intruded by subvolcanic bodies and overlain by andesitic lavas of Hondol–Făierag (hornblende andesites) or Săcărîmb (hornblende+biotite quartz andesites) type (Udubaşa, Istrate, 1981, unpubl. report). The Băiaga and Coranda Mare subvolcanic bodies are strongly affected by hydrothermal alterations, the adularia, silica±clay minerals+baryte facies being widely spread (Udubaşa et al., 1976; 1977). Major base-metal mineralizations associated to the Băiaga subvolcanic body are also known; in the Coranda structure the metallogenetic indications are only sporadic.

The magnetic susceptibility measurements effectuated in the area of study (Ioane et al., 1981, unpubl. report) showed that the strongest contrast of the magnetic properties occurs between the Săcărîmb-type quartz andesites, relatively unaltered, cropping out in the north-eastern extremity (values ranging between 600 and $2100\ 10^{-6}$ uCGS, average value about $1300\ 10^{-6}$ uCGS) and the other rocks and geological formations. The Coranda Mare amphibole andesites, highly hydrothermally altered, display low values (average value of the magnetic susceptibility measurements amounting to 5.10^{-6} uCGS). Similar values have been determined on the sedimentary deposits in the study area, a magnetic delimitation of the amphibole andesites from the adjacent sedimentary formations being not possible. The laboratory gamma-ray spectrometric measurements emphasized, in case of the amphibole andesites, significant variations of the K, Th, U concentrations; certain sectors with average contents of 1.7 ppm U and 3.3 ppm Th, and 1.47–3.66 per cent K fall in the normal field of the amphibole andesites, the potassium amount varying according to the intensity of the potassic metasomatosis; the highest concentrations of U (4.9–8.4 ppm) and K (5.48–10.32 per cent) have been obtained on amphibole andesites, argillized and silicified, with pelitic enclaves. The presence of these enclaves of hornfelsed sedimentary rocks within the andesites of the Coranda Mare structure explains the high values of the U component measured, and the high K content is due to the neoformation minerals from the hornfelsed pelites (biotite, muscovite, sericite) and to the strong adularization of the andesites. As for the sedimentary rocks, mention should be made of the Cretaceous hydrothermalized sandstones (Th = 8.6 ppm) and the Carpathian microconglomerates with elements of altered crystalline schists and andesites (Th = 23.8 ppm and K = 9.01 per cent).

limited and fracture lines within them could be emphasized (Fig. 2).

In the Coranda Mare zone the intense alterations in potassic facies facilitated the representation of the

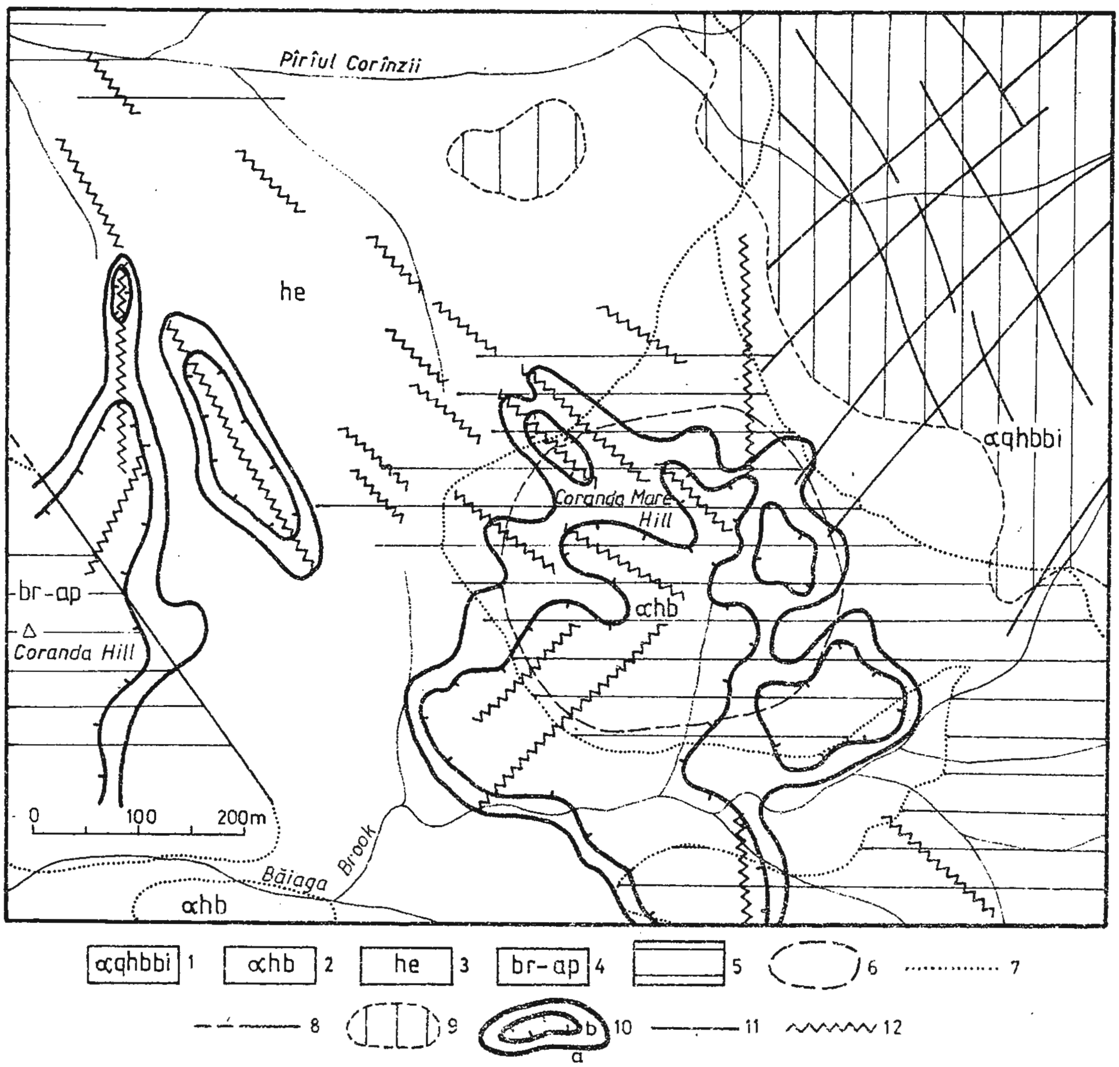

Fig. 2 – Structural and metallogenetical sketch-map of the Coranda Mare zone, elaborated on the basis of ΔT magnetic and gamma-ray spectrometric data.
Neogene volcanics: 1, hornblende+biotite quartz andesites (Săcărîmb type); 2, hornblende andesites (Hondol–Făcrag type); Carpathian: 3, Almaşu Mare gravels complex; Barremian-Aptian: 4, Căbeşti Beds: sandstones, silts, argillites; 5, intense hydrothermal alterations (silicifications, argillization, adularization); 6, subvolcanic body; 7, geological boundary; 8, fault, geologically traced; 9, area with hydrothermally unaltered volcanics inferred from ΔT magnetic data; 10, potassium hydrometasomatosis halo, inferred from gamma-ray spectrometric data: a, intense; b, highly intense; 11, fractures inferred from ΔT magnetic data; 12, fractures with metallogenetic functions inferred from gamma ray spectrometric data.

The magnetic map evidenced a low regional anomaly in the area with hydrothermally altered andesites and sedimentary deposits, the absence of a contrast of magnetic properties making impossible the mapping of the Coranda Mare subvolcanic structure using this method. However, on the basis of magnetic data, the area with Săcărîmb-type quartz andesites could be de-

hydrothermal halo on the potassium component map, this mapping representing the basis for the structural-metallogenetic sketch-map. Thus, two areas of maximum have been located, situated in the easternmost part of the Băiaga-Coranda structure and on the Coranda Mare subvolcanic body, mainly determined by the mentioned adularization phenomena.

The higher intensity from the central-western part points to a structural cause concerning the westward enrootment of the Coranda Mare andesitic structure. One can also observe lineaments of NW–SE trending longitudinal anomalies, that might represent the result of the alterations in potassic facies associated to vein fractures. This hypothesis is based on the electrometric (Josan et al., 1980, unpubl. report) and mercurometric (Ioane et al., 1981, unpubl. report) data from the study area. The drawing up of the maps with the K/U and K/Th ratios has not brought further information, images similar to that on the map with the potassium component being obtained in the area of the hydrothermalized amphibole andesites. The only exception, without a metallogenetic significance, is represented by the effect of the hornfels enclaves with a high-U content which generates areas of minimum on the map with the K/U ratio. In the sedimentary domain, the existence of lithologic variations which correspond to significant differentiations of the K, U, Th content complicates the interpretation of the gamma-ray spectrometric data, particularly on the maps with the K/U and K/Th ratio.

Pîrîul lui Avram zone

Pîrîul lui Avram zone is situated mostly on the Coasta Mare andesitic body, being constituted of biotite+hornblende quartz andesites. In the northwesternmost part Carpathian sedimentary deposits crop out, represented by Almaşu Mare gravels (conglomerates, microconglomerates, sandstones). In the upper basin of the Pîrîul lui Avram zone hydrothermal alterations of argillization-silicification type (Haiduc, 1963, unpubl. report) are observed, the most important ones occurring in the area of the vein fracture. Within it, the gangue minerals are represented by quartz, dickite, sericite, the mineralization being formed of Cu, Te and Ge sulphosalts. The halo of this vein is characterized by an intense silicification, the clay minerals containing K practically lacking.

The petrophysical study (Ioane et al., 1982, unpubl. report) showed that the Coasta Mare quartz andesites display a wide range of magnetic susceptibility values ($0-1300.10^{-6}$ uCGS) in comparison with the intensity of the hydrothermal alterations underwent, a quite significant aspect in case of this zone. The laboratory gamma-ray spectrometric determinations showed that the andesitic rocks have relatively high contents of U and Th (4–6 ppm, 15–20 ppm, respectively) and low contents of K (1–2 per cent). The decrease of the K amount is the result of the hydrothermal alteration processes which determined the transformation of the primary biotite and did not lead to the occurrence of neoformation potassic minerals but to an intense silicification.

Considering the particular petrophysical conditions of this zone, the detailed ΔT magnetic map contributed to the outlining of the hydrometasomatosis areas and to the drawing up of the structural-metallogenetic sketch-map (Fig. 3), due to the magnetic properties of the rocks which are closely linked with their degree of hydrothermal alteration. Thus, a good magnetic mapping of the vein fracture has been achieved and its southward continuation, after a small shifting due to E–W faults, has been pointed out. The information given by the gamma-ray spectrometrical maps in the area of study has not metallogenetic implications (the causes being already explained), the lack of alterations in the potassic facies being correlated here with the low-grade mineralization of the Pîrîul lui Avram vein fracture. The superposition of some minimum anomalies of the K/Th ratio over hydrothermal circulated fractures is unsignificant for the metallogenetic potential of this zone.

Conclusions

The experimental geophysical researches carried out in the Metaliferi Mts highlighted the opportunity to use the gamma-ray spectrometrical methodology in the study of the hydrothermal haloes, the enrichment of these data with detailed magnetic measurements being necessary.

The areas with Neogene volcanics affected by hydrothermal alterations of argillization-sericitization-adularization-silicification type are mostly revealed on magnetic images by quite low anomalies in contrast with the adjacent unaltered zone strongly disturbed magnetically. Locally, e.g. in the Pîrîul lui Avram zone, the existence of a narrow hydrothermal halo, closely linked with the vein fracture, made possible its magnetic mapping. In cases in which the strongly hydrothermally altered andesites are in contact with sedimentary deposits, the efficiency of the magnetic survey is much diminished.

In most cases, the base-metal and/or auro-argentiferous hydrothermal mineralizations in the Metaliferi Mts have been accompanied by a potassic metasomatosis which facilitated a correlation of the gamma-ray spectrometric anomalies of the potassium radiation or of the K/U and K/Th anomalies with mineralized fractures or stocks. The aspects revealed in the Bocşa–Săcărîmb zone emphasize the efficiency of the K/U and K/Th ratio images in areas with andesitic rocks with a high biotite content, the map with the potassium component cumulating the effect of the primary minerals (biotite) with that of the neoformation minerals (sericite, illite). More seldom, the metallogene products were not accompanied by a potassic metasomatosis, silicification representing the

Fig. 3 – Structural and metallogenetic sketch-map of the Pîrîul lui Avram zone inferred from ΔT magnetic and gamma-ray spectrometric data.
Neogene volcanics: 1, biotite+hornblende quartz andesites; Carpathian: 2, Almaşu Mare gravels complex; 3, geological boundary; 4, vein fracture; 5, hydrothermal alteration halo inferred from ΔT magnetic data: a, moderate; b, intense; 6, fractures with metallogenetic functions inferred from ΔT magnetic data; 7, lineaments of K/Th minimum inferred from gamma-ray spectrometric data; 8, fractures deduced from ΔT magnetic data.

predominant alteration type; in such cases the K, K/U or K/Th maximum anomalies no longer emphasize the vein fracture, minima of these images, related to the metallogene products, could be thus observed.

The examples presented in this paper pointed out quite different situations in areas situated at several kilometres one from another, the efficiency of these two methods being unequal, due to the specific geological and petrophysical conditions. Taking into account the complementary character of the information supplied by the magnetic and gamma-ray spectrometric researches, their conjugated use is compulsory in the study of the hydrothermal haloes and implicitly of the base-metal and/or associated auro-argentiferous mineralizations.

References

Calotă C., Romanescu Dr. (1963) Asupra aplicabilităţii metodelor gravimetrice şi magnetice în cercetarea erupţiilor neogene şi a mineralizaţiilor legate de acestea. *Probl. geofiz.*, II, Bucureşti.

Ghiţulescu T. P., Socolescu M. (1941) Étude géologique et minière des Monts Métallifères. *An. Inst. Géol. Roum.*, XXI, Bucureşti.

Ianovici V., Giuşcă D., Ghiţulescu T. P., Borcoş M., Savu H. (1969) Evoluţia geologică a Munţilor Metaliferi. Edit. Acad. R. S. România.

Romanescu Dr. (1963) Cercetări magnetice asupra eruptivului neogen din partea de est a Munţilor Metaliferi (Baia de Arieş, Zlatna). *Asoc. geol. carp.-balc., Congr. V.*

Udubaşa Gh., Istrate Gh., Dafin E., Braun A. (1976) Mineralizaţiile polimetalice de la Bocşa (N de Săcărîmb, Munţii Metaliferi). *D. S. Inst. Geol. Geofiz.*, LXII, 2, p. 97–124, Bucureşti.

Received: December 5, 1991
Accepted: January 17, 1992

Rom. J. Geophysics, 1993, 16, p. 23–28

METODE BIOGEOFIZICE DE IDENTIFICARE A MINERALIZAŢIILOR POLIMETALICE ŞI A GENERAŢIILOR DE FALII, APLICATE ÎN ZONELE ZEBRAC–MERMEZEU (MUNŢII CĂLIMANI DE SUD) ŞI JOLOTCA (MASIVUL ALCALIN DE LA DITRĂU)

Lucian IONESCU, László ZÓLYA

I.P.E.G. - Harghita, Str. Gh. Doja 6, 4100 Miercurea Ciuc.

Key words: Geophysical methods. Gravity surveys. Magnetic surveys. Electrical surveys. Geochemical methods. East Carpathians.

Abstract: *Biogeophysical Methods for the Identification of the Base-Metal Mineralizations and of the Faults Generations in the Zebrac-Mermezeu (South Călimani Mountains) and Jolotca (Ditrău Alkaline Massif) Zones.* These biogeophysical methods (dowsing) have been used in areas with a different geological structure. In the Zebrac-Mermezeu zone, characterized by a Tertiary andesitic structure affected by hydrothermal alterations, the biogeophysical method clearly revealed the mineralized and hydrothermally altered zones. The biogeophysical anomalies can be correlated with the geological boundaries as well as with the geophysical and geochemical anomalies. In the Jolotca zone, constituted of Jurassic hornblendites, diorites and syenites, the biogeophysical method (dowsing) evidenced several fractures of different age.

Cercetările actuale privind identificarea şi interpretarea unor semnale de natură biogeofizică reiau, pe o bază ştiinţifică, practici tradiţionale milenare. Biogeofizicieni din C. S. I., Franţa, S. U. A. au dovedit existenţa obiectivă a acestor semnale şi marea lor utilitate în cercetarea geologică.

Iniţierea autorilor lucrării în acest domeniu a fost făcută de Ioan Seghedi de la Institutul de Geologie şi Geofizică din Bucureşti, căruia îi mulţumim pe această cale.

Avînd în vedere rezultatele deosebite obţinute cu ajutorul metodelor biogeofizice descrise în această lucrare, considerăm utilă prezentarea lor. În literatura de specialitate studiată pînă în prezent nu am găsit descrise aceste metode.

Prezentarea metodelor de cercetare biogeofizică

Identificarea anomaliilor biogeofizice pe o suprafaţă de circa 6 km^2 din zona structurii eruptive Zebrac-Mermezeu s-a efectuat prin aproximativ 50 km de profile pe văi, creste şi poteci, parcurse cel puţin o singură dată. În zona cercetată au rămas mici areale insuficient acoperite. Instrumentul radiestezic folosit pentru semnalarea anomaliilor biogeofizice a fost o baghetă unghiulară confecţionată dintr-o ramură de arţar.

Cei doi autori receptează o serie de semnale biogeofizice în mod diferit, iar altele în mod identic.

a. Astfel, la primul dintre autori, semnalul biogeofizic, pe baza căruia s-au obţinut anomaliile biogeofizice, se manifestă prin ridicarea şi coborîrea alternativă a baghetei în timpul parcurgerii unui anumit profil. Lungimea intervalelor succesive, în care bagheta se ridică sau coboară, prezintă tendinţe de creştere sau micşorare treptată şi constantă a semnalului. Pe aceste semnale s-au suprapus şi altele, de exemplu cele cauzate de falii şi galerii. Pentru a aprecia lungimea intervalelor am folosit pasul, care în unele condiţii poate deveni o unitate de măsură destul de exactă. Apostol (1976) a constatat "un automatism al ritmului respirator şi frecvenţa paşilor" în timpul parcurgerii profilului de către operator.

Acest semnal prezintă un caracter sinusoidal, cu punctul zero cînd bagheta are poziţie orizontală, sinusul pozitiv – cînd bagheta este ridicată – şi sinusul negativ – cînd bagheta este coborîtă.

Primele observaţii biogeofizice au evidenţiat valori mici sau nule ale semnalelor în afara structurii eruptive Zebrac-Mermezeu, în general pînă la 50 paşi. Pe măsura intrării în zona structurii, aceste valori cresc foarte repede, ajungînd la 100 paşi, 200 paşi şi, rar, mai mari – între 250–300 paşi. Harta anomaliilor biogeofizice a rezultat prin interpolarea zonelor cu aceeaşi valoare (în paşi) a semnalelor, în valoare absolută, deci indiferent dacă ele sînt pozitive sau negative.

Am constatat că semnalele mai lungi sînt mai puternice. In acest caz bagheta trebuie blocată cu degetele pentru a nu se pierde controlul asupra ei. Trecerea de la o tendinţă de ridicare la aceea de coborîre sau invers, se face repede. Un profil reluat de mai multe ori în decursul aceleiaşi zile a prezentat o configuraţie identică a succesiunii semnalelor pozitive şi negative; lungimea lor, precum şi localizarea limitei dintre ele rămîn neschimbate, cu condiţia ca starea timpului să nu se modifice esenţial. Dacă măsurătoarea este întreruptă, dar se reia din acelaşi punct, datele înregistrate au continuitate. În timpul ploilor torenţiale valoarea semnalelor este diminuată, dar zăpada nu le afectează. Frigul şi oboseala operatorului pot denatura semnalele biogeofizice.

Pot fi făcute unele comparaţii între metoda descrisă de Matveev (1967) şi cea folosită de noi: Matveev foloseşte cadre metalice care se rotesc în sens pozitiv, corespunzînd unei ridicări a baghetei noastre de lemn, sau se rotesc în sens negativ, corespunzînd unei coborîri a baghetei. Matveev a întrebuinţat cadre din metale diferite cu care a obţinut semnale diferite, iar noi am întrebuinţat baghete din lemn de diferite esenţe, cu care am obţinut, practic, rezultate identice. Matveev a determinat intensitatea semnalelor biogeofizice prin raportarea numărului de rotiri (însumat algebric) pe o distanţă constantă, măsurată pe teren (de exemplu 5 m sau 20 m), iar noi – prin măsurarea lungimii pe care bagheta prezintă aceeaşi tendinţă de ridicare sau coborîre. In această privinţă metoda noastră este mult mai operativă, deoarece nu necesită jalonarea profilelor.

Semnalele biogeofizice generate de faliile verticale, în momentul traversării lor, prezintă o configuraţie specifică şi simetrică (Apostol et al., 1972). Simetria scade pe măsură ce faliile trec de la poziţia verticală la cea orizontală. Prin măsurarea asimetriei celor două flancuri se poate preciza sensul înclinării faliilor şi se poate estima unghiul înclinării. Centrul de simetrie al acestor semnale se suprapune pe axul faliilor. Determinarea direcţiei acestora se realizează fie prin intersectarea lor în cel puţin două puncte, fie prin deplasarea pe direcţie, urmărindu-se încadrarea permanentă pe semnalul de minim sau maxim (în funcţie de operator) existent în centrul de simetrie al semnalului biogeofizic. Dacă în timpul deplasării în lungul faliei, pe axul de simetrie al semnalului se interceptează un alt semnal de falie, înseamnă că falia urmărită este intersectată de către o falie mai tînără. Prin deplasarea în lungul unei falii mai tinere nu vor fi sesizate semnale provocate de intersecţia cu falii mai vechi.

b. La al doilea autor, semnalele biogeofizice marchează cu exactitate limitele dintre diferitele tipuri petrografice, prin ridicarea sau coborîrea baghetei. In cadrul aceluiaşi petrotip, bagheta îşi păstrează poziţia. In cazul mineralizaţiilor apropiate de suprafaţă, semnalul biogeofizic este foarte intens.

c. Ambii autori receptează semnale biogeofizice provocate de golurile subterane şi de galerii, care se manifestă prin coborîrea baghetei deasupra acestora.

Compararea rezultatelor metodei biogeofizice de identificare a zonelor mineralizate cu datele prospecţiunilor geologice, geofizice şi geochimice din zona Zebrac-Mermezeu (munţii Călimani de Sud)

1. Prospecţiunea geologică

Regiunea bazinelor superioare ale văilor Zebrac şi Mermezeu prezintă o structură geologică complicată, determinată de participarea formaţiunilor sedimentare miocene şi a celor eruptive pannoniene (Balla, 1980, 1981, date nepubl.). Structura eruptivă Zebrac-Mermezeu are o alcătuire complexă, ca urmare a edificării ei în mai multe momente de activitate magmatică. Manifestări postvulcanice au condus la intense transformări hidrotermale±mineralizare. Mineralizaţia prezintă un caracter filonian aurifer sau diseminat plumbo-zincifer.

În afara structurii eruptive Zebrac-Mermezeu, semnalele biogeofizice nu apar sau au o valoare foarte redusă. Pe structura eruptivă semnalele cresc pînă spre 300 paşi (fig. 1). Se pot contura cîteva zone anomale biogeofizice: Dealul Ursului, izvoarele pîriurilor Păltiniş, Mermezeu şi Popii. Toate aceste zone au fost anterior cercetate cu foraje şi galerii scurte, dar dintre ele se detaşează Dealul Ursului, cu valori de peste 250 paşi, zonă în care sînt concentrate majoritatea lucrărilor miniere. Zonele enumerate sînt caracterizate de intense transformări hidrotermale, în special argilizări (fig. 2).

În Vîrful Ursului apare o zonă moderat anomală biogeofizic, înconjurată de o centură de maxime intense (fig. 1). Acestă situaţie este identică cu aceea descrisă de Balla (1981, date nepubl.), în care andezitele slab transformate din Vîrful Ursului, reprezentînd probabil o ultimă erupţie, sînt înconjurate de o centură cu argilizări intense. Pe pîrîul Zebrac, în amonte de confluenţa cu Pîrîul Ursului, apare o anomalie biogeofizică intensă, orientată nord-sud, reprezentînd un fragment din centura amintită anterior. Ea este cauzată de un filon care a fost identificat la suprafaţă, în talvegul pîrîului şi în subteran. Filoanele mineralizate din Dealul Ursului sînt instalate pe falii şi, de asemenea, se consideră că zonele afectate hidrotermal±mineralizate, peste care se suprapun anomaliile biogeofizice de pe pîriurile Păltiniş, Mermezeu şi Popii, sînt datorate circulaţiei hidrotermale în lungul unor falii.

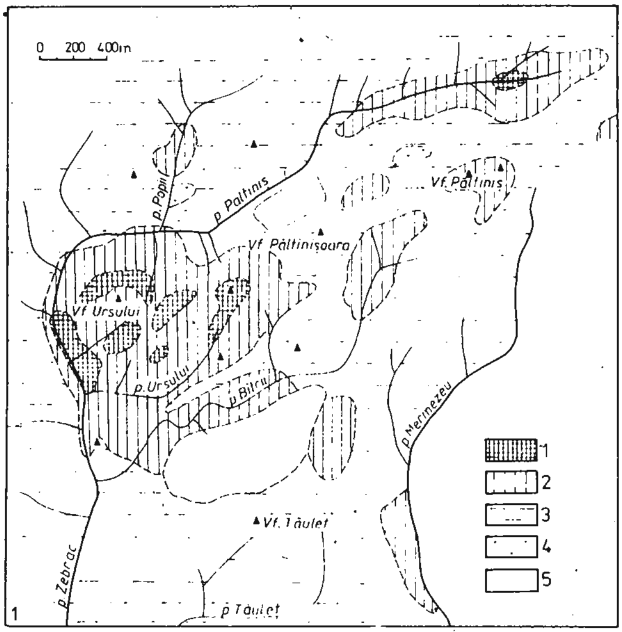

Fig. 1 – Harta anomaliilor biogeofizice din zona Zebrac-Mermezeu.
1, 201–300 paşi; 2, 101–200 paşi; 3, 1–100 paşi; 4, semnal nul; 5, zone neacoperite.

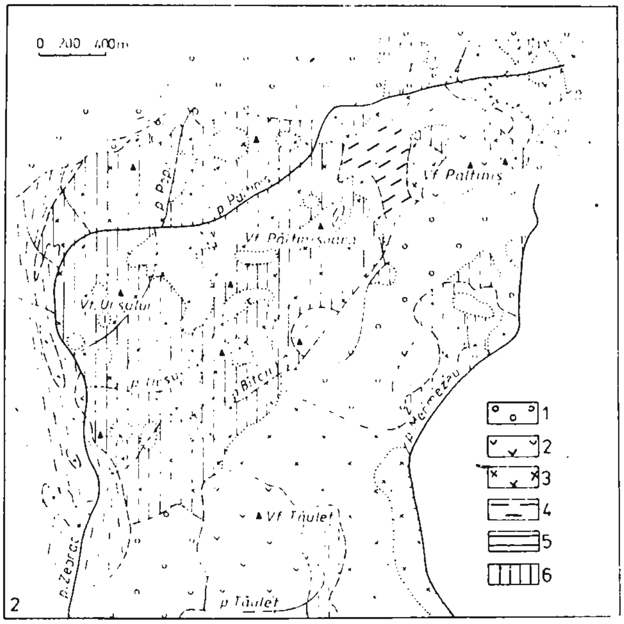

Fig. 2 – Harta geologică a zonei Zebrac-Mermezeu (după Balla în Brotea et al., 1985, date nepubl., cu simplificări).
1, piroclastite; 2, andezite de Tăuleţ; 3, structura eruptivă Zebrac-Mermezeu; 4, fundamentul sedimentar; 5–6, transformări hidrotermale: 5, argilizări; 6, propilitizări.

In cadrul structurii eruptive, se remarcă patru zone de minim biogeofizic. Două dintre acestea (prima în malul drept, amonte de pîrîul Bîtcii şi, cea de-a doua, la nord de vîrful Păltinişoara) corespund apariţiei la zi a depozitelor sedimentare miocene. Pentru zonele fără semnal biogeofizic de pe pîrîul Popii şi pîrîul Păltiniş trebuie găsite alte explicaţii (vezi prospecţiunea electrometrică).

2. Prospecţiunea gravimetrică

Harta anomaliilor gravimetrice Bouguer (fig. 3), cu izolinii care converg spre centrul structurii eruptive, reflectă contrastul de masă dintre andezitele acestui corp şi formaţiunile înconjurătoare (Ioane în Brotea et al., 1985, date nepubl), fără a avea o legătură directă cu anomaliile biogeofizice.

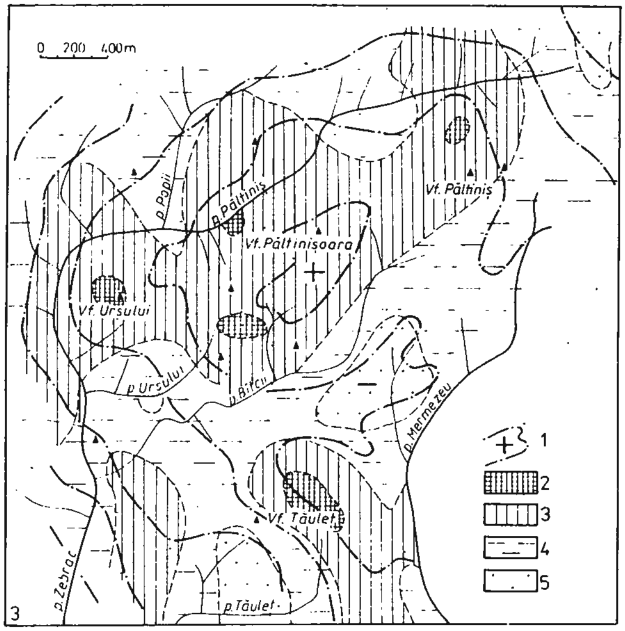

Fig. 3 – Harta anomaliilor gravimetrice din zona Zebrac-Mermezeu (după Ioane în Brotea et al., 1985, date nepubl., cu simplificări).
1, anomalia gravimetrică Bouguer: 1, izolinii gravimetrice; 2–5, anomalii gravimetrice reziduale: 2, 3, 4, 5, izozone gravimetrice.

Harta anomaliilor gravimetrice reziduale (fig. 3) conturează intruziunile corpurilor microdioritice prin anomaliile locale de maxim, iar zonele transformate hidrotermal sau cele scufundate tectonic (pîrîul Bîtcii) prin cele de minim. Corelaţiile care se pot face cu anomaliile biogeofizice constau în valorile generale de maxim ale celor două măsurători în zona structurii eruptive Zebrac-Mermezeu, precum şi în dispunerea asemănătoare a acestor anomalii.

3. Prospecţiunea radiometrică

Deşi maximele radiometrice (Onescu în Brotea et al., 1985, date nepubl.) se suprapun peste formaţiunile sedimentare, la rîndul lor caracterizate de minime biogeofizice, în cadrul structurii eruptive nu se poate face nici o corelaţie între cele două tipuri de anomalii.

4. Prospecţiunea magnetometrică

Anomaliile magnetometrice de minim (fig. 4) din zona Dealul Ursului, amonte pe pîriurile Păltiniş, Mermezeu, Popii şi Bitcii (Onescu în Brotea et al., 1985), reflectînd intensitatea transformărilor hidrotermale, se corelează foarte bine cu anomaliile biogeofizice existente în aceleaşi zone.

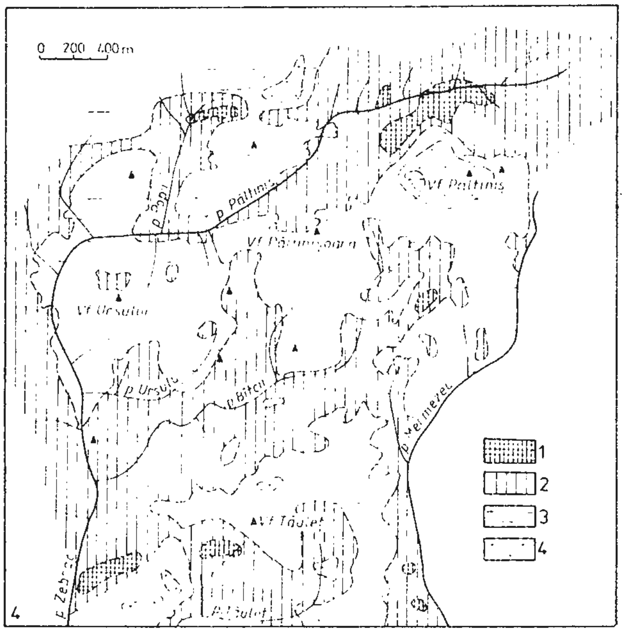

Fig. 4 – Harta anomaliilor magnetometrice din zona Zebrac-Mermezeu (după Onescu în Brotea et al., 1985, cu simplificări).
1–4, izozone magnetometrice (Δ T): 1, sub 300 γ; 2, 0–300 γ; 3, 0–500 γ; 4, peste 500 γ.

5. Prospecţiunea electrometrică

O situaţie interesantă, care ar putea lămuri o problemă pusă anterior, se referă la cele două zone de nul biogeofizic care apar pe structura eruptivă, una pe pîrîul Păltiniş şi a doua pe Pîrîul Popii. Comparînd cu datele prospecţiunii electrometrice (Rusu in Brotea et al., 1985) se constată că acestea se înscriu într-un culoar de minim electric (fig. 5).

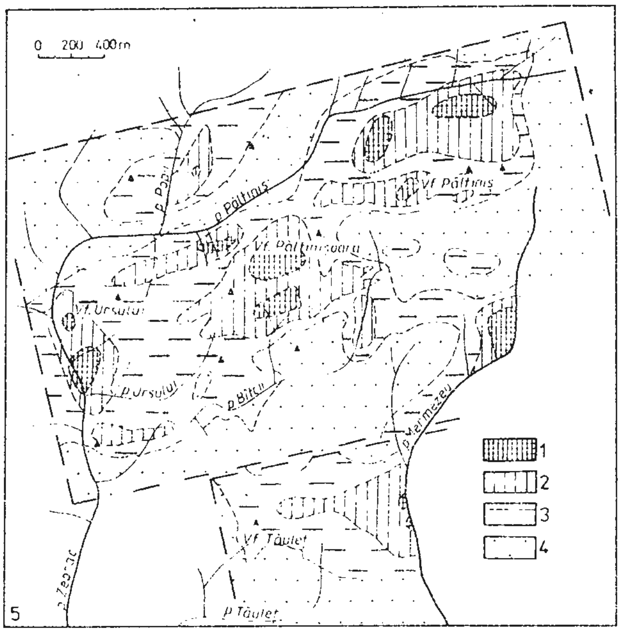

Fig. 5 Harta anomaliilor geoelectrice din zona Zebrac-Mermezeu (după Rusu în Brotea et al., 1985, cu simplificări). Perimetrul nordic, Ursu-Păltiniş: 1–4, izozone geoelectrice, metoda polarizabilităţii în domeniul timp, ma(msec): 1, peste 20; 2, 15–20; 3, 10–15; 4, sub 10. Perimetrul sudic, Tăuleţ: 1–4, izozone geoelectrice, metoda polarizaţiei induse, M(mv/v): 1, peste 80; 2, 60–80; 3, 40–60; 4, sub 40.

Anomaliile de maxim geoelectric apar în zona Dealul Ursului, amonte pe pîrîul Păltiniş, pe pîrîul Mermezeu şi mai slab pe pîriurile Popii şi Bitcii. Dispunerea acestora reflectă o corelaţie bună între anomaliile electrometrice şi cele biogeofizice

6. Prospecţiunea litogeochimică

În zona Dealul Ursului se observă dispunerea anomaliilor litogeochimice selectiv cumulative sub forma unei centuri de maxim în jurul unei zone centrale de minim (fig. 6) (Balla, 1981, date nepubl.). Un aspect identic prezintă şi anomaliile biogeofizice. După opinia lui Balla (1981, date nepubl.), valorile lui A mai mari de 800 ppm sînt datorate unor filoane mineralizate.

Alte zone de maxim litogeochimic, care se corelează cu cele biogeofizice, sînt în amonte pe pîriurile Păltiniş şi Bitcii. Deşi în unele zone mai apar diferenţe între datele celor două metode de prospecţiune, datorate culegerii nesistematice a probelor sau nereprezentativităţii acestora, se poate aprecia că există o corelaţie bună a anomaliilor litogeochimice şi biogeofizice.

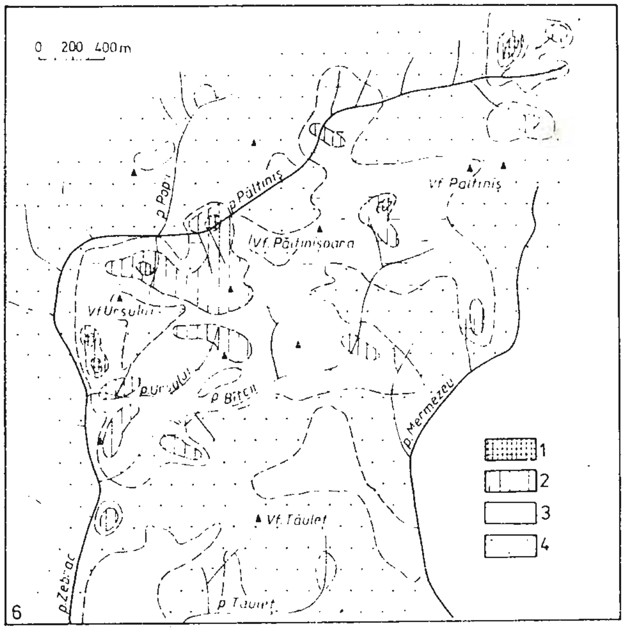

Fig. 6 - Harta anomaliilor litogeochimice din zona Zebrac-Mermezeu (după Balla, 1980, 1981, cu simplificări).
1-4, anomalii litogeochimice selectiv-cumulative, in ppm (A = 100 Ag+As+B+100 Bi+Cu+Mo+Pb+10 Sn): 1, A = peste 700; 2, A = 400-700; 3, A = 100-400; 4, A = sub 100.

Generaţii de falii identificate cu ajutorul metodei biogeofizice în zona Jolotca (Masivul alcalin de la Ditrău)

Zona Jolotca este situată in partea de NNV a masivului alcalin de la Ditrău şi cuprinde cea mai mare parte a ariei de aflorare a rocilor ultrabazice şi bazice.

Primele observaţii biogeofizice le-am efectuat acolo unde a fost posibilă verificarea lor in aflorimente sau in lucrări miniere. Folosind metoda detectării faliilor prezentată anterior, am putut localiza fracturile, precizind direcţia, sensul inclinării şi succesiunea in timp a acestora. Prin localizarea exactă a semnalelor pe hartă sau chiar pe teren, am reuşit să determinăm sensul şi amplitudinea decroşărilor. Faliile din zona Jolotca aparţin cel puţin la la patru generaţii (fig. 7).

Există un sistem de falii orientat NV-SE, avind inclinări diferite. Relaţiile lor cu celelalte sisteme incă n-au fost verificate. Acestea sint mai vechi decit faliile cu direcţia N-S, care le intersectează. Acestui sistem NV-SE ii aparţin faliile de pe piriurile Filip şi Gudu (in amonte).

Urmează o generaţie mai nouă reprezentată prin falia situată in lungul primului afluent sting al piriului Teasc. Falia are direcţia NNE-SSV şi inlinare spre NNV.

Faliile aparţinind generaţiei a treia au direcţia aproximativă N-S şi căderi estice. Acestui sistem aparţin falia de pe piriul Simo, faliile Teasc T, T_1, T_2, T_3, partea sudică a faliei Filip, faliile de pe piriurile Tarniţa de Sus, Tarniţa de Jos, Pietrăriei de Sus, Pietrăriei de Jos. Aceste falii sint foarte importante deoarece ele controlează dispunerea spaţială a mineralizaţiilor de la Jolotca şi influenţează evoluţia geomorfologiei din zonă.

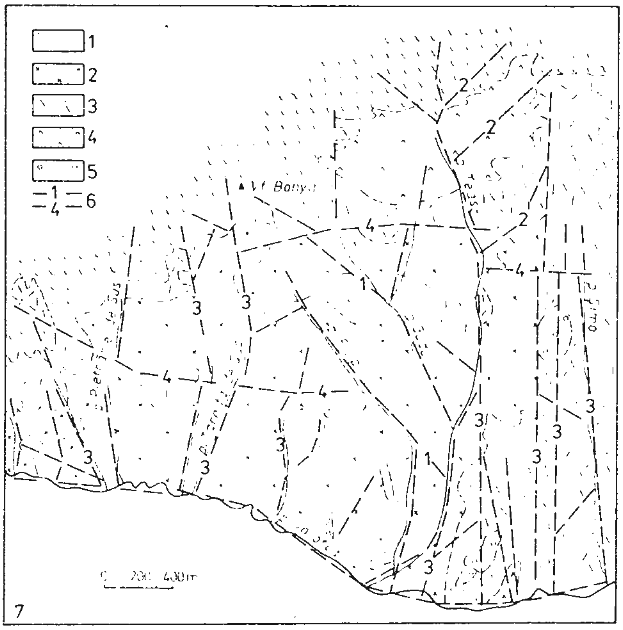

Fig. 7 - Generaţii de falii detectate biogeofizic în zona Jolotca. 1, şisturi cristaline; 2, hornblendite şi diorite; 3, sienite şi monzonite; 4, sienite nefelinice; 5, depozite vulcano-sedimentare; 6, generaţii de falii.

Faliile din generaţia a patra reprezintă cel mai tînăr sistem detectat pînă acum. Au direcţia aproximativă E-V şi inclinări nordice. Ele descroşează compartimentul sudic al faliilor din generaţia a treia spre vest cu circa 20-30 m. Cu toate că şi falia mare de pe pîriul Jolotca are direcţia E-V, nu avem suficiente date ca s-o incadrăm in acest sistem. Ea decroşează puternic spre vest compartimentul sudic.

Pe lingă aceste sisteme de falii au fost identificate mai multe fracturi de sprijin care au lungimi şi importanţă mai redusă.

In stadiul actual de cunoaştere nu ne putem pronunţa cu certitudine asupra virstei fiecărui sistem de falii şi nici asupra apartenenţei lor la anumite faze orogenetice. Putem insă susţine că majoritatea faliilor prezentate se continuă, intersectind şi rocile cristaline din jur (seriile de Rebra şi Tulgheş), deci nu sint proprii masivului. Acestea sint generate de faze tectonice post-jurasice, după intruziunea masivului alcalin de la Ditrău. Mai mult, unele sisteme sint foarte tinere, de exemplu faliile din generaţia a treia şi a patra, care deranjează formaţiunile vulcano-sedimentare neogene, deci par a fi postneogene.

Concluzii

Metodele prezentate le-am aplicat ulterior şi în studierea altor zone, în condiţii geologice foarte diferite. Rezultatele obţinute au confirmat caracterul de sinteză al metodei biogeofizice, reflectînd concomitent structura geologică, anomalii geofizice şi geochimice. Majoritatea cercetărilor noastre au fost axate pe identificarea semnalelor biogeofizice, care apar în zonele mineralizate cunoscute, şi pe verificarea extinderii acestora în zonele limitrofe aflate în curs de cercetare sau necunoscute. De fiecare dată am efectuat cercetările fără a fi studiat în prealabil geologia perimetrului respectiv. Compararea rezultatelor s-a făcut după terminarea măsurătorilor biogeofizice.

Semnalele biogeofizice ale autorilor acestei lucrări sînt, în mare parte, deosebite, dar ele se completează reciproc şi pe baza interpretării lor pot fi rezolvate următoarele probleme:

– identificarea şi determinarea cu precizie a conturului, direcţiei şi înclinărilor structurilor mineralizate;

– identificarea limitelor dintre diferite tipuri petrografice;

– identificarea şi determinarea direcţiei, sensului de înclinare, succesiunii în timp a faliilor;

– identificarea şi conturarea galeriilor recente şi vechi sau a golurilor subterane.

Received: April 25, 1988
Accepted: May 15, 1988
Presented at the scientific session of I.P.E.G. Harghita: May 27, 1988

Dacă în momentul de faţă această metodă nu este încă suficient de riguros pusă la punct pentru a putea plasa o lucrare minieră numai pe baza informaţiilor biogeofizice, reiese clar rolul ei în evitarea localizării greşite a acestora. Noi nu cunoaştem toate cauzele geologice care pot genera anomalii biogeofizice, dar susţinem că nu poate exista o mineralizaţie metalică lipsită de o anomalie de acest gen.

Avînd în vedere dotarea tehnică necesară foarte modestă, cheltuielile minime, operativitatea deosebită, precum şi caracterul foarte complex al observaţiilor biogeofizice, rezultă marea eficienţă a acestei metode de cercetare.

Bibliografie

Apostol A., Ionescu Fl., Pricăjan A., Săhleanu V. (1972) Asupra unor informaţii de natură biologică obţinute în practica geologică. *Rev. Minelor*, 7, Bucureşti.

Apostol A., Dumitrescu I. Fl. (1976) Măsurători radiotelemetrice ale variaţiei diurne a semnalului dowsing. *St. tehn. econ.*, Inst. Geol. Geofiz., D, 11, Bucureşti.

Matveev V. S. (1967) O biofizicescom metode v gheologhii. Izv. Acad. Nauk. Kazah. S.S.S.R., Ghcol., 3, Alma Ata.

x x x (1986) Biolocaţie. Rev. "Aurora", 6, Bucureşti.

Rom. J. Geophysics, 1993, 16, p. 29–35

POSSIBILITIES OF DETERMINING THE INFLUENCE OF THE PROSPECTING ARRAYS ON INDUCED POLARIZATION ANOMALIES USING PHYSICAL MODELLING

Mitrofan JOSAN, Liviu CORCIMARU, Mihalache ROMAN

"Prospecţiuni" S. A. Str. Caransebeş 1, 78 344 Bucureşti 32.

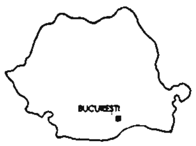

Key words: Electrical anomalies. Induced polarization. Physical models. Three-dimensional models.

Abstract: The simulation of the induced polarization anomalies is often necessary for the geoelectrical prospectings. The present paper is an attempt to illustrate the possibilities of IP anomalies simulation using physical modelling. The results obtained on two types of three-dimensional models – inclined homogeneous plate and vertical unhomogeneous cylinder – by means of longitudinal gradient arrays and electrical sounding are presented, too.

Introduction

For modelling simulation of the resistivity and induced polarization anomalies several methods can be used such as: numerical or analytical modelling and physical modelling.

Physical modelling of the geoelectrical anomalies, also known as scale modelling, have been dealt with by several researchers in two variants: resistivity two-dimensional modelling on conducting paper (Aiken et al., 1973; Avdevici et al., 1978) and vat modelling (Aiken et al., 1973; Hallof, 1961–1971; Komarov, 1969; Veşev, 1965).

Following the Romanian tradition of physical modelling (Stoica et al., 1972, unpubl. data; Georgescu et al., 1974) the present paper is an attempt to illustrate the possibility of envicing the dependence of the elements specific to a IP anomaly corresponding to a geological object, on the type and dimensions of the prospecting array using the vat scale modelling.

Although the previous papers dealt with diverse cases, they generally discussed profile anomalies. Hallof (7) presented images of IP anomalies in vertical section but only for the dipole-dipole array, and Scupin et al. (1976) achieved, by simulation on a reduced model, geoelectrical sections of resistivity and polarizability with a Wenner array.

This paper presents the results of the IP anomalies simulation by vat physical modelling on two model types: inclined plate and vertical cylinder. The results are presented as maps and vertical sections of apparent polarizability.

Results obtained

The laboratory tests have been effectuated on models with volume polarization only.

The induced potential measured by a time domain technique corresponds to a reference time of 0.91 sec after the current pulse interruption and to an integration interval of 0.52 sec.

The parameter of polarizability M_{4232} represents thousandths of the potential induced from the primary potential. It has been recorded using a Scintrex IPR–8 receiver and is expressed as mV/V.

It is thought that the method used ensures a good accuracy. Figure 1 presents a comparison between a vat physical modelling and a computer 2–D modelling. The simulation of the IP model by physical modelling was effectuated on a 3–D model, the square plate size being 15 u and 2 u thick (1 u = 1 cm).

The profiles presented represent the variation of the apparent polarizability recorded by a longitudinal gradient array (AB = 60 u, MN = 2 u) perpendicular to the elongation trend of the plate.

Between the obtained profiles, as for their shape and position of the maxima and minima, a good correlation is to be noticed. The differences of intensity of the anomalies are due to the finite length of the model in the physical modelling and to the different depth at the top of the bodies.

The contrasts of the electrical properties between the model and the environment for both modellings (physical and theoretical) were, as follows:

$$\frac{\rho medium}{\rho model} = \frac{35 ohmm}{15 ohmm} \text{ and } \frac{M medium}{M model} = \frac{0.5 mV/V}{65 mV/V}$$

For the same model (3–D) vat recordings with the gradient array have been carried out further on by using a measuring lay-out with the size equal to the mid-length of the AB line.

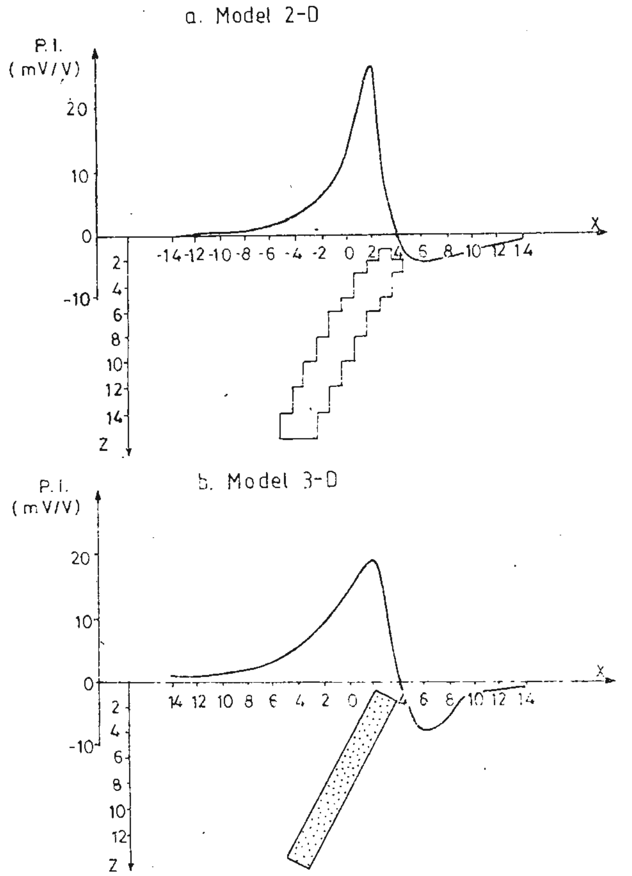

Fig. 1 – Profiles of apparent polarization, longitudinal gradient array AB = 60 u, MN = 2u; a, theoretical modelling 2–D; b, physical modelling; 3–D, central profile; strike extension of the model is 15 u.

Figures 2a and 2b present polarizability maps for an approximately central position of the body, in cases in which the polarizing field is perpendicular to the elongation direction of the body and parallel to it, respectively. It is of note that the elongation of the anomaly perpendicular to the AB line is first of all the result of the direction of the polarizing field (Fig. 2b).

The maximum of the positive values is superposed to the body, that is to the portion near the surface, whereas the IP minima highlight the marginal parts of the body, situated on the AB line.

The anomaly morphology suggests the body shape only in the first case, where the array is perpendicular to the body elongation.

A special case is presented in Figure 2c, in which the same disturbing body is situated in the contact zone of two measuring panels and the elongation direction of the body forms an angle of ca 45^0 with the AB directions of each panel. The influence of the AB line manifests by the outlining of a regional anomaly (M—4 mV/V) extended along a strike perpendicular to the AB line. Although the total volume of the body is equally distributed to the two panels, the maxima on each panel show different strikes and intensities.

Without averaging the values on the tie-profile, the two anomalies show only a part of the real situation, namely in the southern panel (M = 22 mV/V) only, where two thirds of the upper part of the body occur and where the body is closer to the AB emission line. On the northern panel the top of the body (about one third), situated farther from the AB line, generates an anomaly about 30 per cent reduced (M = 14 mV/V), striking strictly perpendicular to the direction of the polarizing field AB. For both plates the minima with negative IP values point out the edges of the body parallel to the AB line. If we use the averaging method at the limit between the panels, quite frequently used in practice, only the apex of the anomaly with values of 14–22 mV/V occurs above the body, namely in the area close to the surface.

The polarizability cross-section obtained with a Schlumberger array is shown in Figure 3. The anomaly obtained presents a specific shape of this array which consists in the outlining of a central maximum, strongly elongated on the vertical and two maxima of a lower intensity extended laterally. The central maximum is located strictly at the top of the body, whereas the lateral branches overpass the body. The results of the carried out modellings, in case of other models too, showed the same characteristic shape of the IP anomaly, for the Schlumberger-type array, regardless of the shape of the modelled body.

The shape of the IP anomaly, in case of the same model, recorded with the axial dipole array (x = 1 u) is characteristic of this technique (Fig. 4). The two maxima symmetrically situated as against the top of the body show different intensities. The higher intensity of the western maximum points out the dipping of the body in this direction. The position of the body is well determined in case of the axial dipole array only for the anomalous values recorded at the levels 1–3.

Further on a second model is described for which recordings with the gradient and Schlumberger array have been effectuated in the basin. The model consists of two mediums with volume polarization and it simulates a mineralized subvolcanic body of porphyry copper type (Figs. 5, 6). The two coaxial cylinders, at about 1 u from the surface, simulate the central part of a volcano, less mineralized (M = 40 mV/V) and the "internal" and "external" zones where the accumulations of metallic sulphides are maximum (M = 160

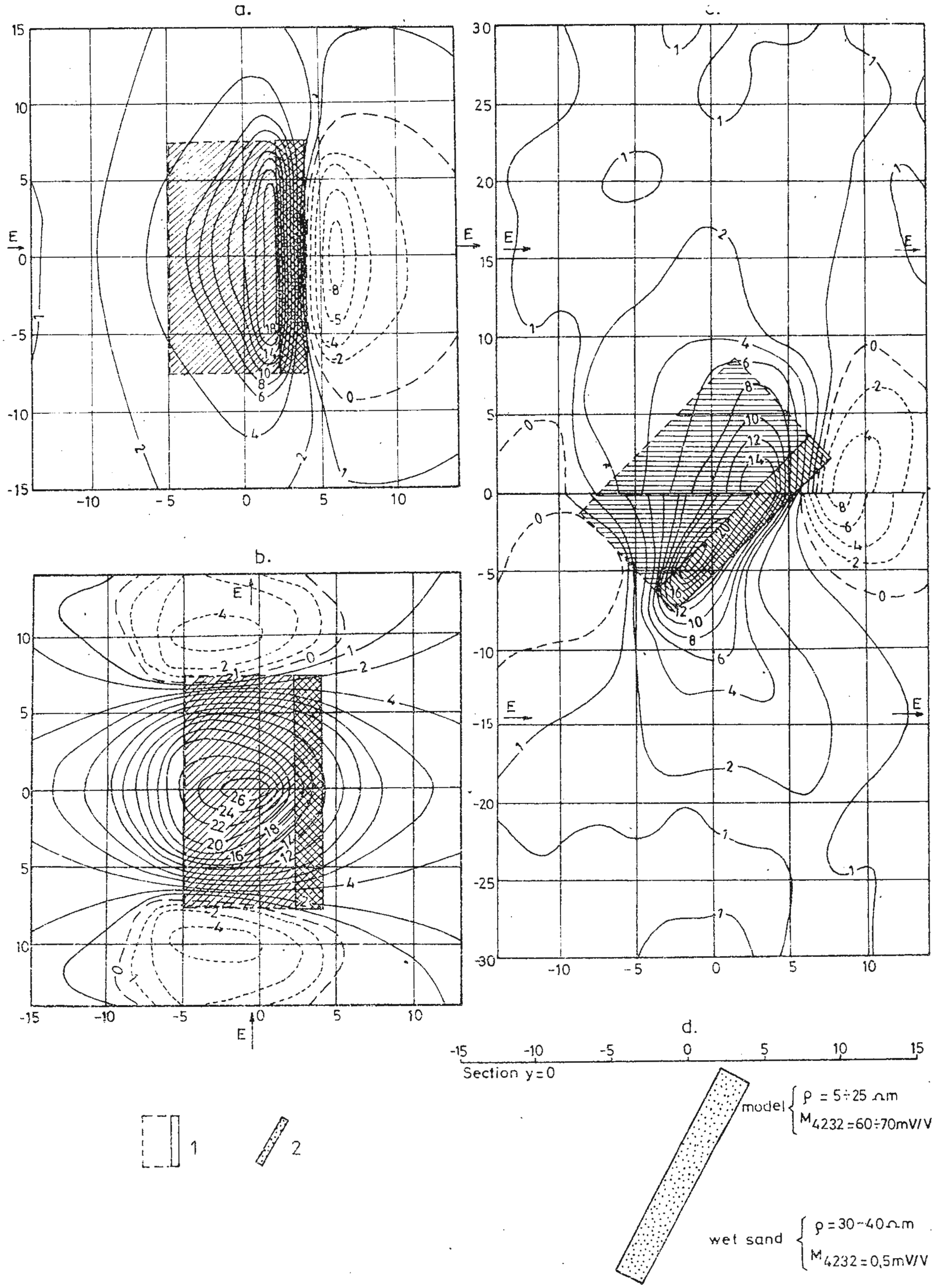

Fig. 2 – Maps of apparent polarization M_{4232}(mV/V) on a square plate model dipping 65°. (a), longitudinal gradient array perpendicular to the AB line; (b), parallel; (c), at 45° versus the elongation strike of the plate; (d), vertical section through the model. 1, prolongation of the model on the observation surface; 2. cross section projection of the model.

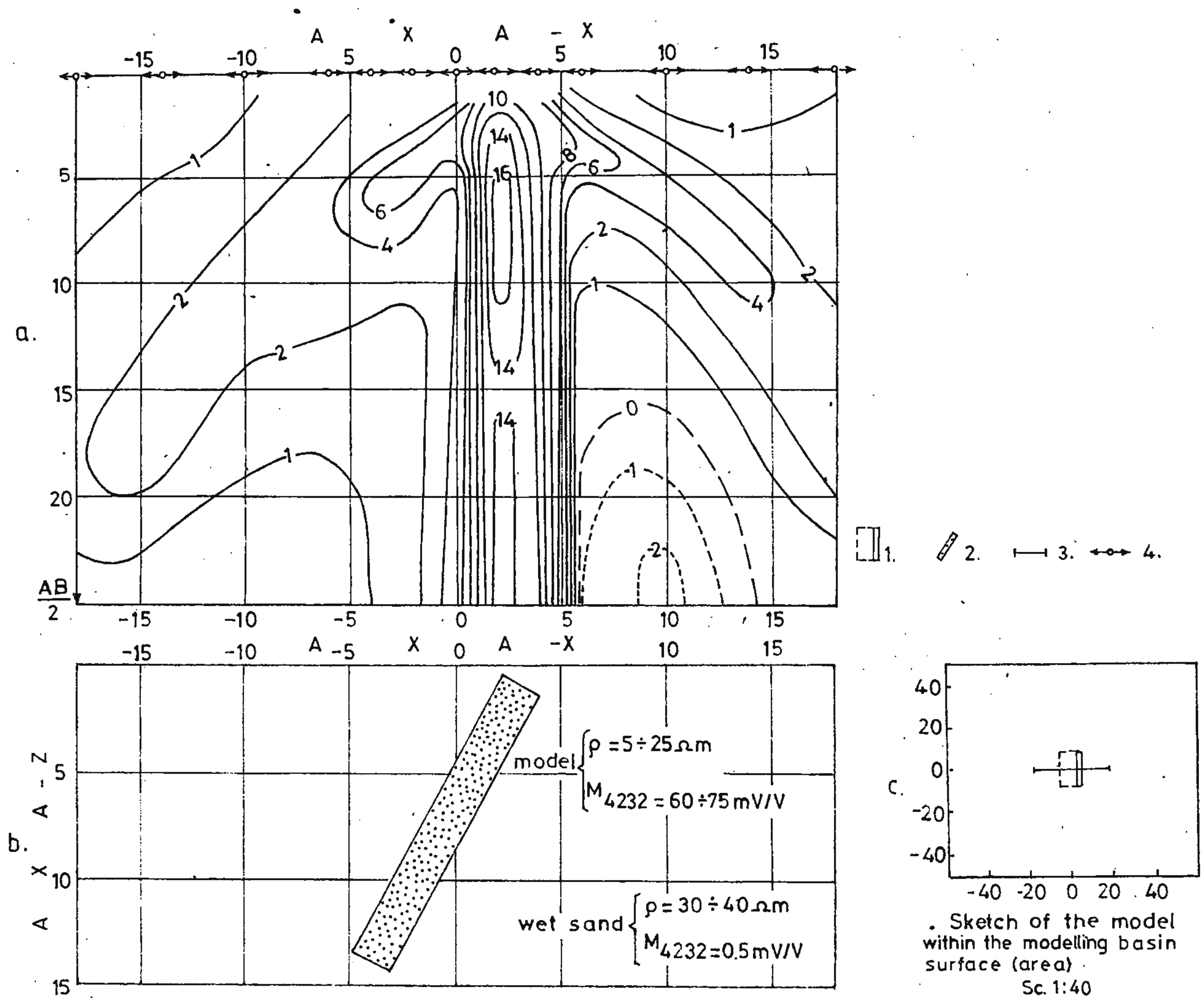

Fig. 3 – VES section of M_{4232}(mV/V) polarization on the central profile. (a), model draft – square plate dipping 65^0; (b), model draft on the surface of the modelling basin.

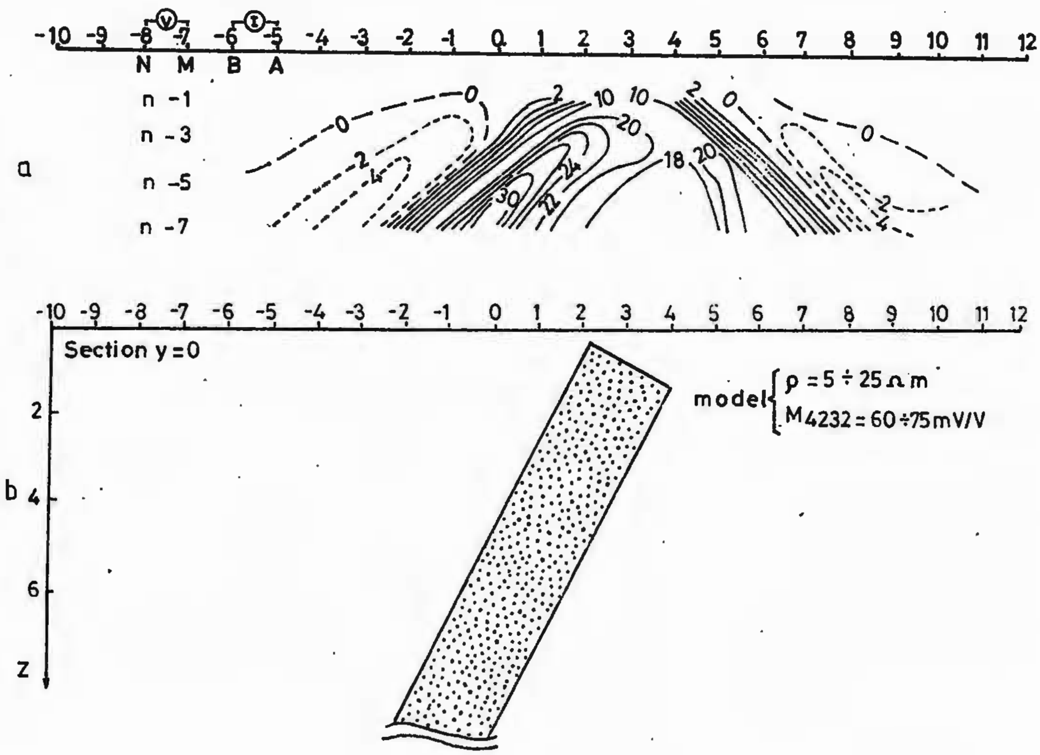

Fig. 4 – Axial dipole section of apparent polarization M_{4232}(mV/V) on the central profile y = 0 – (a); model draft on cross section square plate dipping 65^0 – (b).

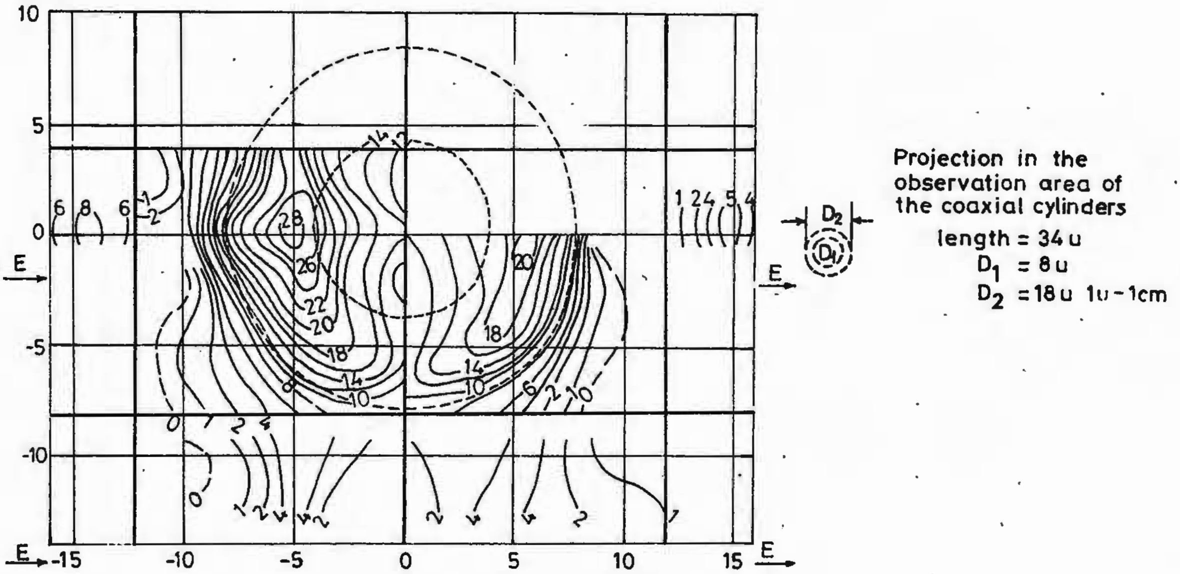

Fig. 5 – Map of apparent polarization M_{4232}(mV/V) on the model of the two vertical coaxial cylinders for the gradient array.

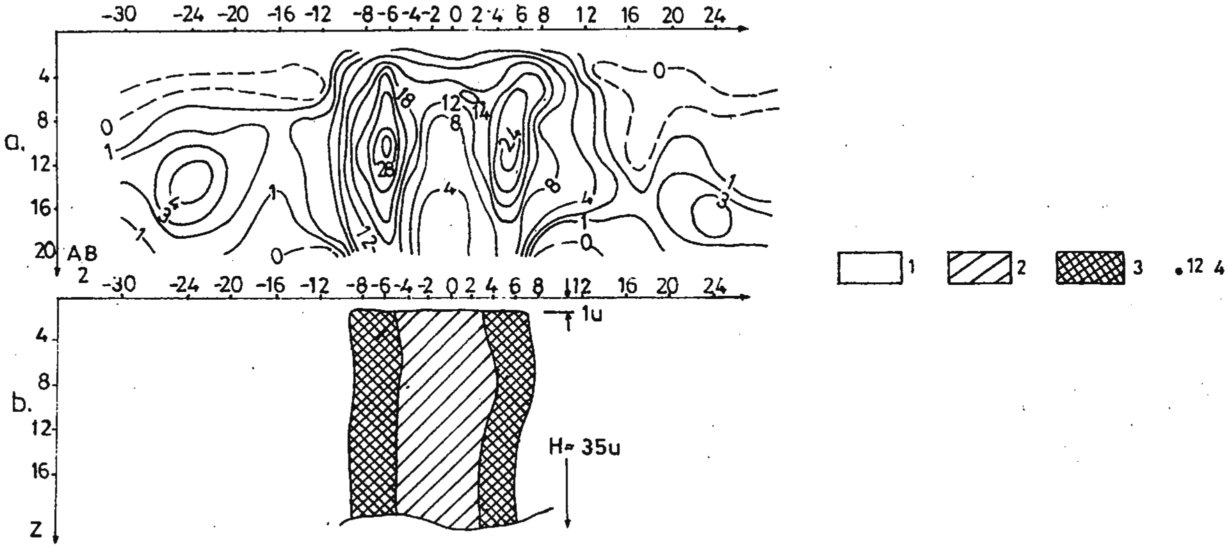

Fig. 6 – VES section of polarization M_{4232}(mV/V) on the central profile (a); model draft – coaxial cylinders (b). 1, sand and clay wet mixture (M = 0.5 mV/V); 2, internal zone (M = 40 mV/V); 3, external zone (M = 160 mV/V); 4, VES station.

mV/V). The IP contrasts were established on the basis of the petrophysical analyses effectuated on rock samples from the Zlatna-Stănija zone, at the surface, from boreholes and mine workings.

Interesting data were obtained with the longitudinal gradient array (AB = 24 u, MN = 1u), the body occurring on several work panels (Fig. 5). From objective reasons the recordings were interrupted before studying the whole area of interest. The image of the IP anomaly can be however completed by symmetry. Thus, a regional anomaly is outlined, marking the limits of the body, which presents two maxima elongated perpendicular to the profiles. The values of the apparent polarizability in the contact zone of the work panels are different.

The recordings carried out on some profiles in the lateral panels point to anomalous values of a lower intensity, at relative great distances from the body.

In case of the Schlumberger array the anomalous image presented in Figure 6 was obtained. The section of apparent polarizability was recorded on a profile which contains the center of the body.

The maximum anomaly connected with the body presents a particular shape, constituted of two branches, elongated vertically, corresponding to the external cylinder with a higher proper polarizability. The fusion tendency of the two anomalies toward the upper part of the section and the outlining of two "false" lateral anomalies can be noticed.

Conclusions

The simulation of the IP anomalies on the two 3-D models presented in this paper offers interesting data which draw the attention on the possibilities of utilizing the physical modellings both in the elaboration phase of the field electrometric measurements and in the interpretation stage of the results.

It is of note that the apex of the IP anomalies, generated by simple and homogeneous inclined bodies, is situated in the zone corresponding to the body section closer to the surface. The observation can be generalized to all the arrays with which the square plate model – longitudinal gradient, VES and axial dipole – has been studied with the specification that as to the axial dipole array we refer only to the upper levels at which the anomaly appears (Figs. 2a, 3 and 4).

The study of the anomalies obtained on the inclined plate model, in case of the gradient and VES Schlumberger arrays points out a possible valuation of the IP minima. They emphasize the body extremes parallel to the AB line. A detail study shows that these IP maxima make possible an estimation of the dipping trend of the body, the minimum of the highest intensity marking the footwall zone of the body (Figs. 2c and 3).

The modellings effectuated for the same model (inclined square plate) by measurements with gradient array, in panels corresponding to a certain trend of the array versus the body elongation, show that in order to establish the position and shape of the polarizing bodies it is necessary to effectuate measurements in the same area of a single panel with several trends of the measuring array (Figs. 2a, 2b, 2c). A first study of the polarizability anomalous image, obtained for a disposition of the array parallel to the elongation trend of the body, does not suggest any real shape of the polarizing body (Fig. 2b).

For the unhomogeneous body modelled by the two vertical coaxial cylinders, the regional anomaly recorded with the gradient array is circumscribed to the surface projection of the body. An interesting result is represented by the two maxima elongated perpendicular to the measurement profiles (Fig. 5). They are generated by the exterior cylinder with a higher proper polarization.

The vertical section of apparent polarizability recorded for this particular model (nonhomogeneous body) is quite suggestive in order to estimate the position and shape of the body on the basis of the study of the anomalous image (Fig. 6).

A significant conclusion is drawn up for the anomalies simulated with the VES Schlumberger array; the vertical elongation of the IP maxima is rather a characteristic of the measuring array without any connection with the shape of the bodies (Figs. 3 and 6).

The coincidence noticed in case of the unhomogeneous cylinder model is due to its verticality (Fig. 6).

It is also of note that the gradient and VES Schlumberger recorded, in the lateral areas of the bodies, anomalies of a lower intensity – false anomalies – as a result of the appearance of a further polarization in cases in which one of the A or B current electrodes are situated nearby the polarizing bodies (Figs. 5 and 6).

References

Aiken C. L., Hastings D. A., Sturgul J. R. (1973) Physical and Computer Modeling of Induced Polarization. *Geophysical Prospecting*, 21, 4, p. 763–782, Haga.

Avdevici M. M., Fokin A. F. (1978) Electrical modelling of potential geophysical fields. Nedra Press. Leningrad (in Russian).

Georgescu P., Gavrilă I., Ion G. (1986) Influence of Gradient Arrangement on Apparent Rezistivity Anomalies. *Rev. roum. géol., géophys. géogr., Géophysique*, p. 45–58, Bucureşti.

Georgescu P., Ionescu V. (1974) Proiect de diplomă, archives of the University of Bucharest.

Komarov V. A., Hlaponina L. S., Balaşev A. N., Popov I. I., Safarenco V. A. (1969) Electrical sounding by induced polarisation method. Nedra Press, Leningrad (in Russian).

Komarov V. A. (1980) Electrical sounding by induced polarisation method. Nedra Press, Leningrad (in Russian).

Mihail C. (1973) Aspecte moderne ale prospecţiunii electrice prin metoda polarizaţiei induse în domeniul frecvenţă. Oficiul de informare şi publicaţii tehnice, Bucureşti.

Scupin N., Niţică C. (1976) Cercetări geoelectrice privind mineralizaţiile de sulfuri polimetalice legate de activitatea magmatismului neogen din zona Cisma-Coasta Ursului, judeţul Maramureş. *St. tehn. econ.*, D, 11, p. 103–110, Bucureşti.

Veşev A. V. (1965) Electrical working in direct and alternating current. Nedra Press, Leningrad (in Russian).

Received: November 8, 1989
Accepted: November 8, 1989
Presented at the XIV-th Symposium of Earth's Physics and Applied Geophysics: July 2–4, 1987

Rom. J. Geophysics, 1993, 16, p. 37–44

GRAVITY EFFECT OF THE NORTH DOBROGEA LOESS; TEMPLATES FOR ITS QUICK EVALUATION

Amuliu PROCA, Angela PROCA
S.C. "PROSPECŢIUNI" S.A. Str. Caransebeş 1, 78 344 Bucureşti 32.

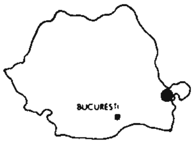

Key words: Gravity surveys. Gravity anomalies. Direct problem. Two-dimensional models. Loess. Dobrogea.

Abstract: The limits within which vary the elements (depth, shape and dimensions) which define the loess accumulations in North Dobrogea as sources of gravity anomalies have been determined using information obtained by drillings and vertical electrical soundings. On these bases, geometrical bidimensional models have been elaborated and their gravity effects computed. Finally, templates which connect the defining elements of the sources with those of the corresponding gravity anomalies have been elaborated. The templates may be used in the direct and quick interpretation of the anomalies caused by paleovalleys filled up with loess, a very important step in the complex interpretation of the geophysical anomalies in the North Dobrogea.

Most of the North Dobrogea territory is overlain by loess. The intense geophysical activity carried out in this area in recent years brought into discussion the problem of the disturbing influence induced in almost all geophysical fields by the variation of thickness of the loess accumulations. In particular, this influence on the gravity field is obvious in all very detailed gravity or microgravity maps of Somova-Tulcea (Ciuta, 1978, 1979; Proca, 1980; Maxim, 1981, 1982; Boboc, 1983, unpubl. reports), Iulia (Ciuta, 1973; 1974, 1978, 1979; Ioane, 1975, 1976; Proca, 1980; Maxim, 1981, unpubl. reports) or Turcoaia (Boboc, 1982, unpubl. report) zones.

In fact, the gravity effect of the loess accumulation represents a particular case of the influence of the shallow geological structure which disturbs the geophysical signals that come from deeper zones (Botezatu, 1987). Besides the loess accumulations such a disturbing zone may consist of: laterite accumulations in certain African areas, ice from the permafrost regions, sand and dunes in the deserts, lava flows overlying sedimentary formations etc.

For a correct estimation of the gravity effect several key parameters defining the source have to be known (Romberg, 1958): density contrast, volume, depth, shape and isolation degree. On the other hand, based on the known gravity anomaly and on some of the key parameters, the unknown parameters may be determined, a common process in the physico-geological interpretation of the anomalies.

The present paper is an attempt to elucidate these problems; based on the general features of the sources (depressions filled up with loess) geometrical models have been elaborated and their gravity effect has been computed; finally, templates which connect the defining elements of the sources with the corresponding gravity anomalies have been elaborated.

Considering the physical properties, the loess contrasts with the overlying rocks as regards density, magnetic susceptibility, seismic wave propagation velocity etc.

Loess density is quite low; the average of recent direct determinations is 1.77 g/cm^3; therefore, there is a strong negative density contrast versus any underlying formation. The value of the contrast varies according to the petrographic constitution of the basement whose density ranges from more than 2.80 g/cm^3 (Precambrian amphibolites, Jurassic dolomites) to less than 2.30 g/cm^3 (Turonian sandstones in the Babadag Basin).

In order to determine the shape, depth and extension of the depressions filled up with loess numerous vertical electrical soundings have been carried out in the study area (Balint, 1983; Roşca, 1984, 1985, unpubl. reports). Using the information obtained by vertical soundings and by drillings, maps with the thickness variation of the loess accumulations have been elaborated. After correlation with Bouguer gravity the loess isohypse map was produced (Proca, 1985, unpubl. report).

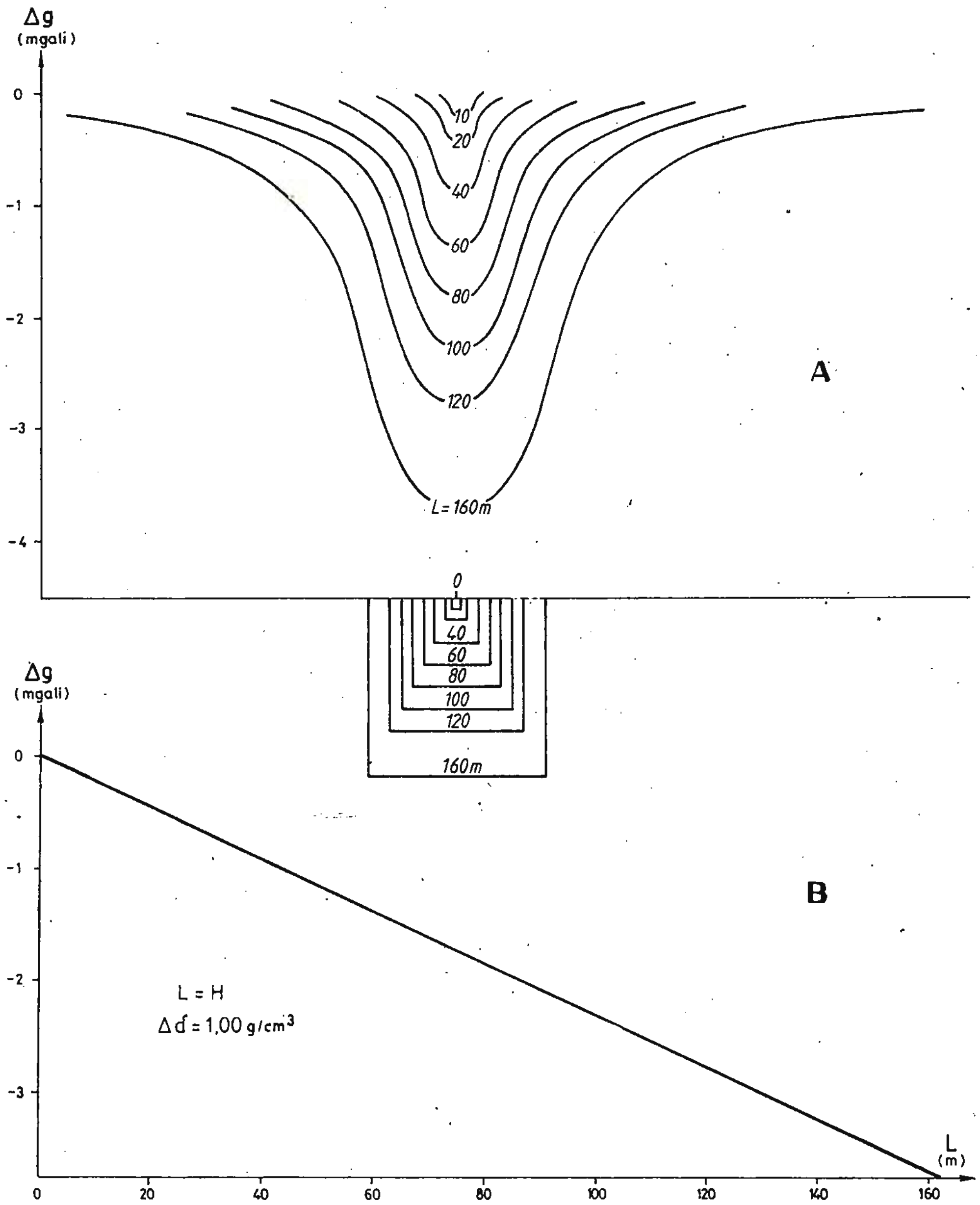

Fig. 1 – Gravity effect of a square bidimensional depression filled up with loess.
A, variation of the anomaly shape; B, variation of the maximum effect as a function of the depression side.

It has a high certainty degree as it incorporates data obtained by three entirely different investigation methods (electrometric, gravimetric, drilling).

This map shows that loess fills up depressions of a relief which existed at the time of its deposition. The paleodepressions have the shape of paleovalleys which quite often follow closely the courses of the present-day valleys; they have tributaries and most of them trend and deepen towards the present course of the Danube. It is of note that these paleovalleys are bidimensional: length reaches several kilometers or tens of kilometers, width rarely exceeds 1–2 km and depth varies between 100 m and 160–180 m. The cross-section of these paleovalleys filled up with loess may be represented geometrically by a square, rectangle, trapezium or even triangle.

To study the gravity influence of such paleovalleys, the gravity effect of several bidimensional geometrical

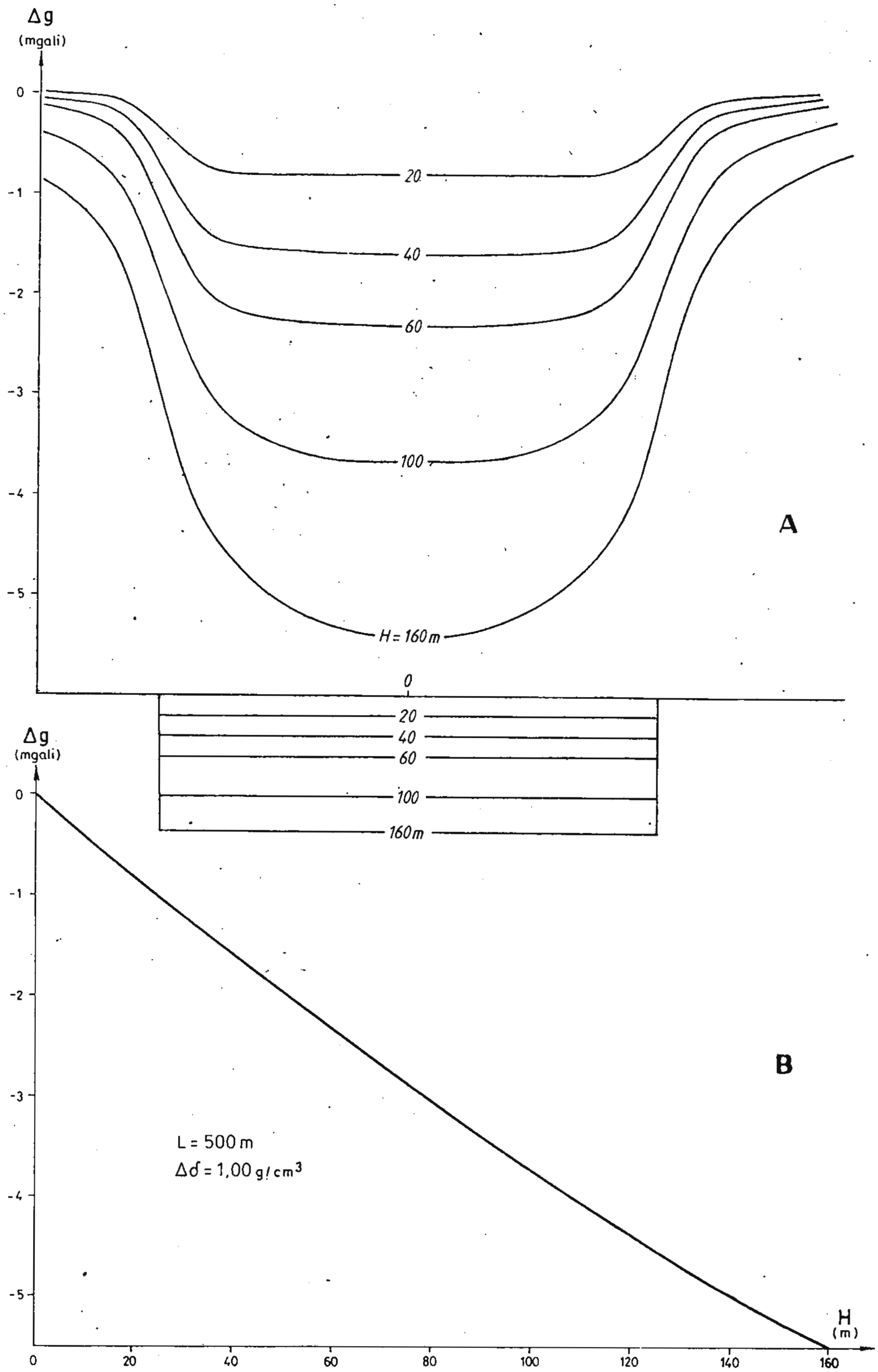

Fig. 2 – Gravity effect of a rectangular bidimensional depression filled up with loess.
A, variation of the anomaly shape; B, variation of the maximum effect as a function of the depression depth.

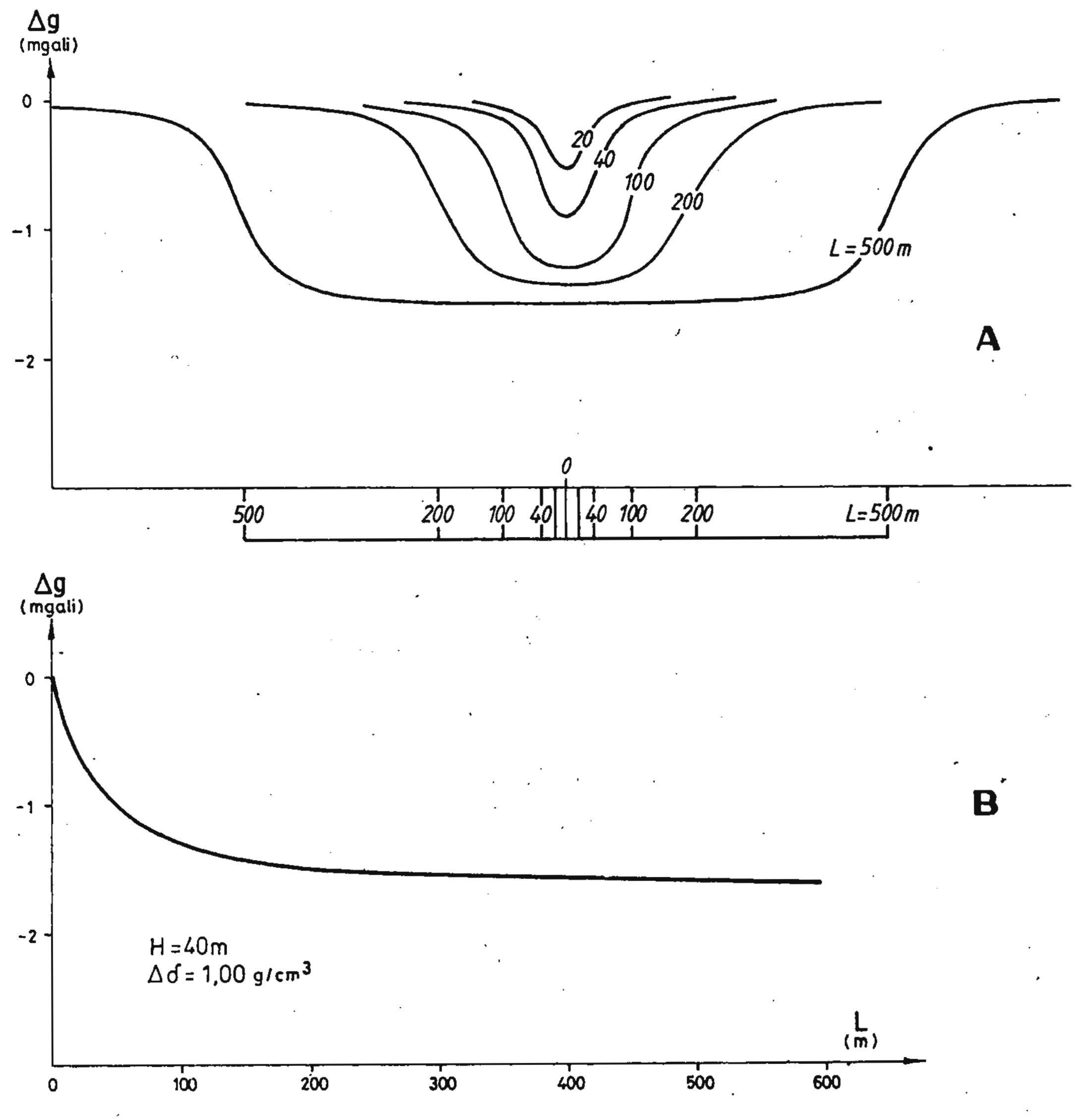

Fig. 3 – Gravity effect of a shallow (H = 40 m) rectangular bidimensional depression filled up with loess.
A, variation of the anomaly shape; B, variation of the maximum effect as a function of the depression width.

models has been computed, observing the changes of different anomaly elements (shape, extension, amplitude, sharpness) as a result of the modifications of the model parameters (shape, depth, width). The density contrast was kept constant and equal to 1.00 g/cm^3.

The calculations have been carried out by means of Talwani methods using a Wang 2000 computer. The results are presented in Figures 1–5 as variation curves of the anomaly shape and of the maximum effect.

For a square depression (Fig. 1) the shape of the anomaly remains the same when the square side varies. Therefore, the anomaly has a characteristic shape with strong gradients above the depression margins. The maximum amplitude varies lineary with the variation of the side dimensions (0.20 mgal at 10 m; 3–7 mgal at 160 m).

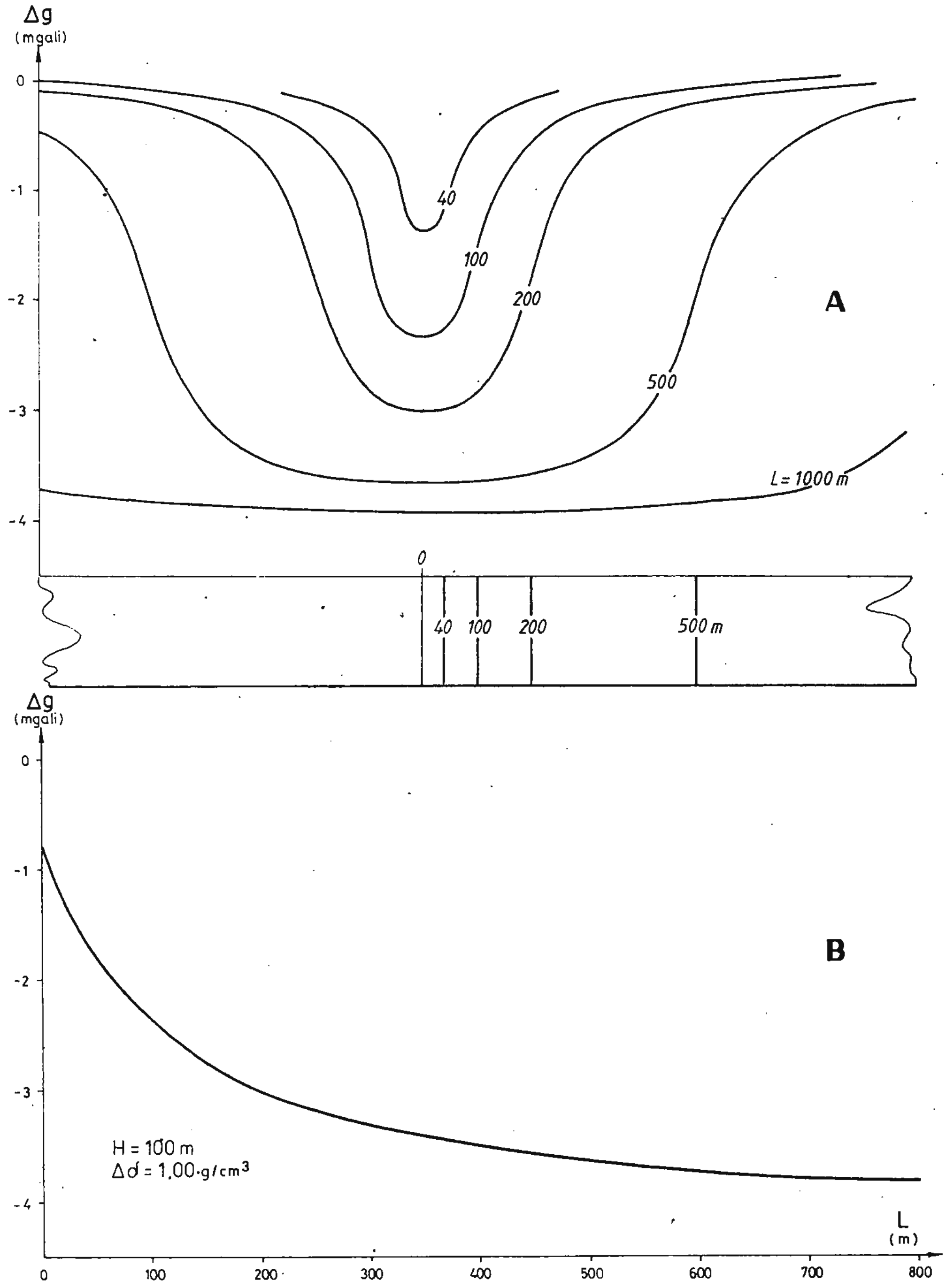

Fig. 4 – Gravity effect of a deep (H = 100 m) rectangular bidimensional depression filled up with loess.
A, variation of the anomaly shape; B, variation of the maximum effect as a function of depression width.

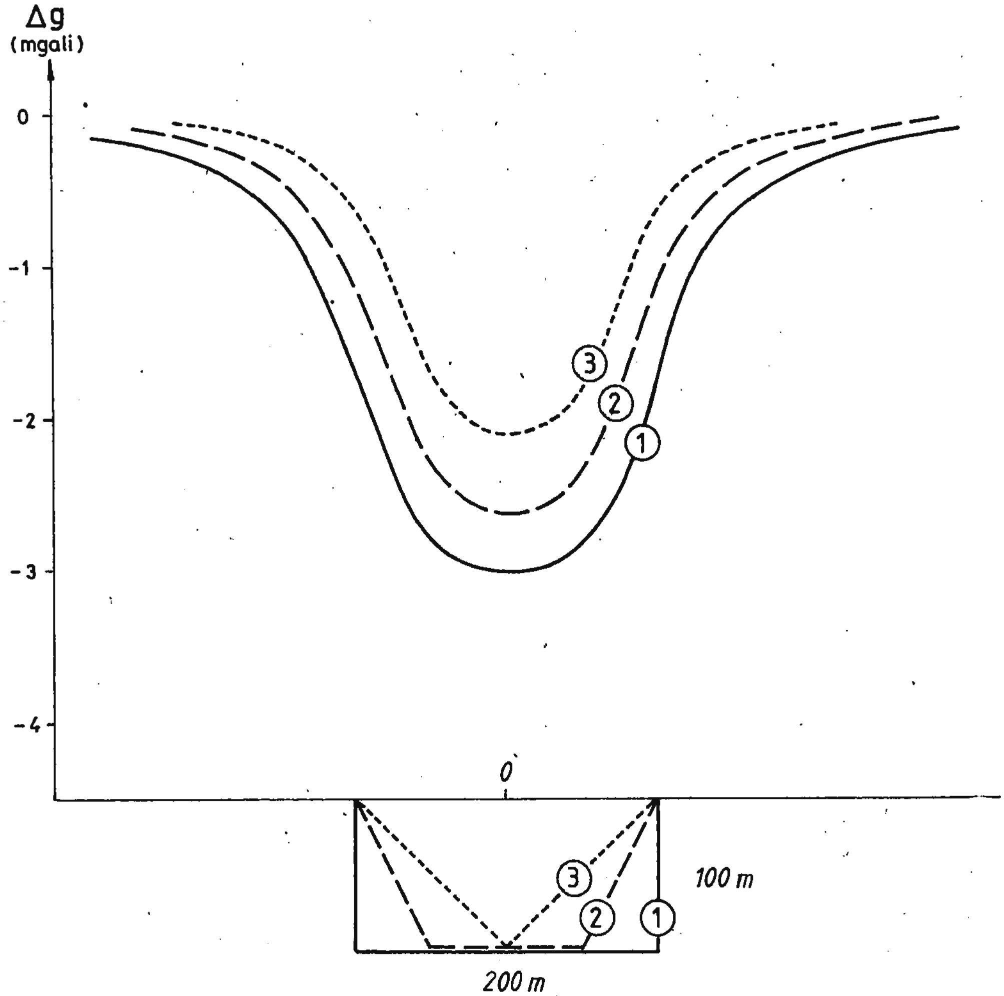

Fig. 5 – Variation of the gravity effect of a depression filled up with loess as a function of the shape of the cross-section.
1, rectangular section; 2, trapezoid section; 3, triangular section.

In case of the rectangular depression gravity effects depend on its width and depth. Figure 2 shows the anomaly modification as the depth varies for a depression with constant width (L = 500 m). It is of note the linearity of the dependence between the maximum effect and the depression depth as well as the characteristic shape of the anomaly: a central part limited by abrupt flanks situated above the depression margins. The central part is well developed if the depth (H)/width (L) ratio is small.

Figures 3 and 4 illustrate the anomaly dependence on the depression width for two constant depths (H). For shallow depth (H = 40 m) the maximum effect in the anomaly axis varies asymptotically with the increase of the depression width (Fig. 3), culminating with the moment when, regardless of the depression width, the maximum effect is practically the same and equal to the effect of an infinite horizontal plate.

The anomaly is sharp for small widths and it becomes flat, with a wide central part, for greater widths of the depression.

Similar conclusions can be inferred from the analysis of a deeper depression (H = 100 m), the absolute values being obviously different (Fig. 4). At a depth of 40 m the maximum effect is of ca 1.6 mgal whereas at 100 m deep the effect is of almost 4 mgal.

Figure 5 represents the anomaly variation concomitantly with the modification of the depression shape, width and depth being constant. The effect of rectangular, trapezoidal and triangular depressions have been calculated as well. The shape of the anomaly changes very little (the value of the flanks gradient changes slightly) but the anomaly amplitude is significantly modified.

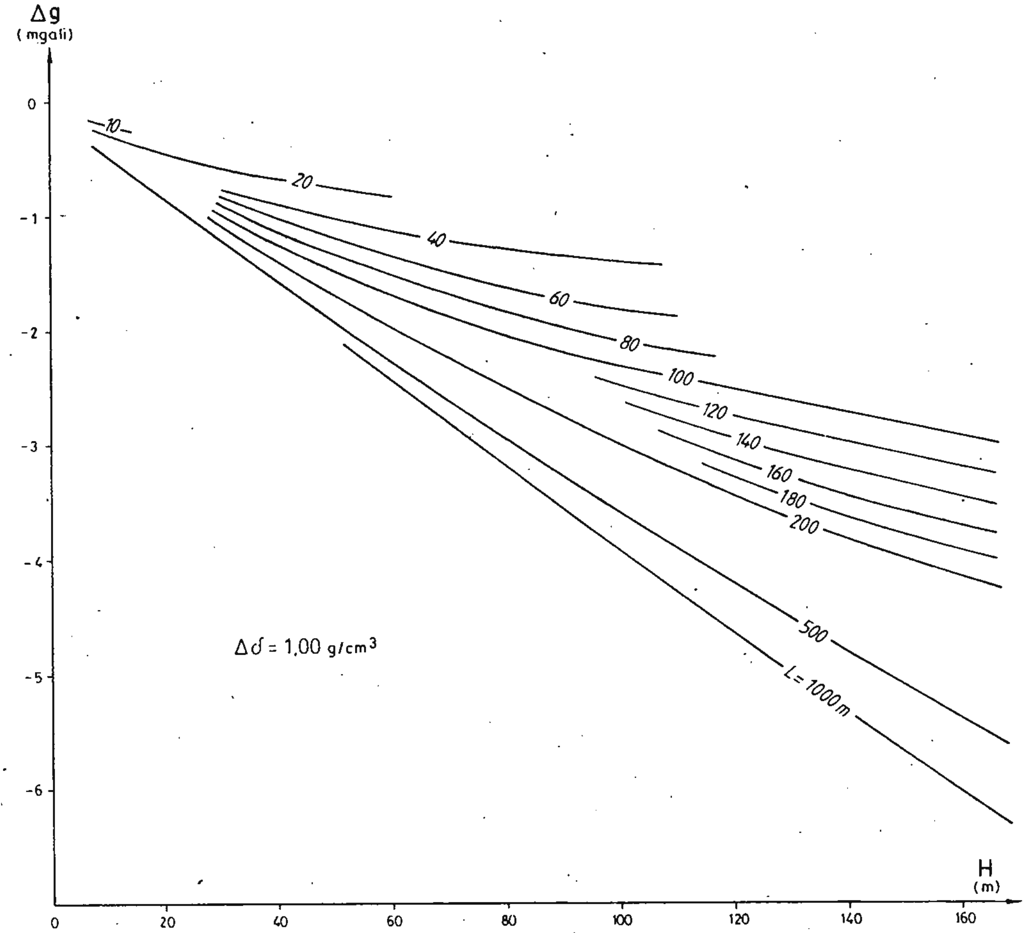

Fig. 6 Template for determining the maximum amplitude of the gravity effect as a function of depth (H) for different widths (L) of a rectangular bidimensional depression filled up with loess.

The last two figures (Figs. 6 and 7) show templates of the variation of the anomaly maximum amplitude as a function of depth H and width L of a rectangular depression for common values.

Figure 6 illustrates the variation depending on the depth H, width L being regarded as a parameter. Their representation can be used for the quick evaluation of the maximum effect for rectangular depressions (up to 160 m deep and 1000 m wide).

Figure 7 represents the variation controlled by width L, in this case depth H being the parameter. The logarithmic scale of the width has been used in order to include the whole interval. This template can be used for the interpretation of gravity anomalies determined by loess. On the gravity map the depression width L can be measured as the distance between the middle of the gradient belts of the anomaly which delimits it. The maximum amplitude Δ g is the difference between the anomaly values in the apex and that at the flanks margins. Introducing the two values (Δ g and L) in the template one can immediately obtain the depression depth (H).

Thus the template can be used in the direct and quick interpretation of the anomalies caused by paleovalleys filled up with loess, a very important step in the complex interpretation of the geophysical anomalies of

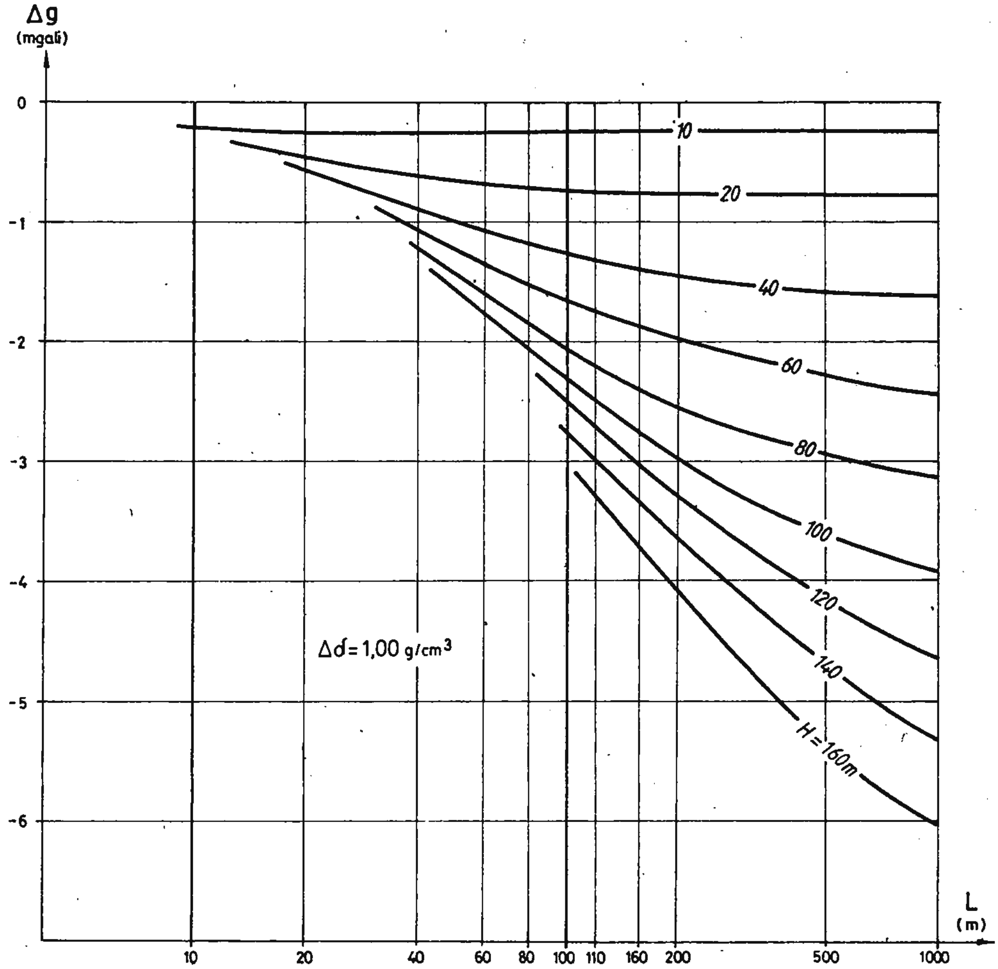

Fig. 7 - Template for determining the depth (H) knowing the width (L) and maximum gravity effect of a rectangular bidimensional paleovalley filled up with loess.

North Dobrogea.

The H values of the paleovalleys depth obtained by the above-mentioned method represent maximum values as the template has been calculated for a rectangular depression and for a relatively high density contrast (1.00 g/cm^3). For more accurate estimations corrections may be applied for the depression shape (Fig. 5) and for the density contrast.

References

Botezatu R. (1987) Bazele interpretării geologice a informaţiilor geofizice. Edit. tehn., Bucureşti.

Romberg F. E. (1958) Key Variables of Gravity. *Geophysics*, 23, 4, Tulsa.

Talwani M., Worzel J. L., Landisman L. (1959) Rapid Computation of Two-Dimensional Bodies with Application to the Mendocino Submarine Fracture Zone. *Journ. Geophys.*, 64, 1, Hague.

Received: September 4, 1989
Accepted: September 5, 1989
Presented at the scientific session of the "Al. I. Cuza" University of Iaşi: October 28, 1989

Rom. J. Geophysics, 1993, 16, p. 45–51

FAULTS IN THE CIUC BASIN DEPICTED BY GRAVITY AND GEOTHERMICS

Amuliu PROCA, Valentin NICOLAU
S. C. "Prospecţiuni" S. A. Str. Caransebeş 1, 78344 Bucureşti 32.

Şerban VELICIU
Institutul de Geologie şi Geofizică. Str. Caransebeş 1, 78344 Bucureşti 32.

Key words: Gravity surveys. Geothermics. Gravity anomalies. Faults. East Carpathians.

Abstract: Integrated interpretation of the gravity and geothermic data obtained in 1988 from a complex survey performed in the Upper Ciuc Basin has indicated the presence of three faults that affect the basin basement and allow the upward circulation of the thermalised waters coming from the depth. The faults manifest themselves by both maximum of gravity horizontal gradient and positive anomalies of temperature measured at a depth of 40 m. The overlapping of the two different types of geophysical anomalies is remarkable.

Introduction

The neovolcanic area of the East Carpathians has been the object of numerous investigations by means of various geophysical methods and techniques used for solving the geological or hydrogeological problems and, more recently, for the identification of geothermal resources.

In the upper Ciuc Depression located between the parallels of Sîncrăieni and Racu villages and surrounded by the Hăghimaş, Ciuc and Harghita Mountains an outstanding coincidence between gravity and geothermic anomalies mapped in 1989 has been observed.

The aim of this paper is to introduce the gravity and geothermic data from the upper Ciuc Depression, their correlation type as well as the geological significance assigned to the superposition of the anomalies of the two fields with different physico-geological background.

Geological setting

The morphological aspect of the region lying between the Călimani-Gurghiu-Harghita neovolcanic chain and the Hăghimaş and Ciuc Mountains is the result of the recent evolution of an area affected by important disjunctive tectonic events. Both the emplacement of eruptive masses and the sinking of the parts belonging to the Central East Carpathians Nappes (Crystalline Mesozoic Zone) and the Outer Dacids (Ceahlău Nappe) led to the formation of post-tectonic depressions at the interior of the East Carpathians. One of these depressions is located on the upper segment of the Olt valley being confined to the north by the crystalline rocks of the Central East Carpathians Nappes and to the south by the Jigodin ridge.

Data supplied by the geological maps of Romania (scale 1:50.000) supplemented with information from Săndulescu (1984), Ştefănescu (1980) and Kusko (1989) led to the following main features of the study area.

The basement of the Ciuc Depression is mostly constituted of the metamorphic formations of the Bucovinian and sub-Bucovinian Nappes, on which patches of sedimentary rocks (Triassic-Lower Cretaceous) belonging to these two tectonic units have been found. On the south-eastern side of the Ciuc Basin, flysch formations of the Ceahlău Nappe constitute the basement.

From the petrographic point of view, within the Bucovinian and sub-Bucovinian Nappes of the study area several metamorphic series have been distinguished, as follows: Bretila Series (gneissic and paragneissic formations intruded by granitoids), Rebra Series (represented by thick terrigene deposits with carbonatic and basic magmatogene rocks), Negrişoara Series (represented by mesometamorphic schists and metavolcanic dacites), Tulgheş Series (comprising mainly terrigene rocks with acid and basic volcano-sedimentary interbeddings metamorphosed in the greenschist facies). These series overthrust each other during the pre-Alpine tectogenesis.

Sedimentary formations of the Bucovinian Nappes, cropping out north-west of Delniţa and in the southernmost part of the Hăghimaş syncline, comprise deposits of Upper Paleozoic (breccias), Lower and Middle Triassic (sandstones, dolomites and limestones), Lower and Middle Jurassic (limestones), Callovian (silts and sandstones), Tithonian-Neocomian (mainly marly limestones) age.

Mesozoic formations of the sub-Bucovinian Nappe crop out north of Tomeşti, in the tectonic window with the same name. They belong to the Lower and Middle Triassic (quartzitic sandstones, dolomites and jaspers) and to the Lower and Middle Jurassic (detrital limestones, black schists and sandstones).

On the eastern margin of the Ciuc Depression, flysch deposits of Tithonian-Lower Cretaceous age were encountered, all of them belonging to the Outer Dacids (Ceahlău Nappe). Within this tectonic window two digitations have been separated: Ciuc, to the west, and Bodoc, to the east.

The western and north-eastern cartographic limits of the Ciuc Basin are constituted not only of the volcano-sedimentary formation but also by the massive andesitic rocks developed in the axial zone of the neovolcanic chain.

Drilling data from the Ciuc Basin indicate that the filling of this depression is mainly formed of aggiomerates with tuffs, gravels and clays interstratifications. Westward, the frequency of extrusive interbeddings (agglomerates or even lava flows) increases resulting in a higher average density for the basin filling. All these deposits belong to the Upper Pliocene, except for a discontinuous basal level with marls and sideritic sandstones referred to the Miocene.

From the hydrogeologic point of view, two aquifers with hydrodynamic inter-relations have been distinguished. The first one is developed within the filling of the depression exhibiting a remarkable permeability. The recharging of this aquifer is acomplished by the meteoric waters as well as by the underground waters from the western prolongation of the volcanics.

A second aquifer is developed within the Cretaceous flysch formations (Sinaia Beds) which are intensely folded and fissured. The recharge takes place either in the outcropping area of the flysch deposits from meteoric water or through the deep faults circulated by the underground waters coming from the depth.

Chemical analyses of the waters from numerous mineralized springs emerging in the region indicated that these springs are supplied by both aquifers. An argument in this respect is the thermalization of some springs which exhibit temperatures ranging from 14 to 27^0 C.

The Ciuc Basin has been subject to many geological surveys by means of practically all measuring techniques. Thus, the regional and local gravity investigations covered the whole neo-volcanic area of the Gurghiu-Harghita Mts (Suceavă, Proca, 1970, unpubl. reports), revealing the gravity anomalies and their correlation with the geological structure. Gravity data made possible the achieving of several generalized models (Proca, 1981; Botezatu, 1987).

In order to depict the structure of the basement Popescu et al. (1963) performed a seismic study. Recently, Stanchievici et al. (1988, unpubl. report) made seismic records and drew up a structural map of the basement on which the position of several faults was indicated.

In the frame of a complex investigation for geothermal resources assessment, apart from gravity and geothermic studies, which are the subject of this work, the magneto-telluric, geoelectric resistivity and self potential surveys were carried out, too (Visarion et al., 1989, unpubl. report). Geological and geophysical exhaustive syntheses were subsequently performed (Ionescu et al., 1985; Visarion et al., 1989, unpubl. report) on the basis of the results obtained from the surveys mentioned above.

Gravity Data

The detailed gravity survey carried out in 1988 covered the middle and upper part of the Ciuc Basin with a network having a station density of 15 stations per sq.km. The primary processing of the field gravity and topographic data enabled to produce the Bouguer gravity map for a density of 2.40 g/cm^3.

As in other intramountainous basins, the gravity anomaly in the Ciuc Basin is strongly dependent of the basement topography because on the one hand its depth is rather small (up to 800 m) and on the other hand a strong density contrast (of over 0.50 g/cm^3) exists on its surface.

Generally speaking, the basin reflects itself in the gravity anomaly as a minimum of over 15 miligals with an asymmetrical shape. The anomaly apex corresponds to the maximum depth area and it lies between the town of Miercurea-Ciuc and the Olt River.

The gravity anomaly has been subjected to secondary analytical processing in order to increase its expressiveness. Thus, the regional/residual analyses were carried out either by the running average method (for various grid sizes) or by applying "geological corrections" by an original method (Proca and Nicolau, 1989, unpubl. report). Very useful proved to be the analysis of statistical correlation between the primary and corrected Bouguer anomalies and the basin depth obtained by drilling data.

A widely accepted fact is that fractures are sources of the step-type structure which produces particular gravity anomalies whose main characteristic is the steep horizontal gradient. The gradient maximum value is situated above the trace of the step.

In order to point out more clearly the gravity effect of the fractures, the total horizontal gradient map of the Bouguer gravity anomaly was calculated and drawn up. In each calculation point the N-S and E-W components of the gradient were determined by simply dividing the differences in gravity to the distance on the two directions. The absolute value of the total gradient resulted as the square root of the squares sum of the two components. Thus, a scalar value results showing only the size of the gradient without its orientation. Although the information referring to the gradient direction in each point is lost (Botezatu, 1986, personal communication), the map obtained by contouring the gradient values contain information on the absolute dimension of this component and implicitly on the positions, sizes and orientations of its maxima.

In the study area, the map of the horizontal gradient of the gravity anomaly (Fig. 1), on which only the contours above 30 E at a spacing of 20 E were traced, shows several maximum alignments which might be interpreted in the above-described manner.

The most conspicuous alignment is the East Miercurea Ciuc-Păuleni-Delniţa-Nicoleşti one, which lies near the eastern side of the Ciuc Basin. It trends almost north-southwards and along it the horizontal gradient reaches values of 70 E in the Şumuleu quarter of the Miercurea Ciuc town and even 90 E at Delniţa. A NE-SW branch of this lineament starts from Şumuleu, goes to the western side of the town, crosses the Miercurea Ciuc resort and continues over the Olt River. Its maximum intensity is 70 E.

South of Miercurea Ciuc, another alignment, less intensive (50 E), is situated at Sîncrăieni and shows a NW-SE trending parallel, in this area, with the Olt River.

Westwards, on the right bank of the Olt, another gradient anomaly is outlined south of Ciceu; it trends north-southward, have intensities around 50 E, but reaches 70 E in the southernmost part where its direction changes. There are two smaller and less intense anomalies north-east of this anomaly. The parallel anomalous alignments with a NE-SW trending mark the flanks of the Racu uplifted block. The outstanding gradient intensities found here (over 110 E) suggest not only the very existence of basement fractures, but also a significant displacement produced by them. In this respect it might be stated that the resolution of the total horizontal gradient map in pointing out the basement faults is better if the faults exhibit a bigger displacement and are shallower. The down or uplifted position of various blocks limited by fractures might be established by correlation with Bouguer map.

East of Miercurea Ciuc two semicircular anomalies of over 70 E can be seen on the horizontal gradient map. They do not mark faults, but rather the borders of the Şumuleu intrusive body which is in a strong mass contrast against its host rocks.

Geothermic data

The regional geothermic data for the Gurghiu-Harghita area (Veliciu, Peter, 1985, unpubl. report) pointed out that the Neogene volcanic area has associated high terrestrial heat flow values ranging from 70 to 118 mWm^{-2}. The amplitude of this regional anomaly decreases slightly from north to south but it shows an important reduction westward (in the Transylvanian Basin) and eastward (in the Crystalline Mesozoic and Flysch zones).

The heat flow values measured in the wells in the Ciuc Basin range from 65 to 70 mWm^{-2}, which correspond to a conductive geothermal gradient of 4.5–5.0^{0}C/100 m (or cca 30–40^{0}C at the depth of 600 m).

A detailed study performed by means of 35 short drill-holes (Veliciu, Zamfir, 1989, unpubl. report) supplied new information on the temperature distribution at the depth of 40 m in the Miercurea Ciuc-Jigodin-Sîncrăieni area. These data have been supplemented with temperature values from observations in 8 wells drilled for mining prospecting between Miercurea Ciuc and Racu.

The temperature maps for the depth of 40 m (Fig. 2) showed the existence of several local positive anomalies surrounding the Miercurea Ciuc town. These anomalies outlined by the geoisothermal line of 12^{0}C (mean annual temperature at the earth surface is 7^{0}C) are located as follows: west of Miercurea Ciuc between Miercurea Ciuc resort and the town limit, south of Miercurea Ciuc near Jigodin and in the Şumuleu district.

A less intense anomaly (14^{0}C) but with a wider extent is situated west of the Olt Valley. Positive anomalous temperature values were recorded north and south, respectively, of Racu.

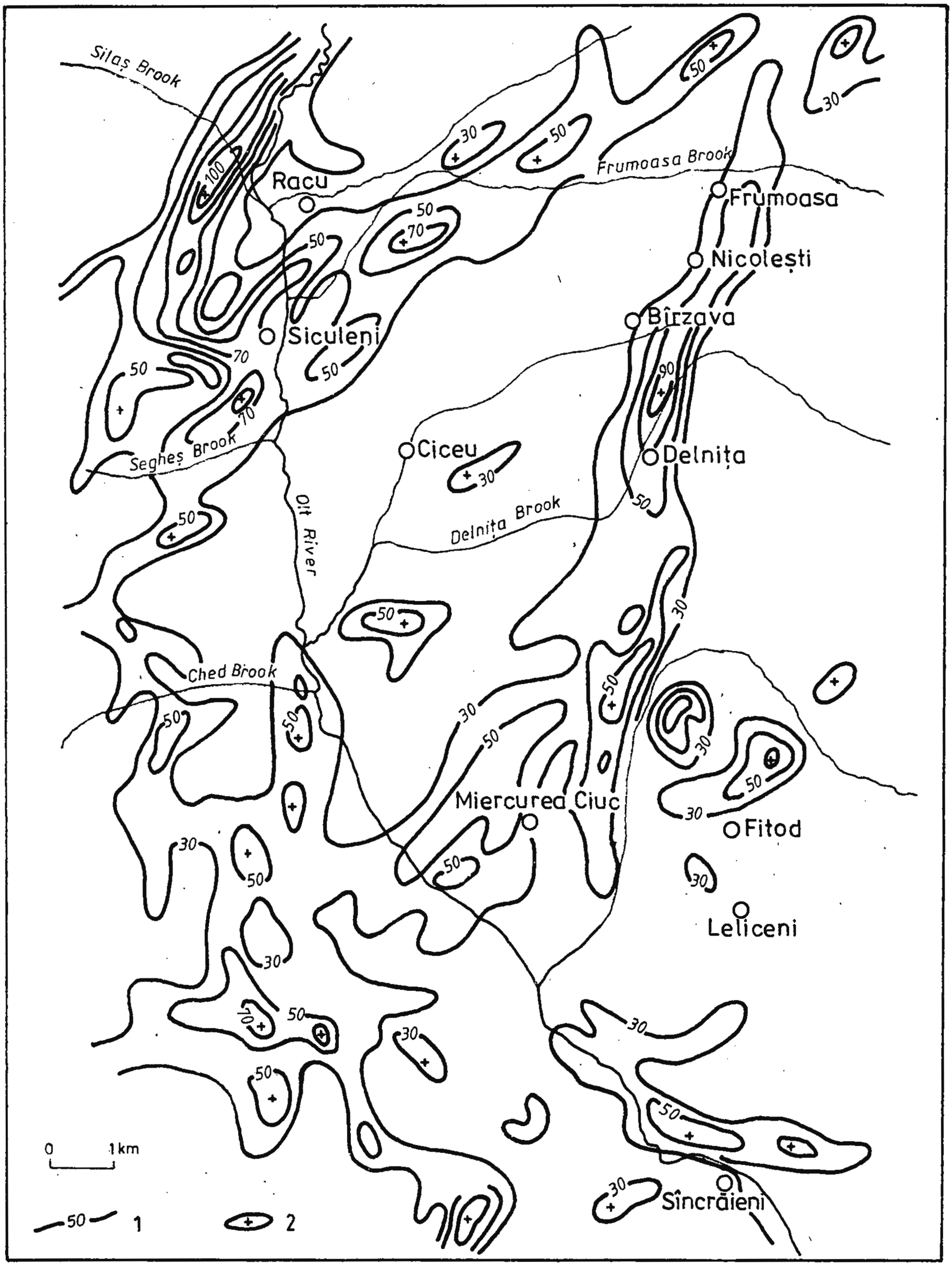

Fig. 1 - Horizontal gradient of the gravity anomaly map in the Upper Ciuc Basin. 1, horizontal gradient contour for 20 Eötvös interval; 2, maxima of horizontal gradient.

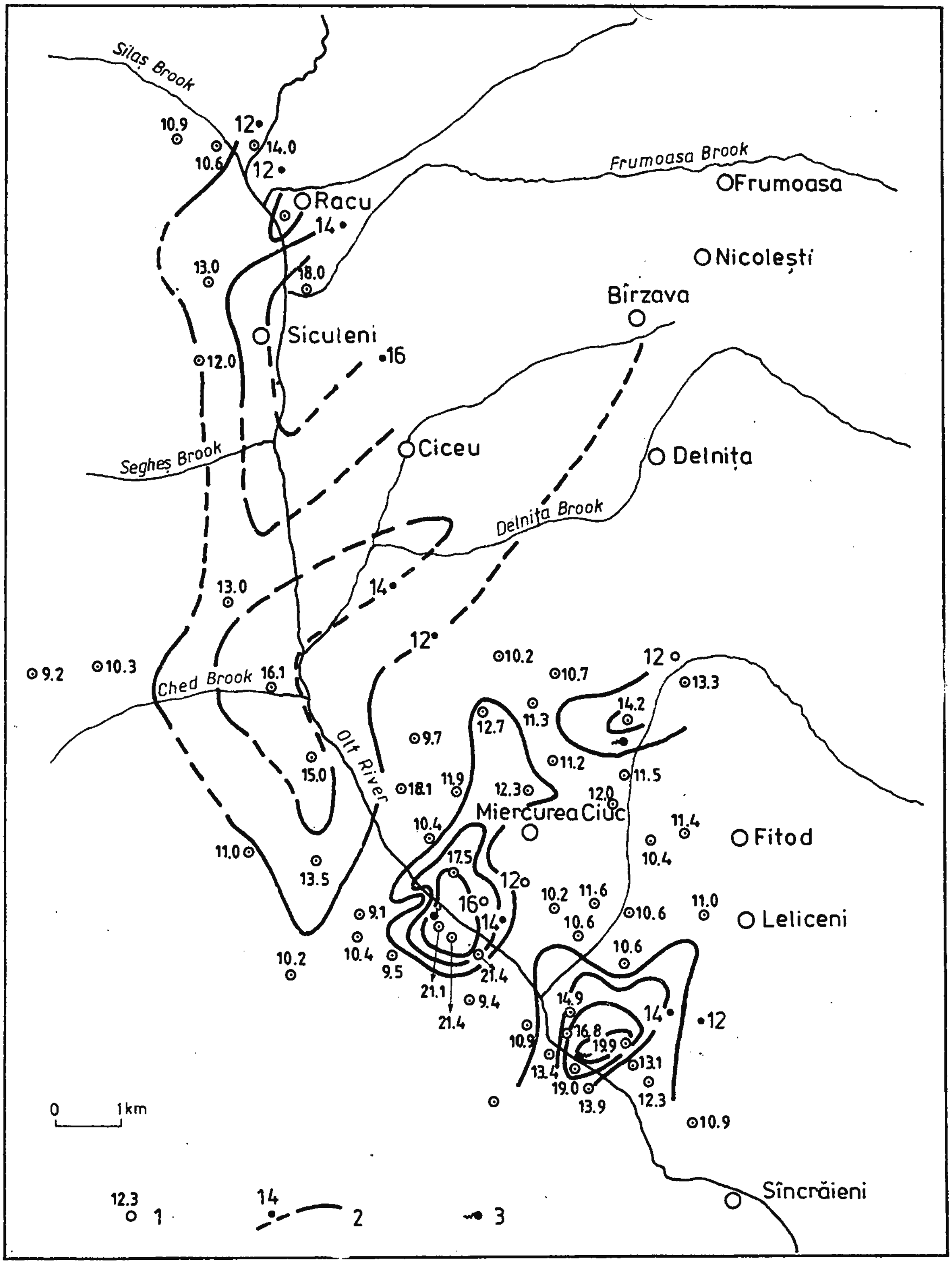

Fig. 2 - Temperature distribution map at a depth of 40 m in the Upper Ciuc Basin: 1, geothermic drill hole and measured temperature at a depth of 40 m; 2, geoisothermal line; 3, thermal emergence.

Integrated interpretation of gravity and geothermic data

The analysis of both gravity data (horizontal gradient of the Bouguer anomaly) and of geothermic data (temperature at 40 m deep) shows a good correlation between two types of anomalies: the maxima of temperature measured in shallow drill-holes are superimposed on the horizontal gradient maxima.

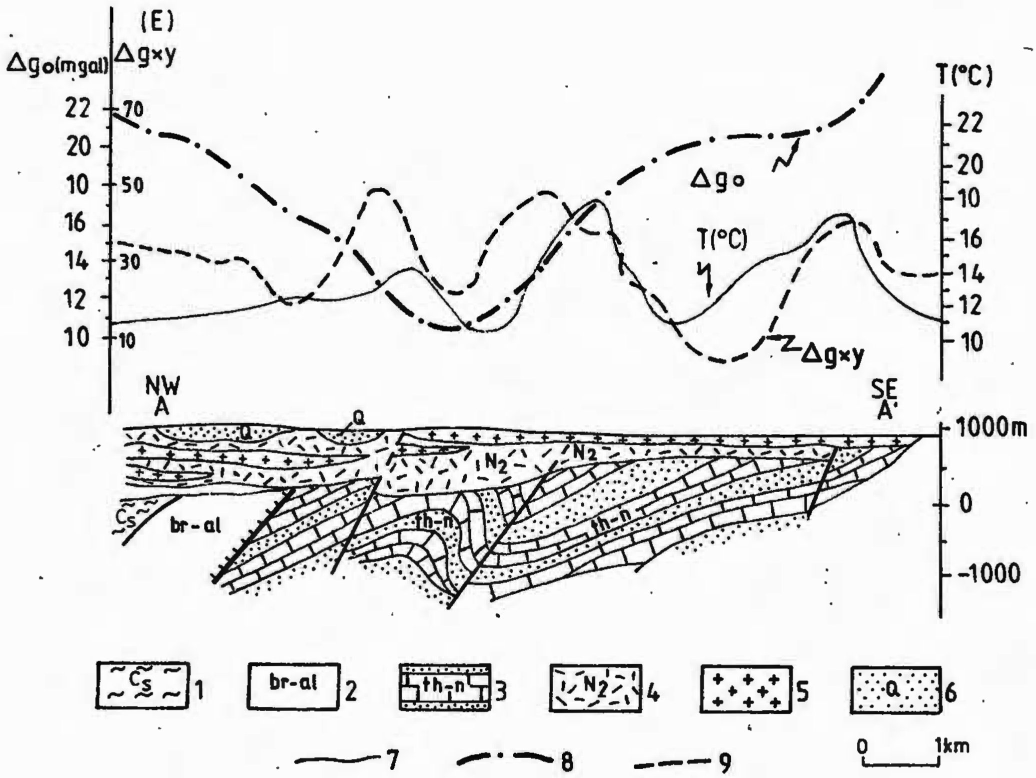

Fig. 3 – Geological cross-section (M. Ştefănescu, 1988), gravity and geothermic profiles in the Upper Ciuc Basin: 1, Bretila Series; 2, Wildflysch formation (Barremian-Albian) from the Bucovinian Nappe; 3, Sinaia Beds (Tithonian-Neocomian); 4, volcano-sedimentary formation (Upper Pliocene); 5, andesitic lavas; 6, Quaternary deposits; 7, temperature profile; 8, Bouguer anomaly profile; 9, horizontal gradient profile of the gravity anomaly.

Such a correlation is obvious around Miercurea Ciuc where the most important geothermic anomaly, that of Miercurea Ciuc resort, is superposed on the NE-SW gradient alignment that passes west of the city. The anomaly from the Şumuleu district superposes the East Miercurea Ciuc-Păuleni-Delniţa-Nicoleşti alignment whereas the Jigodin geothermic anomaly lies on the NW-SE Sîncrăieni-Jigodin alignment.

Although the superposition is obvious the temperature anomalies do not follow the gradient anomalies on their entire length but they are rather situated preferentially on zones where such alignments intersect themselves. It is worth mentioning that the apexes of the two types of anomalies are not always in the same place.

Accepting that the gravity anomaly gradients are generated by displacements caused by faults at the basement level and that the geothermic anomalies are generated by circulation towards the surface of the thermalized waters coming from the depth, it results that the two geophysical methods show two complementary features of the same tectonic element.

Moreover, the fact that the directional extension of the two types of anomalies are not equal (the gradient alignment being usually longer) proves that the fractures pointed out by gravity are not circulated on all their length but rather preferentially on zones where two or more fractures intersect.

The differences in the location of the anomaly apexes may give indications on the dipping of the fault planes: the geothermic anomaly shows the shallow trace (down to 100 m) of the fracture plane whereas the gravity gradient corresponds to the step at the basin basement level (several hundreds of metres). The dip of the fracture may be seen by joining the two traces on a transverse cross-section (Fig. 3).

In the study area, the majority of fractures dip westward; this observation is confirmed by the geological mapping.

Finally, the combined analysis of the two geophysical fields points out that the geothermic anomalies do not correspond to all gravity gradient anomalies. This may be caused by the lower density of the geothermic observation points (about one drill-hole per 2-3 sq.km.) or by the fact that not all the faults are circulated by thermalized fluids or because of the decrease of the initial temperatures during the upward circulation, or even because the faults are not permeable enough to allow a fluid circulation.

Conclusion

The gravity and the geothermic surveys in the Ciuc Basin area have contoured superposed anomalies. Although they have a different physico-geological background, they show two complementary aspects of the same tectonic element, namely faults.

The gravity data expressed by the horizontal gradient of the Bouguer anomaly show sharp displacements caused by faults at the basin basement level. The geothermic anomalies (temperature at 40 m, measured in drill holes) point out zones where there is an upward circulation of thermalized waters coming up from depth.

The traces of fractures affecting both the basin basement and its filling sediments have been outlined by the correlation of the gravity and geothermic data. The most important faults are those which form a triangle around Miercurea Ciuc town and which intersect themselves at Miercurea Ciuc resort, Jigodin and Şumuleu. Thermalized waters from depth circulate upward through these faults, preferably at their intersection. They are probably the most promising areas for economic development of geothermal waters in this region.

References

Botezatu R. (1987) Bazele interpretării geologice a informaţiilor geofizice. Edit. tehn., Bucureşti.

Ionescu Fl., Polonic P., Teodorescu Vl. (1985) Structura adîncă a ariei ocupate de vulcanitele neogene din zona munţilor Călimani-Gurghiu-Harghita. *St. cerc. geol., geofiz. geogr., Geofizică*, 23, p. 44–52, Bucureşti.

Proca A. (1981) Modele fizico-geologice de interpretare a anomaliilor gravimetrice din munţii Harghita de Nord. *St. tehn. econ.*, D, 13, Bucureşti.

– , Nicolau V. (1989) The separation and significance of a regional gravity anomaly in the Ciuc depression. *Rev. roum. géol., géophys. géogr., Géophys.*, 33, p. 95–100, Bucarest.

Săndulescu M. (1984) Geotectonica României. Edit. tehn., Bucureşti.

Suceavă M., Proca A. (1970) Prospecţiuni gravimetrice în munţii Gurghiu şi Harghita de Nord. *Stud. tehn. econ.*, D, 7, p. 89–106, Bucureşti.

Visarion M., Săndulescu M., Atanasiu L. (1988) An improved geotectonic model of the East Carpathians. *Rev. roum. géol., géophys. géogr., Géophys.*, 32, Bucureşti.

Veliciu S. (1987) Geothermics of the Carpathian area. *An. Inst. Geol. Geofiz.*, 67, p. 81–116, Bucureşti.

– , Visarion M., Ghenea C., Peltz S., Opran G. (1983) Assessment of the geothermal resources of the Harghita-Gurghiu Mountains (East Carpathians). *An. Inst. Geol. Geofiz.*, 63, p. 292–301, Bucureşti.

Received: December 14, 1989
Accepted: December 15, 1989
Presented at Geological Symposium organized by IPEG Harghita at Miercurea Ciuc: September, 1–3, 1989.

Rom. J. Geophysics, 1993, 16, p. 53–58

UN MODÈLE GRAVIMÉTRIQUE DE LA DOBROGEA

Vlad ROŞCA, Ligia ATANASIU

Institutul de Geologie şi Geofizică. Str. Caransebeş 1, 78344 Bucureşti 32.

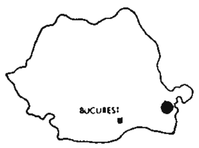

Key words: Gravity surveys. Gravity anomalies. Gravity field. Three-dimensional models. Physical models. Simulation. Dobrogea.

Abstract: *A Gravimetric Model of Dobrogea.* A configuration of straight rectangular prisms has been used to reproduce the major regional anomalies known in Dobrogea. Based on the modelling process the whole morphology of the gravity field can be explained by density contrasts situated on the first 5 km of the crust. Elements of a deep-seated basic eruptive structure and of an E-W trending zonation in Central Dobrogea has also been obtained.

Introduction

Les levés gravimétriques régionals et sémirégionals, effectués dans la Dobrogea entre les années 1950 et 1965 ont évidentié les principaux traits structuraux reflétés dans l'anomalie de la gravité, pratiquement en même temps ou à une courte période après l'achèvement des respectifs travaux.

Morphologiquement, la Dobrogea est une région faiblement élevée, qui émerge des terrains alluvionnaires de la Plaine Roumaine, du Delta du Danube, ainsi que des sédiments du plateau continental de la Mer Noire. Les investigations géologiques et géophysiques à caractère régional ont relevé le fait que cette région est partagé par deux unités tectoniques majeures: l'Orogène nord dobrogéen et la Plate-forme Moesienne, la limite entre les deux unités étant marquée par la ligne de chevauchement de Peceneaga-Camena. Le domaine moesien de la Dobrogea est traversé par une importante dislocation, la ligne de Capidava-Ovidiu qui sépare le domaine des schistes verts ou la Dobrogea Centrale de la Dobrogea Méridionale. La signification géologique des images gravimétriques correspondantes tant aux deux lignes majeures de chevauchement qu'au principaux éléments structuraux présents dans l'unité dobrogéenne aussi, a été relevé par les auteurs mêmes des cartes qui comportent ces images.

Ainsi, pour l'Orogène nord-dobrogéen on a évidentié la signification du minimum intense et à un large développement, situé surtout dans le territoire de l'unité de Tulcea et attribué à une dépression synclinale majeure du fondement cristallin développée dans tout le territoire de la Dobrogea septentrionale (Botezatu et al., 1961). Les lignes de maximum qui entourent ce minimum ont été, à leur tour, attribuées à certains "plis anticlinaux du soubassement cristallin". Même si de nouveaux modèles tectoniques apportent des correctifs à cette formation, ainsi que des correctifs de détail imposés par l'enrichissement de l'information pétrophysique, on peut affirmer que l'étude susmentionnée a attribué déjà à certaines roches paléozoïques et prépaléozoïques denses, trouvées en position élevée, le rôle de source des maximums gravimétriques régionales de la Dobrogea septentrionale.

Ainsi, pour la Dobrogea Centrale les schistes verts denses sont reconnus comme responsables pour le contraste de masse engendrant la large anomalie de maximum développée vers le plateau continental (Airinei, 1967; Botezatu, Băcioiu, 1957).

Dans la Dobrogea méridionale l'interprétation des données gravimétriques a été concentrée notamment sur la zone de Palazu Mare (Visarion et al., 1979), mais des certaines références recouvrent une zone plus large au sud de la ligne de Capidava-Ovidiu, en remarquant l'effet de l'épaississement de la couverture mésozoïque (Băcioiu, 1957; Botezatu, 1982).

On a présenté sommairement les interprétations données jusqu'à présent à la carte gravimétrique régionale de la Dobrogea pour mentionner dès le début que le modèle proposé par nous ne peut pas apporter des éléments essentiels nouveaux. Mais il favorise la mise en discution de certains traits structuraux profonds sur la base des informations quantitatives fournies par le processus de modélisation même.

Le modèle proposé a un caractère tridimensionnel, c'est à dire il essaie de reproduir à l'aide d'une configuration de masses prismatiques, des anomalies à caractère isométrique en général. Pour calculer l'effet cumulé de la configuration de prismes on a utilisé un programme de calcul automatique écrit en langage Fortran IV. Le calcule a été effectué dans un réseau carré avec le côté de 10 km. Cette dimension a été adoptée en accord avec le degré relativement réduit de fidélité qui peut être exigé d'un modèle à une géométrisation prohibitive et en accord avec le fait qu'on a eu pour but la reproduction d'une carte gravimétrique régionale.

Pour réaliser le modèle on a adopté comme hypothèse de travail la limitation des contrasts de densité responsables pour la présence des anomalies gravimétriques cartographiées sur le territoire de la Dobrogea, à une zone superficielle de la croûte, épaisse de 5 km. L'hypothèse s'apuie sur l'intégration des informations sur la densité, la telluroélectrométrie, la sismométrie et la géologie.

Des données sur la densité

Les informations sur la densité sont synthétisées dans le diagramme de la planche I, qui nous offre une image du paramètre respectif pour les principaux lithotypes connus dans les affleurements et forages de la Dobrogea. Il est nécessaire de souligner que l'information pétrophysique provient de la surface ou d'une faible profondeur. Par conséquent, dans l'investigation de la structure profonde l'utilisation de ces données doit être faite sous la reserve d'importantes transformations que celles-ci puissent subir dans les conditions de gisement profond. Pour les schistes verts et la série des schistes mésozoïques d'Altın-Tepe le diagramme met en évidence une difference qui peut atteindre 0,10 g/cm^3 entre la densité observée dans les affleurements et sur les carottes extraites des profondeurs de jusqu'à 1700 m.

Pour évidencier les contrastes pétrophysiques importants pour l'étude de structure profonde, on doit remarquer dès le commencement une certaine uniformité dans le sens que tant les roches cristallines et éruptives de l'unité de Măcin, que les carbonatites de l'unité triasique aussi, présentent des densités rapprochées dans la Dobrogea septentrionale, les contrastes importants se réalisant au compt des densités plus faibles des formations jurassiques (flysch de Nalbant et de Denis-Tepe). Des faibles densités ont été enregistrées aussi dans les formations siluriennes et les schistes cristallins de la colline de Horia et la colline de Rediu, mais le degré avansé d'altération supergène de ces roches conduit à l'attribution d'une signification réduite à la valeur obtenue pour les lithotypes mentionnés. Des densités plus réduites sont attribuées aux magmatites acides triasiques. En contraste de densité faiblement négatif avec la masse des roches paléozoïques et prépaléozoïques se trouve aussi la formation de Carapelit et le Dévonien de l'unité triasique. Les densités les plus élevées rencontrées dans la Dobrogea septentrionale, chose à prévoire d'ailleurs, caractérisent les magmatites basiques triasiques.

Dans la Dobrogea Centrale, tant les schistes verts que les schistes mésozonaux d'Altîn-Tepe aussi, ont des densités supérieures par rapport à la plupart des roches paléozoïques et prépaléozoïques de la Dobrogea septentrionale, étant comparables avec la série de Palazu Mare de la Dobrogea Méridionale. Cette dernière réalise, à son tour, un contraste de densité positif avec les gneiss basaux sous-jacents, ainsi qu'avec toutes les formations plus jeunes surjacentes.

Pour la Dobrogea Méridionale on peut remarquer aussi quelques contrastes de densité, le plus important étant, certainement, celui engendré par la disposition de la couverture de roches terrigenes et carbonatées quaternaires, caïnozoïques et mésozoïques non affectées tectoniquement, au-dessus du socle paléozoïque et prépaléozoïque à une tectonique compliquée et peu connue (Paraschiv et al., 1983). Bien que ce contraste arrive jusqu'à 0,5 g/cm^3, la disposition quasi-horizontale de sa surface d'existence nous empêche de lui attribuer une signification importante dans la détermination de la morphologie du champ de la pésanteur observée.

Pour la morphologie de la carte gravimétrique de la Dobrogea Méridionale nous considérons essentiels les rapports densimétriques entre les divers types paléozoïques et prépaléozoïques. Ces rapports sont évidentiés par les données publiées (Visarion et al., 1979), ainsi que par les déterminations effectuées sur les échantillons prélevés de l'affleurement et sur les carottes renfermées dans la lithothèque[1]. Dans ces conditions on doit considérer comme seul contraste de densité certe celui observé entre les dépôts carbonifères pélitomorphes et les carbonatites de la formation de Călăraşi (dévonienne), qui est supérieur à 0,1 g/cm^3, en faveur de ces dernières. Pour les quelques échantillons où nous croyons d'avoir reconnu le grès quartzeux de Smirna et les argilites de Ţăndărei (dévoniennes) on retient seulement des densités inférieures par rapport à celles des roches paléozoïques susmentionnées. Avec quelques reserves on retint aussi la valeur de 2,71 g/cm^3 pour les schistes verts.

[1] La détermination litho-stratigraphique d'après Gh. Vasilescu et C. Dragomirescu, 1977; V. Carp et Gh. Pitulea, 1985, données nonpubl.

Données télluroélectrométriques, sismométriques et géologiques

Une information extra-gravimétrique considérée importante, conduit vers la délimitation du modèle proposé à la profondeur de 5 km. Cette information est fournie par la section des résistivités électriques obtenues par la méthode des courants télluriques le long d'un profil qui traverse la Dobrogea orienté NNE-SSV (Stănică, 1987).

La section géoélectrique mentionnée met en évidence des variations de la résistivité obtenues par la méthode des courrants telluriques tant dans la Dobrogea Centrale que dans celle Septentrionale aussi, jusqu'à la profondeur de 5 km. Les facteurs pétrophysiques qui déterminent les variations de la résistivité électrique diffèrent des ceux qui déterminent les variations de la densité. Pour les profondeurs prises en considération la micro et la macroporosité ensemble avec la résistivité des fluides qui occupent les espaces poreux, jouent un rôle primordiale pour la résistivité électrique apparente. La microporosité, qui diminue jusqu'à des valeurs négligeables à travers les premiers deux à trois kilometres de profondeur, même dans le cas des roches jeunes, peut jouer un rôle moins important pour la densité, la composition minéralogique devenant décisive à des profondeurs plus grandes. Malgré cela, au moins comme hypothèse de travail, nous considérons qu'on peut accepter une corrélation entre les limites majeures résistivimétriques et densimétriques, surtout s'il s'agit d'une macroporosité qu'on peut, dans une première approximation, considerer comme équivalente au degré de tectonisation. Ainsi, la section tellurométrique de la Dobrogea a été adopté comme argument en faveur de la limitation du modèle gravimétrique à la profondeur de 5 km. Vers la meme profondeur conduisent aussi les observations géologiques effectuées dans la Dobrogea centrale (Mirăuţă, 1969), qui indiquent pour toute la formation des schistes verts une épaisseur de 5000 m. Nous considérons aussi que l'onde continue réfractée dans la Dobrogea centrale (Constantinescu, Spînoche, 1967) peut être interprétée comme l'expression de la homogénéité des schistes verts au moins jusqu'à la profondeur de 5 km. La présence des formations cristallophyliennes à des propriétés élastiques similaires à celles des schistes verts, sous la profondeur mentionnée, ne serait pas infirmé par les observations sismométriques citées.

Dans la Dobrogea méridionale nous savons seulement qu'on se trouve dans la présence d'un développement du Paléozoïque vers la limite méridionale du territoire, pour lequel on a pu élaborer, a l'aide des données de forage, une coupe synthétique correspondant à une colonne de 3000 m (Paraschiv et al., 1983).

En ce qui concerne la Dobrogea septentrionale, les données des courants telluriques, ainsi que les considérations d'ordre géotectonique suggèrent, au contraire, l'existence des certains contrasts de densité à des profondeurs dépassant les 5 km. La faille de Peceneaga-Camena, évidentiée au N du Danube comme déterminant un affaissement de jusqu'à 6 ou 7 km (Constantinescu et al., 1970; Constantinescu et al., 1972) du compartement au niveau de la surface de Conrad et à la base de la croûte, constitue évidemment la source de quelques effets gravimétriques qui s'ajouttent à ceux engendrés par des néhomogénéités trouvés au dessus des limites susmentionnées. La valeur de ces effets profonds étant réduite par rapport aux effets des contrastes de densité des premiers 5 km, on a considéré qu'un premier modèle tridimensionnel peut être limité à la profondeur déjà mentionnée.

Le modèle

Nous avons abordé ce modèle tridimensionnel par l'intermède d'un profil orienté N-S, situé dans la partie est de la Dobrogea (fig. 1). On a réalisé le long de ce profil un modèle gravimétrique tridimensionnel intégré par la méthode Talwani (Talwani et al., 1959), pour lequel les coupes géologiques d'où on est parti ont été celles qui accompagnent les cartes à 1:200.000 publiées par l'Institut de Géologie, ainsi que la carte du soubassement préjurassique de la Dobrogea méridionale publiée par Paraschiv et al. Ce modèle bidimensionnel a constitué une première confirmation du fait que l'anomalie de Bouguer sur le territoire de la Dobrogea, peut être réproduite à l'aide de quelques contrastes de densité placés dans l'interval des premiers 5 km de la croûte et a indiqué en même temps la corrélation entre les contrastes de densité offerts par les déterminations sur les échantillons et ceux acceptés par le modèle gravimétrique.

Pour réaliser le modèle on a juxtaposé, initialement, un nombre réduit de prismes grandes correspondant aux anomalies principales. On a attribué aux prismes des densités compatibles aux données pétrophysiques, en modifiant les densités jusqu'on a obtenu les amplitudes des variations extrêmes présentes sur la carte observée. Dans cette étape on a déterminé aussi la densité unique (2,55 g/cm^3), attribuée aux zones limitrophes au modèle. Après avoir obtenu cette première approximation nous avons détaillé le modèle par la division des prismes appartenant à cette première approximation dans les deux sens verticale et horizontale. Parallèlement aux transformations spatiales du modèle on a effectué aussi les modifications des densités exigées soit par la correspondance du nouveau arrangement géométriques à des formations bien déterminées densimétriquement, soit seulement par la morphologie du champ anomal observé.

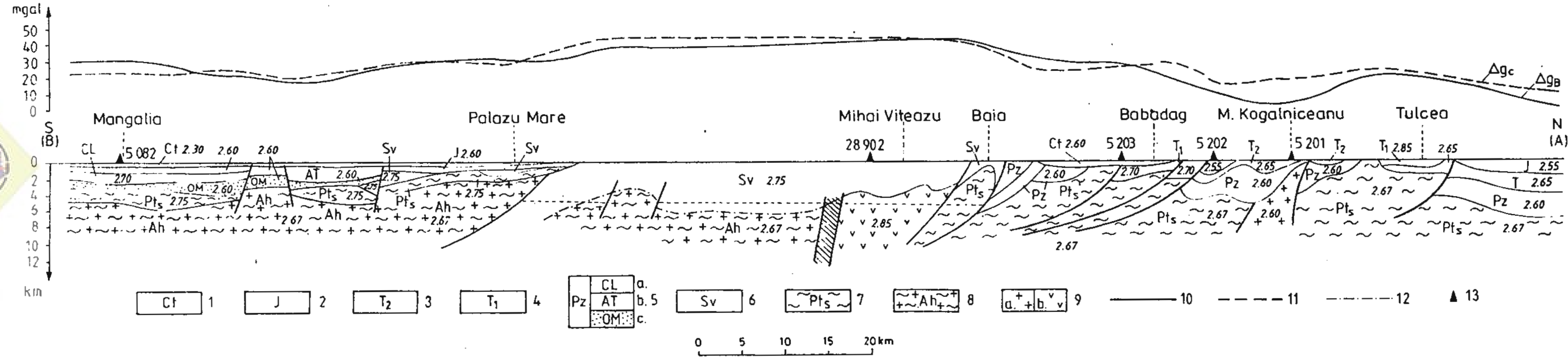

Fig. 1 – Modèle gravimétrique le long du profile Tulcea-Baia-Palazu Mare-Mangalia.
1. Cretacé; 2. Jurasique; 3. Triasique supérieur; 4. Triasique supérieur et moyen; 5. Paleozoïque: a. Série de Călăraş; b. argilites de Ţăndărei; c. orthoquartzites de Mangalia;6. Cambrien, Infracambrien; 7. Protérozoïque supérieur: séries de: Orliga, Megina, Boclugea, Altîn Tepe, Palazu Mare; 8. Archaïque, série gneissique; 9 a. granites; 9 b. métamorphites basiques; 10. Anomalie gravimétrique observée; 11. Anomalie gravimétrique calculée; 12. Limite de résistivité éléctro-tellurique (d'après D. Stănică, 1987); 13. Forages.

Tenant compte du but proposé, ce processus de modelage s'est arrété à la douzième itération, en obtenant le résultat présenté dans la carte annexée (Pl. II).

Cette carte comporte tant des isolignes du champ gravitationnel de modelage, aussi bien que des isolignes appelées "de qualité" du modèle, et qui représentent des isolignes de la difference d'entre l'anomalie observée et celle calculé pour le modèle tridimensionnel auquel nous nous sommes arrêtés.

En observant ces isolignes de qualité on constate que le modèle comportant des prismes reproduit les anomalies observées avec une approximation de jusqu'à 30% de l'amplitude de celles-ci, la déviation maximum se situant dans la zone de minimum nord-dobrogéen. Pour la plupart du territoire les déviations sont de l'ordre de 10%, les meilleures correspondances étant observées dans la zone de l'unité de Măcin, dans la Dobrogea centrale, ainsi que dans la zone du minimum gravimétrique de la Dobrogea méridionale. Implicitement, du point de vue physique la fiabilité du modèle est plus grande pour les zones susmentionnées. Les significations géologiques de ce fait résultent de la correspondance densité-lithofaciès attribuée à chaque prisme-modèle en partie.

Pour l'unité de Măcin, l'existence de diverses roches, à des densités compatibles à celles des roches précambriennes et paléozoïques connues à la surface, jusqu'à la profondeur de 5 km, peut constituer l'indice d'une allochtonie réduite de cette unité. Au contraire, la qualité faible du modèle pour le territoire de l'unité de Tulcea, où pour les prismes qui devraient modeler le minimum central on a adopté une densité inférieure à celle connue pour les roches de la surface, indique l'existence d'une structure plus compliquée, à sources d'anomalie trouvées à des profondeurs de plus de 5 km.

Pour la Dobrogea centrale le modèle tridimensionnel constitue le support physique de l'emplacement de la source du maximum de Sinoe à l'intérieur des schistes verts. Cette source peut être identifiée à l'aide de la densité, avec un important massif de roches erruptives basiques métamorphosées. La partie supérieure de ce massif serait situé à une profondeur de 2700 m et sa conformation le place suivant les directions disjonctives majeurs (les failles de Peceneaga-Camena et Capidava-Ovidiu). Dans la zone centrale le massif présente aussi un développement selon une direction perpendiculaire sur celle des lignes tectoniques majeures.

On doit mentionner qu'au nord de la faille de Peceneaga-Camena, dans la zone lagunaire, se situe un maximum pour lequel le modèle indique, aussi, des densités compatibles avec les roches erruptives basiques. L'avancement d'une liaison structurale avec le massif de Sinoe est, cependant, hasardé et en tout cas en dehors des modèles géologiques conçus dans le cadre des connaissances actuelles.

Toujours pour la Dobrogea centrale le processus de modelage a conduit à l'identification d'un compartiment nord-occidental (à l'ouest de la ligne de Topolog -ouest Băltăgeşti) à une densité inférieure à celle retenue pour les schistes verts percés par les forages du nord et de l'est. Jusqu'à présent nous ne disposons pas de données géologiques corrélables avec ce résultat de la modélisation physique.

Dans la Dobrogea méridionale le modèle tridimensionnel suggère la présence, dans la zone de Cobadin, d'une dépression comportant des roches paléozoïques à densité réduite, compatibles avec celles percées par le forage 3 Dobromiru (cité à l'occasion de la présentation pétrophysique), ainsi qu'avec celles attribuées aux formations terrigènes dévoniennes.

Conclusions

De l'interprétation quantitative de la carte gravimétrique de la Dobrogea, a résulté un modèle géométrisé comportant 34 prismes. Celles-ci correspondent à des divers volumes de roches considérées homogènes quant à la densité. Le modèle réalisé est, par essence, correlable avec tous les éléments structuraux majeurs de la Dobrogea. On peut signaler cependant 3 éléments que le modèle gravimétrique tridimensionnel met en discussion:

1 – La présence, dans la zone centrale de l'unité de Tulcea, au moins à travers les premiers 5 km, de diverses roches moins denses que celles connues à la surface;

2 – La présence, dans la zone de Sinoe, d'un massif eruptif basique profond, située à une profondeur de plus de 2700 m. Pour le développement du maximum de Sinoe au nord de la faille de Peceneaga-Camena, suggéré par le modèle, on ne peut pas donner une interprétation géologique en accord avec les connaissances actuelles. On signale seulement cette extension comme simple observation;

3 – Dans la partie occidentale de la Dobrogea centrale on a séparé un compartiment à dénsité inférieure à celle spécifique des schistes verts des zones centrale et orientale.

Jusqu'à présent on ne dispose pas des connaissances géologiques qui puissent donner une signification lithofaciale ou structurale à cette séparation.

Note. Les auteurs remercient les collegues Gabriela Cucu et Gheorghe Ionescu pour l'assistence accordée dans l'utilisation des programmes de calcul automatique.

Bibliographie

Airinei St., Stoenescu Sc., Velcescu G. (1966–1968) Harta gravimetrică a R. S. R., sc. 1:200.000. σ=2.67 g/cm^3. Foile: 38 Tulcea (L-35-XXIX), 39 Sulina (L-35-XXX), 45 Călăraşi (L-35-XXXIV), 46 Constanţa (XXXV), 50 Mangalia (K-35-V).

– (1967) Cupluri de anomalii gravimetrice-magnetice deschise pe litoralul românesc al Mării Negre. *St. cerc. geol. geofiz., geogr., Geofizică*, 5, 1, Bucureşti.

– , Botezatu R. (1977) Contribuţii geofizice la cunoaşterea geologică a Dobrogei. *St. cerc. geol., geofiz., geogr., Geofizică*, 15, p. 13–17, Bucureşti.

Băncilă I. (1958) Geologia Carpaţilor Orientali. Edit. Ştiinţifică, Bucureşti.

Botezatu R., Băcioiu Tr. (1957) Anomalia gravităţii în Dobrogea centrală. *Bul. ştiin., Acad. R.P.R., Secţ. geol. geogr.*, 2, 2, p. 237–252, Bucureşti.

– , Băcioiu Tr., Andrei J. (1961) Relaţiile dintre anomalia gravităţii şi structura geologică a Dobrogei de Nord şi a regiunilor limitrofe din Moldova de Est. *St. cerc. geol.*, VI, 1, Bucureşti.

– (1971) Sur la nature de certaines anomalies gravimétriques dans les régions à dépôts carbonates épais de Roumanie. *Acta Geol. Acad. Sci. Hung.*, 15, p. 351–356, Budapest.

– (1982) Modele geofizice ale alcătuirii geologice a României. Edit. Acad. R. S. R., Bucureşti.

Constantinescu P., Spânoche S. (1967) Unde continuu refractate şi unde de schimb P. S. P. în înregistrările seismice din Dobrogea centrală (zona şisturilor verzi). *Stud. cerc. geol., geofiz., geogr., Geofizică*, 5, 2, Bucureşti.

– , Spânoche S., Scurtu Fl. (1970) Utilizarea undelor seismice continuu refractate pentru stabilirea distribuţiei de viteze în Dobrogea Centrală. *Stud. tehn. econ.*, D, 7, Inst. Geol., Bucureşti.

– , Cornea I., Enescu D., Pătruţ St., Rădulescu Fl., Spînoche S. (1970) Evaluations préliminaires de l'épaisseur de la croûte terrestre sur le territoire de la Roumanie. *Rev. roum. géol., géophys., géogr., Géophys.*, 14, 1, p. 3–14, Bucarest.

Constantinescu L., Cornea I., Enescu D. (1972) Structure de la croûte terrestre en Roumanie d'après les données géophysiques. *Rev. roum. géol., géophys., géogr., Géophysique*, 16, 1, p. 3–20, Bucarest.

Dumitrescu I., Săndulescu M., Lăzărescu V., Mirăuţă O., Pauliuc S., Georgescu C. (1962) Mémoire à la carte tectonique de la Roumanie. *An. Com. Geol.*, 32, p. 5–97, Bucureşti.

Gavăt I., Airinei St., Botezatu R., Socolescu M., Stoenescu Sc., Vencov I. (1963) Structura geologică profundă a teritoriului R. P. R. după datele actuale geofizice (gravimetrice şi magnetice). *Stud. cerc. geofiz.*, 1, 1, p. 7–34, Bucureşti.

Mirăuţă O. (1969) Tectonica Proterozoicului superior din Dobrogea centrală. *An. Inst. Geol.*, XXXVII, p. 7–36, Bucureşti.

Paraschiv D., Dăneţ N., Popescu M., Dumitrescu V. (1983) The present stage of the pre-jurassic deposits knowledge in South Dobrogea. *An. Inst. Geol. Geofiz.*, LIX, Bucureşti.

Săndulescu M. (1984) Geotectonica României. Edit. tehn., Bucureşti.

Stănică D. (1987) Contribuţii la descifrarea structurii geologice profunde a Platformei Moesice prin metoda curenţilor telurici. Teză de doctorat. Universitatea din Bucureşti.

Talwani M., Worzel J. L., Landisman M. (1959) Rapid gravity computations for three-dimensional bodies with application to the Mendocino submarine fracture zone. *Jour. Geophys. Res.*, 64, 1, p. 49–59.

Visarion M., Maier O., Nedelcu I. C., Alexandrescu R. (1979) Modelul structural al metamorfitelor de la Palazu Mare, rezultat din studiul integrat al datelor geologice, geofizice şi petrofizice. *Stud. cerc. geol., geofiz., geogr., Geofiz.*, 17, 1, p. 95–113, Bucureşti.

– , Săndulescu M., Stănică M., Veliciu S. (1988) Contributions à la connaissance de la structure profonde de la Plate-forme Moesienne en Roumanie. *Stud. tehn. econ.*, D, 15, p. 211–222, Bucureşti.

Received: June 9, 1989
Accepted: June 12, 1989
Presented at the XIV-th Symposium of Earth's Physics and Applied Geophysics: July 2, 1987

DIAGRAMME DE LA DISTRIBUTION DES DENSITÉS DES PRINCIPAUX LITHOTYPES DE LA DOBROGEA

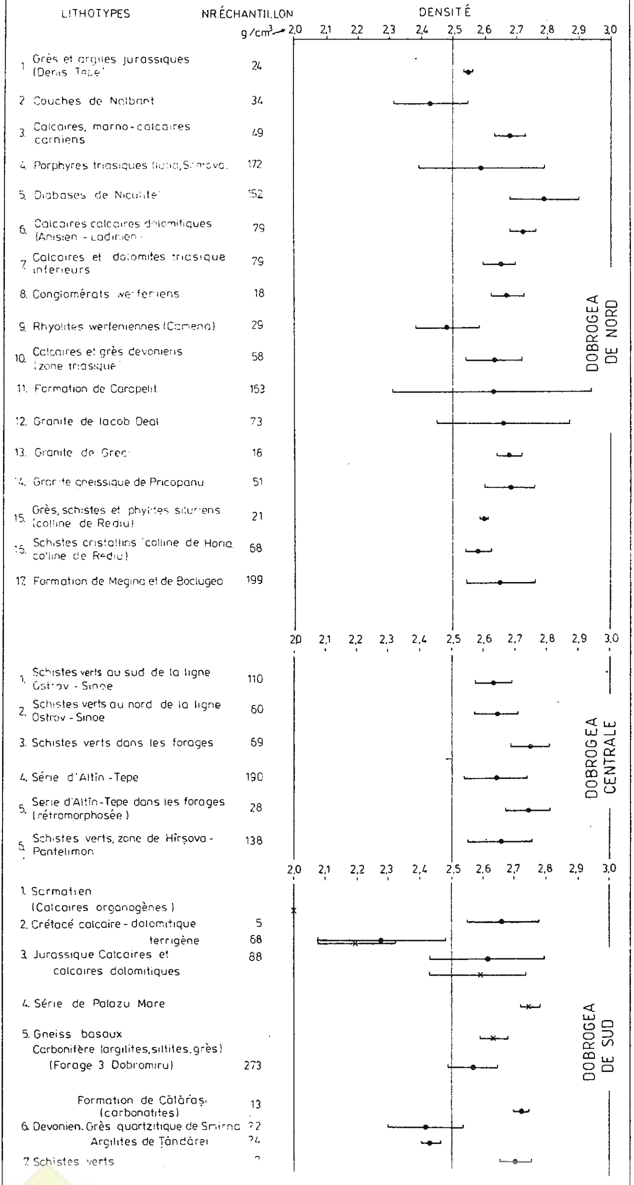

Rom. J. Geophysics, 1993, 16, p. 59-66

SOURCE OF THE CĂZĂNEŞTI-CUIAŞ GRAVITY ANOMALY IN THE DROCEA MOUNTAINS OPHIOLITES (MUREŞ ZONE) AND ITS METALLOGENIC IMPLICATIONS

Haralambie SAVU, Justin ANDREI
Institutul de Geologie şi Geofizică. Str. Caransebeş 1, 78 344 Bucureşti 32.

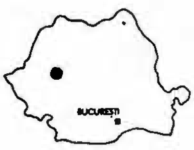

Key words: Gravity anomalies. Magnetic anomalies. Ophiolite. Gabbro. Mineralization. Apuseni Mountains.

Abstract: In the Liassic ophiolite megaslab of the Mureş Zone (Drocea Mts) there are several major gravity anomalies, e.g. the high gravity anomaly (25 km long) lying between Căzăneşti and Cuiaş. This anomaly is determined by the north-eastern segment of a deep-seated dyke of gabbroic and peridotitic rocks intruded parallel with the sheeted dykes of the ophiolitic complex (O_2). Its apophyses are represented by the Căzăneşti, Almăşel and Cuiaş gabbroic bodies which contain liquid-magmatic concentrations of vanadiferous Ti-magnetite. Along the gravity anomaly two metallogenic fields with hydrothermal mineralizations have been separated: a cupriferous field and a pyrite one. For detailed information on the structure of the anomaly zone, the petrographic constitution of the great deep-seated dyke (about 500 m) and on the metallogenic implications a structural borehole has to be drilled.

Introduction

In the Liassic ophiolites (180 Ma, Herz et al., 1974) in the Drocea Mts occurs a major high gravity anomaly (Andrei, 1964, 1969; Andrei et al., 1970, unpubl. reports) lying between Căzăneşti and Cuiaş (Plate). As numerous occurrences and major iron and sulphide concentrations occur along this anomaly, we considered of interest a study on the source of this anomaly and on the characteristics of the different mineralization types situated in the area. Data concerning the mineralizations included in the gravity anomaly zone are provided by reports and papers published by Socolescu (1944), Cioflică (1962), Popescu et al. (1969, unpubl. report), Corbu et al. (1969), Gheorghiţescu (1970), Savu (1954, 1962, 1963, 1974, 1986), Savu et al. (1988 a, 1989), Andrei et al. (1984), as well as in other materials in the archives of I.G.G., I.P.G.G. and I.F.L.G.S. of Bucharest.

Origin and position of the Mureş Zone ophiolites

As mentioned earlier (Savu, 1983; Savu et al., 1987) the Liassic ophiolites in the Mureş ophiolitic suture (Mureş Zone) represent vestiges of an ocean crust megaslab obducted from the Mureş Ocean on the convergent tectonic plates from the north (Apuseni Mountains Plate) and from the south (Transylvanian Plate) during the Upper Jurassic and the Neocomian. At present the tectonic plates are collided under the ophiolitic slab of about 3000 m thick in this western part of the Mureş Zone (Fig. 1). According to this model, concomitantly with the beginning of the bilateral subduction and the closure of the Mureş Ocean (Savu, 1983, 1990) in the ophiolitic suture area the eugeosyncline stage settled, during which the Late Kimmerian calc-alkaline volcanism manifested along two island arcs and began the Tithonian-Neocomian flysch sedimentation. The Late Kimmerian volcanics and the flysch unconformably overlie the ophiolite megaslab. Due to the Mesozoic tectonic movements the flysch deposits, the Late Kimmerian volcanics and their allochthonous ophiolitic basement have been folded, overthrust and then faulted. Thus, several tectonic units occur, some of them including an ocean crust slab torn off from the mentioned ophiolitic megaslab.

The major tectonic unit including the largest mass of Liassic ophiolites in the base is the Căpîlnaş-Techereu Unit, separated by Lupu (1975). It has formed at the end of the Neocomian and extends on the whole length of the Mureş Zone, from south of Lipova up to north-east of the Trascău Mts (Savu, 1983, 1990). Nowadays in the Mureş Zone occur the remains of the initial ophiolitic suture. To the south-west, in the connection zone with the Sumadia ophiolitic suture (Serbia), the Alpine formations of the Mureş ophiolitic suture have been entirely eroded, so that at present only the suture or collision line between the two convergent plates is preserved. Consequently, Bleahu's theory (1989) referring to four subduction planes cannot be sustained because all the Alpine ophiolites occur in an obducted position.

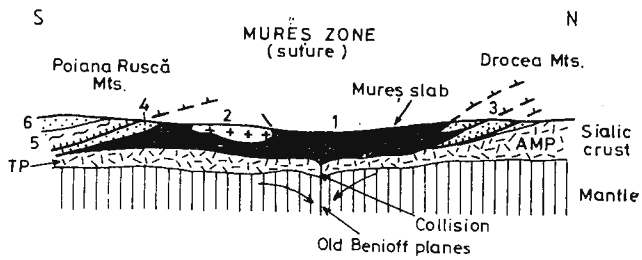

Fig. 1 Model for the position of the Liassic ophiolitic megaslab in the Mureş suture and its modifications after obduction (after Savu et al., 1987, completed).
1, Mureş ophiolitic megaslab; 2, volcanics from the southern volcanic arc; 3, Tithonian-Neocomian flysch deposits with Late Kimmerian volcanics from the northern island arc, including the Barremian-Aptian and Senonian deposits in the northern imbricated marginal area of the Mureş Zone, included into the Criş, Groşi and Highiş-Drocea units; 4, Barremian-Aptian deposits; 5, Tisa Unit; 6, Laramian volcanics and Tertiary deposits in the Lăpugiu basin; TP, Transylvanian Plate; AMP, Apuseni Mountains Plate.

There are two more opinions concerning the tectonic position and the origin of the Mesozoic eruptive rocks in the Mureş Zone. Thus, Cioflică et al. (1980) and Lupu et al. (1990) presumed a unilateral subduction from the east and the ocean floor Liassic ophiolites and the Late Kimmerian volcanics would represent products of an arc volcanism, manifested on the Apuseni Mts sial. Another model (Stănică et al., 1989, unpubl. report) presents the tectonic position of the Alpine ophiolitic rocks in the Mureş Zone and the presumed suture line of this zone, starting from a unilateral subduction from west-north-west. The authors of the two above-mentioned opinions have not taken into account that within the Mesozoic eruptive rocks ("ophiolites") in the Mureş Zone they include both the Liassic ophiolites – ocean floor rocks – and the Late Kimmerian island arc volcanics, rocks series which present different geochemical and petrophysical characteristics.

Gravity and aeromagnetic anomalies in the Drocea Mts and their causes

The westernmost part of the Techereu-Căpîlnaş Unit as well as its westward prolongation masked by Neogene deposits of the Pannonian Basin have been prospected gravimetrically in a detailed network (Andrei, 1964, 1965, unpubl. reports) and aeromagnetically in a research (Cristescu et al., 1964, unpubl. report) and detailed network (Cristescu et al., 1972, unpubl. report). The petrophysical study of the formations occurring in this areal have been carried out either on the occasion of gravimetric prospectings, or within geophysical and geological-geophysical synthesis papers (Andrei, 1969; Andrei et al., 1970; Andrei, Bălan, 1978; Andrei et al., 1979; Andrei et al., 1984, unpubl. reports).

The ocean floor and island arc magmatic rocks show a significant excess of the magnetic intensity in comparison with the crystalline basement formations and of their cover of Mesozoic deposits. Consequently, the aeromagnetic images reflect very well the location of the Căpîlnaş-Techereu Unit. Usually, the structural aspects of this unit are better cleared up based on gravity images than on magnetometric ones due to a more homogeneous distribution of the density of different magmatic lithotypes of their magnetic intensity.

The main components of the ocean floor magmatic rocks show the following bulk densities: basalts - 2.82 g/cm^3; tachylites and amygdaloid basalts - 2.70 g/cm^3; basaltic pyroclastics - 2.60 g/cm^3; dolerites - 2.88 g/cm^3; gabbros - 2.90 g/cm^3. Therefore, the basic intrusive bodies show an excess of density and mass in comparison with the adjacent volcanics and they can be rendered evident by gravity highs.

The Late Kimmerian island arc volcanics (andesite and basalt flows - 2.65 g/cm^3; their pyroclastics - 2.55 g/cm^3) display generally a significant mass deficit as compared to the subjacent ocean floor rocks. Consequently, the thickening zones of calc-alkali volcanics determine gravity lows. Also by gravity lows are emphasized the Late Kimmerian island arc granitoid intrusions which penetrate the ocean floor rocks due to the significant deficit of density achieved.

The magnetization intensity of different types of Mesozoic magmatic rocks which constitute the Căpîlnaş-Techereu Unit show quite large variations due to the ununiform distribution of the ferromagnetic minerals (especially magnetite). For this reason sometimes no significant differentiations occur between the average values of the magnetization intensity in different types of rocks, the intraformational contrasts being more important. Such contrasts are determined by the initial distribution of magnetite but particularly by the effect of the postmagmatic processes. In the first case the excess of magnetization of the Ti-magnetite

(χ = 10000–50000 μ CGS units) versus diopside gabbros (χ = 50–500 μ CGS units) has to be mentioned.

The postmagmatic alterations (autometamorphic and hydrothermal) locally determine a decrease of the magnetite content in the magmatic rocks by sulphidization or, in our case, especially by oxidation with martite formation. Other autometamorphic processes, such as uralitization or certain forms of chloritization determine an increase of the initial magnetite content in the magmatic rocks by the oxidation of the iron released as a result of pyroxene alteration. Such processes (especially uralitization) which determine the formation of secondary magnetite seem to be more active at the periphery and in the vicinity of the basic intrusive bodies as well as around the Late Kimmerian or Laramian arc granitoid intrusions which penetrate the ocean floor magmatic rocks. These considerations make possible a better understanding of the particularities of the aeromagnetic anomalies in the western segment of the Căpîlnaş-Techereu Unit.

The Cuvejdia-Bruznic-Juliţa-Corbeşti-Vorţa-Techereu-Presaca Ampoiului regional aeromagnetic anomaly, sigmoidal flattened in shape, extending WSW- ENE on about 135 km and about 25 km wide, is determined by the ocean floor and island arc magmatic rocks of the Căpîlnaş-Techereu Unit. The respective anomalous source was defined in the past as "The ophiolitic trench of the Metaliferi Mts" (Andrei, 1969, unpubl. report; Andrei et al., 1975); at present it is known as the Mureş ophiolitic suture (Savu et al., 1987) or the Mureş Zone (Savu, 1983). First of all, this regional anomaly specifies the concealed western and eastern extension of the Căpîlnaş-Techereu Unit. Also by its morphologic particularities the Cuvejdia-Corbeşti-Presaca Ampoiului regional anomaly attests the tectonic relationships of the Căpîlnaş-Techereu Unit with the Groşi, Criş and Bucium units of the Mureş Zone and suggests a significant southward sinking of the magmatic rocks from the Căpîlnaş-Techereu Unit (Cristescu et al., 1964, unpubl. report; Andrei, 1969, unpubl. report; Andrei in Borcoş et al., 1987, unpubl. report etc.) below the Tisa Unit (Savu et al., 1988 b) (Fig. 1).

In the westernmost segment of the Căpîlnaş-Techereu Unit two major gravity highs are found: (1) Vîrful Măgurilor-Troaş-Juliţa-Bruznic-Labaşinţ; (2) Căzăneşti (Tătăroaia Valley)-Almăşel-Corbeşti-Cuiaş and one gravity low; (3) Bunea Mică-Ardeu.

(1) The major western gravity high, trending NE-SW, north of the Mureş, and ENE-WSW, south of it, presents a lenght of about 55 km, a width of 10 km and an intensity of about 15 mgal. This major gravity high is determined by the dolerite and gabbro masses from the Juliţa-Vîrful Măgurilor and south of Bruznic (Andrei, 1964, 1965) situated in the sheeted dyke complex (Savu in Savu et al., 1979, 1981) west of the considered region. Within this major gravity high the aeromagnetic images show a complicated anomalous regime. Thus, generally speaking, at the periphery of the major gravity high, aeromagnetic high are found and in the axial zones at Juliţa-Ţela-south of Ohaba Română and south of Bruznic negative anomalies are observed. The magnetic highs mentioned above are probably determined especially by the uralitization processes. The aeromagnetic lows at Juliţa and south of Bruznic can be partly assigned to some gabbroic bodies with a low magnetite content and partly to martitizations, possibly sulphidizations of the basic magmatic rocks determined by autometamorphic and hydrothermal alterations (Andrei et al., 1979, unpubl. report).

(2) The eastern major gravity high Căzăneşti (Tătăroaia Valley)-Almăşel-Corbeşti-Cuiaş-south of Valea Mare (Plate), which is described in this paper, has a NE-SW trending; it is about 25 km long, about 4 km wide and has an intensity of 5 mgal. This gravity high is determined by a gabbroic intrusive mass unitary at depth (Andrei, 1964, 1969; Andrei et al., 1973, 1979, unpubl. reports). The gabbroic bodies of Almăşel, Corbeşti, Cuiaş and Valea Mare represent culminations of the deep-seated intrusive mass. The axis of the major gravity high Almăşel-Cuiaş is closely correlated with an alignment of aeromagnetic high mapped by a detailed network. It is only in the area of the Cuiaş gabbroic body that the gravity high axis is situated on an aeromagnetic low, due to the diopside-bearing gabbros with a magnetite content lower than that in the adjacent basic rocks. The respective magnetic highs can be partly determined by a high content of primary magnetite, but they probably reflect a martitization aureole controlled by exposed or concealed gabbroic intrusions.

(3) The major gravity low Bunea Mică-Căpîlnaş-Vorţa-Ardeu (east of the considered region) is determined by the obvious thickening of the Late Kimmerian volcanics from the southern island arc of the Mureş Zone. This major gravity low intersects obliquely the major gravity high Căzăneşti-Almăşel-Cuiaş, which indicates that the gabbroic intrusive mass may extend south-westwards, below the pile of island arc volcanics.

The Late Kimmerian granitoid bodies of Săvîrşin, Cerbia and Pietroasa Hill-Căzăneşti (Plate) determine strong gravity lows, conjugated with intense aeromagnetic lows. On aeromagnetic images the gravity lows at Săvîrşin and Cerbia are bordered by rings of magnetic highs, determined by the uralitization of the adjacent ocean floor magmatic rocks.

Structure of the ophiolitic slab in the Căzăneşti-Cuiaş gravity anomaly zone

The ophiolitic rocks from the ocean crust fragment situated at the lower part of the Căpîlnaş-Techereu Unit belong to two complexes characteristic of an ocean crust (Savu, 1983; Savu et al., 1981) as follows: (1) the sheeted-dyke complex (O_2) and the ocean floor basalts complex (O_1). These complexes are penetrated by the Late Kimmerian magmatic rocks and east of Ilteu they are overlain by an outlier of Laramian volcanics (60 Ma, Herz et al., 1974).

(1) The sheeted dyke complex is the lowermost complex known in the Mureş Ocean Crust. It develops in the area west of the ocean floor basalts complex (Pl. and Fig. 2). This complex originates in a normal-type ridge (N-type MORB, Savu, Stoian, 1988). It consists 100 per cent of dykes of intergranular basalts and dolerites with chill margins, with a NE-SW trend, therefore at an angle of about 45^0 versus the present elongation of the ocean crust slab and of the Mureş Zone ophiolitic suture, which in this area trends approximately E-W. It shows, beside the above presented geophysical data, that the ophiolitic megaslab has its own structure formed on the Mureş ocean floor during the Liassic which differs from the structure of the Mureş ophiolitic suture determined by the subduction/obduction processes and by the Alpine tectonic movements.

The development area of the complex is correlated, as known, with the major gravity and magnetic anomaly Vîrful Măgurilor-Bruznic, wider and more intense than the Căzăneşti-Cuiaş anomaly.

(2) The area of the Căzăneşti-Cuiaş gravity anomaly (Plate) is overlain by the ocean floor basalts complex (O_1). This complex is more varied petrographically than the former. It consists mainly of basalts in pillow lava facies originating in the basic lava flows which were erupted on the Mureş Ocean floor from the spreading centre, where took place the ascension of the tholeiitic magma (Macdonald, 1982) formed at about 100–125 km deep (Savu et al., 1981; Savu, 1983). Locally the basaltic flows are associated with basaltic pyroclastics – especially agglomerates and volcanic breccia or tachylites.

In the middle part of the area overlain by the basaltic complex is situated the Căzăneşti-Cuiaş gravity anomaly (Pl.). This quite elongate anomaly is parallel to the normal contact between the two complexes of Liassic ophiolitic rocks mentioned above. Two major gabbroic bodies appear along the anomaly alignment: the bodies of Almăşel and Cuiaş, as well as several smaller bodies of gabbros at Căzăneşti (Vaţa valley) and south-east of Almăşel and a small peridotite body situated north-east of Corbeşti (Savu, 1962). These petrological relationships and the trend of the gravity anomaly parallel to the primary structural elements of the allochthonous fragment of Liassic ophiolitic rocks show that this anomaly is determined by elements which occurred during the Liassic, concomitantly with the formation of the Mureş Ocean Crust. Taking into account the very small width of the anomaly and the very great elongation it results that this anomaly is determined by an intrusion with a great dyke aspect (Fig. 2). This dyke occurred due to the uplift towards the surface of the ocean floor of the more dense materials from the upper mantle or from the gabbro (O_3) and peridotite (O_4) complexes as a narrow (about 2 km) and very elongated intrusion whose apophyses at the level of the ocean floor basalts complex are represented by the mentioned gabbroic bodies and the small peridotitic body of Corbeşti, exposed by erosion.

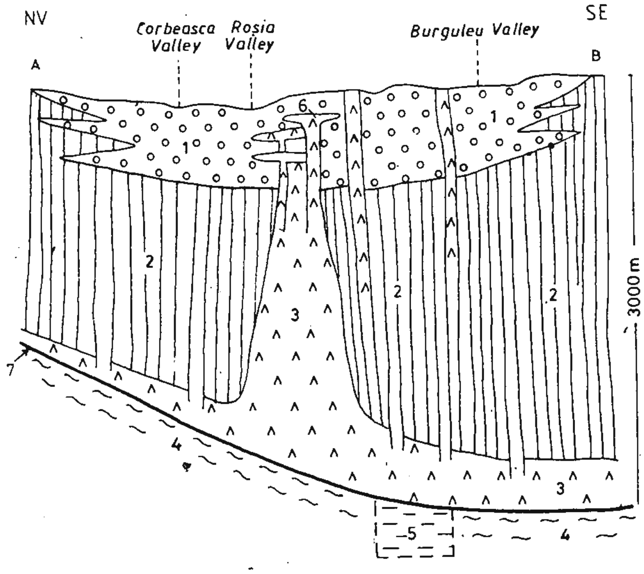

Fig. 2 – Hypothetical geological section through the Liassic ophiolitic megaslab in the Căzăneşti-Cuiaş gravity anomaly in the Colbeşti area.
1, Ocean floor basaltic complex (O_1); 2, sheeted dyke complex (O_2); 3, gabbro-peridotitic complex (O_3+O_4); 4, sedimentary and metamorphic formations from the tectonic plates in the north (Apuseni Mountains Plate) and the south (Transylvanian Plate); 5, collision zone (suture line); 6, apophyses of the great dyke; 7, obduction and/or overthrust plane.

The small gabbroic bodies of Căzăneşti crop out on the Vaţa valley, north-east of Căzăneşti, and on the Ponorul valley, south-east of the locality. They probably represent small apophyses of the north-eastern extremity of the great dyke which determines the gravity anomaly. The intrusive nappe of Căzăneşti-Ciungani, located north-west of the gravity anomaly area, might be generated by a dyke enrooted in the great dyke. This intrusive nappe presents at the lower part a discontinuous level of ferrogabbros with vanadiferous Ti-magnetite (Cioflică, 1962) like the other two major gabbroic bodies in the gravity anomaly area.

The gabbroic body of Almăşel represents, according to its shape, a composite dyke, resulting from several successive parallel intrusions of gabbroic magma. The body consists of diopside gabbros, dolerites, ferrogabbros, olivine gabbros, gabbroporphyrites and albitic granophyres (Savu, 1954, unpubl. report; 1962; 1986; Savu et al., 1970). It is intruded by numerous hydrothermal veins of sulphides.

From the gabbroic body of Cuiaş, located in the south-westernmost part of the gravity anomaly only its north-eastern half is cropping out, the rest of it being destroyed by the intrusion of the Late Kimmerian Săvîrşin granite and by the erosion of the Mureş valley (Pl.). This body was also yielded by a dyke of gabbroic magma which widened toward the upper part like a trough with asymmetrical flanks (Savu, 1953, unpubl. report; Savu, Udrescu, 1967; Savu et al., 1990). The main mass of gabbroic body is mostly constituted of diopside gabbros with a heterogeneous structure. This structure represents the result of the "in situ" differentiation of the main tholeiitic magma intrusion. Due to this gravity differentiation a discontinuous level of ferrogabbros with vanadiferous Ti-magnetite formed at the lower part of the intrusion and is found again on the north-western margin of the body. The body was penetrated by small intrusions of melagabbros and olivine gabbros, troctolites and hyperites. Some dykes are represented by albitic plagioaplites and granophyres. The gabbroic body is penetrated by numerous veins and dykes of dolerites and gabbroporphyrites. Hydrothermal mineralizations are quite rarely found.

Metallogenetic aspects of the first depth step

The concentrations of mineral resources known in the first depth step (about 350 m) in the area of the Căzăneşti-Cuiaş high gravity anomaly are of two kinds: (1) liquid-magmatic and (2) hydrothermal. These mineralizations belong to the metallogenic province associated to the Alpine ocean floor magmatism in the Mureş Zone (Savu, 1972).

(1) The liquid-magmatic concentrations are represented by vanadiferous Ti-magnetite accumulations in ferrogabbros levels formed at the bottom of the gabbroic bodies by the "in situ" differentiation process of the tholeiitic magma (Cioflică, Savu, 1960). These concentrations are referred to the liquid-magmatic ferriferous district Drocea-Roşia Nouă (Savu, 1972). The iron and titanium concentrations are included in several minerals which crystallized last from the basic tholeiitic magma (Savu, 1973, 1986). The series begins with Ti-magnetite and ulvospinel which have ilmenite exsolutions and continues with the formation of ilmenite and rutile, the last mineral of the series being sphene which is quite seldom found. These minerals form at different temperatures (Savu, Udrescu, 1967) depending on the gabbroic body crystallization (see Table). Being the last minerals crystallized from the magma they are usually anhedral and contain solid drops of sulphides (Savu, 1973).

The Fe and Ti mineral concentrations in ferrogabbros are variable (Tab.) and it seems that they depended first on the amount of magma differentiated and its oxidation degree (Cioflică, Savu, 1960; Savu, 1986). There also vary from one gabbroic body to another the TiO_2 and V_2O_3 contents in magnetite (Tab.).

The content of vanadiferous Ti-magnetite in the Mureş Zone ferrogabbros (max. 25 per cent at Dumbrăviţa) constitutes, for the time being, a problem as regards the exploitation of this mineral and the extraction of its components. In Finland, at Otanmäki, the exploitation of metamorphosed gabbroic rocks with vanadiferous Ti-magnetite and the ore recovery for the final extraction of Fe, Ti and V started after the Second World War. The differences between the ferrogabbros from Finland and those in the Drocea Mts consist in the different amount of vanadiferous Ti-magnetite. In the first case, the average value of this mineral in the rocks was more than 25 per cent in 1973, whereas in the Drocea Mts it hardly reached 15 per cent.

(2) Hydrothermal mineralizations occur along the high gravity anomaly as numerous sulphide depositions, especially pyrite and chalcopyrite, some of which were previously exploited (Transylvania and Tătăroaia mines). These mineralizations were determined by postmagmatic processes which yielded hydrothermal alteration processes. The rocks altered under the influence of this hydrothermal metamorphism, later named also ocean floor metamorphism, belong to three characteristic facies (Savu, 1967; Coleman, 1977). All these facies have been recognized in the gravity anomaly zone, e.g. albite-epidote-amphibolite facies, greenschists facies and zeolitic facies, characterized by the following parageneses:

(1) Albite-actinolite (uralite)-epidote-quartz-calcite;

(2) Albite-chlorite-calcite-prehnite;

(3) Zeolites-quartz-calcite.

According to their position, the sulphide mineralizations belong to two main types: (a) copper mineralizations; (b) pyrite mineralizations (Socolescu, 1944; Savu, 1954, unpubl. report, 1972). The former develop in the north-eastern part of the high gravity anomaly, where they form a metallogenic field lying between Căzăneşti, Almăşel and Corbeşti; the latter are more frequently found in the south-western part of the anomaly where they form a metallogenic field lying between Pietriş, Toc and Cuiaş. The cupriferous

ous or pyritiferous characteristic of the mineralizations from these metallogenic fields was determined by the emplacement conditions of the host rock. The copper mineralizations are connected with the emplacement of the gabbroic bodies, whereas the pyrite mineralizations are correlated with the effusive rocks, which belong to the ocean floor basaltic complex (O_1).

Table
Ti-magnetite concentrations in the gabbroic bodies in the gravity anomaly zone and their TiO_2 and V_2O_3 contents and formation temperature

No.	Gabbroic body	Thickness of the ferrogabbroic level	Ti-magnetite content	TiO_2	V_2O_3	Formation temperature
1	Căzăneşti-Ciungani	30–40 m	5–15 %	7,2–12,40 %	0,18–0,61 %	850^0–950^0
2	Almăşel	10 m	10–20 %			
3	Cuiaş	8 m	10–20 %	5,04 %		790^0

The copper mineralizations are spread around and inside the gabbroic bodies, especially that of Almăşel. This body includes numerous low mineralized copper veins in the Bălan Brook (Transylvania mine), Gura Cailor, Rîpilor, Butaşului, Padinii Brooks, which have been illustrated on the detailed maps of the region (Socolescu, 1944; Savu, 1954, unpubl. reports) and later explored by I.F.L.G.S. (Popescu, 1969, unpubl report). The mineralization occurrences are located on two alignments situated along the N-W and S-E contacts of the gabbroic body. Similar mineralizations are more rarely found inside the gabbroic body as well as outside it or in farther zones, e.g. the copper mineralizations in the Lupoaia valley nearby Roşia Nouă and those south-east and north-east of the body which crop out along the gravity anomaly toward Căzăneşti and Corbeşti.

The exploration works carried out by I.F.L.G.S. (Corbu et al., 1969; Popescu et al., 1969, unpubl. report; Gheorghiţescu, 1970) and our observations pointed out that on the north-western contact plane occur mineralized veins with chalcopyrite and pyrite, locally magnetite, in a quartz and calcite gangue, which are associated in some places with chlorite, epidote and actinolitic amphibole. On the south-eastern contact the mineralization in the Gura Cailor Brook consists of magnetite, pyrite and chalcopyrite and it is similar with that in the Lupoaia valley (Savu, 1954, unpubl. report, 1972). The mentioned mineralizations are characterized by two parageneses typical of this metallogenetic field:

(1) Magnetite-pyrite-chalcopyrite;

(2) Pyrite-chalcopyrite.

After Gheorghiţescu (1970) these main minerals occur in association with accessory minerals which crystallize together with them as follows: quartz-magnetite-hematite-pyrite-chlorite-epidote-sphalerite- chalcopyrite-galena-tetrahedrite-oligiste-calcite- marcasite-bornite-chalcosine; malachite and azurite occur in the oxidation zone.

The paragenesis of sulphides with magnetite was mentioned by Socolescu since 1944. The formation of such a paragenesis was explained by Betehtin (1950) by the change of the O and S concentration in the hydrothermal solution during the crystallization of the minerals, according to the evolution of the Cu-Fe-S-O system. In our case, if we consider the crystallization succession of the minerals, it results that at the beginning of their deposition there was a higher oxigen concentration in the solution which in time became lower, so that the sulphur concentration prevailed. These processes took place at temperatures ranging between 210 and 230^{0}C; correlated with the above-mentioned parageneses, they show that the copper mineralization deposited in the first part of the mesothermal stage.

Hematite presence in the copper mineralizations associated with the Liassic ocean floor rocks in the Mureş Zone was also found in the Cyprus-type stratiform deposit of Pătîrş (Savu et al., 1982). It has been ascertained that the presence of magnetite or hematite in these mineralizations depended also on the depth at which they deposited. In the Pătîrş mineralization, deposited between the ocean floor basaltic flows of the upper complex (O_1), hematite formed, whereas in the Almăşel mineralizations, formed at great depth, at the level at which the gabbroic body crystallized, magnetite formed.

The occurrence of Pb and Zn minerals in a reduced amount is possible in the ore deposits formed in the ocean crust, as it was the case of the Cyprus-type deposit at Baia de Aramă (Savu et al., 1985). Moreover, the geochemical studies (Savu et al., 1981) showed that the ocean floor basalts always include small amounts of Pb and Zn, which can explain the formation of sphalerite and galena in the associated copper mineralizations.

The major copper mineralization in the Almăşel gabbroic body was at Transylvania mine, nowadays closed, which is situated in the Bălan Brook, at the north-western contact of the gabbroic body. The mineralization consists of veinlets and nests of pyrite and chalcopyrite±magmatite in a kaolin gangue with quartz, calcite, epidote and altered faldspar. Impregnations of sulphides in the host rock are also found.

Another mineralization mined out in the past in the northern part of the metallogenic copper field was that at the Tătăroaia mine, represented by a NE-SW trending vein with a variable thickness. In the north-eastern part of the metallogenic copper field Socolescu (1944) mentioned the mineralizations in the Gruiu Valley and some other occurrences, recently studied by Andrei et al. (1984, unpubl. report). They are characterized by the same parageneses as those mentioned before.

The mineralizations of pyrite and rarely of chalcopyrite are represented by isolated hydrothermal veins or stockworks with quartz, calcite and zeolite gangue, seldom in association with epidote, on the account of which gossans formed. The most frequent mineralizations of this type occur in the north-eastern part of the pyrite metallogenic field west of Pietriş, in the basin of the Fugii and Sălişte valleys (Pl.) where a wide zone of gossan formed on their account, which was worked out in the past. The chemical analysis of the ore in the gossan indicated contents of Fe_2O_3 - 7–30 per cent and FeO - 0.11–1 per cent (Savu et al., 1988 a, unpubl. report). Such gossans are still found at Toc.

Metallogenic aspects of the second depth step

The mineralizations in the first depth step are known on the basis of the direct observations, at the surface or in boreholes and galleries; unlike them, the possible mineralizations situated at depth below 800 m in the high gravity anomaly zone are only hypothetical. A structural borehole south of Corbeşti (Pl.) might clear up this problem. These mineralizations might be connected with the lower part of the ocean floor basalts complex (O_1), the sheeted-dyke complex (O_2), possibly with the gabbroic bodies, like those at the surface, as well as with the deep-seated great dyke (Fig. 2) which determines the gravity anomaly.

The possible mineralizations associated with the first three ophiolitic rocks formation would certainly display the characteristics of the mineralizations of the first depth step mentioned before. The mineralizations of the great dyke obviously depend on the characteristics of the rocks forming it. Thus, the gabbros might include concentrations of vanadiferous Ti-magnetite beside concentrations of Ni-pyrrhotite in association with chalcopyrite. Peridotites might contain concentrations of chromite, pyrrhotite and other Ni-minerals and platinum minerals.

Conclusions

The Căzăneşti-Cuiaş high gravity anomaly in the Liassic ophiolites of the Drocea Mts is determined by a great dyke of gabbroic and peridotitic rocks, situated at about 500 m deep. This dyke was intruded parallel to the sheeted dykes of the complex O_2; its apophyses are the gabbroic bodies of Căzăneşti, Almăşel and Cuiaş which are associated with vanadiferous Ti-magnetite concentrations (Fig. 2).

Along the gravity anomaly two metallogenic fields with concentrations of hydrothermal sulphides have been separated: a cupriferous field to the north-east and a pyrite one to the south-west.

The cupriferous mineralizations in these metallogenic fields have been generated by post-magmatic solutions released both from the rocks of the gabbroic bodies and from the deep-seated magmatic chamber, the origin place of the magmas forming the great dyke and its apophyses – the satellite gabbroic bodies.

Below 800 m deep there might exist both mineralizations similar with those found at 500 m deep and mineralizations of Cr, Ni and platinic elements.

For detailed information on the structure of the high gravity anomaly zone, the petrographic constitution of the great deep-seated dyke and of its metallogenetic implications a structural drilling has to be carried out.

References

Andrei J., Calotă C., Scurtu Fl. (1975) Considérations structurales sur le sillon ophiolitique des Monts Métallifères à l'aide des données géophysiques et des certains éléments quantitatifs obtenus grâce au modellage. *Rev. roum. géol., géophys. géogr., Géophysique*, 19, p. 101–111, Bucureşti.

Betehtin A. G. (1950) Paragenezisî rudnîh mineralov v sistemah Fe-S-O i Cu-Fe-S-O. Izv. Akad. Nauk. SSSR, Gheolog., 5, Moskva.

Bleahu M. (1989) Tectonica globală, II, 491 p., Bucureşti.

Cioflica G. (1962) Studiul petrografic al formaţiunilor eruptive din regiunea Căzăneşti-Ciungani (Munţii Drocea). *An. Com. Geol.*, XXXII, p. 257–424, Bucureşti.

– , Savu H. (1960) Noi contribuţii la cunoaşterea posibilităţilor de formare a titanomagnetitelor din Munţii Drocea. *St. cerc. geol.*, V, 4, p. 693–709, Bucureşti.

– , Lupu M., Nicolae I., Şerban V. (1980) Alpine Ophiolites of Romania: Tectonic Setting, Magmatism and Metallogenesis. *An. Inst. Geol. Geofiz.*, LVI, p. 79–96, Bucureşti.

Coleman R. S. (1977) Ophiolites – Ancient oceanic lithosphere? Spring Verlag, 229 p., Berlin.

Gheorghiţescu D. (1970) Aspecte cristalo-fizice ale piritei din mineralizaţiile cuprifere de la Almăşel (Munţii Drocea). *Stud. cerc. geol., geofiz., geogr., Geologie*, 15, 1, Bucureşti.

Herz N., Jones R. M., Savu H., Walker R. L. (1974) Strontium Isotope Composition of Ophiolitic and Related Rocks, Drocea Mountains, Romania. *Bull. Volc.*, XXXVIII-4, p. 1110–1124, Napoli.

Lupu M. (1975) Einige Bemerkungen zur Tektonik des südlichen Apuseni Gebirge (Siebenbürgisches Erzgebirge). *Rev. roum. géol., géophys., géogr., Géologie*, 19, p. 95–104, Bucureşti.

– , Avram E., Antonescu E., Dumitrică P., Lupu D., Nicolae I. (1993) Neojurasicul şi Cretacicul munţilor Drocea; stratigrafia şi structura unui basin marginal ensialic. *Rom. J. Tectonics & Reg. Geol.*, 75, p. 53–66, Bucureşti.

Macdonald K. G. (1982) Mid-Ocean Ridges: Fine Scale Tectonic, Volcanic and Hydrothermal Processes within the Plate Boundary Zone. *Ann. Rev. Earth Planet Sci.*, 10, p. 155–191, Palo Alto, California.

Savu H. (1962) Corpul gabbroic de la Almăşel şi contribuţii la cunoaşterea chimismului şi petrogenezei ofiolitelor din Masivul Drocea. *An. Com. Geol.*, XXXII, Bucureşti.

– (1967) Die mesozoischen Ophiolithe der rumänischen Karpaten. *Acta Geol. Sci. Hung.*, XI, 1–3, Budapest.

– (1972) Metalogeneza asociată magmatismului ofiolitic din Munţii Drocea. *D. S. Inst. Geol.*, LVIII/2, p. 94–119, Bucureşti.

– (1973) Succesion dans la separation des oxides et des sulfures des magmas ophiolitiques de la Zone de Mureş (Monts Apuseni). *Rev. roum. géol., géophys. géogr., Géologie*, 17, p. 15–20, Bucureşti.

– (1983) Geotectonic and Magmatic Evolution of the Mureş Zone (Apuseni Mountains). *An. Inst. Geol. Geofiz.*, LXI, p. 253–262, Bucureşti.

– (1986) Concentrations of Fe, Ti and V in the Alpine Ophiolites from the Mureş Zone, Romania. In Metallogeny of Basic and Ultrabasic Rocks. *Theophrastus Publ. S. A.*, p. 99–120, Athens.

– (1990) Remarks on the Mesozoic Tectonomagmatic Activity in the Trascău Mountains (Mureş Zone). *Rev. roum. géol., géophys. géogr., Géologie*, 34 (sub tipar).

– , Udrescu C. (1967) Paleotemperatura şi geochimia gabbrourilor de la Cuiaş (Munţii Drocea). *D. S. Com. Geol.*, LII, Bucureşti.

– , Stoian M. (1988) REE Contents in the Sheeted Dyke Complex of the Mureş Zone and Their Petrogenetic Significance. *Rev. roum. géol., géophys. géogr., Géologie*, 32, Bucureşti.

– , Vasiliu C., Udrescu C. (1970) Geochimia şi petrologia ofiolitelor din prima etapă de evoluţie a magmatismului iniţial alpin din Masivul Drocea (Munţii Apuseni). *D. S. Inst. Geol.*, LVI, 1, Bucureşti.

– , Lupu M., Lupu D., Ştefan A. (1979) Harta geologică a R. S. România, scara 1:50000, foaia Roşia Nouă, I.G.G., Bucureşti.

– , Udrescu C., Neacşu V. (1981) Geochemistry and Geotectonic Setting of Ophiolites and Island Arc Volcanics of the Mureş Zone (Romania). *Ophioliti*, 6 (2), p. 269–286, Bologna.

– , Berbeleac I., Udrescu C., Neacşu V. (1982) Basalt – spilitic (ophiolitic) Complex of Pătîrş (Mureş Zone) and the Associated Sulfide Mineralizations. *D. S. Inst. Geol. Geofiz.*, LXVII/2, p. 161–195, Bucureşti.

– , Andăr P., Gaftoi F. (1985) The Copper and Pyrite Ore Deposit Associated with Ophiolites of Baia de Aramă (South Carpathians). *D. S. Inst. Geol. Geofiz.*, 70–71 (1983; 1984), p. 125–140, Bucureşti.

– , Udrescu C., Neacşu V., Nacu D. (1987) Mid-Ocean Characteristics of Ophiolites in Baia-Lupeşti-Vărădia Area (Drocea Mountains), their Tectonics and Petrology. *D. S. Inst. Geol. Geofiz.*, 72–73 (1985–1986), p. 161–180, Bucureşti.

– , Udrescu C., Neacşu V., Stoian M. (1988 b) Petrology, Geochemistry and Origin of the Laramian Volcanics from the Mureş Couloir, between Zam and Gurasada. *Rom. J. Petrology*, 75 , p. 117–130, Bucureşti.

– , Udrescu C., Neacşu V., Stoian M. (1989) Structure, Petrology and Geochemistry of the Gabbroic Body of Cuiaş (Mureş Zone). *Rom. J. Petrology*, 75, p. 85–96, Bucureşti.

Socolescu M. (1944) Les affleurements de minérais de la région de Vaţa-Şoimuş-Buceva-Săvîrşin-Zam. *C. R. Inst. Géol. Roum.*, XXVIII, Bucureşti.

Received: November 13, 1989
Accepted: May 17, 1990
Presented at the scientific session of the Institute of Geology and Geophysics: October 30, 1990

Rom. J. Geophysics, 1993, 16, p. 67–76

DEEP STRUCTURE OF THE INNER CARPATHIANS IN THE MARAMUREŞ–TISA ZONE (EAST CARPATHIANS)

Mircea SĂNDULESCU, Marius VISARION, Dumitru STĂNICĂ, Marcela STĂNICĂ, Ligia ATANASIU

Institutul de Geologie şi Geofizică. Str. Caransebeş 1, 78 344 Bucureşti 32.

Key words: Tectonic units. Nappe. Faults. Mohorovicic discontinuity. Models. East Carpathians.

Abstract: The structural model elaborated based on the geological and geophysical data in Maramureş and the Subcarpathian Ukraine reveals the existence of two consumption paleoplanes of the primary basements of the flysch and Pieniny nappes between which lies the sialic block corresponding to the Median Dacides. The relative closeness of the two planes suggests the more restricted initial width of the Median Dacides and their transversal shortening. From W to E the blocks separated are characterized by different thicknesses of the crust: 25–26 km, 30–33 km and 50–52 km. The tectonic draft elaborated reveals the marked bent of the Pienides in the terminal zone of the Gutîi-Maramureş determined by the Tertiary overthrust of the Inner Dacides. The separation of the Băbeşti-Tiacovo Nappe, consisting of Mesozoic formations and ophiolitic rocks, and the prolongation of the Kricevo Nappe in Romania represent new elements.

The Maramureş-Oaş area and the Subcarpathian Ukraine, situated south and north, respectively, of the upper Tisa Valley, correspond to a part of the Inner Carpathians realm. It is possible to distinguish a lower tectonic stage (following Wegman's deffinition), consisting of the deformed Cretaceous and Lower Miocene units (Inner, Median and Outer Dacides as well as the Pienides), and the upper tectonic stage, consisting of the Neogene molassic depressions and the Neogene calc-alkaline volcanic arc. The aim of this note is to analyse the correlation between the different Cretaceous and Lower Miocene deformed units and the deep structure of the crust, taking into account the correlation between the geological, drilling and geophysical data.

The geological investigations in Maramureş have a relatively long history. The latest information concerning the lithostratigraphy of the Mesozoic and Paleogene formations belongs to Antonescu et al. (1975), Dicea et al. (1980), Săndulescu et al. (1982), Săndulescu, Bratu (1984), Săndulescu et al. (1989a, 1991). The general structure of the area and the correlations with the Ukrainian Carpathians are due to Săndulescu (1975, 1980a, 1984).

Major contributions on the deep structure, particularly of the Neogene volcanics structure, have been brought by gravimetric and magnetic surveys accomplished during several stages (Fotopolos, 1962–1970; Cristescu, Ştefănciuc, 1968) by petrophysical studies effectuated on different types of rocks and geological formations (Botezatu et al., 1970) as well as by synthesis works based on them (Andrei et al., 1970; Borcoş et al., 1979). On small areas the seismic surveys carried out in the eastern part of the Pannonian Depression, in the Sighet and Văratec Mts-Rodnei Mts areas (Stanchievici et al., 1983; Ionescu, Popovici, 1979; Milea, Popescu, 1988) have brought sound evidence on the Neogene formations structures as well as a few disparate data on deeper levels. The results obtained have been taken over and reinterpreted within regional studies based on the integrate analysis of the geological and geophysical data (Visarion et al., 1979, 1988).

Several studies referred to the specification of the position of the Mohorovičič discontinuity (Enescu et al., 1967; Rădulescu et al., 1976), the establishing of the horizontal nonhomogeneities of the electric conductivity by the geomagnetic sounding method, the simplified version represented by Wiese induction vectors (Calotă et al., 1971; Soare, 1989), the particularities of the regional flux (Veliciu, 1987), and the seismicity of the northern part of Romania (Polonic, 1980).

Researches effectuated by the magnetotelluric sounding method in the Medieşul Aurit-Remetea Oaşului-Cîmpulung la Tisa profile provided new information concerning the deep structure of the area. Their integration in the actual structural model allowed some important specifications mostly about the position and mutual relations between the crystalline (crustal) block and the position of the suture zones.

For correlations with the Subcarpathian Ukraine we have taken into account the geological and tectonic maps (scale 1:200,000) (Krugliov et al., 1977), the structural map of the pre-Neogene formations of the Solotvino depression (Katîlk et al., 1974), data on gravity and electromagnetic induction surveys (Melniciuc et al., 1974; Burianov et al., 1980; Adam, Wallner, 1981), as well as the results of seismic surveys carried out on the international profiles IP-III and NP-17 (Beránek et al., 1972).

Overlook on the Geological Structure

The correlation of the geological and geophysical data in the Oaş-Maramureş zone with those in the Tiacovo-Sockyrnitza-Teresva Valley area in the Subcarpathian Ukraine made possible the elaboration of a tectonic draft (Plate I) which includes several new elements.

The major structural group of units presented on this map belongs to the Inner Dacides, Pienides, Median and Outer Dacides up to the boundary of the last ones with the Moldavides (Fig. 1).

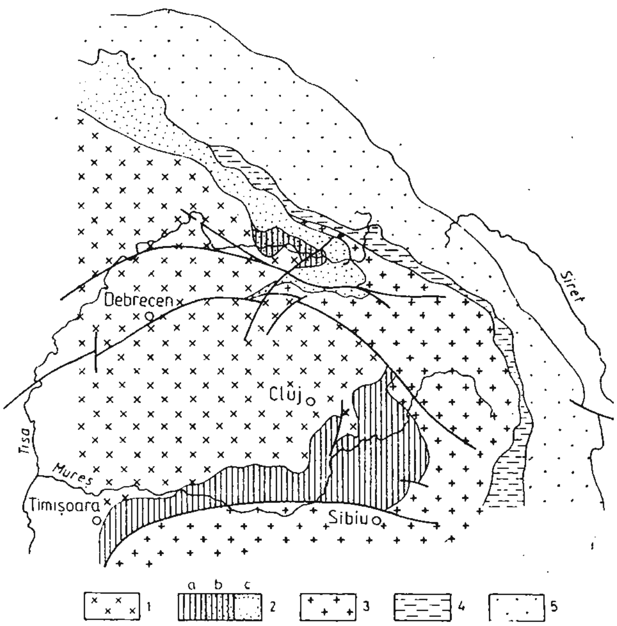

Fig. 1 - Tectonic sketch showing the position of the Main Tethyan Suture (MTS).
1, Pre-Apulian continental plate (Inner Dacides); 2, Main Tethyan Suture: a, Transylvanides; b, Băbeşti-Tiacovo Nappe; c, Pienides; 3, Continental Median Dacides; 4, Outer Dacidian Suture; 5, Moldavides.

The Pienides belong to the Major Tethyan Suture, squeezed between the Inner Dacides and the Median Dacides, both continental crusts bearing groups of units. The Pienidian units are cover nappes, whereas the Inner and Median Dacides group together continental basement shearing nappes. In an outer position is respect with the Median Dacides develop units – the Outer Dacides – which come from a satellite suture generated within an intracontinental rift zone (with Jurassic thinned or/and oceanic-type crust).

The main deformation periods of the different major groups of tectonic units are different in age. The oldest – Mid-Cretaceous – deformations have structured the Median Dacides and involved at least a part of the Major Tethyan Suture, corresponding to the obductions of Transylvanian elements known mostly southeast and south of the Maramureş area (Săndulescu, 1975, 1984). The Inner Dacides were structured during the Turonian (Late Turonian ?) time, while the Outer Dacides recorded the Mid-Cretaceous deformations and also the End-Cretaceous ones (Late Senonian). The Pienides show in their actual shape the traces of important Early Miocene deformations, but within some of their units traces of End-Cretaceous deformations are also preserved.

The I n n e r D a c i d e s extend from the Apuseni Mts and north-west Transylvania up to the westernmost Slovakia; they correspond to the Austro-Alpine nappe system of the Eastern Alps. In the area presented in this note the Inner Dacides are mostly represented by the Bihor Unit, which is their most external, consequently the deepest zone. The metamorphic formations, of Precambrian age (Someş Series), are largely developed in the Bihor Unit, intruded in places by Paleozoic granitic massifs. In the area under discussion the Someş Series crops out in the Ticău and Făget "crystalline islands" from under the molassic Neogene deposits of the Pannonian Depression and, practically, represents by itself the whole Bihor Unit. This situation is determined by an important pre-Paleogene (probably pre-Senonian) erosion which removed the Mesozoic envelope of the unit, preserved in its southern areas (Apuseni Mts). In the Preluca "massif" metamorphic formations crop out, which have been correlated (Rusu et al., 1983) with the Baia de Arieş Series of the Apuseni Mts or with the Rebra Series of the East Carpathians. This problem, as well as the correlation of the Pietriş "massif" situated north of Preluca, is a more complex question concerning the Paleozoic geotectonic history, the Tethyan rifting and oceanic spreading and the actual position of the Major Tethyan Suture.

The M a j o r T e t h y a n S u t u r e (MTS) groups together the units which proceed from the oceanic Tethys. Following the age of their main deformations (tectogeneses) the Transylvanides (Cretaceous deformations exclusively) and the Pienides (Cretaceous and Early Miocene deformations) have been distinguished

(Săndulescu, 1984). The Pienides develop north of the North-Transylvanian Fault only. The Transylvanides represent the whole MTS south of the North-Transylvanian Fault. Nevertheless, north and north-east of this fault Cretaceous obducted (above the European continental margin represented by the Median Dacides) units (the Transylvanian nappes) proceeding from the oceanic Tethys (=MTS) are known; this fact suggests that Transylvanidian elements take part in the building of the MTS together with the Pienides in parallel positions. In this discussion significant data were supplied by the borehole 2805 Băbeşti. At 2620 m deep below Badenian deposits, it penetrated a carbonatic sequence with dolomites and limestones assigned to the Middle Triassic (or Upper Jurassic ?). Below this rocks a dark-coloured clayey breccia with elements of eruptive rocks and mafic cinerites was drilled. At about 2875 m deep, the borehole intercepted basic and ultrabasic (picrite) eruptive rocks, which could be observed up to the bottom of the drilling (2909 m). This last sequence drilled in the Băbeşti borehole can be referred to a Mesozoic ophiolitic complex lithostratigraphically covered by the carbonatic (Triassic or Jurassic) sequence; both belong to the MTS and must be situated in front of (and below) the Inner Dacides with continental crust (as represented on the tectonic sketch). In a relatively close vicinity with the Băbeşti borehole several boreholes (Tiacovo, Sokyrnitza) are known in the southern Subcarpathian Ukraine, which have drilled Mesozoic (Triassic and Jurassic) formations constituted of clayey-calcareous sequences with intercalations of blackish siltic limestones; basic and alkaline magmatic rocks are associated (in an imbricated structure ?). We group together the formations occurring in the Băbeşti, Tiacovo and Sokyrnitza boreholes in a Băbeşti-Tiacovo Nappe, the innermost unit of the MTS situated in front of the Inner Dacides. The age of the tectogenesis which yielded the Băbeşti-Tiacovo Nappe is, however, difficult to specify; it can be Cretaceous only or Cretaceous and Early Miocene.

External in respect with the Băbeşti-Tiacovo Nappe another tectonic unit develops, that belongs to the Pienides (and consequently to the MTS) – the Kricevo Nappe. First identified in the Subcarpathian Ukraine (Jivko, Petrashkevici, 1971), its prolongation south of the Tisa River was supposed (Săndulescu, 1980b) below the Neogene molasses and volcanics. This supposition was confirmed by the borehole 4201 Sarasău (Fig. 2). The Kricevo Series, intercepted in the Subcarpathian Ukraine in boreholes (1 and 3 Tereblea, 11 Teresova, 2 Irshava, 4 and 5 Solotvino), consists of dark-grey calcareous clays with interbeds of grey sandstones, marls and limestones. Its age extends from Aptian to Senonian. The borehole 4201 Sarasău crossed between 2250 m and 2740 m a pelitic sequence of grey-blackish colour, perfectly comparable with those in boreholes 4 and 5 Solotvino (Fig. 2). Starting with the Sarasău area the Kricevo Nappe displays a major south-west bending.

One of the most specific element of the Pienides is represented by the Pieniny Klippen Zone which in Romania's territory crops out only in the Poiana Botizei-Strâmbu Băiuţi area, in the frontal part of the Botiza Nappe (the "frontal scales" which involve Pieniny-type klippen with Jurassic-Cretaceous formations and an End-Cretaceous tectogenesis). This element was intercepted in a borehole at the western periphery of the Baia Mare locality. North of Romania, the Pieniny Klippen Zone can be traced, across Ukraine, Slovakia and Poland, up to Vienna. In Ukraine, as in the Poiana Botizei-Strâmbu Băiuţi area, this zone is characterized by a very imbricated tectonic structure in a relatively narrow strip. The first compressions are Meso(?)- and End-Cretaceous, the second one Early Miocene. In some places a gap is known between the Cretaceous and the Paleogene. The same tectogenesis seems to be recorded in the Kricevo Nappe, too, a Paleogene (Eocene ?) sandy flysch overlying the Cretaceous Kricevo Series.

The Botiza Nappe, cropping out south of the Bogdan Vodă Fault and carrying in its frontal part the Poiana Botizei-Strâmbu Băiuţi Pieniny-type klippen, has apparently the same tectonic position as the Kricevo Nappe, but the lithostratigraphic succession is, at least partially, different. The most important volume of the Botiza Nappe is represented by an Eocene flysch succession, with variegated Paleocene shales and Turonian(?)-Senonian red marls, at its base. In front and below the Botiza Nappe develops the Wildflysch Nappe, constituted of Middle and Upper Eocene formations, with alternating levels of flysch, olistostromes, massive sandstones, sedimentary breccias and polymictic conglomerates, and of Oligocene sandy flysch. Both the Botiza and the Wildflysch nappes were recognized (Săndulescu et al., 1983, 1984) below the Neogene volcanic chain, in boreholes and mine workings, south of the Bogdan Vodă Fault, west of their outcropping area.

The Petrova Nappe is the most external unit of the Pienides; it corresponds westwards to the Măgura Nappe of the Slovakian-Polish Carpathians. The main part of the Petrova Nappe is represented by an Eocene (Middle and Upper) flysch. The Petrova Nappe develops only north of the Bogdan Vodă Fault; south of the fault it possibly corresponds (at least as regards the tectonic position and with some lithofacial changings) to the Wildflysch Nappe (Săndulescu in Săndulescu et al., 1989b).

The M e d i a n D a c i d e s belong to the deformed European continental margin and rep-

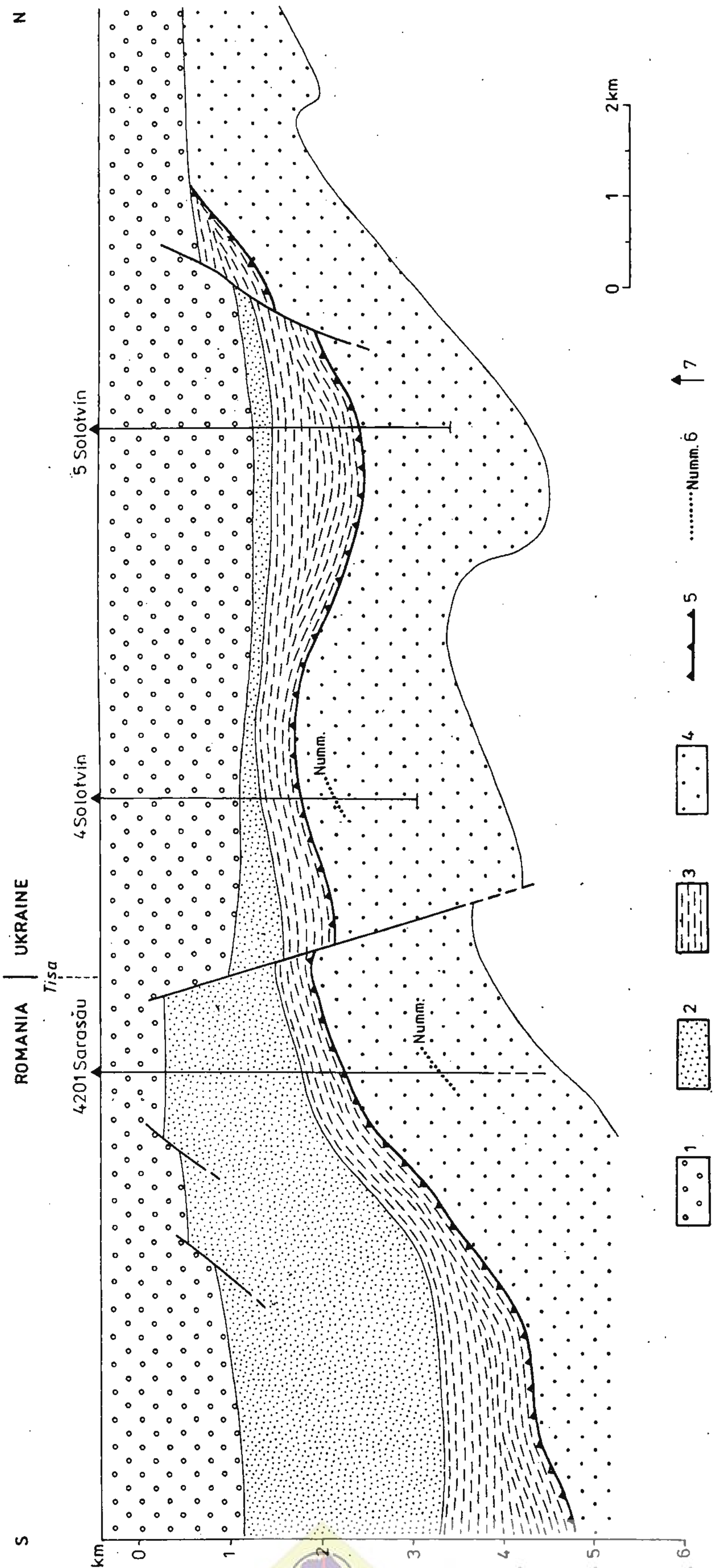

Fig. 2 – Geological cross-section in the Sarasău-Solotvino area.
1, Neogene molasses; 2, Barlov Series – Upper (?) Eocene; 3, Kricevo Series (Aptian-Senonian); 4, Eocene sandy flysch; 5, Overthrust; 6, Nummulitic-bearing levels; 7, Drillings.

resent the proximal group of units of this margin, in respect with the Major Tethyan Suture. The Median Dacides group together basement shearing nappes (with Precambrian and/or Paleozoic metamorphic formations and Triassic-Lower Cretaceous sedimentary formations) overthrust each other during the Meso-Cretaceous tectogenesis. The Post-Tectogenetic Cover of the Median Dacides, which largely develops in Maramureş area, shows two main sedimentary cycles: Cenomanian-Senonian and Eocene-Lower Miocene. The former starts with conglomerates, followed by a marly sequence (Turonian-Senonian). The latter starts also with conglomerates, followed by detrital sequences, carbonates and marls (Priabonian) and thick Oligocene formations (pelitic, alternating with massive sandy sequences). In some distal parts of the sedimentary basin of the Post-Tectogenetic Cover of the Median Dacides a continuous sedimentation develops from the Cenomanian up to the Oligocene, with a condensed pelagic succession during the Turonian-Priabonian time; the Oligocene formations are similar to the marginal facies mentioned above. The youngest levels of the Post-Tectogenetic Cover (Borşa Sandstone) may be Early Miocene in age. The Post-Tectogenetic Cover of the Median Dacides is tectonically overthrust by the Pienidian units during the Lower Miocene (Intra-Burdigalian). The formations of the cover were deformed during the same time (folds and scales partly detached from their substratum).

The O u t e r D a c i d e s are represented by a group of nappes with Cretaceous (Meso-Cretaceous and End-Cretaceous) tectogeneses. They proceed from an intracontinental rift, situated within the European continental margin (Săndulescu, 1980b, 1983), where thinned and/or oceanic type crust developed. This crust (and lithosphere) was consumed (by subduction) below the continental Median Dacides, generating a "satellite suture" in respect with the MTS. In Maramureş and the Subcarpathian Ukraine the Outer Dacides include the Black Flysch Nappe (=the Kameny Potok Unit=Civcin Unit) and the Cehlău Nappe (=Rahov and Burkut units). They are built up mostly of flysch formations (Jurassic-Lower Cretaceous or only Cretaceous) which, in some areas, preserved at their bottom mafic complexes.

Outside the Outer Dacides develop the M o l d a v i d i a n N a p p e s with a Miocene tectogenesis.

M o l a s s i c D e p r e s s i o n s develop since the Middle Miocene above the deformed Inner Carpathians. In the study area there is the north-east corner of the Pannonian Depression and the Transcarpathian Depression (different from the Transcarpathian Flysch Zone which groups the outcropping Pienides and the Median Dacides post-tectogenetic cover) which is a sort of gulf of the former one. Partly contemporaneous and partly above these depressions develops a V o l c a n i c C h a i n generated in connection with subduction processes.

Main Deep Fault Systems

The most expressive fractures are those which were active during the Neogene time; some of them can be older but were reactivated.

One of the most important deep fracture, reaching the Moho, is the N o r t h - T r a n s y l v a n i a n F a u l t (NTF) (Săndulescu, Visarion, 1978). It extends along about 800 km from eastern Transylvania up to south Hungary and crops out on the northern border of the Preluca "massif" (Plate I), where it is known as Preluca Fault. The transcrustal character of the North-Transylvanian Fault was assigned by deep seismic soundings (Rădulescu et al., 1976); the displacement at the Moho level is of about 5 km. This character is stressed out also by the seismic activity in the Tg. Lăpuş-Copalnic-Criscior area, characterized by earthquakes of low magnitude (Polonic, 1980) and by the high content of the endogene helium in the Coaş, Copalnic-Mănăştur and Brabeni areas (Veliciu et al., 1982). The displacements along the fracture show a composite and long activity. The significant role of the North-Transylvanian Fault is stressed out, among other facts, by the different tectonic evolution of the structural units situated on either part of the fracture. North of the fault the Cretaceous tectogeneses were followed in the Pienidian realm by the Early Miocene ones, whereas south of it only Cretaceous deformations are recorded (Săndulescu, 1975, 1984; Săndulescu, Visarion, 1978). The actual shape of the NTF is that of a normal fault with downward northern block. In fact, strike-slip components were active during the Cretaceous and the Early Miocene.

North and generally parallel to NTF develops another important fracture: the B o g d a n V o d ă F a u l t (BVF) (Săndulescu, 1975). This is also a transcrustal fault, still seismically active, with composite displacements – left-lateral strike-slip fault in the Early Miocene and normal fault with downward southern block during the Middle and Upper Miocene BVF can be traced in outcrops east of the volcanic chain; it continues below the Neogene volcanics where it was traced using the drilling and mining data (Săndulescu et al., 1983, 1984) as well as satellite images and gravity anomaly (Vâjdea et al., 1983). Its trend is marked also by epicenters of crustal earthquakes in the Racşa, Livada, Oraşul Nou and Nisipeni areas.

Between NTF and BVF develops the Neogene Satu Mare Graben sharply subsequent in respect with the deformed units of the Inner Dacides and Pienides. The graben is divided by NE–SW and ENE–WSW transversal faults into several blocks. The Făget Fault is one of the most important one, extending largely north and south of the graben boundary. West of the Făget Fault the Andrusat-Urmeniş Block is the main sunk one, with important Sarmatian-Pannonian subsidence. Another young subsided elongated area, with a transversal position in respect with the Satu Mare Graben, is the Baia Sprie (transversal) Graben generated between the Mara and Săsar faults, within which the pre-Badenian basement was drilled at depths of more than 2500 m (Săndulescu et al., 1983).

North of BVF and west of the Făget Fault the post-tectogenetic (Neogene) block-faulted style is largely developed (Plate I). One of the relatively most elevated blocks is the Oraşul Nou-Negreşti Block where metamorphic formations of the Inner Dacides were drilled at 675 m (Oraşul Nou borehole) and which is clearly outlined by a major gravity maximum with an east-west trending. The gravity maximum closes abruptly in the Livada area, on the Halmeu Fault. This fracture is relatively young, with right-lateral strike-slip translations and marked actually by epicentres of crustal earthquakes (Oraşul Nou, Livada and Halmeu).

Geotectonic Model

The geotectonic model of the study area, showing the deep structure of the crust, is based on the data supplied by the magnetotelluric surveys on the Medieşul Aurit-Tisa Valley profile correlated with the seismic information obtained on the international profile III, the Ukrainian profile NP-17 (Beranek et al., 1972), the local seismic soundings carried out in the north of Romania (Enescu et al., 1967) as well as with the geomagnetic, gravity and geothermal data in the Baia Mare-Sighet and Solotvino-Sockyrnitza in the Subcarpathian Ukraine. An attempt of geological interpretation of a profile which begins at Oradea in the Inner Dacides area and reaches the flysch zone of the Ukrainian Carpathians has also been taken into consideration (Rădulescu et al., 1976).

The geotectonic model elaborated (Plate II) emphasizes two gaps of the Mohorovičič surface: one situated under the development area of the Pienides and the other in the frontal part of the Inner Dacides. From NE to SW, in the three compartments separated, the average thicknesses of the crust are, as follows: 50-52 km, 30-32 km and 26-27 km. The most conclusive data have been obtained from the south-western area, corresponding to the Pannonian realm with thinned crust, where the elements supplied by the interpretation of the magnetotelluric soundings are grouped satisfactorily and they coincide with those obtained to the west and north by seismic surveys. The strong thickening of the crust toward NE is suggested by the regional decrease of the gravity values on this trend and it is confirmed by the gravity modelling carried out in correlation with the seismic data in the Subcarpathian Ukraine (Melniciuc et al., 1974).

The fracture situated at the Moho level below the external part of the Pienides (the eastern deep fracture on Plate II) has been considered as representing the suture of the Outer Dacides, corresponding to an old plane of crustal consumption of the primary basements of the flysch nappes. From this point of view it is comparable with that emphasized on several geological profiles in the East Carpathians (Săndulescu, 1975, 1980, 1984; Rădulescu et al., 1976, 1983; Stănică et al., 1986; Visarion et al., 1988) under the frontal part of the Central East Carpathian Nappes. This interpretation was also confirmed by the distribution of the Wiese vectors, computed for 20-30 minutes magnetic field variations in the Carpathian area (Calotă et al., 1971; Rokitianski, 1975; Adam, Wallner, 1981). The results obtained made possible the accurate outlining of an alignment which marks the direction change of the induction vectors, materializing the existence of the conducting zone in the crust (Fig. 3). The calculations effectuated by bidimensional modelling indicated depths of 16-25 km for the conducting zone. Although there were different opinions versus a certain point of view (Visarion et al., 1988), we consider that the mentioned alignment, located in the study area below the frontal part of the Pienides, corresponds to the consumption paleoplane of the primary basement of the flysch nappes. This interpretation is also based on the hypothesis formulated by Rokitianski (1975), with the specification that the depth where the conductive-zone is situated may be explained only by subduction processes. This solution is also accepted in other studies on the Carpatho-Pannonian area (Adam, Wallner, 1981). It was also illustrated the development toward depth of the Outer Dacides, represented by the Black Flysch Nappe, equivalent with the Civcin-Kameny Potok Nappe in the Subcarpathian Ukraine, and by the Ceahlău Nappe, corresponding to the Rahov and Porculeţ nappes, as well as of the Moldavides represented by the section through the Dukla Nappe. Below these nappes, at 9-10 km deep, is situated the basement of the underthrust platforms overlain by a relatively thin sedimentary cover and also possibly a part of the continental cordilleras of the flysch basins.

The second fracture rendered evident by the magnetotelluric surveys is located below the frontal part of the Inner Dacides. It must correspond to the MTS and consequently to the subduction and consuption paleoplane of the oceanic-type primary basement of the Pienidian cover-type nappes. The collision along this paleoplane occurs between the deformed continental crust of the Median Dacides (European continental margin) and that of the Inner Dacides (Preapulian

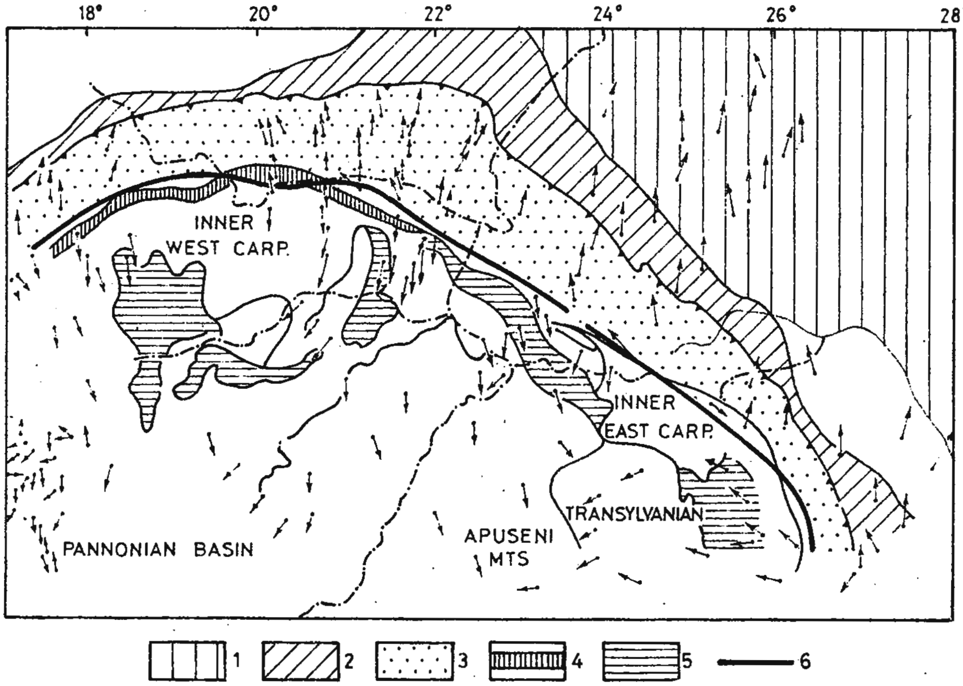

Fig. 3 – Wiese induction vectors on a tectonic map of the Inner Carpathians-Pannonian region (acc. to Adam, Wallner, 1981 and Soare, 1989).
Legend: 1, East European Platform; 2, Foredeep; 3, Flysch nappes; 4, Pieniny Klippen Belt; 5, Neogene calk-alkaline volcanic rocks; 6, Turn of direction of the Wiese vectors.

continental margin).

The continental crust segments, corresponding to the Median Dacides and lying between the two consumption paleoplanes, are situated at 7 km deep, in the elaborated model, and are successively overlain by their post-tectonic cover, the Pienidian nappes and the Neogene molasse.

The area situated SW of the MTS is characterized by a thin Pannonian-type crust. The continental crust of this area corresponds to the Inner Dacides group of units. Their present position is the result of some Miocene translations directed by the North-Transylvanian Fault.

A similar situation was observed on the Beregovo-Dolhina segment (Fig. 4) of the international profile III (Beránek et al., 1972) for which a seismo-tectonic section was elaborated. The NE extension of the profile emphasized the strong thickening zone of the crust noticed below the flysch nappes and the foredeep of the East Carpathians. It is worth mentioning the existence of a transition layer (about 10 km thick) at the lower part of the crust, characterized by propagation speeds of 7.2–7.3 km/s, which extends on a width of about 100 km. Considering the westward prolongation of the underthrust platform elements up to the Outer Dacides suture, it is possible that the Tornquist-Teisseyre Zone, in its actual acceptance, might be situated between the crustal fractures which delimit this transition layer.

In the actual acceptance the Tornquist-Teisseyre Zone (TTZ) represents a transcontinental zone (from the Baltic Sea to the Black Sea), at this scale relatively narrow zone, delimited toward north-east by the Tornquist-Teisseyre Fault and grouping together horst and graben structures, parallel and close to this fault. The flysch nappes of the East Carpathians cover, by overthrust, approximately the whole TTZ (in the Ukrainian East Carpathians and the northern Romanian East Carpathians). Consequently the south-western border of the TTZ has in this sector a very close position in respect with the subduction zone of the primary basements of the flysch nappes (the satellite suture).

The direct comparison of the results presented, with those obtained on the international profile XI, shows that the crustal block, implicitly the lithosphere one, which separates the two consumption zones, is twice narrower northwards than southwards (central part of the East Carpathians). This situation might be explained following several hypotheses:

– primary width (previous to the crustal shortening determined by the overthrust processes) of the Median Dacides was smaller northwards than southwards;

– the overthrust processes were "absorbed" in depth leading to the thickening of the crust in the north-western area.

recorded on the external subduction plane. The crust between the two subduction planes is of about 30–35 km thick, whereas south-west of the MTS it decreases at 25 km (Pannonian-type crust). A comparable situation is recorded also south of the study area on the East Carpathian-Transylvanian cross-section.

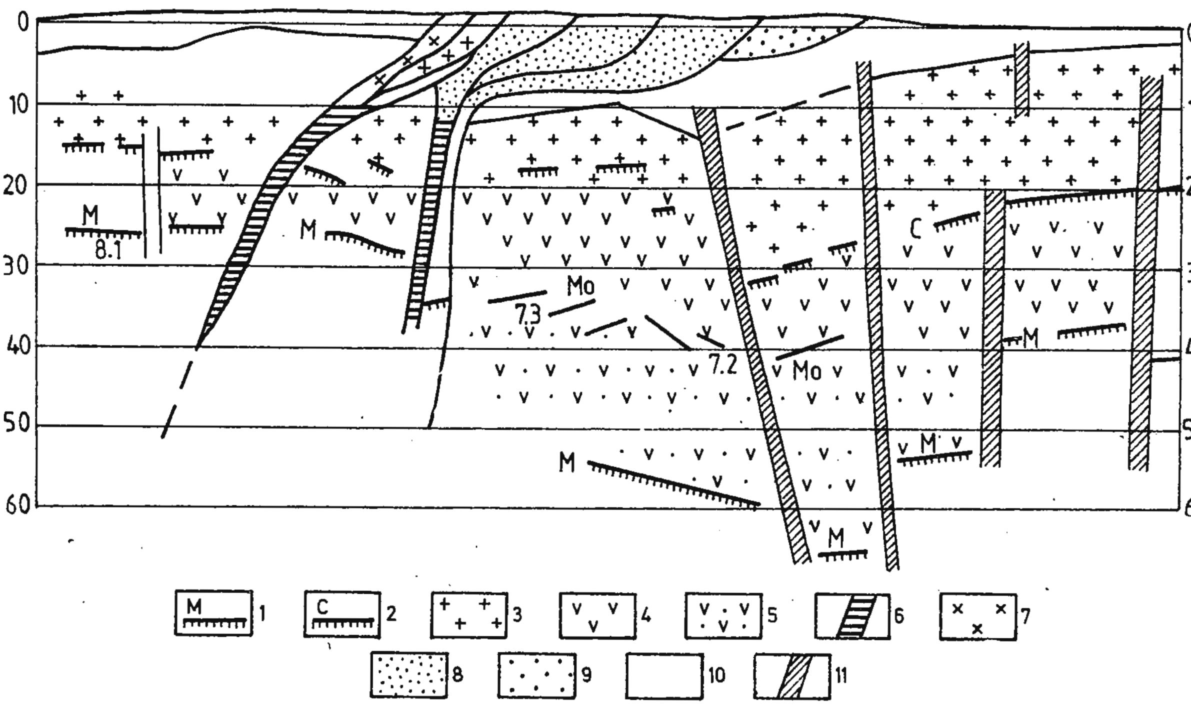

Fig. 4 – Crustal geological section Beregovo-Dolina along the profile of IP–III (seismic data acc. to Beránek et al., 1972, position and interpretation of the ophiolitic sutures acc. to the authors).
Legend: 1, Moho discontinuity; 2, Conrad discontinuity; Crustal layers: 3, Upper layer; 4, Lower layer; 5, Crust-mantle transition layer; 6, Ophiolitic sutures; 7, Pieniny Klippen Belt; 8, Flysch Nappes; 9, Foredeep; 10, Post-nappe and platform covers; 11, Crustal fault.

On the basis of the available data a structural sketch-map was elaborated at the level of the Mohorovičić discontinuity (Fig. 5) for the northern part of Romania and Subcarpathian Ukraine. It was elaborated on the basis of the regional gravity anomaly, calculated for a square net with 20 km each side. The position of the Mohorovičić discontinuity was established, based on a formula elaborated by the authors taking into account the seismic soundings and deep magnetotelluric data. This map shows the positions of the two consumption paleoplanes, the deep crustal fractures as well as the distribution of the crustal earthquake epicentres. By a general analysis of this map it is clearly possible to stress out the different thicknesses of the crust in the Carpathian area. Outside the external subduction paleoplane a thick crust of about 60 km develops in a north-western block and 45–50 km in a south-eastern one, the two blocks being separated by a deep transversal fault. An important displacement (15–20 km) of the Mohorovičić discontinuity is

Conclusions

This study brings new elements for a better knowledge of the structure of the Inner Carpathians by correlating geological and geophysical data from Romanian and the Subcarpathian Ukraine. A special significance in structural respect shows the spectacular bent of the Pieniny Klippen Zone in the Maramureş-Gutîi area, the separation of the Băbeşti-Tiacovo Nappe included in the units of the major Tethyan suture and the continuation of the Kricevo Nappe in the Romanian territory.

In this paper stress was laid on the specification of the deep-seated fracture systems and on the role played by it in the finishing off of the structural edifice. The different tectonic evolution of the structural units separated by the North-Transylvanian fracture is also revealed.

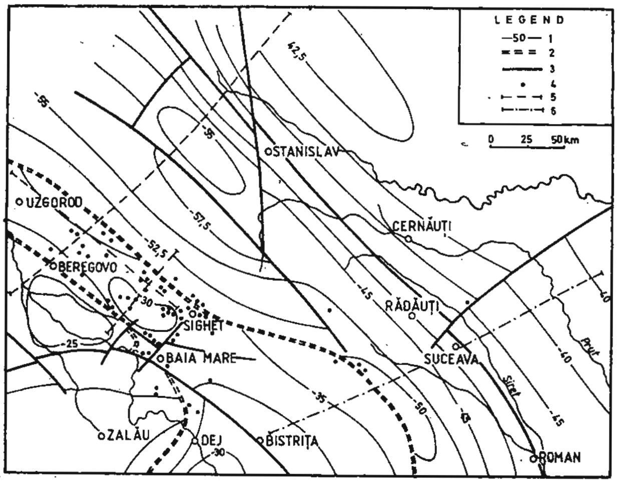

Fig. 5 - Moho structural map in North Romania and Subcarpathian Ukraine areas.
Legend: 1, Moho depth (in km); 2, Ophiolitic suture; 3, Crustal fault; 4, Macroseismic epicentre; 5, DDS profile; 6, MTS profile.

Considering all the data known so far a representative geotectonic model has been elaborated, which reveals the small horizontal distance between the consumption paleoplanes of the primary basements of the flysch and of the Pienides, as well as the probable existence of the Tornquist-Teisseyre Zone, as it is defined in the present international research programmes.

References

Adám A., Wallner A. (1981) Information from electromagnetic induction data on Carpatho-Pannonian geodynamic. *Earth Evol. Sci.*, 1, p. 3–4, Berlin.

Antonescu F., Mitrea Gh., Năstase N. (1975) Contribuţii la cunoaşterea stratigrafiei şi tectonicii zonei Poiana Botizei-Ieud. *D. S. Inst. Geol. Geofiz.*, LXI, 5, p. 3–35, Bucureşti.

Beráneck B., Weiss J., Hrdlicka A., Dudek A., Zounkova M., Suk M., Feifer M., Militzer H., Knothe H., Mituch E., Poszgay K., Uchman J., Sollogub V. B., Chekunov A. V., Prosen D., Milovanovici B., Roksandic M. (1972) The crustal structure of central and southeastern Europe based on the results of explosion seismology. *Geofizik Közlemények, Special Edition*, Budapest.

Borcoş M., Fotopolos S., Peltz S., Socolescu M., Stan N. (1979) Observaţii preliminare asupra structurii regiunii vulcanice neogene Oaş-Gutîi dedusă din corelarea datelor geologice şi geofizice. *St. tehn. econ.*, I, 15, Bucureşti.

Botezatu R., Andrei J., Calotă C., Visarion M. (1970) Studiul densităţii rocilor din eruptivul neogen de la Baia Mare. *St. tehn. econ.*, D, 7, p. 59–70, Bucureşti.

Burianov V. D., Gordienko V. V., Kulik S. N., Livanova L. P., Logvinov I. M., Paschievici I. K., Sollogub V. B., Cekunov A. V. (1980) Kompleksraia geofiziceskaia modeli stroienia i razvitiia litosferî Karpati i Sredneevropeiskih Gertinid. In: *Tektonosfera Ukrainî i drugi regionov SSSR*, Kiev.

Calotă F., Câltan I., Ionescu A., Soare A., Steflea V. (1971) Inregistrări de variaţii geomagnetice pe teritoriul României. *St. cerc. geol., geofiz., geogr., Geofizică*, 9, 2, Bucureşti.

Cristescu Tr., Stefănciuc Al. (1968) Prezentarea hărţii aeromagnetice a teritoriului României. *Al V-lea Simp. prosp. geofiz. fiz. scoarţei glob.*, Bucureşti.

Dicea O., Duţescu P., Antonescu F., Mitrea G., Botez R., Donos I., Lungu V., Moroşanu I. (1980) Contribuţii la cunoaşterea stratigrafiei Zonei transcarpatice din Maramureş. *D. S. Inst. Geol. Geofiz.*, LXV, 4, p. 21–85, Bucureşti.

Enescu D., Cornea I.,Constantinescu P. (1967) Primele încercări de evaluare a grosimii scoarţei terestre pe teritoriul României prin sondaje seismice punctuale. Consideraţii asupra mantalei superioare. *St. cerc. geol., geofiz., geogr., Geofizică*, 5, 2, Bucureşti.

Jivko A. M., Petroskeoici M. T. (1971) Gheologhiceskoe stroenie zakarpatskovo vnutrenovoproghiba. In: "Gheologhiceskoe stroenie i gorincie iskopaemîe Ukrainiski Karpat", Trud. UKRNigri, XXV, Ed. "Nedra", Moskva.

Katîik V. I., Bokun A. N., Filistinskii L. E. (1974) Strukturnîe osobennosti neogenobîh otlojenii Solotvinskoi vpadinî. *Geol. Geochim. Gor. Iskop*, 39, Kiev.

Krugliov S. S. (1977) Gheologhiceskaia Karta Ukrainskih Karpat, Lvov.

Krugliov S. S. (1977) Tektoniceskaia Karta Ukrainskih Karpat, Lvov.

Melniciuc M. I., Kuzneţova V. G., Rahimova I. S. (1974) Nekotorîe voprosî kompleksnogo izuceniia glubinogo stroeniia Vostocinîh Karpat. *Geol.-Geochim. Gor. Iskop.*, 41, Kiev.

Polonic G. (1980) Seismicity and tectonics of Baia Mare-Sighetul Marmaţiei area. *Rev. roum. géol., géophys. géogr., Géophysique*, 24, 2, Bucureşti.

Rădulescu D. P., Cornea I., Săndulescu M., Constantinescu P., Rădulescu F., Pompilian A. (1976) Structure de la croûte terrestre en Roumanie. Essaï d'interpretation des études sismiques profondes. *An. Inst. Geol. Geofiz.*, L, p. 5–36, Bucureşti.

– , Săndulescu M., Veliciu S. (1983) A Geodynamic Model of the East Carpathians and the Thermal Field in the Lithosphere. *An. Inst. Geol. Geophys.*, LXIII, p. 135–144, Bucureşti.

Rokitianski I. I. (1975) Investigation of anomalies of electro-conductivity by method of magnetovariational profiling. Nauk. Dumka, Kiev.

Rusu A., Balintoni I., Bombiţă G., Popescu Gh. (1983) Harta geologică a României, scara 1:50.000, foaia Preluca. Inst. Geol. Geofiz., Bucureşti.

Săndulescu M. (1975) Essaï de synthèse structurale des Carpathes. *B.S.G.F.*, 7, XVII, 3, Paris.

– , Visarion M. (1978) Considérations sur la structure

du soubassement de la Dépression de Transylvanie. *D. S. Inst. Geol. Geofiz.*, LXIV, Bucureşti.
– (1980 a) Sur certaines problèmes de la corrélation des Carpathes Orientales roumaines avec les Carpathes ucrainiennes. *D. S. Inst. Geol. Geofiz.*, LXV, 5, Bucureşti.
– (1980 b) Analyse géotectonique des chaînes alpines situées autour de la Mer Noire occidentale. *An. Inst. Geol. Geofiz.*, LVI, p. 5–54, Bucureşti.
– , Neagu Th., Antonescu E. (1982) Contributions à la connaissance des klippes de type pienin de Poiana Botizei (Maramureş). *D. S. Inst. Geol. Geofiz.*, LXVII, 4, p. 79–96, Bucureşti.
– (1983) Le problème de la marge continentale européenne dans l'areal carpatho-balcânique. *An. Inst. Geol. Geophys.*, LX, p. 199–208, Bucureşti.
– (1984) Geotectonica României. 336 p., Ed. tehn., Bucureşti.
– , Bratu E. (1984) Nouvelles données pour des formations paléogènes des unités allochtonnes de la zone du Flysch Transcarpathique (Maramureş). *D. S. Inst. Geol. Geofiz.*, LXVIII, 4, p. 119–135, Bucureşti.
Soare A. (1989) Preliminary results of some tectomagnetic researches at the Surlari Geophysical Observatory. *Rev. roum. géol., géophys., geogr., Géophysique*, 33, Bucureşti.
Stănică D., Stănică M., Visarion M. (1986) The structure of the crust and upper mantle in Romania as deduced from magnetotelluric data. *Rev. roum. géol., géophys., géogr., Géophysique*, 30, Bucureşti.
Vâjdea V., Bercia I., Săndulescu M., Veliciu S., Zincenco D., Ignat V. (1983) Uses of Landsat data to structural study of the Romanian East Carpathians. *An. Inst. Geol. Geofiz.*, LXIII, Bucureşti.
Veliciu S. (1987) Geothermics of the Carpathian area. *An. Inst. Geol. Geofiz.*, Bucureşti.
Visarion M., Polonic P., Ali-Mehmed E. (1979) Contribuţii geofizice la cunoaşterea structurii sectorului de NE al Depresiunii Pannonice şi a unităţilor limitrofe. *St. tehn. econ.*, D, 12, Bucureşti.
– , Săndulescu M., Stănică D., Atanasiu L. (1988) An improved geotectonic model of the East Carpathians. *Rev. roum. géol., géophys., géogr., Géophysique*, 32, Bucureşti.
– , Săndulescu M., Constantinescu P., Atanasiu L. (1989) The structure of the Pannonian Depression in Romania (II. Northern Area). *The XIV-th Symposium of Earth's Physics and Applied Geophysics*, June 1989, Bucureşti.

Received: 5 December, 1991
Accepted: 7 December 1991
Presented at the XVI-th Symposium of Earth's Physics and Applied Geophysics: December 1991, Bucureşti.

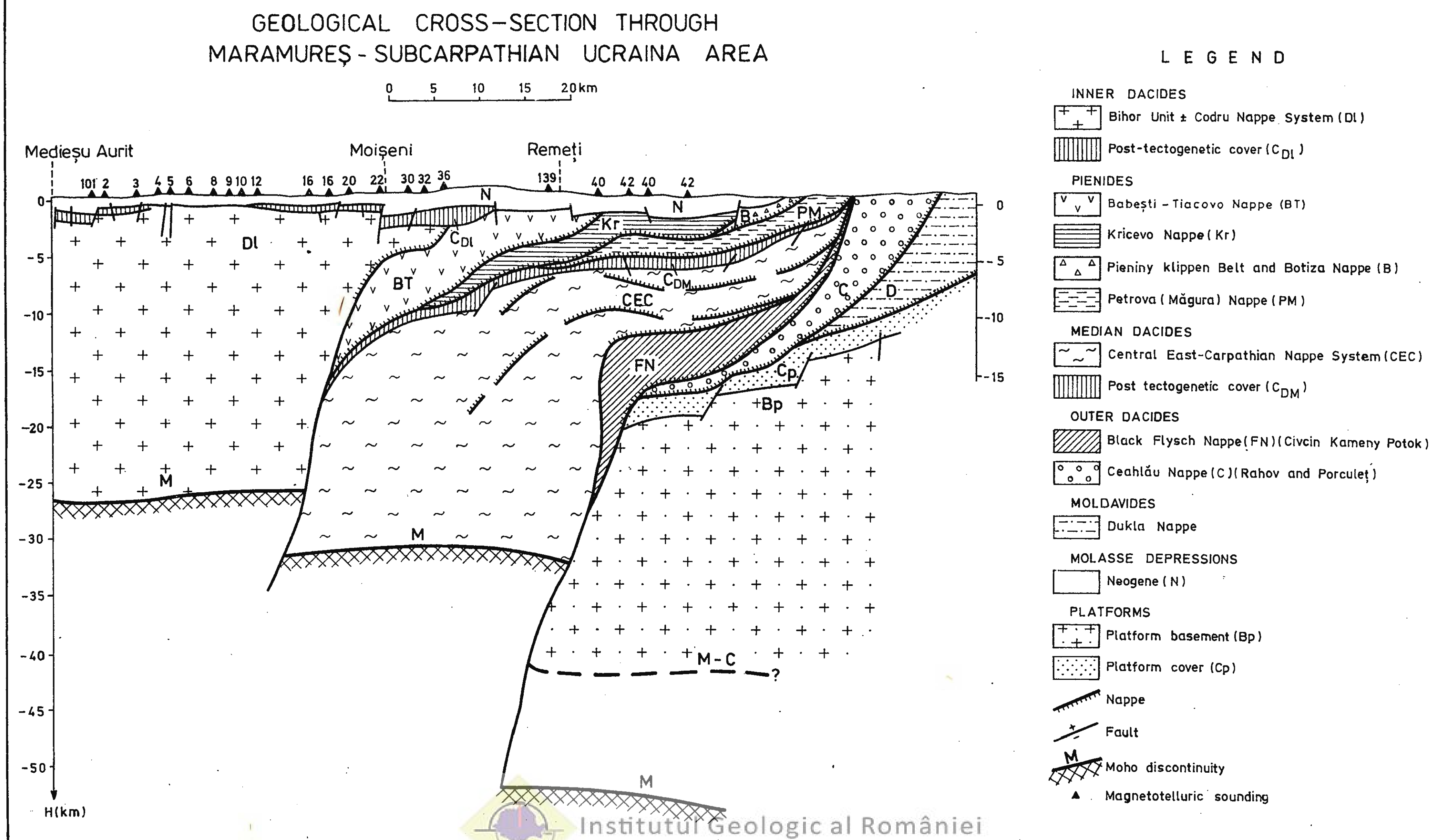

 Imprim. Atel. Inst. Geol. Geofiz.

Rom. J. Geophysics, 1993, 16, p. 77–82

THE INTERNATIONAL ADOPTION OF THE DREPTU GEOMAGNETIC STATION (POIANA TEIULUI, NEAMŢ DISTRICT)

Andrei SOARE, Mioara ALEXANDRESCU, Dan ALEXANDRESCU

Institutul de Geologie şi Geofizică. Str. Caransebeş 1, 78344 Bucureşti 32.

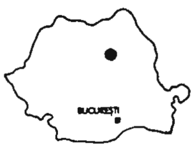

Key words: Observatories. Magnetic field. Magnetic surveys. Correlation. East Carpathians.

Abstract: Dreptu geomagnetic station is located in the northern part of the East Carpathians. This station is equiped with a recording system of four elements of the geomagnetic field. The correlation between the information obtained at the Surlari Observatory with the one obtained at the Dreptu Station, the necessity of this station for the study of the geomagnetic field and for the magnetic prospecting are to be emphasized.

The recordings of the geomagnetic variations date back in the mid of the last century but their systematic use developed only in the last decades. That is why out of the two hundred permanent observatories which constitute the survey network of the magnetic field evolution only a few celebrated fifty years of uninterrupted activity.

In Romania, Ştefan Hepites put into operation the first magnetic observatory in the present-day building of the Astronomic Observatory in 1897. The rapid ceasing of its activity was obviously due to the urban development so that its mentioning is only of a historic significance (Constantinescu, 1977).

In 1943 the Geological Institute of Romania proposed the foundation of the Surlari Geophysical Observatory ($\Lambda=26^0 15.2$ E, $\Phi=40^0 40.8$ N), a station equiped at that time at the level of the best similar stations in Europe. This observatory is still in operation as national fundamental station integrated since 1957 in the complex of observatories coordinated by IAGA.

The development of prospectings and magnetometric mappings raises the problem of the study of the spatial distribution of the transitory geomagnetic field and of the utilization of the natural electromagnetic induction phenomenon in the study of the geological deep-structure. Under these circumstances a new geomagnetic observation station situated in another geologic province in the Romanian territory at least 300 km far from the Surlari Observatory was necessary. Thus, in 1981 a new station for permanent magnetic recordings began its activity in the area of the Poiana Teiului village - Neamţ district (Dreptu station $\Lambda=25^0 50.5$ E, $\Phi=47^0 07.1$ N).

The significance of the location of this station results also from the fact that it can become a study place of the earth's magnetic evolution, well situated within the network of the geomagnetic observatories in the South-East Europe (Fig. 1) and of those along the meridian 30^0 long E (Fig. 2).

A geomagnetic observatory records the variations of the geomagnetic field on short or long time intervals so that the information obtained to be representative for a wide area (Chapman, 1951). For the location of a permanent geomagnetic station in the north-eastern part of Romania several factors have been taken into consideration.

The first condition required for a geomagnetic observatory was its location in a zone without geological anomalies. As shown on the aeromagnetic map of the area, scale 1:200,000 (Fig. 3) and the two aeromagnetic profiles N-S and W-E, scale 1:200,000 (Fig. 4), in the Poiana Teiului zone the geomagnetic field has a quite regular distribution.

This condition could be checked up by a simple magnetic prospecting. In the area of the Dreptu station measurements were carried out toward NNW and SSE and two profiles situated along the Dreptu Brook, the second one perpendicular to it. Observations on the variation of the vertical component ΔZ were effectuated with a "Scintrex" magnetometer, in 60 observation points on the basis of which a draft, scale 1:500, being elaborated (Fig. 5). The two profiles measured (Figs. 6 and 7) point out the regular structure of the magnetic field in the area of the Dreptu geomagnetic station.

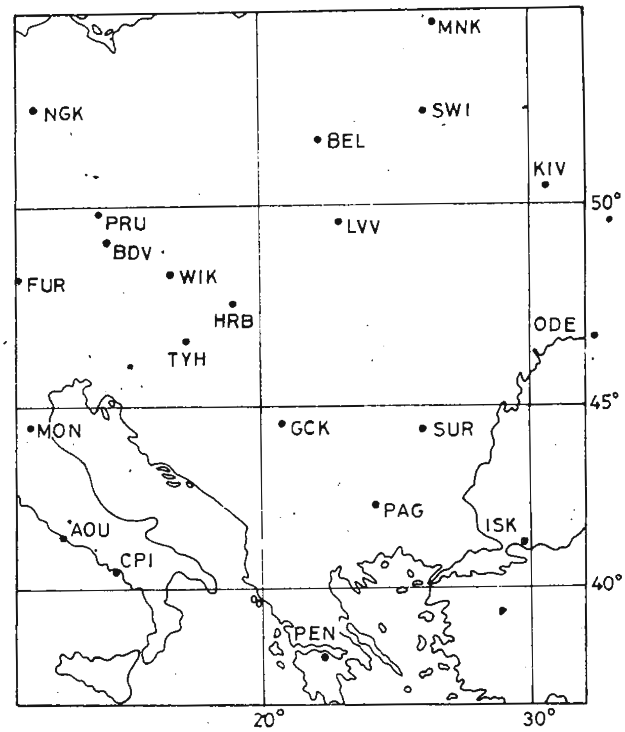

Fig. 1 – Spreading of the geomagnetic observatories in South-East Europe. AQU=L'AQUILA, BDV=BUDKOV. BEL=BELSK, CPI=CAPODIMONTE, FUR=FURSTENFELDBRUCK, GCK=GROCKA, HRB=HURBANOVO, ISK=KANDILLI, KIV=KIEV, LVV=LVOV, MNK=MEANOOK. MON=MONTE CAPELLINO, NGK=NIEMEGK, ODE=ODESSA, PAG=PANAGJURISTE, PEN=PENDELI, PRU=PRUHONICE, SUR=SURLARI, SWI=SWIDER, TYH=TIHANY, WIK=WIEN, KOB=KOBENZL.

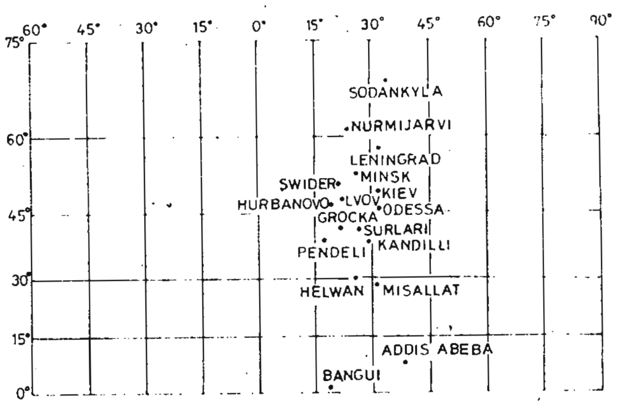

Fig. 2 – Spreading of the geomagnetic observatories between 15^0–45^0 long. E.

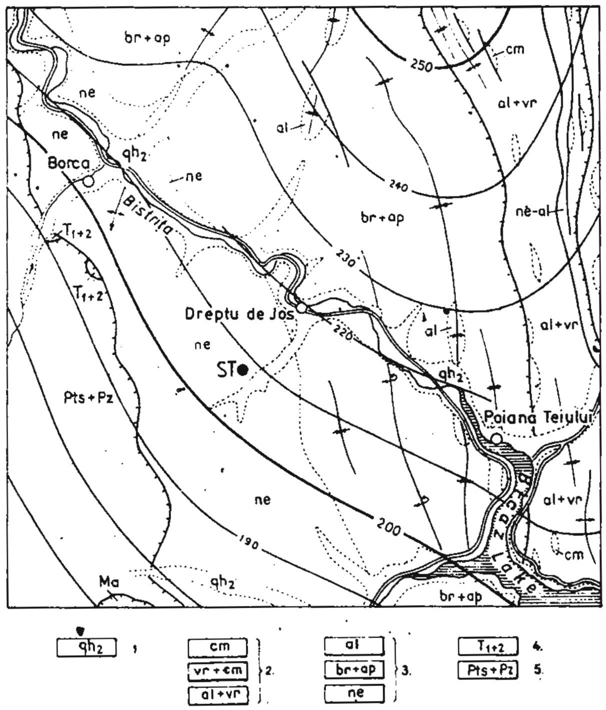

Fig. 3 – ΔT_a aeromagnetic map of the Borca-Poiana Teiului area (sc. 1:200,000). 1, Upper Holocene; 2, Upper Cretaceous; 3, Lower Cretaceous; 4, Middle and Lower Triassic; 5, Paleozoic and Upper Proterozoic.

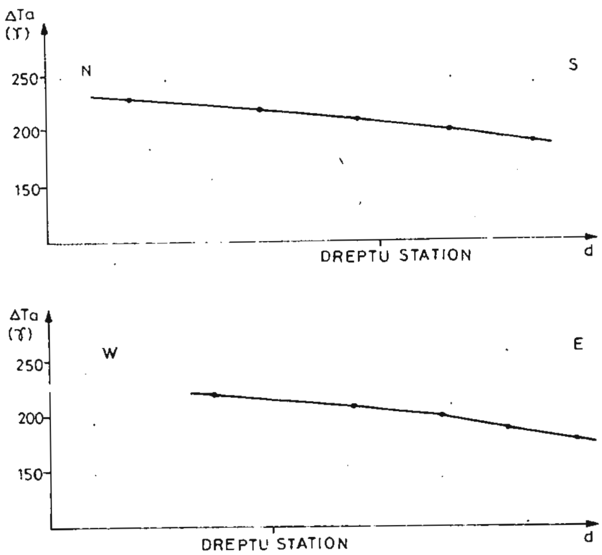

Fig. 4 – N-S and W-E aeromagnetic profiles in the area of the Dreptu aeromagnetic station (sc. 1:200,000).

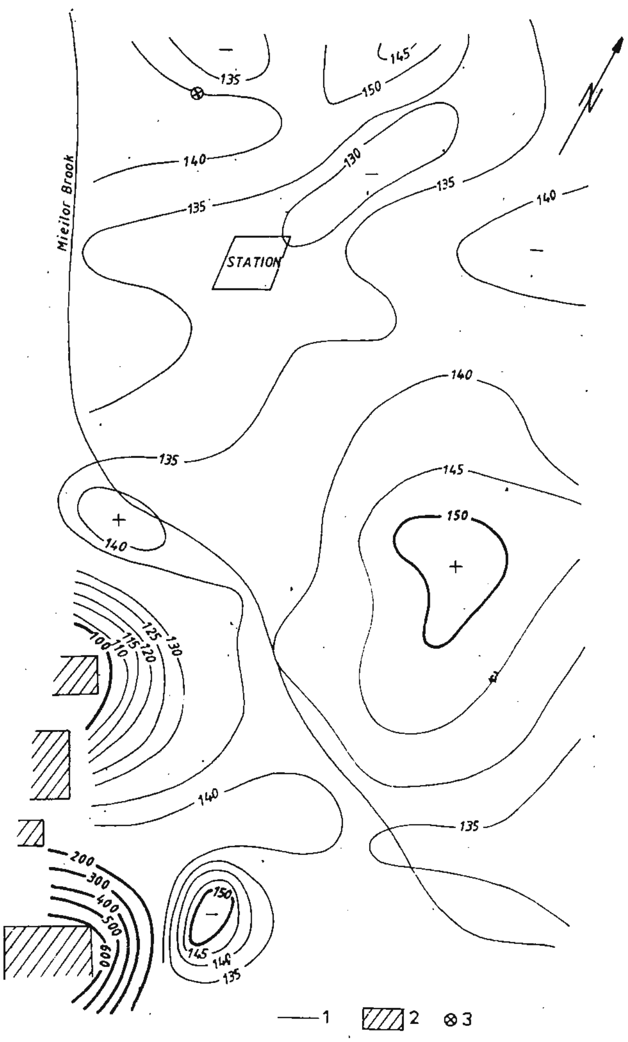

Fig. 5 – Detailed magnetometric sketch in the Dreptu Station area (sc. 1:200,000). 1, isolines ΔZ_a, 2, annexed buildings; 3, pillar.

The Dreptu geomagnetic station is situated on Lower Cretaceous formations of the internal flysch. The basement rocks are represented by different types of sandstones and frequent calcite diaclases belonging to the Bistra Beds. The magnetic susceptibility of these rocks varies between 10 and 20.10^{-6}uCGS, rarely reaching 28.10^{-6} uCGS and the density between 2.6 and 3.7 g/cm^3.

This station lies at about 3.5 km east of the anomalous contact between the inner flysch, developed eastward, and the Tulgheş metamorphic series – westward – represented in this area (Dreptu Brook basin – Grinţieş Mount) by the acid series (quartz prevailing): sericite schists with a high quartz content, chlorite-sericite schists, also with a high quartz content, metaquartzites (finely bedded, sericitous, graphitous, ferromanganoan), as well as frequent quartz veins. The magnetic susceptibility of these rocks varies between $0-30.10^{-6}$ uCGB, frequently $5-15.10^{-6}$ uCGB, and density ranges from 2.53 to 2.75 g/cm^3 (Romanescu, 1987, unpubl. data).

In conclusion, both the sedimentary rocks on which the Dreptu station is located and the adjacent metamorphic ones are practically nonmagnetic or very poorly magnetic.

The artificial perturbations of the geomagnetic field (railway, high voltage network, buildings etc.) do not occur in the area of the Dreptu station. The draft of the vertical component variation Δ Za (Fig. 5) shows in the SW part a deformation of the isolines due to the perturbatory sources (buildings) which, however, do not affect the course of the isolines nearby the station situated at about 60–70 m from it.

The building for variometers has been erected so that to ensure a good temperature stability. It is difficult, even for well-equiped observatories, to obtain a relative constant temperature, with exclusive seasonal variations. The residual temperature coefficients can be determined and consequently correlations could be made when necessary (Iliceto, 1972–1975).

The humidity control raises the same problems as that of temperature. The quartz thread of the variometers D and H are sensitive to a higher humidity. Humidity also affects the sensitivity of the photographic paper.

Dreptu geomagnetic station disposes of a recording system of four elements of the geomagnetic field (D, H, Z, T), situated in a nonmagnetic place. The system consists of four Bobrov variographs and a Matting & Wiesemberg recorder.

The technical parameters of the recording system are: unrolling rate of the photographic paper 20 mm/h, scale values ranging between 1.97 and 2.56 uT/mm. The supply is a 12 V direct current obtained by transforming the main power supply.

In case of electric current interruptions an accumulator (12 V) is automatically switched on and supplies the lights. The recording system functions continuously, excepting the cases when interventions are required for the readjustment of the light spots for the resetting of the basic lines or for the cleaning of the equipment.

In order to check up the veridicity of the geomagnetic recordings at Dreptu station comparisons have been made with the data obtained at the Surlari Geophysical Observatory. This comparison was made in several directions, each of them emphasizing the high quality of the magnetic recordings at the Dreptu Station.

The geomagnetic field changes continuously under the influence of different factors. The major variation is the daily one – S_q – which originates in the

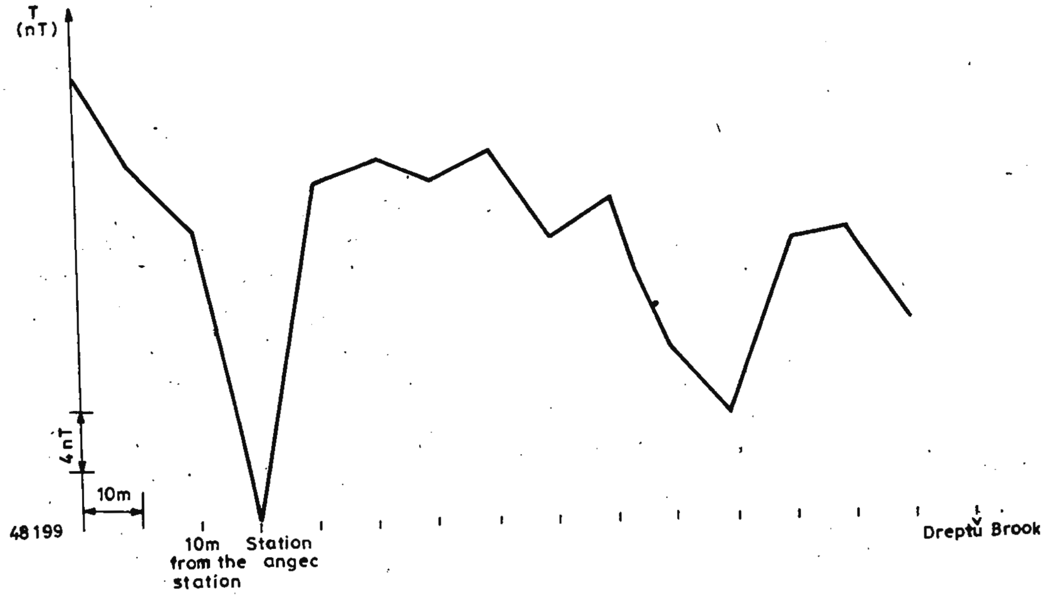

Fig. 6 – NNW-SSE magnetometric profile perpendicular to the Dreptu Brook.

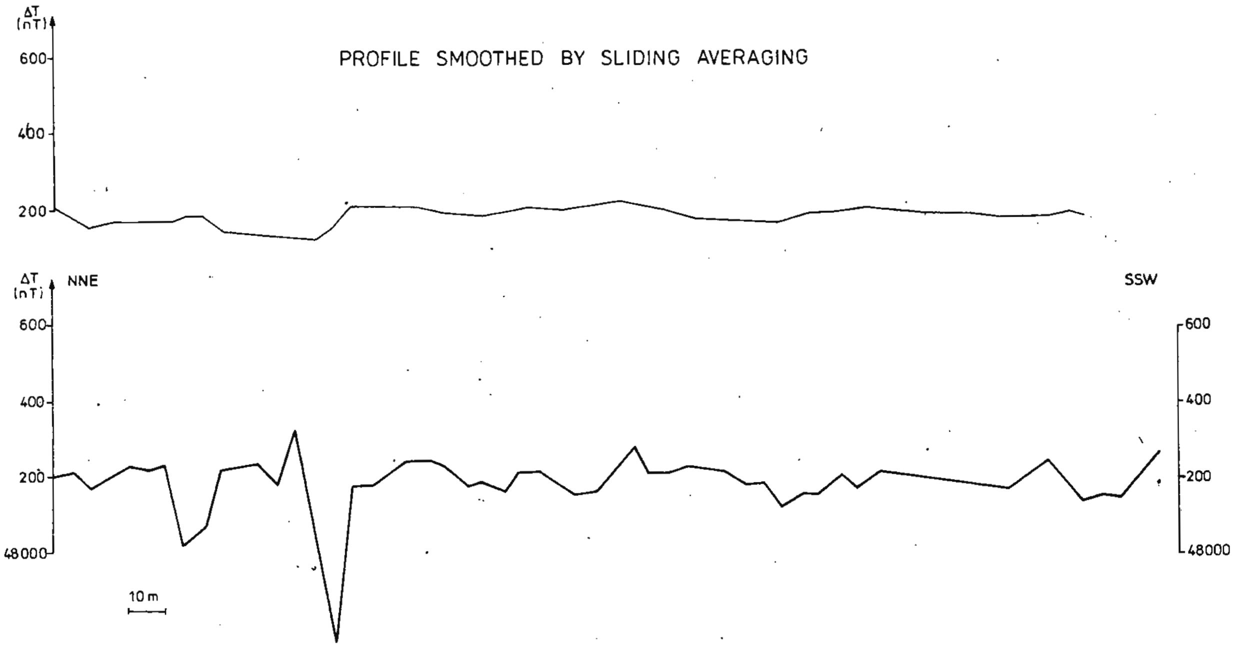

Fig. 7 – NNE-SSW magnetometric profile in the Dreptu Station area.

electromagnetic solar radiation which yields a system of currents in the ionosphere at about 100 km above the Earth's crust (Wienert, 1970). S_q variation for H, D, Z function of latitude is presented in Figure 8 which shows that the data obtained in our country are well placed within the general framework.

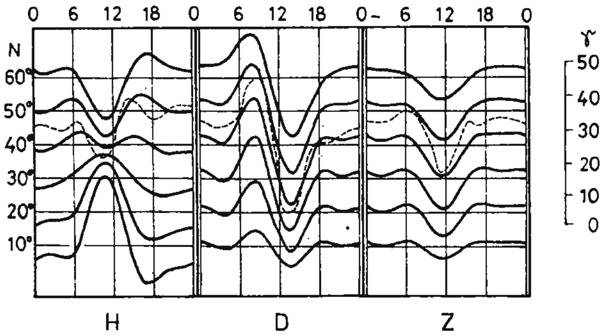

Fig. 8 – S_q variation in H, D, Z depending on latitude

The recordings made at the Dreptu Station and those at the Surlari Geophysical Observatory were also correlated statistically. The correlation coefficient r and the covariant S_{xy} for a succession of given data (x_i, y_i), i = 1, 2, ... n were established.

$$r = \frac{S_{xy}}{S_x S_y} \qquad -1 \leq r \leq 1$$

where

$$S_x = \sqrt{\frac{\Sigma x_i^2 - (\Sigma x_i)^2/n}{n-1}}$$

$$S_y = \sqrt{\frac{\Sigma y_i^2 - (\Sigma y_i)^2/n}{n-1}}$$

$$S_{xy} = \frac{1}{n-1}(\Sigma x_i y_i - \frac{1}{n}\Sigma x_i \Sigma y_i) \quad \text{or}$$

$$S_{xy} = \frac{1}{n}(\Sigma x_i y_i - \frac{1}{n}\Sigma x_i \Sigma y_i)$$

Using these relations for the geomagnetic recordings at the Surlari and Dreptu stations computations were made using a Hewlett-Packard computer. The digitizing of the recordings from tape recorders were made manually using a sampling interval of one hour, thus a set of 24 values and an end value for each geomagnetic component being observed (Tab. 1).

Table 1

Correlation of the scc phenomena at the Surlari Geophysical Observatory and the Dreptu Geomagnetic Station

Date	ΔD_S (mm)	ΔD_D (mm)	dD_S/dD_D	ΔZ_S (mm)	ΔZ_D (mm)	ΔH_S (mm)	ΔH_D (mm)	dZ_S/dH_S	dZ_D/dH_D
20–21 I - B	2.0	2.0	0.80	2.5	1.0	8.5	1.0	0.19	0.31
27–28 I - C	2.5	2.0	0.99	2.5	1.5	3.5	1.0	0.47	0.46
14–15 II - A	3.0	3.0	0.80	4.0	2.0	8.5	1.5	0.31	0.41
20–21 II - B	1.5	1.5	0.80	1.5	1.0	2.0	0.5	0.49	0.62
06–07 III- B	8.0	7.5	0.85	6.0	2.5	11.0	2.0	0.36	0.38
09–10 IV - A	3.0	2.0	1.23	4.0	2.0	8.0	1.5	0.33	0.29
04–05 V - A	10.0	9.0	0.91	8.0	5.0	21.5	4.0	0.25	0.29
07–08 VI - C	3.0	3.0	0.82	4.5	2.0	7.5	3.5	0.40	0.30
12–13 VII- C	2.0	2.0	0.82	4.0	2.5	10.5	5.0	0.25	0.27
14–15 VIII-A	3.0	2.5	0.97	6.0	3.0	10.5	4.5	0.38	0.36
20–21 VIII-A	5.5	5.5	0.90	6.5	3.0	14.5	5.5	0.30	0.29
23–24 VIII-A	4.5	4.0	0.93	7.5	2.5	12.0	5.5	0.41	0.27
28–29 VIII-A	2.0	1.5	1.10	5.0	2.0	8.5	3.5	0.39	0.31
11–12 IX - A	5.0	3.5	1.17	13.0	7.0	31.5	12.5	0.27	0.32
15–16 IX - C	2.0	2.0	0.82	3.0	2.0	7.0	3.0	0.28	0.38
26–27 IX - C	10.0	10.0	0.82	4.0	2.5	11.5	4.5	0.23	0.32
10–11 XI - C	2.5	1.5	0.92	4.0	2.0	9.0	11.7	0.29	0.17

Other phenomena under study were the sudden beginnings of a storm (*scc*). In 1986, about 33 events were recorded by the Surlari Geophysical Observatory and had correspondents at the Dreptu Station. Table 1 shows the representative results of the study effectuated, a good correlation between the recordings of the phenomena at the two observatories being observed.

The scale values of the Bobrov recorders at the two stations are presented in Tables 2 and 3 for each geomagnetic component.

The correlation of the ΔZ recordings at the Dreptu Station with those at the Surlari Geophysical Observatory was made for a period of six months (June-December, 1986) and the correlation of the geomagnetic components ΔD, ΔH and ΔT for a period of three months (October-December). The results of these correlations are given in Table 4.

Table 2
Scale values for 1986 at the Surlari Geophysical Observatory

T nT/mm	D ^{0}/mm	H nT/mm	Z nT/mm
1.969	0.324	1.766	1.164

Table 3
Scale values for 1986 at the Dreptu geomagnetic station

Month	T nT/mm	D ^{0}/mm	H nT/mm	Z nT/mm
June		0.394	4.73	2.46
July		0.394	4.69	2.56
August		0.394	4.59	2.47
September		0.394	4.46	2.56
October	2.93	0.394	4.46	2.56
November	2.58	0.585	2.05	1.97
December	2.56	0.560	2.01	2.13

Table 4
Statistic correlation between the data recorded at the Surlari Geophysical Observatory and the Dreptu geomagnetic station

Z						T			D			H		
June	July	Aug.	Oct.	Nov.	Dec.	Oct.	Nov.	Dec.	Oct.	Nov.	Dec.	Oct.	Nov.	Dec.
0.85	0.95	0.90	0.72	0.89	0.88	xx)	0.98	0.95	0.98	0.99	0.97	0.95	0.91	0.99
0.95	0.73	0.84	0.95	0.86	0.89	0.98	0.94	0.98	0.91	0.94	0.97	0.77	0.95	0.91
0.84	0.85	0.91	0.98	0.93		x)	0.97		0.92	0.98		0.91	0.99	
0.87	0.84		0.89	0.95					0.90			0.89		
	0.84		x)	0.87					0.98					
	0.81			0.80										
	0.72			0.81										
0.88	0.82	0.88	0.89	0.87	0.89	0.98	0.96	0.97	0.94	0.97	0.97	0.88	0.95	0.95

$r_Z = 0.87$; $r_T = 0.97$; $r_D = 0.96$; $r_H = 0.93$
x) Correlation obtained after the intervention....
xx) Lack of correlation

The data presented point out a good correlation between the recordings of the two stations.

Considering the good correlations and the protection conditions against the artificial perturbations, one may state that the new station entered into current operation in 1987.

In the near future a nonmagnetic pavilion, which has to protect the absolute measurements pillar and the organization of regular measurements for determining the recordings level are taken into account.

The fitting of a secondary equipment to ensure the mutual control and the continuity of the recordings in case of damage or technical intervention are also considered.

References

Chapman S., Bartels J. (1951) Geomagnetism. University Press, Oxford.

Constantinescu L. (1977) Contribuţia lui Ştefan Hepites la dezvoltarea geofizicii. *St. cerc. geol. geofiz. geogr., Geofiz.*, 15, p. 179–185, Acad. R. S. România, Bucureşti.

Iliceto V., Norinelli A., Soare A. (1972–1973) Indagini geofisiche per una stazione geomagnetica. *Atti e Memorie dell'Academia Pataniana*, LXXXV/II, Padova.

Wienert K. A. (1970) Méthodes d'observation et de prospection géomagnétiques. *Sciences de la terre*, 5, Paris.

x x x (1974) Harta aeromagnetică ΔT_a, foaia Topliţa, sc. 1:200.000, Institutul de Geologie şi Geofizică, Bucureşti.

x x x (1968) Harta geologică, foaia Topliţa, sc. 1:200.000, Institutul de Geologie şi Geofizică, Bucureşti.

Received: February 1, 1989
Accepted: February 1, 1989
Presented at the XIV-th Symposium of Earth's Physics and Applied Geophysics: July 1987

Rom. J. Geophysics, 1993, 16, p. 83–88

BIOGEOPHYSICAL METHOD IN HYDROGEOLOGY WITH APPLICATIONS IN THE IULIA ZONE (NORTH DOBROGEA)

Dan SVORONOS, Adrian NICOLESCU

Institutul de Geologie şi Geofizică. Str. Caransebeş 1, 78344 Bucureşti 32.

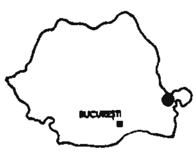

Key words: Geophysical methods. Biogeophysical reaction. Hydrodynamics. Ground water. Dobrogea.

Abstract: In the period 1971–1991 and especially after the year 1986 many papers dealt with "dowsing". As a result of these studies, at the Institute of Geology and Geophysics a new working method based on the biogeophysical reaction was introduced and tested (Patent no. 102 971, OSIM Romania). This paper deals with the biogeophysical method and its applications in the study of the water flows in porous-permeable mediums, of the active fractures and, generally, of the tectonic discontinuities in the geological environment. The biogeophysical method represents an efficient, rapid and cheap prospection way, which can be used either by itself or complementary to the geological and geophysical methods. Biogeophysics has many aspects in common with the traditional geoanthropogenous method but it is not identical with it. The biogeophysical surveys effectuated in North Dobrogea, in an areal overlain by cover deposits of the Babadag Basin, led to the drawing up of the map of the preferential circulation of the groundwater in the area of the study. A circulation was highlighted mostly on fractures which, older or younger, are hydrologically active only on certain portions; this makes difficult their identification by means of other methods, even by the classical hydrogeological ones.

General considerations

The present paper analyses theoretical and practical aspects of employment of a "biogeophysical" method. It is described the application of this method at the locating of water flows and hydrologically active fractures within the cover deposits of the Babadag Basin. In the Iulia-Nicolae Bălcescu zone of this basin the observation data led to the elaboration of a pattern of groundwater circulation.

The term "biogeophysics" was introduced in the Romanian literature after 1970, as a result of the surveys carried out at the Institute of Geology and Geophysics (Apostol et al., 1972; Svoronos, 1981, 1988; Svoronos et al., 1989). At present, by convention, biogeophysics represents the location techniques using as operators human sensors who are able to convey rationally interaction phenomena between human organisms, as unitary and integrable systems, and certain stressing physico-geological situations existing in the geological-geophysical medium (water flows in porous-permeable medium and the hydrogeologically active fractures are the most important). The biogeophysics cannot be mistaken for other methodologies based on the individual sensitivity of the subjects to the geological, physico-chemical, sanogenetic etc. stimuli (e.g. divining rod – Y-rod, L-rod a.s.o.). The difference between biogeophysics and dowsing consists first of all in the working method used during the first stage of the data perception (Svoronos et al., 1987–1990, unpubl. reports). The underground physico-geological systems, which may represent sources of the signals received by biological information, have been identified unequivocally – using the correlation between the geophysical observation and the geophysical data and using also the checking by means of the mine workings and drillings – and they have been named biologically disturbant geological bodies (Svoronos, 1988).

Biogeophysical prospecting principle

The movement of a human being along a course at the Earth's surface, in case of crossing the vertical of a disturbing geological body (water flow or circulated fracture), between the receiving biological system and the physico-geological system can become sentient under certain circumstances and it can be used in the geological prospecting.

The living-non-living interaction phenomena are known since earlier times: for their application our forefathers proved an unlimited cleverness although the natural explanations of the physico-biological mechanisms were entirely lacking or had no scientific substratum.

A study of the old methodologies used in the field (Y-rod, L-rod, Virgula divina, rhabdomancy, radiesthesia and in Romania the craft of the well sinkers or courciers or Wünchelrüte) can confirm that all the attempts (to find out springs, groundwaters, metalliferous veins) have various stages belonging to a long and complicated causative chain: geological stimulus – sensorial translation – rational translation – final response (at the level of the forearms), then again geological object a.s.o. For sensorial implication and highlighting of the results of the intercalations, the operator uses adequate working instruments, the V- or Y-shaped wooden rod handled on both ends is most often used (Fig. 1 a, b, c).

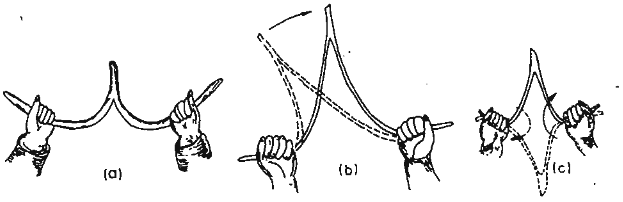

Fig. 1 Wooden rod and the traditional geoanthropogenous practice. (a), handling position; (b), (c), movement of the instrument and outlining of the effects of the interaction between the human organism and the disturbant geological body.

From the point of view of the field practice, between biogeophysics and the older or more recent techniques no essential differences have been observed, at least as regards the working instruments which remained the same (Fig. 2). The differences observed refer to the cause-effect (Svoronos et al., 1987–1988; unpubl. reports) relation and they originate in the working techniques by which certain weight is *a priori* attributed to the mental component as well as to the geological setting scientifically proved in which such investigations are used.

At present, it is well known that any method based on interaction phenomena with human implication relies on the operation mechanism within which the cortex is involved to a certain extent and this particularity makes the respective methods more or less active. The specification of the participation of the cortex in the development of such a phenomenon can be indicated only qualitatively and for this reason up till now there has been no systematic approach of the working methodology. That is why for the researcher in this domain the field practice consists not only in establishing the phenomena (it occurs operationally at about 25 per cent of the individuals) but also the working methodology, the separation of the sources and interpretation of the observations within a given geological framework.

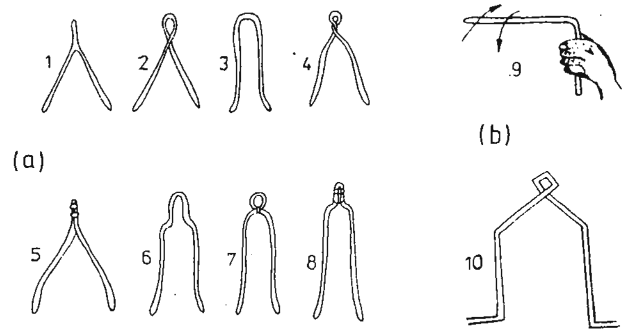

Fig. 2 – Types of instruments known in the geological biolocation. (a), old: wooden (1); wire of the same metal (2, 3, 4); wire of different metals (5, 6, 7, 8). (b), recent: metallic frames or glass fibres (9, 10).

The biogeophysical practice has been introduced for experimental reasons: the repetatibility and reproduction of the observations, the specific content of the biogeophysical information, the acceptable accuracy, the relatively low cost price and the necessity of a complex and unitary interpretation of a large bulk of data (Stoici et al., 1979; Bulgăreanu et al., 1987; Svoronos et al., 1989). As regards the biogeophysical technique, it marks and delimits the receiver quality of the human organism unlike other working techniques which do not make such a distinction and are based mostly on the human organism as a transmitter (Svoronos et al., 1989).

When the human operator effectuates the crossing of the chosen working profile (at random or possibly relying on general geological-geophysical data, without preconceived ideas) he does not expect it to happen certainly. However, regardless of his will, at a certain moment he finds out that the working instrument starts moving. This way of undeliberate manifestation is typical of an interaction between human organism and disturbing geological body and it is called biogeophysical reaction (Svoronos, 1988).

Practising this method the individual who effectuates the biolocation learns from his own experience, which suggests that a feed-back circuit between him and the environment is established. This feed-back probably operates with the participation of the unconscious part of the brain, the movement of the working instrument facilitating the rational translation of the signals received by sensors. The phenomenon takes place only if the intensity of the stimuli from the geological framework overpasses a certain threshold and it ceases when it decreases below the threshold.

Therefore, the prospection is based on the biogeophysical reaction which takes place when the operator comes closer, crosses or goes farther from the disturbing geological body in the profile, when he is able to understand an interaction phenomenon highlighted and even amplified by the movement of the instrument that is used. This phenomenon is fairly complex, the biogeophysical reaction described by the movement of the working instrument being decomposed into a regular succession of biological signals to each element corresponding to a certain muscular tonus of the operator's arms.

A study of this phenomenon from the biomechanical point of view at the level of the operator's hand will show that the forearm handles the instrument in two different ways: by a flexion and extension movement at the level of the elbow, and by a rotation movement of the forearm around the longitudinal axis – the pronosupination movement. Considering the energetic aspects of the muscular activity generated by the two simultaneous movements, the specific energetic features of the subsoil sources and the experiments effectuated with the view of objectivity of the biogeophysical reaction, we inferred that the connection between a disturbant geological body and the human organism (operator) is of energo-informational type (Svoronos, 1988).

Working methods

The field measurements technique consists in the covering of the profile by two or more operators with a view to highlighting and recording the biogeophysical reaction according to known working techniques (Apostol et al., 1972; Stoici et al., 1979; König, Betz, 1989).

Before starting the measurements, the prospector establishes an initial standardization position of the instrument or of the framework within which he will operate (Figs. 1, 2) trying to maintain the same position of the forearms. This can be achieved only within certain limits imposed by the handling position of the instrument used and by the relatively unstable character of the biophysical system in the course of movement with a relatively constant speed (Fig. 1 b, c).

The receiving instrument is considered to consist of an active part – the human organism – and a passive part – the working rod held by the operator in a certain position. The receiver line is represented by the forearm and its prolongation up to the edge of the working instrument, and the feed line by the disturbant geological body and its projection on the surface. In case of the utilization of the wooden rod, the receiver contains two identical channels with the top of the rod as common point.

While crossing the vertical projection of an underground water or circulated fracture, a movement of the instrument can be noticed in relation to the initial standardization position; graphically, it can be compared with a network of topographic markings taking into account the rotation sense of the working instrument.

The characteristic parameters I_s, m, M, S_s and D, d and L (see Fig. 3) represent the elements of a biogeophysical reaction; as a rule, they are enough for a general presentation of the interaction phenomenon in relation to the distance covered. The symmetry axis of the diagram coincides with the projection on the surface of the water flow or circulated fracture.

The recording of the elements rendered in Figure 3 does not refer directly to the amplitude of the biogeophysical reaction (that is the number of the rotations effectuated in one sense or another); it is related to the modification of the state of the initial standard contraction of the arm muscles that cannot be sufficiently controlled. However, usually the operator feels easily that the muscular contractions are spontaneous impulses, strictly connected one to another and in a logical succession. Concurrently with the perception of an impulse at a certain time, the human operator tries to maintain the state muscular contractions at the level considered at the beginning of the observations. The way of development of the driving act decisive for the movement of the instrument highlights a group of chain reflexes. The diagram in the figure represents such a conventional model for the complex movements of the work instrument resulting from the estimation of the stimuli – response relation (S_1 - R_1; S_2 - R_2.....S_n - R_n) from the point of view of the feedback adherence. The map location of the parameters I_s, m, M, S_s means in fact the identification of the main stages of an energo-informational process of the human operator involved in action. Consequently the movement senses of the work instrument are regarded as the "parameter" of the measurement, namely the information useful for the pointing out and identification of the source.

The choosing of the work profiles, the thickness of the network, and the direction of the profiles represent problems raised and dealt with similarly with those known in the geophysical prospecting. The operator pursues that the direction of the work profile should preserve its perpendicular position in relation to the projection on the surface of the disturbant geological source.

The particularity of an underground water flow to have a sinuous course requires often the reorientation of the work profiles; this presumes the carrying out of a large number of profiles and shows the adaptability of the method to a real geological situation.

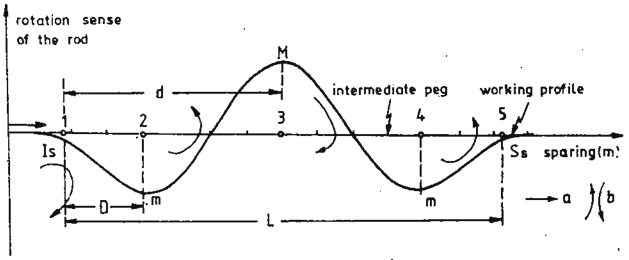

Fig. 3 – Graphic representation of the biogeophysical reaction in case of water flows or circulated fractures.
1, beginning of signals (I_s); 2, first minimum; 3, maximum; 4, second minimum; 5, end of signals (S_s); L = width; a, moving direction along the profile; b, rotation senses of the work instrument versus the initial position.

The field practice points out the possibility to estimate the sense of the water flow in accordance with biodynamic effects observed by the human operator when he is using a specific work method.

Biogeophysical model of the underground water circulation in the Iulia Zone

The study area lies in the interference zone between the southern frontal part of the Măcin Nappe and the Niculiţel Nappe, on the one hand, and the post-tectonic cover, on the other hand (Săndulescu, 1984), in the area of the localities of Iulia and Nicolae Bălcescu, being bordered by the Consul Hill northwards, the Taiţa Valley eastwards, and the Carierii–La Carieră Hill south and south-westwards.

The biogeophysical mapping of this zone and the correlation of the results with the geological evidence made possible the elaboration of an improved structural-tectonic image (Fig. 4).

The disposition of the fractures according to the draft led to the confirmation by biogeophysics of some major NW-SE trending tectonic accidents and at the same time to detailed information concerning the delimitation of the main units: the Măcin Unit from the Consul Unit, marked by Luncaviţa-Consul tectonic line, and the Consul Unit from the Niculiţel Unit, marked by the Meidanchioi-Iulia tectonic line. As compared with the course indicated by geophysical data, the Luncaviţa-Consul line is outlined farther westwards up to the Nicolae Bălcescu locality, where the Consul Unit becomes narrower until it vanishes.

A system of NE-SW-NS trending tectonic accidents has been identified. The faults constituting it are younger as indicated by the biogeophysical results on the two major lines mentioned above. Most of these tectonic accidents do not show important slips or falls; there are, however, some exceptions e.g. the main faults which crosses approximately NNE-SSW the zone of the Iulia ore deposits and delimits an uplifted northwestern area from a sunk southeastern one (Fig. 4). The known iron ores are represented by six groups of mineralized bodies occurring in the uplifted compartment, most of them concealed by cover deposits. According to the strike-slips of the major fault, three segments have been delimited, among them the central one is found in the mining field area, nearby the southeastern end of the trend line of horizon – 246.

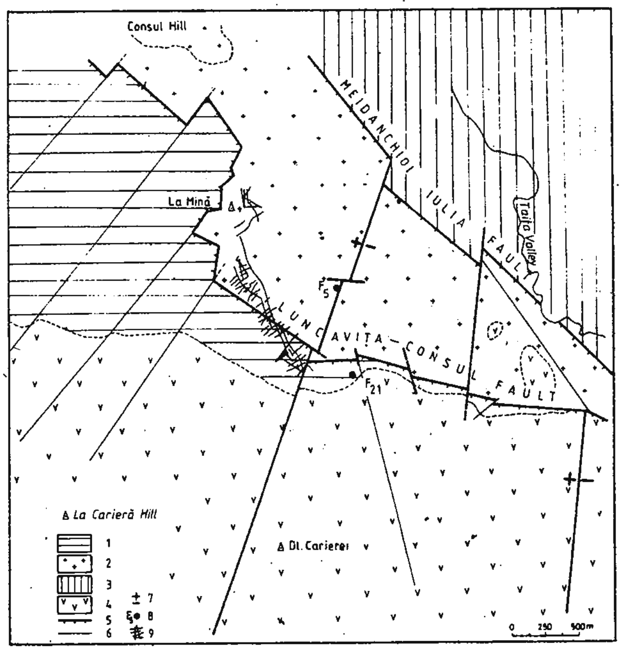

Fig. 4 – Tectonic structural draft of the Iulia Zone.
1, Măcin Unit; 2, Consul Unit; 3, Niculiţel Unit; 4, post-tectonic cover; 5, reverse longitudinal faults from the major NW-SE structure; 6, recent (transcurrent) faults; 7, uplifted compartment/sunk compartment; 8, F_5, F_{21} structural boreholes; 9, projection of the mine workings on the Earth's surface.

The initial structural-tectonic image has been completed with biogeophysical data with the view of locating fractures, water flows and estimating the direction of the water flow on fractures. Thus, the hydrogeological map has been elaborated (Fig. 5).

The correlation of the geological and partially geophysical (electrometric) data with the biogeophysical measurements made possible the identification of the water sources and the elaboration of a pattern for the underground waters circulation, as follows:

a) In the study area the water flows in the cover deposits of the Babadag Basin are active in the spreading area of the Coniacian deposits. The Coniacian limestones are porous-permeable rocks which can form aquifers when they are delimited by imprevious rocks as hydrologic protection screens, the latter consisting of Turonian limestones.

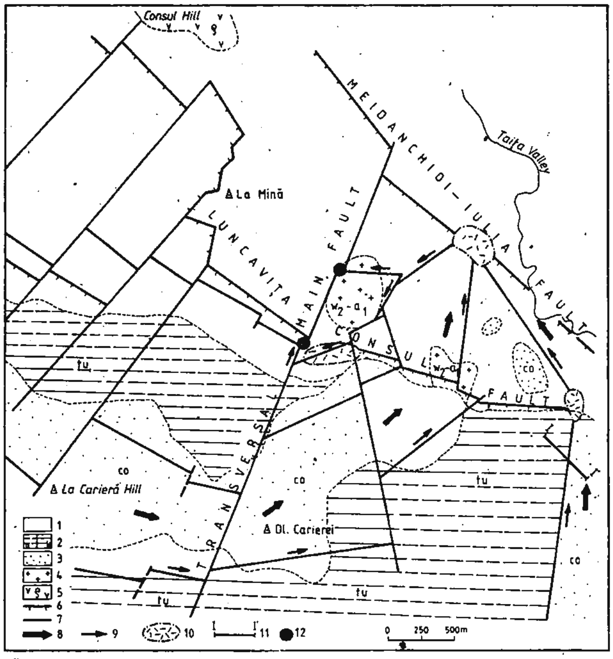

Fig. 5 – Geological map with hydrological elements in the Iulia Zone.
1, loess deposits; 2, Turonian limestones (tu): a, loess subcover; b, exposure; 3, Coniacian limestones (co); 4, Triassic (Lower + Middle, w_2-a_1) limestones; 5, rhyolites; 6, reverse faults; 7, hydrologically active tectonic accidents; 8, water flows; 9, sense of the water flow along the fracture; 10, areas of high fissure permeability; 11, VES cross-section; 12, places of the ground waters in-put in the ore deposit.

The flow is in accordance with the hydrodynamic laws, towards more and more sunk deposits, as pointed out also by the correlation with geomorphologic elements (Fig. 6). The main supply zones are represented by the areal north and northwest of the Carierii Hill, including La Carieră Hill-Carierii Hill and the zone in the vicinity of the locality of Nicolae Bălcescu comprising the Cazu Mare Hill.

b) A gradual circulation of the underground waters related to structural-tectonic features is highlighted on fractures.

The tectonic lines from the major structure are generally less circulated, even not circulated except for certain restricted areals, such as those nearby the thrust line Meidanchioi-Iulia where the identified fractures are active on some portions.

The faults of the NE-SW up to NS system are more intensely circulated; however, two situations can be distinguished: the former refers to the tectonic accidents in the uplifted compartment, where the water circulation is usually superficial, mostly at the base of the loess; the latter refers to the tectonic accidents in the sunk compartment where the circulation is usually deeper depending on the degree of the fracture development on the vertical (Fig. 7).

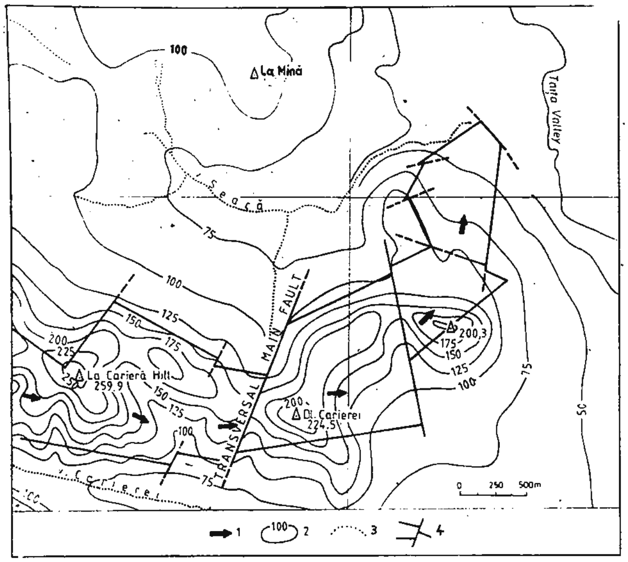

Fig. 6 – Preferential flow of the groundwater in correlation with geomorphological elements in the La Carieră Hill-Carierii Hill-Taița Valley Zone.
1, flow sense by infiltration; 2, level curve; 3, paleovalley; 4, tectonic accidents.

Most intensely circulated are the tectonic accidents in the interference zone of the two fracture systems mentioned: longitudinal and transversal. It is notable the median segment of the major fault and some faults in the narrowing zone of the Consul Unit, west of the locality of Nicolae Bălcescu.

The biogeophysical stability of the underground circulation made possible the identification of the influx ways of the superficial and underground water in the known ore deposit (Fig. 5).

The pattern presented before is in agreement with the results of the previous hydrogeological surveys; however, it brings further detailed data concerning the clearing up of the hydrogeological conditions of the Iulia ore deposit and, generally, on the underground water circulation in the cover deposits of the Babadag Basin.

Conclusions

The biogeophysical method consists in the pointing out of involuntary effects, induced and perceived by a human operator under certain conditions, when coming closer, crossing or going farther from a disturbant geological body.

For the application of the biogeophysical methodology adequate instruments are used, which represent a real prolongation of the human organism (receiver).

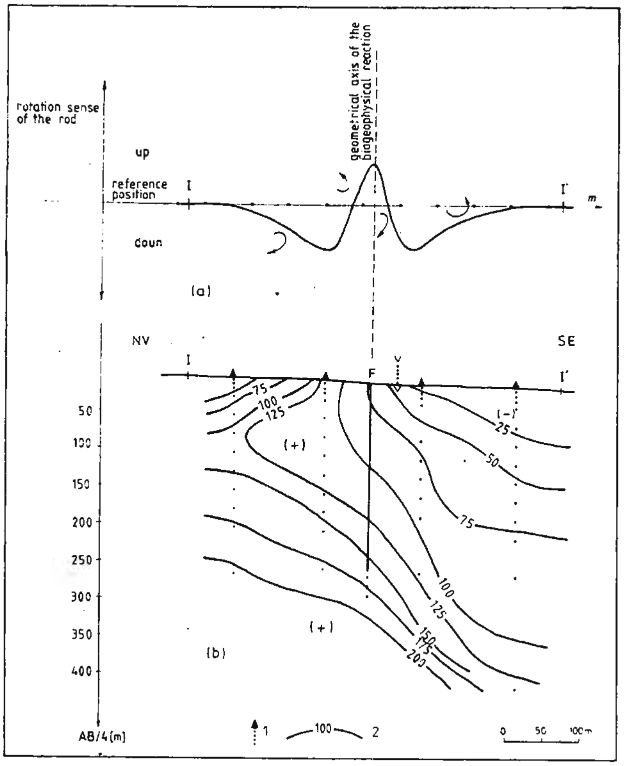

Fig. 7 Preferential flow of the groundwater along a fracture in the southeast of the Iulia Zone (profile I-I in Fig. 5). (a), biogeophysic profile; (b), section of vertical electrical soundings; F, circulated fracture; 1, sites of the electrical soundings on the topographic profile; 2, isoohm.

Concomitantly with the sensorial implication in the course of the dowsing process an ordered movement or the work instrument occurs, which facilitates the rational translation of the effects of an interaction living-geological medium which finally makes possible the location of the active discontinuities in the subsoil mainly of the tectonic accidents and of the water flow in porous-permeable mediums.

The interaction phenomenon on which the method is based is known as biogeophysical reaction and the rotation sense of the work instrument is considered the parameter of the prospection.

Received: Mars 4, 1993
Accepted: October 12, 1993

The field application in the Iulia-Nicolae Bălcescu zone pointed out the main porous-permeable mediums and the active hydrogeological fractures were located.

A pattern of the underground water circulation in the study zone was elaborated, with economic implications in the solving of the hydrogeological problem of the Iulia mine.

References

Apostol A., Ionescu Fl., Pricăjan A., Săhleanu V. (1972) Asupra unor informaţii de natură biologică întîlnite în practica geologică. *Rev. min.*, XXIII, 7, Bucureşti.

Bulgăreanu V. A. C., Olteanu E., Rădulescu I., Feurdan V., Lascu C., Svoronos D. (1987) Geodynamics and the water circulation in the salt massif lake area Baia Baciului-Baia Neagră-Baia Miresii (Slănic-Prahova, România. *Theoretical and Applied Karstology*, 3, p. 165–174, Bucureşti.

König H. L., Betz H. D. (1989) Der Wünchelruten Report, Wiessenschaftlicher Untersuchungsbericht. München Universität, Germany.

Săndulescu M. (1984) Geotectonica României. Ed. tehn., Bucureşti.

Stoici S. D., Apostol A., Svoronos D., Andriescu Gh. (1979) Asupra unor corelaţii dintre informaţii de natură geologică, geofizică, geochimică şi biogeofizică obţinute în Valea Băii (Munţii Bihor). *D. S. Inst. Geol. Geofiz.*, LXVI, p. 115–122, Bucureşti.

Svoronos D. (1981) Manifestarea fenomenului biogeofizic ca informaţie, în vol.: Fenomene bioenergetice în ecosistem. Al III-lea Simpozion - Bazele biologice ale proceselor de epurare şi protecţia mediului, p. 219–233, Bistriţa.

— (1988) Experimental Researches for Objectifying the Biogeophysical Reaction. *St. tehn. econ.*, D, 15, p. 69–84, Bucureşti.

— , Nicolescu A., Nicolaescu L. (1989) Termeni şi concepte în biodetecţie, în vol.: Realizări în domeniul electronicii profesionale. 2, p. 74–78, Snagov.

— , Nicolescu A. (1991) Method and device for pointing out and discriminate underground discontinuities: R R patent no. 102 971.

Rom. J. Geophysics, 1993, 16, p. 89–99

LE CHAMP NORMAL DE LA PESANTEUR SUR LE TERRITOIRE DE LA ROUMANIE

Marius VISARION

Institutul de Geologie şi Geofizică. Str. Caransebeş 1, 78344 Bucureşti 32.

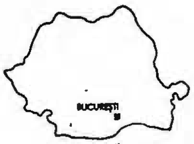

Key words: Gravity surveys. Gravity field. Gravimetry. Geoid. Geodetic coordinates. Geophysical methods. Formula. Romania.

Abstract: *Normal Gravity Field on the Romanian Territory.* The reduction of a normal field is at present differently calculated, either by the Helmert formula (1901), which applies gravity data to physical geodesy, or by the Cassinis formula (1930) for drawing up of the gravimetric maps on different scales. The present paper proposes a unitary reduction system based on the international formula adopted at the 17-th IUGG General Meeting (GRS–1980). Therefore the normal field values have been calculated between $43^0 30'$ and $48^0 30'$ latitudes, which delimits the territory of our country, at $10''$ intervals. Rapid ways for transferring the available values to the new system are presented.

L'élaboration des cartes gravimétriques de divers types (Faye, Bouguer, isostatiques etc.) exige la réduction de champ normal, tant pour les valeurs mesurées dans les réseaux d'ordre supérieur, que pour celles mesurées dans les stations des réseaux afférents aux travaux de prospection aussi. La connaissance du champ normal de la pesenteur est nécessaire aussi pour la résolution des problèmes de géodésie physique. À présent, on utilise, dans l'activité de prospection, la formule de Cassinis, adoptée à la IV-ème Assemblée Générale de l'U.I.G.G. (Stockholm, 1930). Après cette formule, Botezatu et Ştefănescu (1963) ont calculés les valeurs normales pour le territoire de la Roumanie, à des intervalles de latitude de $10''$. Dans l'activité géodésique, qui a adopté l'ellipsoïde de Krasovski (1940) comme ellipsoïde de référence on utilise la formule Helmert (1901).

La présente étude propose un système unitaire d'évaluation du champ normal pour le territoire de la Roumanie, ayant à la base la formule internationale du Système Géodésique de Référence (SRG) 1980, adoptée à la XVII-ème Assemblée Générale de l'U.I.G.G. Dans ce sens nous reproduissons, selon Moritz (1980) la résolution no. 1 de l'Association Internationale de Géodésie (A.I.G.).

"L'association Internationale de Géodésie, en reconnaissant qu'à la XVII-ème Assemblée Générale de l'U.I.G.G., a été introduit un nouveau Système Géodésique de Référence 1980, recommende l'emploi de celui-ci en tant que système officiel de référence pour les travaux géodésiques et encourage le calcul du champ de la pesanteur à la surface ainsi que dans l'espace extérieur, fondé sur ce système."

L'adoption de la formule internationale dans le S.G.R.–1980, pour tous les travaux exécutés, ou à réaliser à l'avenir, rend possible la comparaison des anomalies évaluées et la corrélation de la carte gravimétrique nationale avec celles réalisées dans les pays voisins. Sa détermination à base de l'ellipsoïde géocentrique équipotentiel assure l'utilisation d'une surface de référence unique pour la détermination de toutes les données gravimétriques liées à la direction ou à l'intensité du champ de la pesanteur.

On a apprécié que l'établissement des valeurs du champ normal pour tout le territoire de la Roumanie, à des différentes valeurs de la latitude géodésique et pour des intervalles de $10''$ entre celles-ci contribuirait au développement harmonieu des travaux gravimétriques.

L'évolution des idées concernant le champ normal de la pesanteur

Les formules pour l'évaluation du champ normal ont été modifiées le long du temps, en rapport avec le progrès de la connaissance des paramètres de l'ellipsoïde général de référence et avec les modifications apportées à la valeur absolue de la gravité dans la station fondamentale de Potsdam, qui influence la détermination des valeurs de cette grandeur à l'équateur et au pol.

Le tableau 1 présente quelques formules d'évaluation du champ normal de la gravité. Le plus souvent, dans ces formules, la forme de la Terre a été exprimée par des ellipsoïdes homogènes de révolution. On a proposé aussi des formules où la forme de la Terre a été exprimée par des ellipsoïdes à trois axes, avec l'apparition d'un terme de longitude. Ces formules n'ont pas été largement utilisées. En partant de l'équation fondamentale établie par Clairant on est arrivé donc à des solutions assez simples, représentées par des formules qui décrivent la variation de la gravité normale comme une fonction des paramètres physiques de la terre choisis par chaque auteur. La première solution concernant la liaison entre la gravité normale, la latitude géodésique et les paramètres de l'ellipsoïde terrestre de référence, élaborée par Pizzetti (1894, 1913) a été ultérieurement mise sous une forme mathématique élégante par Somigliana (1929, 1933).

l'ellipsoïde international de référence Hayford, adopté par U.I.G.G. à la deuxième Assemblée Générale de Madrid (1924). D'autres auteurs (Jongolovici, 1952, Heiskanen, 1957) ont employé seulement des données gravimétriques, en utilisant les valeurs moyennes de la pesanteur dans la plupart des secteurs à une surface de $1^0 x 1^0$ (4378 et, respectivement, 6679 secteurs). Ces formules ont été moins utilisées à cause de la distribution non uniforme des mesures gravimétriques sur le globe terrestre, à des espaces non investigués dans les zones océaniques.

Parmi ces formules, une large application, inclusivement dans notre pays ont connu les formules de Helmert (1901) et de Cassinis (1930). Depuis 1967 on a appliqué la formule internationale en SGR–1967, mais ce système ne s'est pas généralisé. Dans certaines pays, parmi lesquels la Roumanie, où l'ellipsoïde de référence est l'ellipsoïde de Krasovski (1940), on a poursouivi l'utilisation de la formule de Helmert (1901) pour résoudre les problèmes de géodésie physique.

Tableau 1

Formules proposées pour le calcul du champ normal de la pésanteur

Auteur	Année	Formule proposée
Helmert	1901, 1909	$\gamma = 978{,}030\ (1 + 0{,}005302 \sin^2 B - 0{,}000007 \sin^2 2B)$
Bowie	1917	$\gamma = 978{,}039\ (1 + 0{,}005294 \sin^2 B - 0{,}000007 \sin^2 2B)$
Heiskanen	1924	$\gamma = 978{,}052\ [1 + 0{,}005285 \sin^2 B - 0{,}000007 \sin^2 2B + 0{,}000027 \cos^2 B . \cos 2(L-18^0)]$
Heiskanen	1928	$\gamma = 978{,}049\ (1 + 0{,}005289 \sin^2 B - 0{,}000007 \sin^2 2B)$
Cassinis	1930	$\gamma = 978{,}049\ (1 + 0{,}0052884 \sin^2 B - 0{,}0000059 \sin^2 2B)$
Berroth	1949	$\gamma = 978{,}03630\ (1 + 0{,}0052884 \sin^2 B - 0{,}0000059 \sin^2 2B)$
Jongolovici	1952	$\gamma = 978{,}0573\ (1 + 0{,}0052837 \sin^2 B - 0{,}0000059 \sin^2 2B)$
Heiskanen	1957	$\gamma = 978{,}0497\ (1 + 0{,}0052902 \sin^2 B - 0{,}0000059 \sin^2 2B)$
Gruşinski	1960	$\gamma = 978{,}0531\ (1 + 0{,}0052883 \sin^2 B - 0{,}0000059 \sin^2 2B)$
Formula internaţională SGR	1967	$\gamma = 978{,}03185\ (1 + 0{,}005278895 \sin^2 B + 0{,}000023462 \sin^4 B)$
Eremeev-Jurkina	1974	$\gamma = 978{,}030\ (1 + 0{,}005280 \sin^2 B - 0{,}000023 \sin^4 B)$

Quelques formules ont été établies uniquement sur la base des données gravimétriques soit par l'emploi des données existents dans un nombre assez grand de points, soit par l'utilisation des valeurs moyennes par secteurs, les systèmes des équations résultés étant résolus par la méthode des plus petits carrées. Ainsi la formule de Helmert (1901) a été établie sur une base de 1803 mesures gravimétriques auxquelles on avait appliqué la réduction Faye. Dans une première variante, Helmert (1884) a appliqué la méthode de la condensation pour la réduction des valeurs de la pesanteur sur la surface de référence. Cassinis (1930) a utilisé les données gravimétriques uniquement pour déterminer la valeur normale à l'equateur, les autres coeficients étant déterminés par rapport aux paramètres de

Pour l'élaboration des cartes gravimétriques nationales on a employé la formule de Cassinis (1930) (tableau 1). Pour la valeur normale à l'equateur on a adopté $\gamma = 9{,}78049\ ms^{-2}$ provenant des études effectuées par Heiskanen (1929), Soler (1931) et d'autres. Ultérieurement on a observé que la valeur adopté n'étant pas adéquate, étant donné les erreurs des mesures absolues à Potsdam, point de référence fondamental du réseau gravimétrique mondiale. À la base des mesures absolues et relatives intercontinentalles effectuées dès 1949, l'Association Internationale de Géodésie a décidé en 1967 la modification de la valeur absolue de la pesanteur dans le point de référence Potsdam avec -14 mgal, de $9{,}81274\ ms^{-2}$ à $9{,}81260\ ms^{-2}$ (AIG, 1971, publication spéciale 3).

De manière subordonnée, l'application de la formule de Cassinis introduit des erreurs, aussi par la modification des paramètres numériques lorqu'on passe de l'ellipsoïde de référence de Hayford à celui de 1967 et ultérieurement à celui de 1980.

• En adoptant la valeur de la pesanteur normale à l'equateur de la formule de Helmert et en calculant, les autres coeficients en accord avec les paramètres géométriques de l'ellipsoïde, Krasovski, Eremeev et Jurkins (1974) ont élaboré une nouvelle formule (tableau 1), recommandée pour être utilisée dans des services géodésiques des pays de l'Europe Orientale.

De cette brève présentation de l'évolution des idées concernant l'évaluation du champ normal de la pesanteur résulte nettement le caractère conventionnel des formules élaborées et la perspective de nouvelles modifications mineures à SGR–1980. L'adoption de ce système est indiqué parce qu'il assure la résolution souple et élégante des problèmes de la géodésie ellipsoïdale, ainsi que le calcul rigoureux du champ normal de la surface terrestre et de l'espace extérieur, comme système de référence pour la gravimétrie et la géodésie physique, inclussivement la géodésie satélitaire. Selon une opinion exprimée, il faut établir un consens pour l'utilisation de cette formule dans les activités de gravimétrie géodésique et de prospection de notre pays (Ghiţău, 1983).

Le système géodésique de référence 1980

Le Système Géodésique de Référence 1980 est fondé sur la théorie de l'ellipsoïde géocentrique équipotentiel. La pésanteur normale sur un ellipsoïde équipotentiel de révolution est déterminée, de manière univoque, par quatre constantes: sémiaxes a, b de l'ellipse méridienne, la vitesse angulaire de rotation ω et la masse totale de la terre M, en accord avec le théorème de Stokes-Poincaré, n'importe quelle soit la distribution des densités à l'intérieur du globe terrestre. Mais on peut utiliser aussi d'autres quatre constantes. U.I.G.G. a élu les suivantes constantes de base:

$a = 6\ 378\ 137$ m – rayon équatorial (sémiaxe grande de l'ellipse méridianne);

$GM = 3\ 986\ 005.10^8$ m^3s^{-2} – constante gravitationelle géocentrique;

$J_2 = 108\ 263.10^{-8}$ – le facteur de la forme dynamique de la Terre;

$\omega = 7\ 292\ 115.10^{-11}$ rad.s^{-1} – la vitesse angulaire de rotation.

Les autres constantes géométriques et physiques dérivent de celles fondamentales. Dans l'annexe 1 sont reproduites, d'après Moritz (1980), les valeurs numériques de ces constantes. Les aspects théoriques concernant les formules de détermination de ces constantes sont largement présentées dans les travaux de spécialité (Heiskanen, Moritz, 1967; Dragomir et al., 1977; Ghitău, 1983).

La théorie standard de l'ellipsoïde équipotentiel considère que le potentiel normal est une fonction harmonique dans l'espace environnant de l'ellipsoïde. Dans ces conditions SGR–80 est ainsi définie qu'il inclut tout la masse de la Terre, y compris l'athmosphère, considérée comme une couche superficielle condensée au-dessus de l'ellipsoïde. Ainsi les formules de calcul pour la détermination des constantes géométriques et physiques ignorent la présence de l'athmosphère. Pour les cas où on doit prendre en considération l'effet de l'athmosfère, on a élaboré des tableaux qui indiquent la correction qu'on doit ajouter aux valeurs mésurées de la pesanteur (A.I.G., 1971; Moritz, 1980).

Les valeurs du champ normal de la pesanteur sur le territoire de la Roumanie

Le calcul de la réduction de champ normal a été réalisé en partant de la formule internationale:

$\gamma = 9{,}780\ 326\ 7715\ (1 + 0{,}005\ 279\ 0414 \sin^2B + 0{,}000\ 023\ 2718 \sin^4B + 0{,}000\ 000\ 1262 \sin^6B + + 0{,}000\ 000\ 0007 \sin^8B)$.

Les résultats obtenus étant données en ms^{-2} en S.I. Etant donné que dans la gravimétrie, tant dans notre pays qu'au plan mondial aussi, on emploi toujours les unités "gal" et "mgal", le passage d'un système a un autre est simple, conformément à la formule de conversion:

$$1 \text{ gal} = 10^{-2} ms^{-2}$$

L'intervalle de latitude choisi pour le calcul est de 10″, fait qui assure une variation linéaire de la réduction de champ normal, en permettant l'interpolation assez précise des valeurs de cette réduction pour les différentes valeurs de la latitude géodésique comprise dans cet intervalle.

Les résultats obtenus sont compris entre $43^0 30'$ et $48^0 30'$. Les valeurs ont été déterminées automatiquement par un ordinateur de type CORAL–4021, ayant comme base quelques programmes élaborés dans le cadre de l'Institut de Géologie et Géophysique. Les calculs ont été exécutés avec une erreur relative de 10^{-10}, correspondant à 10^{-3} $ms^{-2} = 10^{-4}$ mgal et controlées pour la latitude de 45^0 avec la valeur donnée par Moritz (1980). Pour faciliter l'emploi des tableaux, les valeurs du champ normal sont données avec 9 décimales en ms^{-2}.

À la fin du tableau sont présentées aussi les différences tabulaires entre les valeurs successives à 10″ à des intervalles de 5′ où la linéation du champ normal est assurée. De cette manière les valeurs du champ normal peuvent être aisément calculées par l'interpolation pour n'importe quelle station gravimétrique dont la

La réduction de champ normal pour le territoire de la Roumanie, calculée à des intervalles de 10″ latitude, selon la formule internationale en S. G. R.-1980.

γ = 9,80......ms^{-2}						43^0					
30′00″	4 842 307	35′00″	4 917 619	40′00″	4 992 942	45′00″	5 068 277	50′00″	5 143 622	55′00″	5 218 977
10	4 844 817	10	4 920 129	10	4 995 453	10	5 070 788	10	5 146 133	10	5 221 489
20	4 847 327	20	4 922 640	20	4 997 964	20	5 073 299	20	5 148 645	20	5 224 001
30	4 849 838	30	4 925 150	30	5 000 475	30	5 075 811	30	5 151 157	30	5 226 513
40	4 852 348	40	4 927 661	40	5 002 986	40	5 078 322	40	5 153 669	40	5 229 025
50	4 854 858	50	4 930 172	50	5 005 497	50	5 080 834	50	5 156 180	50	5 231 537
31′00″	4 857 368	36′00″	4 932 682	41′00″	5 008 008	46′00″	5 083 345	51′00″	5 158 692	56′00″	5 234 049
10	4 859 879	10	4 935 193	10	5 010 519	10	5 085 856	10	5 161 204	10	5 236 561
20	4 862 389	20	4 937 704	20	5 013 030	20	5 088 368	20	5 163 716	20	5 239 073
30	4 864 899	30	4 940 215	30	5 015 541	30	5 090 879	30	5 166 227	30	5 241 585
40	4 867 410	40	4 942 725	40	5 018 052	40	5 093 391	40	5 168 739	40	5 244 097
50	4 869 920	50	4 945 236	50	5 020 564	50	5 095 902	50	5 171 251	50	5 246 609
32′00″	4 872 430	37′00″	4 947 747	42′00″	5 023 075	47′00″	5 098 414	52′00″	5 173 763	57′00″	5 249 121
10	4 874 941	10	4 950 257	10	5 025 586	10	5 100 925	10	5 176 274	10	5 251 634
20	4 877 451	20	4 952 768	20	5 028 097	20	5 103 436	20	5 178 786	20	5 254 146
30	4 879 961	30	4 952 279	30	5 030 608	30	5 105 948	30	5 181 298	30	5 256 658
40	4 882 472	40	4 957 790	40	5 033 119	40	5 108 459	40	5 183 810	40	5 259 170
50	4 884 982	50	4 960 301	50	5 035 630	50	5 110 971	50	5 186 322	50	5 261 682
33′00″	4 887 493	38′00″	4 962 811	43′00″	5 038 142	48′00″	5 113 483	53′00″	5 188 834	58′00″	5 264 194
10	4 890 003	10	4 965 322	10	5 040 653	10	5 115 994	10	5 191 346	10	5 266 706
20	4 892 514	20	4 967 833	20	5 043 164	20	5 118 506	20	5 193 857	20	5 269 219
30	4 895 024	30	4 970 344	30	5 045 675	30	5 121 017	30	5 196 369	30	5 271 731
40	4 897 534	40	4 972 855	40	5 048 186	40	5 123 529	40	5 198 881	40	5 274 243
50	4 900 045	50	4 975 366	50	5 050 698	50	5 126 040	50	5 201 393	50	5 276 755
34′00″	4 902 555	39′00″	4 977 877	44′00″	5 053 209	49′00″	5 128 552	54′00″	5 203 905	59′00″	5 279 268
10	4 905 066	10	4 980 387	10	5 055 720	10	5 131 064	10	5 206 417	10	5 281 780
20	4 907 576	20	4 982 898	20	5 058 231	20	5 133 575	20	5 208 929	20	5 284 292
30	4 910 087	30	4 985 409	30	5 060 743	30	5 136 087	30	5 211 441	30	5 286 804
40	4 912 598	40	4 987 920	40	5 063 254	40	5 138 598	40	5 213 953	40	5 289 317
50	4 915 108	50	4 990 431	50	5 065 765	50	5 141 110	50	5 216 465	50	5 291 829
Différence tabulaire pour 10″:											
	251_{04}		251_{08}		251_{11}		251_{15}		251_{18}		251_{21}
γ = 9,80......ms^{-2}						44^0					
00′00″	5 294 341	05′00″	5 369 714	10′00″	5 445 095	15′00″	5 520 483	20′00″	5 595 878	25′00″	5 671 279
10	5 296 853	10	5 372 227	10	5 447 608	10	5 522 996	10	5 598 391	10	5 673 793
20	5 299 366	20	5 374 739	20	5 450 121	20	5 525 509	20	5 600 905	20	5 676 306
30	5 301 878	30	5 377 252	30	5 452 633	30	5 528 022	30	5 603 418	30	5 678 819
40	5 304 390	40	5 379 764	40	5 455 146	40	5 530 535	40	5 605 931	40	5 681 333
50	5 306 903	50	5 382 277	50	5 457 659	50	5 533 048	50	5 608 444	50	5 683 846
01′00″	5 309 415	06′00″	5 384 790	11′00″	5 460 172	16′00″	5 535 562	21′00″	5 610 958	26′00″	5 686 360
10	5 311 927	10	5 387 302	10	5 462 685	10	5 538 075	10	5 613 471	10	5 688 773
20	5 314 440	20	5 389 815	20	5 465 198	20	5 540 588	20	5 615 984	20	5 691 387
30	5 316 952	30	5 392 327	30	5 467 711	30	5 543 101	30	5 618 498	30	5 693 900
40	5 319 464	40	5 394 840	40	5 470 223	40	5 545 614	40	5 621 011	40	5 696 414
50	5 321 977	50	5 397 353	50	5 472 736	50	5 548 127	50	5 623 524	50	5 698 927
02′00″	5 324 489	07′00″	5 399 865	12′00″	5 475 249	17′00″	5 550 640	22′00″	5 626 038	27′00″	5 701 441
10	5 327 002	10	5 402 378	10	5 477 762	10	5 553 153	10	5 628 551	10	5 703 955
20	5 329 514	20	5 404 891	20	5 480 275	20	5 555 667	20	5 631 064	20	5 706 468
30	5 332 026	30	5 407 403	30	5 482 788	30	5 558 180	30	5 633 578	30	5 708 982
40	5 334 539	40	5 409 916	40	5 485 301	40	5 560 693	40	5 636 091	40	5 711 495
50	5 337 051	50	5 412 429	50	5 487 814	50	5 563 206	50	5 638 605	50	5 714 009
03′00″	5 339 564	08′00″	5 414 942	13′00″	5 490 327	18′00″	5 565 719	23′00″	5 641 118	28′00″	5 716 522
10	5 342 076	10	5 417 454	10	5 492 840	10	5 568 232	10	5 643 631	10	5 719 036
20	5 344 589	20	5 419 967	20	5 495 353	20	5 570 746	20	5 646 145	20	5 721 549
30	5 347 101	30	5 422 480	30	5 497 866	30	5 573 259	30	5 648 658	30	5 724 063
40	5 349 614	40	5 424 993	40	5 500 379	40	5 575 772	40	5 651 172	40	5 726 577
50	5 352 126	50	5 427 505	50	5 502 892	50	5 578 285	50	5 653 685	50	5 729 090
04′00″	5 354 639	09′00″	5 430 018	14′00″	5 505 405	19′00″	5 580 799	24′00″	5 656 198	29′00″	5 731 604
10	5 357 151	10	5 432 531	10	5 507 918	10	5 583 312	10	5 658 712	10	5 734 117
20	5 359 664	20	5 435 044	20	5 510 431	20	5 585 825	20	5 661 225	20	5 736 631
30	5 362 176	30	5 437 556	30	5 512 944	30	5 588 338	30	5 663 739	30	5 739 145
40	5 364 689	40	5 440 069	40	5 515 457	40	5 590 851	40	5 666 252	40	5 741 658
50	5 367 201	50	5 442 582	50	5 517 970	50	5 593 365	50	5 668 766	50	5 744 172
Différence tabulaire pour 10″											
	251_{24}		251_{27}		251_{29}		251_{32}		251_{34}		251_{35}

Tableau 2 – continue

γ = 9,80......ms^{-2}					44^0						
30′00″	5 746 685	35′00″	5 822 097	40′00″	5 897 512	45′00″	5 972 931	50′00″	6 048 353	55′00″	6 123 777
10	5 749 199	10	5 824 611	10	5 900 026	10	5 975 445	10	6 050 867	10	6 126 291
20	5 751 713	20	5 827 124	20	5 902 540	20	5 977 959	20	6 053 381	20	6 128 805
30	5 754 226	30	5 829 638	30	5 905 054	30	5 980 473	30	6 055 895	30	6 131 320
40	5 756 740	40	5 832 152	40	5 907 568	40	5 982 987	40	6 058 409	40	6 133 834
50	5 759 254	50	5 834 666	50	5 910 082	50	5 985 501	50	6 060 923	50	6 136 348
31′00″	5 761 767	36′00″	5 837 180	41′00″	5 912 596	46′00″	5 988 015	51′00″	6 063 438	56′00″	6 138 862
10	5 764 281	10	5 839 693	10	5 915 110	10	5 990 529	10	6 065 952	10	6 141 376
20	5 766 795	20	5 842 207	20	5 917 624	20	5 993 043	20	6 068 466	20	6 143 890
30	5 769 308	30	5 844 721	30	5 920 138	30	5 995 557	30	6 070 980	30	6 146 405
40	5 771 822	40	5 847 235	40	5 922 651	40	5 998 071	40	6 073 494	40	6 148 919
50	5 774 336	50	5 849 749	50	5 925 165	50	6 000 585	50	6 076 008	50	6 151 433
32′00″	5 776 849	37′00″	5 852 262	42′00″	5 927 679	47′00″	6 003 100	52′00″	6 078 522	57′00″	6 153 947
10	5 779 363	10	5 854 776	10	5 930 193	10	6 005 614	10	6 081 036	10	6 156 461
20	5 781 877	20	5 857 290	20	5 932 707	20	6 008 128	20	6 083 551	20	6 158 975
30	5 784 391	30	5 859 804	30	5 935 221	30	6 010 642	30	6 086 065	30	6 161 490
40	5 786 904	40	5 862 318	40	5 937 735	40	6 013 156	40	6 088 579	40	6 164 004
50	5 789 418	50	5 864 832	50	5 940 249	50	6 015 670	50	6 091 093	50	6 166 518
33′00″	5 791 932	38′00″	5 867 346	43′00″	5 942 763	48′00″	6 018 184	53′00″	6 093 607	58′00″	6 169 032
10	5 794 445	10	5 869 859	10	5 945 277	10	6 020 698	10	6 096 121	10	6 171 546
20	5 796 959	20	5 872 373	20	5 947 791	20	6 023 212	20	6 098 635	20	6 174 061
30	5 799 473	30	5 874 887	30	5 950 305	30	6 025 726	30	6 101 150	30	6 176 575
40	5 801 987	40	5 877 401	40	5 952 819	40	6 028 240	40	6 103 664	40	6 179 089
50	5 804 500	50	5 879 915	50	5 955 333	50	6 030 754	50	6 106 178	50	6 181 603
34′00″	5 807 014	39′00″	5 882 429	44′00″	5 057 847	49′00″	6 033 268	54′00″	6 108 692	59′00″	6 184 117
10	5 809 528	10	5 884 943	10	5 960 361	10	6 035 782	10	6 111 206	10	6 186 632
20	5 812 042	20	5 887 457	20	5 962 875	20	6 038 297	20	6 113 720	20	6 189 146
30	5 814 555	30	5 889 970	30	5 965 389	30	6 040 811	30	6 116 235	30	6 191 660
40	5 817 069	40	5 892 484	40	5 967 903	40	6 043 325	40	6 118 749	40	6 194 174
50	5 819 583	50	5 894 998	50	5 970 417	50	6 045 839	50	6 121 263	50	6 196 688
Différence tabulaire pour 10″:											
	251_{37}		251_{38}		251_{40}		251_{41}		251_{41}		251_{42}

γ = 9,80.....ms^{-2}					45^0						
00′00″	6 199 203	05′00″	6 274 629	10′00″	6 350 056	15′00″	6 425 483	20′00″	6 500 909	25′00″	6 576 333
10	6 201 717	10	6 277 144	10	6 352 571	10	6 427 997	10	6 503 423	10	6 578 847
20	6 204 231	20	6 279 658	20	6 355 085	20	6 430 511	20	6 505 937	20	6 581 361
30	6 206 745	30	6 282 172	30	6 357 599	30	6 433 026	30	6 508 451	20	6 583 875
40	6 209 260	40	6 284 686	40	6 360 113	40	6 435 540	40	6 510 965	30	6 586 389
50	6 211 774	50	6 287 200	50	6 362 627	50	6 438 054	50	6 513 480	40	6 588 903
01′00″	6 214 288	06′00″	6 289 715	11′00″	6 365 142	16′00″	6 440 568	21′00″	6 515 994	26′00″	6 591 417
10	6 216 802	10	6 292 229	10	6 367 656	10	6 443 082	10	6 518 508	10	6 593 932
20	6 219 316	20	6 294 743	20	6 370 170	20	6 445 597	20	6 521 022	20	6 596 446
30	6 221 831	30	6 297 257	30	6 372 684	30	6 448 111	30	6 523 536	30	6 598 960
40	6 224 345	40	6 299 772	40	6 375 199	40	6 450 625	40	6 526 050	40	6 601 474
50	6 226 859	50	6 302 286	50	6 377 713	50	6 453 139	50	6 528 564	50	6 603 988
02′00″	6 229 373	07′00″	6 304 800	12′00″	6 380 227	17′00″	6 455 653	22′00″	6 531 079	27′00″	6 606 502
10	6 231 887	10	6 307 314	10	6 382 741	10	6 458 168	10	6 533 593	10	6 609 016
20	6 234 402	20	6 309 829	20	6 385 256	20	6 460 682	20	6 536 107	20	6 611 530
30	6 236 916	30	6 312 343	30	6 387 770	30	6 463 196	30	6 538 621	30	6 614 044
40	6 239 430	40	6 314 857	40	6 390 284	40	6 465 710	40	6 541 135	40	6 616 558
50	6 241 944	50	6 317 371	50	6 392 798	50	6 468 224	50	6 543 649	50	6 619 072
03′00″	6 244 459	08′00″	6 319 886	13′00″	6 395 312	18′00″	6 470 739	23′00″	6 546 163	28′00″	6 621 586
10	6 246 973	10	6 322 400	10	6 397 827	10	6 473 253	10	6 548 678	10	6 624 100
20	6 249 487	20	6 324 914	20	6 400 341	20	6 475 767	20	6 551 192	20	6 626 614
30	6 252 001	30	6 327 428	30	6 402 855	30	6 478 281	30	6 553 706	30	6 629 129
40	6 254 515	40	6 329 942	40	6 405 369	40	6 480 795	40	6 556 220	40	6 631 643
50	6 257 030	50	6 332 457	50	6 407 883	50	6 483 310	50	6 558 734	50	6 634 157
04′00″	6 259 544	09′00″	6 334 971	14′00″	6 410 398	19′00″	6 485 824	24′00″	6 561 248	29′00″	6 636 671
10	6 262 058	10	6 337 485	10	6 412 912	10	6 488 338	10	6 563 762	10	6 639 185
20	6 264 572	20	6 339 999	20	6 415 426	20	6 490 852	20	6 566 276	20	6 641 699
30	6 267 087	30	6 342 514	30	6 417 940	30	6 493 366	30	6 568 791	30	6 644 213
40	6 269 601	40	6 345 028	40	6 420 455	40	6 495 880	40	6 571 305	40	6 646 727
50	6 272 115	50	6 347 542	50	6 422 969	50	6 498 395	50	6 573 819	50	6 649 241
Différence tabulaire pour 10″:											
	251_{42}		251_{42}		251_{42}		251_{42}		251_{41}		251_{41}

Tableau 2 – continue

γ = 9,80.....ms^{-2}					45⁰						
30′00″	6 651 755	35′00″	6 727 174	40′00″	6 802 589	45′00″	6 878 001	50′00″	6 953 408	55′00″	7 028 809
10	6 654 269	10	6 729 688	10	6 805 103	10	6 880 515	10	6 955 921	10	7 031 322
20	6 656 783	20	6 732 202	20	6 807 617	20	6 883 028	20	6 958 434	20	7 033 835
30	6 659 297	30	6 734 716	30	6 810 131	30	6 885 542	30	6 960 948	30	7 036 349
40	6 661 811	40	6 737 230	40	6 812 645	40	6 888 055	40	6 963 461	40	7 038 862
50	6 664 325	50	6 739 743	50	6 815 158	50	6 890 569	50	6 965 917	50	7 041 375
31′00″	6 666 839	36′00″	6 742 257	41′00″	6 817 672	46′00″	6 893 083	51′00″	6 968 488	56′00″	7 043 888
10	6 669 353	10	6 744 771	10	6 820 186	10	6 895 596	10	6 971 002	10	7 046 402
20	6 671 867	20	6 747 285	20	6 822 700	20	6 898 110	20	6 973 515	20	7 048 915
30	6 674 381	30	6 749 799	30	6 825 213	30	6 900 623	30	6 976 029	30	7 051 428
40	6 676 895	40	6 752 313	40	6 827 727	40	6 903 137	40	6 978 542	40	7 053 941
50	6 679 409	50	6 754 827	50	6 830 241	50	6 905 651	50	6 981 055	50	7 056 454
32′00″	6 681 923	37′00″	6 757 341	42′00″	6 832 755	47′00″	6 908 164	52′00″	6 983 569	57′00″	7 058 968
10	6 684 437	10	6 759 854	10	6 835 268	10	6 910 678	10	6 986 082	10	7 061 481
20	6 686 951	20	6 762 368	20	6 837 782	20	6 913 191	20	6 988 596	20	7 063 994
30	6 689 465	30	6 764 882	30	6 840 296	30	6 915 705	30	6 991 109	30	7 066 507
40	6 691 979	40	6 767 396	40	6 842 809	40	6 918 218	40	6 993 622	40	7 069 020
50	6 694 493	50	6 769 910	50	6 845 323	50	6 920 732	50	6 996 136	50	7 071 534
33′00″	6 697 007	38′00″	6 772 424	43′00″	6 847 837	48′00″	6 923 246	53′00″	6 998 649	58′00″	7 074 047
10	6 699 521	10	6 774 938	10	6 850 351	10	6 925 759	10	7 001 162	10	7 076 560
20	6 702 035	20	6 777 451	20	6 852 864	20	6 928 273	20	7 003 676	20	7 079 073
30	6 704 549	30	6 779 965	30	6 855 378	30	6 930 786	30	7 006 189	30	7 081 586
40	6 707 062	40	6 782 479	40	6 857 892	40	6 933 300	40	7 008 702	40	7 084 099
50	6 709 576	50	6 784 993	50	6 860 405	50	6 935 813	50	7 011 216	10	7 086 612
34′00″	6 712 090	39′00″	6 787 507	44′00″	6 862 919	49′00″	6 938 327	54′00″	7 013 729	59′00″	7 089 126
10	6 714 604	10	6 790 020	10	6 865 433	10	6 940 840	10	7 016 242	10	7 091 639
20	6 717 118	20	6 792 534	20	6 867 946	20	6 943 354	20	7 018 756	20	7 094 152
30	6 719 632	30	6 795 048	30	6 870 460	30	6 945 867	30	7 021 269	30	7 096 665
40	6 722 146	40	6 797 562	40	6 872 974	40	6 948 381	40	7 023 782	40	7 099 178
50	6 724 660	50	6 800 076	50	6 875 487	50	6 950 894	50	7 026 296	50	7 101 691
Différence tabulaire pour 10″:											
	251_{40}		251_{39}		251_{37}		251_{36}		251_{34}		251_{32}

γ = 9,80.......ms^{-2}					46⁰						
00′00″	7 104 204	05′00″	7 179 593	10′00″	7 254 974	15′00″	7 330 347	20′00″	7 405 712	25′00″	7 481 067
10	7 106 717	10	7 182 105	10	7 257 486	10	7 332 859	10	7 408 224	10	7 483 579
20	7 109 230	20	7 184 618	20	7 259 999	20	7 335 372	20	7 410 736	20	7 486 090
30	7 111 743	30	7 187 131	30	7 262 511	30	7 337 884	30	7 413 248	30	7 488 602
40	7 114 256	40	7 189 644	40	7 265 024	40	7 340 396	40	7 415 760	40	7 491 114
50	7 116 769	50	7 192 157	50	7 267 537	50	7 342 908	50	7 418 271	50	7 493 625
01′00″	7 119 282	06′00″	7 194 669	11′00″	7 270 049	16′00″	7 345 421	21′00″	7 420 783	26′00″	7 496 137
10	7 121 795	10	7 197 182	10	7 272 562	10	7 347 933	10	7 423 295	10	7 498 648
20	7 124 308	20	7 199 695	20	7 275 074	20	7 350 445	20	7 425 807	20	7 501 160
30	7 126 821	30	7 202 208	30	7 277 587	30	7 352 957	30	7 428 319	30	7 503 672
40	7 129 334	40	7 204 720	40	7 280 099	40	7 355 469	40	7 430 831	40	7 506 183
50	7 131 847	50	7 207 233	50	7 282 612	50	7 357 982	50	7 433 343	50	7 508 695
02′00″	7 134 360	07′00″	7 209 746	12′00″	7 285 124	17′00″	7 360 494	22′00″	7 435 855	27′00″	7 511 206
10	7 136 873	10	7 212 259	10	7 287 636	10	7 363 006	10	7 438 367	10	7 513 718
20	7 139 386	20	7 214 771	20	7 290 149	20	7 365 518	20	7 440 879	20	7 516 229
30	7 141 899	30	7 217 284	30	7 292 661	30	7 368 030	30	7 443 390	30	7 518 741
40	7 144 412	40	7 219 797	40	7 295 174	40	7 370 543	40	7 445 902	40	7 521 253
50	7 146 925	50	7 222 309	50	7 297 686	50	7 373 055	50	7 448 414	50	7 523 764
03′00″	7 149 438	08′00″	7 224 822	13′00″	7 300 199	18′00″	7 375 567	23′00″	7 450 926	28′00″	7 526 275
10	7 151 951	10	7 227 335	10	7 302 711	10	7 378 079	10	7 453 438	10	7 528 787
20	7 154 464	20	7 229 848	20	7 305 223	20	7 380 591	20	7 455 950	20	7 531 298
30	7 156 977	30	7 232 360	30	7 307 736	30	7 383 103	30	7 458 461	30	7 533 810
40	7 159 490	40	7 234 873	40	7 310 248	40	7 385 615	40	7 460 973	40	7 536 321
50	7 162 003	50	7 237 385	50	7 312 761	50	7 388 127	50	7 463 485	50	7 538 833
04′00″	7 164 515	09′00″	7 239 898	14′00″	7 315 273	19′00″	7 390 639	24′00″	7 465 997	29′00″	7 541 344
10	7 167 028	10	7 242 411	10	7 317 785	10	7 393 151	10	7 468 508	10	7 543 856
20	7 169 541	20	7 244 923	20	7 320 298	20	7 395 663	20	7 471 020	20	7 546 367
30	7 172 054	30	7 247 436	30	7 322 810	30	7 398 176	30	7 473 532	30	7 548 878
40	7 174 567	40	7 249 949	40	7 325 322	40	7 400 688	40	7 476 044	40	7 551 390
50	7 177 080	50	7 252 461	50	7 327 835	50	7 403 200	50	7 478 555	50	7 553 901
Différence tabulaire pour 10″:											
	251_{30}		251_{27}		251_{24}		251_{22}		251_{19}		251_{15}

Tableau 2 – continue

γ = 9,80.....ms^{-2}						46^0					
30′00″	7 556 412	35′00″	7 631 747	40′00″	7 707 071	45′00″	7 782 383	50′00″	7 857 683	55′00″	7 932 969
10	7 558 924	10	7 634 258	10	7 709 582	10	7 784 894	10	7 860 193	10	7 935 479
20	7 561 435	20	7 636 769	20	7 712 092	20	7 787 404	20	7 862 702	20	7 937 988
30	7 563 946	30	7 639 280	30	7 714 603	30	7 789 914	30	7 865 212	30	7 940 497
40	7 566 458	40	7 641 791	40	7 717 114	40	7 792 424	40	7 867 722	40	7 943 007
50	7 568 969	50	7 644 302	50	7 719 624	50	7 794 934	50	7 870 232	50	7 945 516
31′00″	7 571 480	36′00″	7 646 813	41′00″	7 722 135	46′00″	7 797 444	51′00″	7 872 741	56′00″	7 948 025
10	7 573 992	10	7 649 324	10	7 724 645	10	7 799 954	10	7 875 251	10	7 950 534
20	7 576 503	20	7 651 835	20	7 727 156	20	7 802 464	20	7 877 761	20	7 953 044
30	7 579 014	30	7 654 346	30	7 729 666	30	7 804 975	30	7 880 270	30	7 955 553
40	7 581 525	40	7 656 857	40	7 732 177	40	7 807 485	40	7 882 780	40	7 958 062
50	7 584 037	50	7 659 368	50	7 734 687	50	7 809 995	50	7 885 290	50	7 960 571
32′00″	7 586 548	37′00″	7 661 878	42′00″	7 737 198	47′00″	7 812 505	52′00″	7 887 799	57′00″	7 963 080
10	7 589 059	10	7 664 389	10	7 739 708	10	7 815 015	10	7 890 309	10	7 965 589
20	7 591 570	20	7 666 900	20	7 742 218	20	7 817 525	20	7 892 818	20	7 968 099
30	7 594 081	30	7 669 411	30	7 744 729	30	7 820 035	30	7 895 328	30	7 970 608
40	7 596 592	40	7 671 922	40	7 747 239	40	7 822 545	40	7 897 837	40	7 973 117
50	7 599 104	50	7 674 432	50	7 749 750	50	7 825 055	50	7 900 347	50	7 975 626
33′00″	7 601 615	38′00″	7 676 943	43′00″	7 752 260	48′00″	7 827 565	53′00″	7 902 856	58′00″	7 978 135
10	7 604 126	10	7 679 454	10	7 754 770	10	7 830 075	10	7 905 366	10	7 980 644
20	7 606 637	20	7 681 965	20	7 757 281	20	7 832 584	20	7 907 875	20	7 983 153
30	7 609 148	30	7 684 475	30	7 759 791	30	7 835 094	30	7 910 385	30	7 985 662
40	7 611 659	40	7 686 986	40	7 762 301	40	7 837 604	40	7 912 894	40	7 988 171
50	7 614 170	50	7 689 497	50	7 764 812	50	7 840 114	50	7 915 404	50	7 990 680
34′00″	7 616 681	39′00″	7 692 007	44′00″	7 767 322	49′00″	7 842 624	54′00″	7 917 913	59′00″	7 993 189
10	7 619 192	10	7 694 518	10	7 769 832	10	7 845 134	10	7 920 423	10	7 995 698
20	7 621 703	20	7 697 029	20	7 772 342	20	7 847 644	20	7 922 932	20	7 998 207
30	7 624 214	30	7 699 539	30	7 774 853	30	7 850 154	30	7 925 441	30	8 000 716
40	7 626 725	40	7 702 050	40	7 777 363	40	7 852 663	40	7 927 951	40	8 003 225
50	7 629 236	50	7 704 561	50	7 779 873	50	7 855 173	50	7 930 460	50	8 005 733
Différence tabulaire pour 10″:											
	251_{12}		251_{08}		251_{04}		251_{00}		250_{96}		250_{91}
γ = 9,80.....ms^{-2}						47^0					
00′00″	8 008 242	05′00″	8 083 501	10′00″	8 158 744	15′00″	8 233 972	20′00″	8 309 184	25′00″	8 384 379
10	8 010 751	10	8 086 009	10	8 161 252	10	8 236 480	10	8 311 691	10	8 386 885
20	8 013 260	20	8 088 517	20	8 163 760	20	8 238 987	20	8 314 197	20	8 389 391
30	8 015 769	30	8 091 026	30	8 166 268	30	8 241 494	30	8 316 704	30	8 391 897
40	8 018 278	40	8 093 534	40	8 168 776	40	8 244 001	40	8 319 211	40	8 394 403
50	8 020 786	50	8 096 042	50	8 171 283	50	8 246 509	50	8 321 717	50	8 396 909
01′00″	8 023 295	06′00″	8 098 551	11′00″	8 173 791	16′00″	8 249 016	21′00″	8 324 224	26′00″	8 399 415
10	8 025 804	10	8 101 059	10	8 176 299	10	8 251 523	10	8 326 731	10	8 401 922
20	8 028 313	20	8 103 567	20	8 178 807	20	8 254 030	20	8 329 237	20	8 404 428
30	8 030 821	30	8 106 075	30	8 181 314	30	8 256 537	30	8 331 744	30	8 406 934
40	8 033 330	40	8 108 584	40	8 183 822	40	8 259 045	40	8 334 251	40	8 409 440
50	8 035 839	50	8 111 092	50	8 186 330	50	8 261 552	50	8 336 757	50	8 411 946
02′00″	8 038 347	07′00″	8 113 600	12′00″	8 188 837	17′00″	8 264 059	22′00″	8 339 264	27′00″	8 414 452
10	8 040 856	10	8 116 108	10	8 191 345	10	8 266 566	10	8 341 770	10	8 416 958
20	8 043 365	20	8 118 616	20	8 193 853	20	8 269 073	20	8 344 277	20	8 419 464
30	8 045 873	30	8 121 124	30	8 196 360	30	8 271 580	30	8 346 783	30	8 421 969
40	8 048 382	40	8 123 633	40	8 198 868	40	8 274 087	40	8 349 290	40	8 424 475
50	8 050 891	50	8 126 141	50	8 201 375	50	8 276 594	50	8 351 796	50	8 426 981
03′00″	8 053 399	08′00″	8 128 649	13′00″	8 203 883	18′00″	8 279 101	23′00″	8 354 303	28′00″	8 429 487
10	8 055 908	10	8 131 157	10	8 206 390	10	8 281 608	10	8 356 809	10	8 431 993
20	8 058 416	20	8 133 665	20	8 208 898	20	8 284 115	20	8 359 316	20	8 434 499
30	8 060 925	30	8 136 173	30	8 211 406	30	8 286 622	30	8 361 822	30	8 437 005
40	8 063 433	40	8 138 681	40	8 213 913	40	8 289 129	40	8 364 328	40	8 439 510
50	8 065 942	50	8 141 189	50	8 216 420	50	8 291 636	50	8 366 835	50	8 442 016
04′00″	8 068 450	09′00″	8 143 697	14′00″	8 218 928	19′00″	8 294 143	24′00″	8 369 341	29′00″	8 444 522
10	8 070 959	10	8 146 205	10	8 221 435	10	8 296 650	10	8 371 847	10	8 447 028
20	8 073 467	20	8 148 713	20	8 223 943	20	8 299 157	20	8 374 354	20	8 449 533
30	8 075 976	30	8 151 221	30	8 226 450	30	8 301 663	30	8 376 860	30	8 452 039
40	8 078 484	40	8 153 729	40	8 228 958	40	8 304 170	40	8 379 366	40	8 454 545
50	8 080 992	50	8 156 236	50	8 231 465	50	8 306 677	50	8 381 872	50	8 457 050
Différence tabulaire pour 10″:											
	250_{86}		250_{81}		250_{76}		250_{70}		250_{65}		250_{59}

Tableau 2 – continue

γ = 9,80.....ms^{-2}						47°					
30′00″	8 459 556	35′00″	8 534 715	40′00″	8 609 855	45′00″	8 684 976	50′00″	8 760 077	55′00″	8 835 157
10	8 462 061	10	8 537 220	10	8 612 359	10	8 687 480	10	8 762 580	10	8 837 659
20	8 464 567	20	8 539 725	20	8 614 864	20	8 689 983	20	8 765 083	20	8 840 161
30	8 467 073	30	8 542 230	30	8 617 368	30	8 692 487	30	8 767 586	30	8 842 664
40	8 469 578	40	8 544 735	40	8 619 872	40	8 694 991	40	8 770 089	40	8 845 166
50	8 472 084	50	8 547 240	50	8 622 377	50	8 697 494	50	8 772 591	50	8 847 668
31′00″	8 474 589	36′00″	8 549 744	41′00″	8 624 881	46′00″	8 699 998	51′00″	8 775 094	56′00″	8 850 170
10	8 477 095	10	8 552 249	10	8 627 385	10	8 702 501	10	8 777 597	10	8 852 672
20	8 479 600	20	8 554 754	20	8 629 889	20	8 705 005	20	8 780 100	20	8 855 174
30	8 482 105	30	8 557 259	30	8 632 393	30	8 707 508	30	8 782 603	30	8 857 777
40	8 484 611	40	8 559 764	40	8 634 898	40	8 710 012	40	8 785 106	40	8 860 179
50	8 487 116	50	8 562 268	50	8 637 402	50	8 712 515	50	8 787 608	50	8 862 681
32′00″	8 489 622	37′00″	8 564 773	42′00″	8 639 906	47′00″	8 715 019	52′00″	8 790 111	57′00″	8 865 183
10	8 492 127	10	8 567 278	10	8 642 410	10	8 717 522	10	8 792 614	10	8 867 685
20	8 494 632	20	8 569 783	20	8 644 914	20	8 720 025	20	8 795 117	20	8 870 187
30	8 497 138	30	8 572 287	30	8 647 418	30	8 722 529	30	8 797 619	30	8 872 689
40	8 499 643	40	8 574 792	40	8 649 922	40	8 725 032	40	8 800 122	40	8 875 191
50	8 502 148	50	8 577 297	50	8 652 426	50	8 727 535	50	8 802 625	50	8 877 693
33′00″	8 504 653	38′00″	8 579 801	43′00″	8 654 930	48′00″	8 730 039	53′00″	8 805 127	58′00″	8 880 194
10	8 507 159	10	8 582 306	10	8 657 434	10	8 732 542	10	8 807 630	10	8 882 696
20	8 509 664	20	8 584 810	20	8 659 938	20	8 735 045	20	8 810 132	20	8 885 198
30	8 512 169	30	8 587 315	30	8 662 442	30	8 737 549	30	8 812 635	30	8 887 700
40	8 514 674	40	8 589 820	40	8 664 946	40	8 740 052	40	8 815 137	40	8 890 202
50	8 517 179	50	8 592 324	50	8 667 449	50	8 742 555	50	8 817 640	50	8 892 704
34′00″	8 519 685	39′00″	8 594 829	44′00″	8 669 953	49′00″	8 745 058	54′00″	8 820 142	59′00″	8 895 205
10	8 522 190	10	8 597 333	10	8 672 457	10	8 747 561	10	8 822 645	10	8 897 707
20	8 524 695	20	8 599 838	20	8 674 961	20	8 750 064	20	8 825 147	20	8 900 209
30	8 527 200	30	8 602 342	30	8 677 465	30	8 752 567	30	8 827 650	30	8 902 710
40	8 529 705	40	8 604 846	40	8 679 968	40	8 755 071	40	8 830 152	40	8 905 212
50	8 532 210	50	8 607 351	50	8 682 472	50	8 757 574	50	8 832 654	50	8 907 714
					Différence tabulaire pour 10″:						
	250_{53}		250_{47}		250_{41}		250_{34}		250_{27}		250_{20}

γ =9,80.....ms^{-2}						48°					
00′00″	8 910 215	05′00″	8 985 252	10′00″	9 060 266	15′00″	9 135 257	20′00″	9 210 224	25′00″	9 285 166
10	8 912 717	10	8 987 753	10	9 062 766	10	9 137 756	10	9 212 722	10	9 287 664
20	8 915 218	20	8 990 254	20	9 065 266	20	9 140 255	20	9 215 221	20	9 290 162
30	8 917 720	30	8 992 754	30	9 067 766	30	9 142 755	30	9 217 719	30	9 292 659
40	8 920 222	40	8 995 255	40	9 070 266	40	9 145 254	40	9 220 218	40	9 295 157
50	8 922 723	50	8 997 756	50	9 072 766	50	9 147 753	50	9 222 716	50	9 297 654
01′00″	8 925 224	06′00″	9 000 257	11′00″	9 075 266	16′00″	9 150 252	21′00″	9 225 214	26′00″	9 300 152
10	8 927 726	10	9 002 757	10	9 077 766	10	9 152 751	10	9 227 713	10	9 302 649
20	8 930 227	20	9 005 258	20	9 080 266	20	9 155 250	20	9 230 211	20	9 305 147
30	8 932 729	30	9 007 759	30	9 082 766	30	9 157 750	30	9 232 709	30	9 307 644
40	8 935 230	40	9 010 259	40	9 085 266	40	9 160 249	40	9 235 207	40	9 310 141
50	8 937 731	50	9 012 760	50	9 087 765	50	9 162 748	50	9 237 706	50	9 312 639
02′00″	8 940 233	07′00″	9 015 260	12′00″	9 090 265	17′00″	9 165 247	22′00″	9 240 204	27′00″	9 315 136
10	8 942 734	10	9 017 761	10	9 092 765	10	9 167 746	10	9 242 702	10	9 317 634
20	8 945 235	20	9 020 261	20	9 095 265	20	9 170 244	20	9 245 200	20	9 320 131
30	8 947 736	30	9 022 762	30	9 097 764	30	9 172 743	30	9 247 698	30	9 322 628
40	8 950 238	40	9 025 262	40	9 100 264	40	9 175 242	40	9 250 196	40	9 325 125
50	8 952 739	50	9 027 763	50	9 102 764	50	9 177 741	50	9 252 694	50	9 327 622
03′00″	8 955 240	08′00″	9 030 263	13′00″	9 105 263	18′00″	9 180 240	23′00″	9 255 192	28′00″	9 330 120
10	8 957 741	10	9 032 764	10	9 107 763	10	9 182 739	10	9 257 690	10	9 332 617
20	8 960 242	20	9 035 264	20	9 110 263	20	9 185 238	20	9 260 188	20	9 335 114
30	8 962 743	30	9 037 764	30	9 112 762	30	9 187 736	30	9 262 686	30	9 337 611
40	8 965 244	40	9 040 265	40	9 115 262	40	9 190 235	40	9 265 184	40	9 340 108
50	8 967 745	50	9 042 765	50	9 117 761	50	9 192 734	50	9 267 682	50	9 342 605
04′00″	8 970 246	09′00″	9 045 265	14′00″	9 120 261	19′00″	9 195 232	24′00″	9 270 180	29′00″	9 345 102
10	8 972 747	10	9 047 765	10	9 122 760	10	9 197 731	10	9 272 678	10	9 347 599
20	8 975 248	20	9 050 266	20	9 125 260	20	9 200 230	20	9 275 175	20	9 350 096
30	8 977 749	30	9 052 766	30	9 127 759	30	9 202 728	30	9 277 673	30	9 352 593
40	8 980 250	40	9 055 266	40	9 130 258	40	9 205 227	40	9 280 171	40	9 355 090
50	8 982 751	50	9 057 766	50	9 132 758	50	9 207 725	50	9 282 669	50	9 357 587
					Différence tabulaire pour 10″:						
	250_{13}		250_{05}		249_{97}		249_{89}		249_{81}		249_{72}

latitude a un nombre de secondes qui diffère de 10 ou de ses multiples.

Dans l'intervalle de latitude considéré, la différence de tabulation a varié entre 249,72 et $251,72.10^{-8}$ ms^{-2}. Pour attester la précision du calcul des valeurs du champ normal, on présente, dans la figure 1, la variation du gradient horizontal normal le long du méridien géodésique pour les intervalles de 5′ où les valeurs de celui-ci peuvent être considérées constantes. Les déviations par rapport aux valeurs idéales représentées par la courbe continue varie entre 0 et $0,5.10^{-9}$ ms^{-9}, ce qui prouve que la précision exigée est entièrement réalisée.

Il résulte de la figure que la variation idéale du gradient horizontal normal admet un maximum pour la latitude B = 45°07′. La vérification se réalise immédiatement par la résolution de l'équation trigonométrique obtenue par la double dérivation de l'expression γ par rapport à B. Si on note avec B_1, B_2, B_3 et B_4 les coefficients de la paranthèse de la formule qui exprime le champ normal, il résulte:

$$\frac{\delta^2\gamma}{\delta B^2} = \beta_1 + (6\beta_2 - 2\beta_1)sin^2B + (15\beta_3 - 8\beta_2)sin^4B + (28\beta_4 - 18\beta_3)sin^6B - 32\beta_4 sin^8B = 0$$

En introduisant les valeurs numériques des coéficients B_1, il résulte l'équation suivante:

$$0{,}010\,418\,4520\sin^2B + 0{,}000\,184\,2814\sin^4B + 0{,}000\,002\,2520\sin^6B + 0{,}000\,000\,0224\sin^8B = 0{,}005\,279\,0414$$

qui a une racine B = 45°07′10″ dans l'intervalle $0^0 \leq B \leq 90^0$. La différence entre la position du maximum obtenue graphiquement par rapport à celle analithique est insignifiante, fait qui confirme la valabilité de la courbe de la figure.

Conversion des données existents

Le tableau 3 présente les valeurs du champ normal calculées avec les formules de Helmert (1901) et de Cassinis (1930), employées jusqu'à présent dans notre pays, parallèlement à celles déterminées par les formules internationales adoptées en 1967 et 1980. Elles ont été déterminées avec une précision de $10^{-8}ms^{-2}$=10^{-3} mgal, satisfaisante pour réaliser une étude comparative. On peut constater que les déviations les plus importantes apparaissent pour les valeurs calculées avec la formule de Cassinis.

Le tableau 4 présente les corrections éxigées pour le système de référence 1980 des valeurs des anomalies de la pesanteur calculées avec les formules de Helmert (1901) et Cassinis (1930) pour des intervalles de latitude géodésique de 30′. Les valeurs sont données en mgal étant donné que cette unité a été utilisée dans les travaux gravimétriques en Roumanie. On constate que la différence γ_{SGR-67}-γ_{SGR-80} = 0,86 mgal est constante. Le passage de la formule de Helmert (1901), employée à présent dans la géodésie physique, à la formule internationalle SGR (1980) est simple pour les latitudes entre lesquelles se situe notre pays, la différence étant de 0,02 mgal seulement.

Tableau 3

Valeurs du champ normal de la pesanteur calculées avec quelques formules significatives pour des latitudes comprises entre 43°30′ et 48°30′, à des intervalles de 10′ = 9,80....ms^{-2}

Latitude géodésique B	Formule Helmert (1901)	Formule Cassinis (1930)	Formule SGR–1967	Formule SGR–1980
		γ = 9,80....ms^{-2}		
43°30′	480 265	494 053	483 373	484 231
40′	495 327	509 078	498 436	499 294
50′	510 393	524 107	513 504	514 326
44°00′	525 463	539 138	528 576	529 434
10′	540 537	554 174	543 651	544 510
20′	555 614	569 212	558 729	559 588
30′	570 693	584 255	573 810	574 669
40′	585 774	599 297	588 892	589 751
50′	600 857	614 341	603 976	604 835
45°00′	615 941	629 387	619 061	619 920
10′	631 025	644 432	634 146	635 006
20′	646 109	659 478	649 231	650 091
30′	661 193	674 523	664 315	665 176
40′	676 275	689 567	679 399	680 259
50′	691 356	704 609	694 480	695 341
46°00′	706 435	719 649	709 560	710 420
10′	721 511	734 686	724 637	725 497
20′	736 584	749 722	739 710	740 571
30′	751 654	764 752	754 780	655 641
40′	766 719	779 777	769 846	770 707
50′	781 780	794 800	784 907	785 768
47°00′	796 836	809 816	799 963	800 824
10′	811 886	824 827	815 013	815 874
20′	826 929	839 832	830 057	830 918
30′	841 966	854 929	845 094	845 956
40′	856 996	869 819	860 123	860 986
50′	872 018	884 803	875 145	876 008
48°00′	887 032	899 776	890 159	891 022
10′	902 038	914 742	905 164	906 027
20′	917 034	929 700	920 160	921 022
30′	932 020	944 656	935 145	936 008

Des problèmes plus compliqués, au moins en ce qui concerne le volume des données existentes, apparaissent lorsqu'on transcalcule en SGR–80 des valeurs calculées avec la formule de Cassinis (1930), comme il résulte des expressions:

$$(\gamma_C - \gamma_{SGR-80})48^030' = +\ 9{,}82 \text{ mgal}$$
$$(\gamma_C - \gamma_{SGR-80})48^030' = +\ 8{,}64 \text{ mgal}.$$

Pour les cartes gravimétriques existantes, le passage au nouveau système se réalise soit par l'emploi des valeurs du tableau 3 et celles calculées par Botezatu et Ştefănescu (1963) en vue de déterminer des déviations et de les corriger, soit par la formule de transformation avec une structure simple:

$$\Delta\gamma = 16{,}32 - 13{,}70 \sin^2 B$$

qui donne la correction en mgal, qui doit être appliquée aux valeurs de l'anomalie de la pesanteur en employant cette formule dans l'intervalle de latitudes pris en considération, l'erreur maximum ne depasse pas 0,01 mgal.

Tableau 4

Corrections pour le passage des valeurs des anomalies de la pesanteur calculée avec les formules de Helmert (1901), Cassinis (1930) et SGR (1967), en SGR (1980)

B	$\gamma_H - \gamma_{SGR-80}$	$\gamma_C - \gamma_{SGR-80}$ (mgal)	$\gamma_{SGR} - \gamma_{SGR-80}$
43°30′	- 3,97	+ 9,82	- 0,86
44°	- 3,97	+ 9,70	- 0,86
44°30′	- 3,98	+ 9,59	- 0,86
45°	- 3,98	+ 9,47	- 0,86
45°30′	- 3,98	+ 9,35	- 0,86
46°	- 3,99	+ 9,23	- 0,86
46°30′	- 3,99	+ 9,11	- 0,86
46°30′	- 3,99	+ 9,11	- 0,86
47°	- 3,99	+ 8,99	- 0,86
47°30′	- 3,99	+ 8,87	- 0,86
48°	- 3,99	+ 8,75	- 0,86
48°30′	- 3,99	+ 8,64	- 0,86

Le système WGS-84 (WORLD GEODETIC SYSTEM 1984) a été adopté après la conclusion de ce travail. Lors de l'introduction, dans l'équation WGS-84, d'une correction qui tienne compte de l'effet gravimétrique de l'atmosphère, la plus grande différence entre le système GRS-80 et le système WGS-84 est de 0,000018 mgal pour une latitude de 45°.

En conclusion, les tableaux des valeurs de la pesanteur normale qui sont présentées dans ce travail gardent leurs valabilitées et nous pouvons les utiliser pour dessiner des cartes gravimétriques à différentes échelles.

Bibliographie

Botezatu R., Ştefănescu R. (1963) Reţeaua gravimetrică a R.P.R. III. Reduceri de cîmp normal după formula internaţională pentru teritoriul R.P.R. *St. cerc. geofiz.*, 1, 1, p. 217–237, Bucureşti.

Cassinis G. (1930) Sur l'adoption d'une formule internationale pour la pesanteur normale. *Bull. Géod.*, 26, p. 40–49, Paris.

– (1931) Tables des valeurs de la pesanteur normale internationale. *Bull. Géod.*, 32, p. 313–320, Paris.

Dragomir V., Ghiţău D., Mihăilescu M., Rotaru M. (1977) Teoria figurii Pămntului. Edit. tehn., Bucureşti.

Ermeev V. F., Jurkina M. I. (1974) Theorie der Höhen in Gravitationsfeld der Erde. In: "Arbeiten aus dem Vermessungs und Kartenwesen der DDR, 32, Kombinat Geod. und Kartogr., Leipzig.

Ghiţău D. (1983) Geodezie şi gravimetrie geodezică. Edit. did. pedag., Bucureşti.

Heiskanen W. A., Moritz H. (1967) Physical Geodesy. W. H. Freeman, San Francisco.

Moritz H. (1980) Geodetic Reference System 1980. *Bull. Géod.*, 54, 3, p. 395–405, Paris.

– (1980) Advanced physical geodesy. H. Wichmann Verlag, Karlsruhe.

Soler E. (1931) Sur certaines problèmes de gravimétrie. *Bull. Géod.*, 29, p. 27–32, Paris.

Somigliana C. (1933) Les expressions finies de la pesanteur normale. *Bull. Géod.*, 38, p. 178–187, Paris.

x x x (1967) Geodetic Reference System. *Publ. Spéc. no. 3 du Bull. Géod.*, Paris.

x x x (1969) Spravocinik geofizika, Gravirazvedka, pod. red. E. A. Mudreţovoi, Nedra, Moskva.

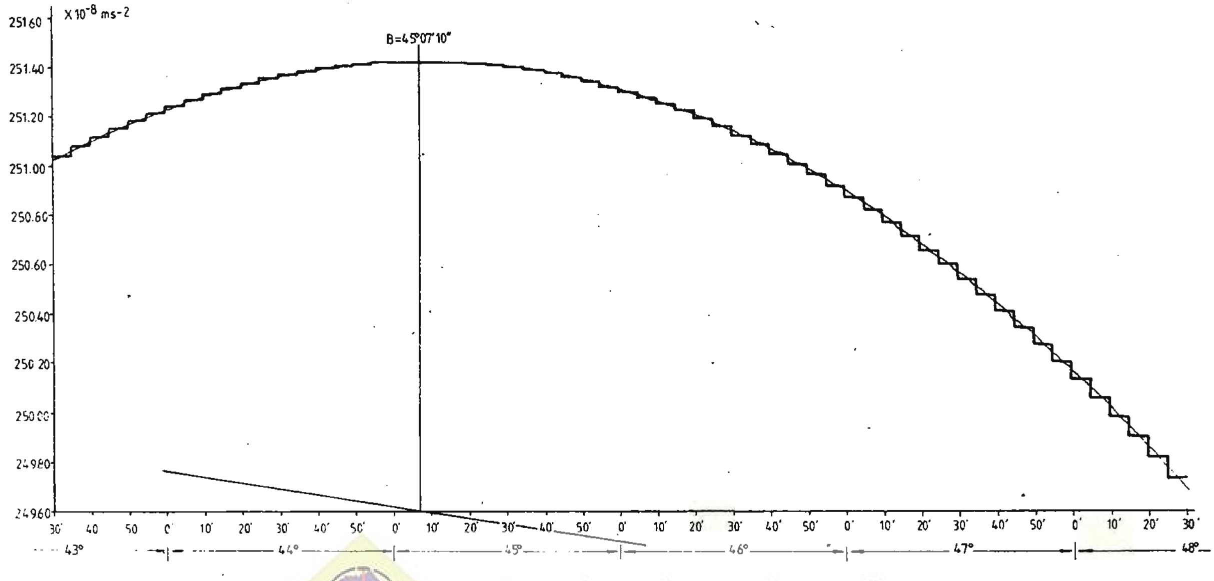

Les constantes de l'ellipsoïde international de réfférence (après H. Moritz, 1980)

Constantes géométriques

b = 6 356 752.3141 m	– sémiaxe .....
E = 521 854.0097 m	– l'excentricité liniaire
c = 6 399 593.6259 m	– le rayon de curbure polaire
e^2 = 0,006 694 380 02290	e = première excentricité
e'^2 = 0, 006 739 496 775 48	e' = la deuxième excenticité
f = 0,003 352 810 681 18	-
f^{-1} = 298,257 223 101	-
Q = 10 001 965,7293 m	
R_1 = 6 371 008,7714 m	$R_1 = (2a+b)/3$
R_2 = 6 371 007,1810 m	
R_3 = 6 371 000,7900 m	

Constantes physiques

U_0 = 6 263 686.0850 x 10 m^2s^{-2}	–
J_4 = -0,000 002 370 91222	
J_6 = 0,000 000 006 08347	
J_8 = -0,000 000 000 014 27	
m = 0,003 449 786 003 08	$m = \omega^2 a^2 b/GM$
γ_e = 9,780 236 7715 ms^{-2}	la pésanteur normale à l'Equateur
γ_p = 9,832 186 3685 ms^{-2}	la pésanteur normale au Pole
f^x = 0,005 302 440 112	$f^x = (\gamma_p - \gamma_e)/\gamma_e$
k = 0,001 931 851 353	$k = (b\gamma_p - a\gamma_e)a.\gamma_e$

Received: February 21, 1989
Accepted: February 22, 1989
Presented at the XVI-th Symposium of Earth's Physics and Applied Geophysics: June 5-6, 1989

INSTRUCŢIUNI PENTRU AUTORI

ROMANIAN JOURNAL OF GEOPHYSICS publică contribuţii ştiinţifice originale în domeniile mineralogiei, cristalografiei, geochimiei mineralelor etc.

Vor fi acceptate numai lucrările care prezintă concis şi clar informaţii noi. Manuscrisul va fi supus lecturii critice a unuia sau mai multor specialişti; după a doua revizie nesatisfăcătoare din partea autorilor va fi respins definitiv şi nu va fi înapoiat.

Manuscrisele trebuie prezentate, de regulă, în engleză sau franceză; cele prezentate în limba română trebuie să fie însoţite de un rezumat, în engleză sau franceză, de maximum 10 % din volumul manuscrisului.

Lucrările trebuie depuse, în două exemplare, la secretariatul Comitetului de redacţie, inclusiv ilustraţiile în original. Manuscrisul trebuie să cuprindă: textul (cu o pagină de titlu, care este şi prima pagină a lucrării), bibliografie, cuvinte cheie, abstract, ilustraţii, explicaţii ale figurilor şi planşelor, şi un sumar cu scop tehnic.

Se va adăuga o filă separată cu un sumar, în care se va indica ierarhia titlurilor din text în clasificarea zecimală (1; 1.1; 1.1.1), care nu trebuie să depăşească patru categorii.

Textul va fi dactilografiat la două rînduri (31 rînduri/pagină şi 64 semne/rînd), pe o singură parte a colii, cu un spaţiu liber de 3–4 cm în partea stîngă a paginii şi nu trebuie să depăşească 20 pagini dactilografiate (inclusiv bibliografia şi figurile).

Prima pagină a textului va cuprinde: a) titlul lucrării (concis, dar informativ), cu un spaţiu de 8 cm deasupra; b) numele întreg al autorului (autorilor); c) instituţia (instituţiile) şi adresa (adresele) pentru fiecare autor sau grup de autori; d) colontitlu de maximum 60 semne. Notele de subsol se vor numerota consecutiv.

Citările din text trebuie să includă numele autorului şi anul publicării. Exemplu: Ionescu (1970) sau (Ionescu, 1970). Pentru doi autori: Ionescu, Popescu (1969) sau (Ionescu, Popescu, 1969). Pentru mai mult de doi autori: Ionescu et al. (1980) sau (Ionescu et al., 1980). Pentru lucrările care se află sub tipar, anul publicării va fi înlocuit cu "in press". Lucrările nepublicate şi rapoartele vor fi citate în text ca şi cele publicate.

Abstractul, maximum 20 rînduri, trebuie să fie în limba engleză şi să prezinte pe scurt principalele rezultate şi concluzii (nu o simplă listă cu subiecte abordate).

Cuvintele cheie (maximum 10) trebuie să fie în limba engleză sau franceză, corespunzător limbii în care este lucrarea (sau abstractul, dacă textul este în română), prezentate în succesiune de la general la specific şi dactilografiate pe pagina cu abstractul.

Bibliografia se va dactilografia la două rînduri, în ordine alfabetică şi cronologică pentru autorii cu mai mult de o lucrare. Abrevierile titlului jurnalului sau ale editurii trebuie să fie conforme cu recomandările respectivelor publicaţii sau cu standardele internaţionale.

Exemple:

a) jurnale:

Giuşcă, D. (1952) Contributions à l'étude cristallochimique des niobates. *An. Com. Geol.*, XXIII, p. 259–268, Bucureşti.

– , Pavelescu, L. (1954) Contribuţii la studiul mineralogic al zăcămîntului de la Muşca. *Comm. Acad. Rom.*, IV, 11–12, p. 658–991, Bucureşti.

b) publicaţii speciale:

Strand, T. (1972) The Norwegian Caledonides. p. 1–20. In: Kulling, O., Strand, T. (eds.) Scandinavian Caledonides, 560 p., Interscience Publishers.

c) cărţi:

Bălan, M. (1976) Zăcămintele manganifere de la Iacobeni. Ed. Acad. Rom., 132 p., Bucureşti.

d) hărţi:

Ionescu, I., Popescu, P., Georgescu, G. (1990) Geological Map of Romania, scale 1:50,000, sheet Cîmpulung. Inst. Geol. Geofiz., Bucureşti.

e) lucrări nepublicate sau rapoarte:

Dumitrescu, D., Ionescu, I., Moldoveanu, M. (1987) Report. Arch. Inst. Geol. Geofiz., Bucureşti.

Lucrările sau cărţile publicate în rusă, bulgară, sîrbă etc. trebuie menţionate în bibliografie transliterînd numele şi titlurile. Exemplu:

Krasheninnikov, V. A., Basov, I. A. (1968) Stratigrafiya kainozoia. Trudy GIN, 410, 208 p., Nauka, Moskow.

Ilustraţiile (figuri şi planşe) trebuie numerotate şi prezentate în original, pe coli separate (hîrtie de calc), bune pentru reprodus. Dimensiunea liniilor, a literelor şi simbolurilor pe figuri trebuie să fie suficient de mare pentru a putea fi citite cu uşurinţă după ce au fost reduse. Dimensiunea originalului nu trebuie să depăşească suprafaţa tipografică a paginii: lăţimea coloanei 8 cm, lăţimea paginii 16,5 cm, lungimea paginii 23 cm, pentru figuri, iar pentru planşele liniare nu trebuie să depăşească dimensiunile unei pagini simple (16,5/23 cm) sau duble (23/33 cm) şi trebuie să fie autoexplicativă (să includă titlul, autori, explicaţie etc.). Scară grafică obligatorie.

Ilustraţiile fotografice (numai alb-negru) trebuie să fie clare, cu contrast bun şi grupate pe planşe de 16/23 cm. In cadrul fiecărei planşe numărătoarea fotografiilor se repetă (de. ex. Pl. I, fig. 1, Pl. II, fig. 1).

Tabelele vor fi numerotate şi vor avea un titlu. Dimensiunea originală a tabelelor trebuie să corespundă dimensiunilor tipografice menţionate mai sus (8/16,5 sau 16,5/23).

Autorii vor primi un singur set de corectură, pe care trebuie să-l înapoieze, cu corecturile corespunzătoare, după 10 zile de la primire. Numai greşelile de tipar trebuie corectate; nu sînt acceptate modificări.

Autorii vor primi gratuit 30 de extrase pentru fiecare lucrare.

Comitetul de redacţie

INSTRUCTIONS TO AUTHORS

ROMANIAN JOURNAL OF GEOPHYSICS publishes original scientific contributions dealing with any subject in the field of mineralogy, crystallography, mineral geochemistry etc.

Only papers presenting concisely and clearly new information will be accepted. The manuscript will be submitted for critical lecture to one or several advisers. Papers will be definitely rejected after a second unsatisfactory revision by the authors. The manuscripts will not be returned to the authors even if rejected.

Manuscripts are prefered in English or French. Manuscripts submitted in Romanian will be accompanied by an abstract in English or French (maximum 10 per cent of the manuscript volume).

Papers should be submitted in duplicate to the secretary of the Editorial Board, including the reproduction rea.y original figures. The manuscript should comprise: text (with a title page which is the first page of it), references, key words, abstract, illustrations, captions and a summary for technical purposes.

The author(s) should add a separate sheet with a summary indicating the hierarchy of headings from the text listed in decimal classification (1; 1.1; 1.1.1) but not exceeding four categories.

The text should be double-spaced typed (31 lines/page with 64 strokes each line) on one side of the paper only, holding an empty place of 3–4 cm on the left side of the page. The text cannot exceed 20 typewritten pages (including references and figures).

The front page (first page of the text) should comprise: a) title of the paper (concise but informative) with an empty space of 8 cm above it; b) full name(s) of the author(s); c) institution(s) and address(es) for each author or group of authors; d) short title (colontitle) of maximum 60 strokes. Footnotes should be numbered consequtively.

Citations in the text should include the name of the author and the publication year. Example: Ionescu (1970) or (Ionescu, 1970). For two authors: Ionescu, Popescu (1969) or (Ionescu, Popescu, 1969). For more than two authors: Ionescu et al. (1980) or (Ionescu et al., 1930). For papers which are in course of print the publication year will be replaced by "in press". Unpublished papers or reports will be cited in the text like the published ones.

Abstract, of maximum 20 lines, must be in English, summarizing the main results and conclusions (not a simple listing of topics).

Key words (max. 10 items), in English or French, following the language used in the text (or the Resumé if the text is in Romanian), given in succession from general to specific, should be typed on the abstract page.

References should be typed in double-line spacing, listed in alphabetical order and chronological order for authors with more than one reference. Abbreviations of journals or publishing houses should be in accordance with the recommendations of the respective publications or with the international practice.

Examples:

a) journals:

Giuşcă, D. (1952) Contributions à l'étude cristallochimique des niobates. *An. Com. Geol.*, XXIII, p. 259–268, Bucureşti.

– , Pavelescu, L. (1954) Contribuţii la studiul mineralogic al zăcămîntului de la Muşca. *Comm. Acad. Rom.*, IV, 11–12, p. 658–991, Bucureşti.

b) special issues:

Strand, T. (1972) The Norwegian Caledonides. p. 1–20. In: Kulling, O., Strand, T. (eds.) Scandinavian Caledonides, 560 p., Interscience Publishers.

c) books:

Bălan, M. (1976) Zăcămintele manganifere de la Iacobeni. Ed. Acad. Rom., 132 p., Bucureşti.

d) maps:

Ionescu, I., Popescu, P., Georgescu, G. (1990) Geological Map of Romania, scale 1:50,000, sheet Cîmpulung. Inst. Geol. Geofiz., Bucureşti.

e) unpublished papers or reports:

Dumitrescu, D., Ionescu, I., Moldoveanu, M. (1987) Report. Arch. Inst. Geol. Geofiz., Bucureşti.

Papers or books published in Russian, Bulgarian or Serbian etc. should be mentioned in the references transliterating the name and titles. Example:

Krasheninnikov, V. A., Basov, I. A. (1968) Stratigrafiya . kainozoia. Trudy GIN, 410, 208 p., Nauka, Moskow.

Illustrations (figures and plates) must be numbered and submitted as originals on separate sheets (tracing papers), ready for reproduction. The thickness of the lines, lettering and symbols on figures should be large enough to be easily read after size-reduction. The original size should not extend beyond the print area of the page: column width 8 cm, page width 16.5 cm, page length 23 cm for figures; the width of line drawings should not extend over a single (16.5/23) or double (23/33 cm) page area and must be selfexplanatory (including title, authors, legend etc.). The graphic scale is obligatory.

Photographic illustrations (black-and-white only) must be of high quality and should be grouped into plates 16/23 cm in size. Each plate should have the photos numbered, i.e. Pl. I, Fig. 1; Pl. II, Fig. 1.

Tables should be numbered and entitled. Original size of the tables should correspond to the above mentioned (8/16.5 or 16.5/23) dimensions of the printing area.

Author(s) will receive only one set of preprint proofs which must be returned, with corrections, 10 days after receiving them. Only printing errors should be corrected, no changes in the text can be accepted.

Thirty offprints of each paper are supplied to the author(s) free of charge.

The Editorial Board